UNIVERSIDAD COMPLUTENSE DE MADRID

FACULTAD DE MEDICINA

DEPARTAMENTO DE MICROBIOLOGÍA

TESIS DOCTORAL

DC-SIGN como modelo de receptor de reconocimiento de patógeno:
Interacción con las glicoproteínas de la envoltura de los virus VIH-1 y Ébola y su papel en la patogénesis viral

DC-SIGN as a model of pathogen recognition receptor:
Interaction with the envelope glycoproteins of HIV-1 and Ebola virus and the role in viral pathogenesis

MEMORIA PARA OPTAR AL GRADO DE DOCTORA
PRESENTADA POR

Joanna Luczkowiak

Director

Rafael Delgado Vázquez

Madrid, 2014

©Joanna Luczkowiak, 2014

UNIVERSIDAD COMPLUTENSE DE MADRID

Facultad de Medicina

Departamento de Microbiología

DC-SIGN como modelo de receptor de reconocimiento de patógenos: interacción con las glicoproteínas de la envoltura de los virus VIH-1 y Ébola y su papel en la patogénesis viral

DC-SIGN as a model of pathogen recognition receptor: interaction with the envelope glycoproteins of HIV-1 and Ebola virus and the role in viral pathogenesis

Tesis Doctoral

Joanna Luczkowiak

Director de la Tesis Doctoral: Dr. Rafael Delgado Vázquez

Madrid 2014

Informe del Director de la Tesis Doctoral

DATOS DE LA TESIS DOCTORAL	
Nombre del Doctorando	Joanna Luczkowiak
Título de la Tesis	DC-SIGN como modelo de receptor de reconocimiento de patógenos: interacción con las glicoproteínas de la envoltura de los virus VIH-1 y Ébola y su papel en la patogénesis viral. DC-SIGN as a model of pathogen recognition receptor: interaction with the envelope glycoproteins of HIV-1 and Ebola virus and the role in viral pathogenesis.
Facultad o Centro	Facultad de Medicina, UCM

DATOS DEL DIRECTOR DE LA TESIS DOCTORAL	
Nombre Completo	Rafael Delgado Vázquez
Centro al que pertenece y dirección	Hospital Universitario 12 de Octubre Facultad de Medicina UCM Avenida de Córdoba sn
D.N.I/Pasaporte	05228085R
e-mail	rafael.delgado@salud.madrid.org

	VALORACIÓN DE LA TESIS			
	Muy Buena	Buena	Suficiente	Deficiente
Originalidad	✓			
Definición Objetivos	✓			
Metodología	✓			
Relevancia Resultados	✓			
Discusión / Conclusiones	✓			

INFORME:

En este trabajo realizado bajo mi supervisión se presentan resultados originales para el desarrollo de una plataforma de cribado de compuestos antivirales basada en un modelo de infección mediado por le receptor DC-SIGN, así como una nueva aproximación al papel que este receptor puede tener en la patogenia de las infecciones por el Virus Ébola y VIH. Los objetivos, metodología, interpretación de resultados y concusiones se han realizado de acuerdo con el método científico y en conjunto reúnen los requisitos para ser presentados como tesis doctoral.

Madrid, a 24 de Abril de 2014

Fdo.: Dr. Rafael Delgado Vázquez

Osobom najbliższym mojemu sercu, rodzicom.

Bardzo Wam dziekuję za ogromną pomoc w zdobyciu wykształcenia,
ale co najważniejsze za Waszą miłość, przyjaźń, ciągłe wsparcie,
niesłabnącą motywację, otuchę i zrozumienie.
Bez Was to wszystko byłoby całkowicie niemożliwe.

To my parents.

Thank you very much for the great help in getting education,
but most importantly for your love, friendship, continuous support,
motivation, encouragement and understanding.
Without you all this would be completely impossible.

Acknowledgments

Above all I would like to gratefully and sincerely thank my supervisor, Dr. Rafael Delgado, for his guidance, understanding, patience, and most importantly, his friendship during my PhD career. His mentorship was paramount in providing a comprehensive experience consistent with my long-term career goals. He encouraged me to not only grow as an experimentalist and biologist but also as an independent thinker. For all of this, thank you Rafael.

Furthermore, I am very grateful to know and collaborate with many brilliant people from the CARMUSYS group, who has become friends over the last years, especially to Dr. Javier Rojo, Dr. Anna Bernardi and Dr. Franck Fieschi.

I also want to thank to Dr. Javier Rojo, Dr. Anna Bernardi, Dr. Benjamin Davis and Dr. Nazario Martín for chemical compounds used in this Thesis. To Dr. Cecilio Lopez Galindez and to Dr. Miguel Thompson for providing HIV envelopes. To Dr. Rafael Rubio and Dr. Federico Pulido for biological samples from Hospital 12 de Octubre.

I would like to thank to the personal of the Laboratory of Molecular Microbiology, to Olalla, Sagrario, Paquita, Lorena, who have been invaluable support during these years, thank you for a pleasant and productive working atmosphere. I am indebted to my friends from Microbiology Department, especially to all resident pharmacists, for their friendship, entertainment and humour in and out of laboratory environment.

I am sincerely grateful to Pancho Pascual-Pareja for providing me with statistical advice. Thank you for your help, suggestions and comments.

Additionally, I want to thank to Paloma Talayero for many FACS analyses and to Dr. Inés García-Consuegra for tips on the WB preparation.

Special thanks are also given to Fabián for standing always by my side. Thank you for continuous support, encouragement, motivation and friendship.

Finally, I am truly grateful to my parents for their support, understanding and endless love through my entire life. I wish to thank also to all my family and friends who were not mentioned before for their infinitive support and care.

I would like to express my appreciation for the financial support of European Union Programme Marie Curie Actions (FP7 PITN-GA2008213592).

Joanna Luczkowiak

TABLE OF CONTENTS

TABLE OF CONTENTS

JUSTIFICACIÓN DE LA TESIS DOCTORAL

JUSTIFICACIÓN DE LA TESIS DOCTORAL

Las lectinas de tipo C juegan un papel importante como receptores de reconocimiento de los carbohidratos derivados de patógenos por el sistema inmunológico. Varios receptores de lectinas de tipo C se han caracterizado previamente, tales como DC-SIGN, L-SIGN, SIGN-R1, Langerina, Siglecs, LSECtin, Mincle, DCIR, DCAR, BDCA-2, DCAL-1, MICL, Dectin-1, DNGR-1/CLEC9A, MR, DEC-205, MMR, MBL. El receptor DC-SIGN fue inicialmente identificado en el año 2000 por Geijtenbeek *y cols*. como el factor de la unión del VIH-1, que capturaba la envoltura viral y facilitaba la infección. Durante años, se llevaron a cabo múltiples estudios para caracterizar el papel biológico de DC-SIGN.

Se ha demostrado que DC-SIGN juega un papel en la respuesta del sistema inmunológico, sin embargo, la importancia biológica de sus funciones no se ha aclarado todavía. DC-SIGN juega un papel substancial en la inmunidad a través del reconocimiento de glicoproteínas propias, como la molécula de adhesión intercelular 2 (ICAM-2) y ICAM-3. Mediante la unión con ICAM-2, DC-SIGN funciona como receptor de adhesión celular que regula la migración de las DCs. La interacción de DC-SIGN con la ICAM-3 tiene un impacto en la agrupación de las células DC-T, en la proliferación inducida por las DCs de las células T en reposo, en la detección de los complejos de péptido-MHC por las células T y en la estabilización del contacto celular de las células DC-T, lo que permite la participación eficiente de los receptores de las células T (TCR). La segunda función de DC-SIGN es su papel como un receptor para patógenos. DC-SIGN reconoce las glicoproteínas que contienen un número relativamente alto de los N-carbohidratos presentes en la superficie de diferentes patógenos: VIH-1, virus del Ébola, citomegalovirus, virus de la Hepatitis C, virus del Dengue, *Helicobacter pylori*, *Klebsiella pneumoniae*, *Mycobacterium tuberculosis*, *Candida albicans*, Leishmania, *Schistosoma mansoni*.

Se ha sugerido que DC-SIGN puede mejorar la entrada viral y la infección directa en el proceso referido como infección en *cis*, así como también puede capturar y transmitir las partículas virales a células susceptibles en el proceso denominado como infección en *trans*.

El objetivo de nuestro estudio fue estandarizar y evaluar el modelo celular de la infección mediada por DC-SIGN por el virus. Queríamos evaluar la consistencia del modelo de infección utilizando diferentes líneas celulares que expresan el receptor DC-SIGN, así como estandarizar el nivel de expresión de DC-SIGN y el título infeccioso de los retrovirus recombinantes para los ensayos de infección. También hemos pretendido establecer las mejores condiciones para los ensayos de infección en *cis* y en *trans* mediadas por DC-SIGN.

Los ensayos *in vitro* presentados por diferentes grupos sugerían que DC-SIGN participa en la difusión del virus en los primeros momentos de la infección, por lo tanto, en los últimos años se diseñaron diferentes estrategias antivirales basados en compuestos de carbohidratos para bloquear la interacción del VIH-1 y Ébola virus con DC-SIGN. En presente estudio hemos evaluado la utilidad del nuestro modelo de infección mediada por DC-SIGN como una plataforma de monitorización de las estrategias antivirales destinadas frente DC-SIGN, incluyendo: las estructuras glicodendríticas, los dendrones tetravalentes, los compuestos basados en dendrímeros, los glicofullerenos y las glicodendrinanoparticulas.

Por otra parte, hemos tratado de estudiar la implicación del receptor DC-SIGN en la patogénesis del virus de Ébola. Se ha descrito que el grupo de filovirus del Ébola comprende cinco subtipos: Zaire, Sudán, Reston, Costa de Marfil, Bundibugyo, entre los cuales la cepa del Ébola Zaire muestra la tasa de mortalidad más alta (50-90%), mientras que la del Ébola Reston nunca ha sido asociada con la enfermedad humana. El fenómeno de las diferencias en la patogénesis del EBOZ y EBOR no ha sido completamente aclarado todavía. Se ha especulado que las glicoproteínas de la envuelta de las dos cepas pueden ser responsables de estas diferencias en la

patogénesis. Sin embargo, estas especulaciones no han sido confirmados aún en un modelo *in vivo*. Por esta razón, en nuestro estudio hemos tratado de analizar las diferencias en la infección en *trans* mediada por DC-SIGN por las dos cepas del virus de Ébola: la cepa patógena Zaire y la cepa no patógena para los humanos Reston.

Por último, hemos investigado la implicación del receptor DC-SIGN en la patogénesis del VIH-1. El VIH es responsable de la causa del síndrome de inmunodeficiencia adquirida (SIDA) caracterizado por un fallo progresivo del sistema inmunitario que resulta en infecciones oportunistas y tumores. La mayoría de los pacientes infectados por el VIH-1 muestran una alta carga viral en plasma y la pérdida de células T $CD4^+$ a lo largo del curso de la infección por VIH-1 en caso de ausencia de la terapia antirretroviral. Gran parte de los pacientes no tratados desarrollan la inmunodeficiencia del sistema inmunológico y mueren a causa de las complicaciones relacionadas con el SIDA en un tiempo aproximado de 10 años tras haberse infectado. Sin embargo, un porcentaje muy pequeño de individuos no tratados permanecen clínicamente y/o inmunológicamente estables durante años. Por este motivo también hemos analizado el proceso de la infección en *trans* en diferentes cepas del VIH-1 y su correlación con el control virológico.

INTRODUCTION

I. INTRODUCTION

1. Immune system: innate and adaptive immunity

All living organisms have evolved many different strategies to defeat pathogen infection (Hoffmann et al., 1999). The mammalian immune system is composed of two types of immunity that are used to protect the host from infections: innate and adaptive immunity (Medzhitov and Janeway, 1999).

The innate immune system is the first line of host defense against pathogens. It is immediate and genetically programmed to detect features of invading microbes. The major components of the innate immunity include epithelial barriers (skin, mucosal epithelia of gastrointestinal, respiratory and reproductive tracks), soluble molecules (antimicrobial peptides, complement, cytokines, natural antibodies), innate immune cells and pattern-recognition receptors (PRRs) (Ip et al., 2009). Innate immune cells include macrophages, neutrophils, natural killer cells (NKs), dendritic cells (DCs). Macrophages are phagocytic cells in lymphoid and non-lymphoid tissues. They are believed to be involved in tissue homeostasis through the clearance of apoptotic cells and the production of growth factors. Macrophages are well equipped with a wide range of PRRs that make them efficient at phagocytosis as well as at production of inflammatory cytokines (Gordon, 2002). Neutrophils are produced in a great number from stem cells in bone marrow and circulate in blood for a few hours. Microorganisms generate substances that guide neutrophils towards the microbe, which are taken up by neutrophils in the process of phagocytosis and exposed to high concentration of bactericidal substances in the phagocytic vacuole. Neutrophils are fully equipped with granules that contain proteins lethal for microbes, but which also cause a tissue damage (Borregaard, 2010). Natural Killer cells are defined as large granular cytotoxic lymphocytes, which differentiate in the bone marrow, lymph nodes, spleen, tonsils and thymus and further enter blood circulation. NK cells provide a rapid response to viral infection as well as to tumor formation. These cells detect pathogen antigens presented on the infected cell sur-

face and release cytokines causing cell lysis and apoptosis (Vivier et al., 2011). NK cells play also a role in the adaptive immunity by formulation of antigen-specific immunological memory fundamental for the second contact with the same antigen (Arina et al., 2007). DCs are heterogeneous population, which is differentiated in lineage, phenotype, location, growth factor requirements and functions. DCs express a wide repertoire of PRRs. Upon pathogen invasion, PRRs send signals to DCs, which result in phenotypic and functional transformation called "DC activation" to become immunogenic antigen-presenting cells (APCs) (Mellman et al., 1998; Reis e Sousa, 2006). Pro-inflammatory mediators are the first molecules to be released after stimulation of innate immunity cells. The major pro-inflammatory cytokines produced by stimulated macrophages are: tumor necrosis factor (TNF), interleukin 6 (IL-6) and interleukin 1 (IL-1). They stimulate the acute phase of immune response, such as triggering phagocytosis by neutrophils and opsonization, activating complement, decreasing bacterial and viral replication, increasing antigen processing, promoting adaptive immune response. Persistent production of those cytokines is often the reason of systemic inflammatory conditions (Crozat et al., 2009). Type I interferon is essential in antiviral immunity and it plays role in inhibition of viral replication, activation of NKs and macrophages, enhancement of class I MHC molecules expression, Th1 polarization and differentiation of DCs (Le Bon et al., 2003).

Adaptive immunity is responsible for the elimination of pathogens in the late phase of infection and the generation of immunological memory. The acquired immune response is highly specific, since it is developed by clonal selection from repertoire of lymphocytes bearing antigen-specific receptors that are not encoded in the germ line but are generated *de novo* in each organism (Akira et al., 2006). The innate phase of immune response in vertebrates is rapidly supplemented by an adaptive response, which is characterized by the activities of pathogen-specific B and T cells. The key role in translating innate information into adaptive immunity plays the members of the dendritic cell family (Reis e Sousa, 2001).

In most tissues, DCs are present in immature state, which is characterized by different features allowing them to capture antigens and take up particles or microbes by phagocytosis (Inaba et al., 1993). Immature DCs can form large pinocytic vescicles, which function in the process of macropinocytosis of extracellular liquids and solutes (Sallusto et al., 1995). DCs can also express receptors that mediate adsorptive endocytosis, including C-type lectin receptors and Toll-like receptors (TLRs). Maturation of DCs is crucial for the initiation of immunity (Fig. 1). Maturation of DCs might be triggered by different factors including microbial and inflammatory products. Upon activation, DCs migrate to the lymphoid tissues (spleen and lymph nodes), where they can complete their maturation process and attract T and B cells by releasing chemokines. DCs activate and expand T-helper cells, which induce B cell growth and antibody production (Kitajima et al., 1996). DCs are efficient stimulators of both B and T lymphocytes. B cells are the precursors of antibody secreting cells and can directly recognize native antigen via their B-cell receptors (BCRs). T lymphocytes need the antigen processing and presentation by APCs for their activation (Banchereau and Steinman, 1998).

The T-cell receptors (TCRs) recognize fragments of antigen bound to the molecules of major histocompatibility complex (MHC) on the surface of APCs. This recognition delivers the first activating signal to T cells (signal 1). Activated by pathogens DCs express a variety of co-stimulatory molecules, which engage receptors on T cells and transmit signals that are important for T cell proliferation and survival (signal 2). The best known co-stimulatory molecules are CD80 and CD86, which trigger CD28 on T cells. Activated DCs produce also mediators that act on T cells to promote their differentiation into effector cells (signal 3) (Joffre et al., 2009). There are two types of MHC peptide-binding proteins: MHC class I and MHC class II. Intracellular antigens are cut into pieces in the cytosol of APCs and then bound to MHC class I molecules that drives cytotoxic T cell (CTLs), which might directly kill a target cell. Extracellular antigens that entered the endocytic pathway of the APCs are processed and presented by MHC class II molecules that stimulate T-helper cells, playing thus role in the immune regulation (Banchereau and Steinman, 1998).

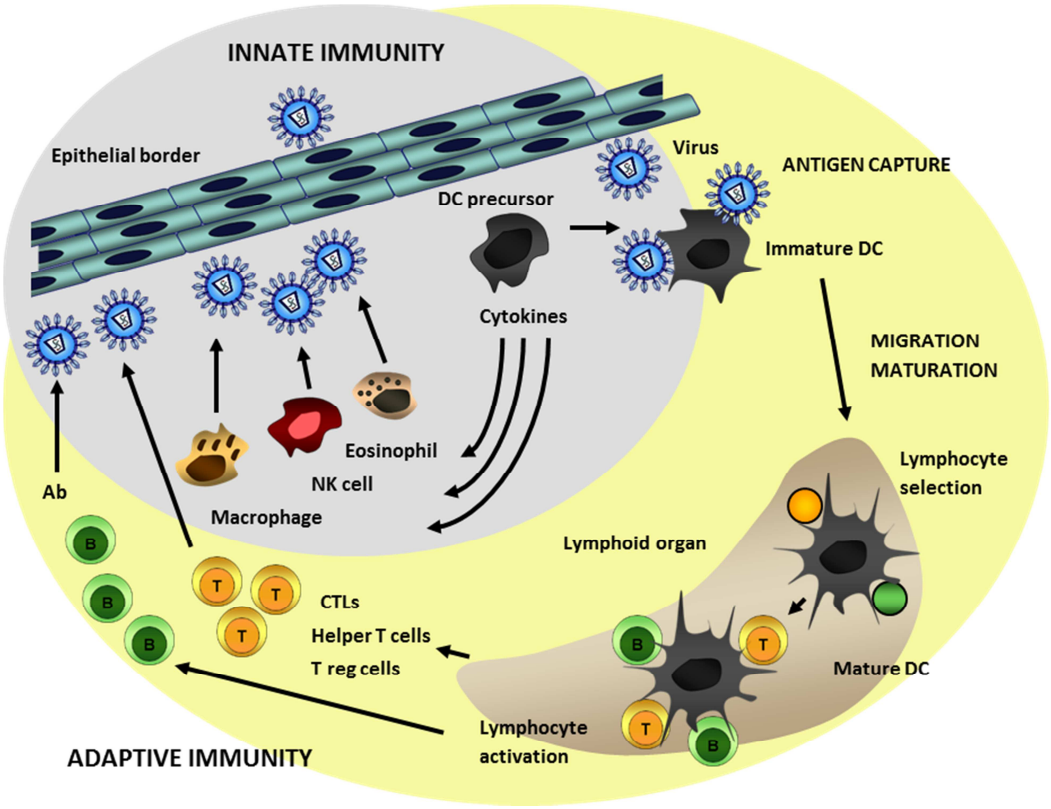

Figure 1. DCs as immunological sensors translating perceived information into efficient adaptive immune response. Modified from Palucka *et al.* (Palucka and Banchereau, 2002).

2. Pattern recognition receptors and the innate immunity

The innate immune system senses the presence of infection through the recognition of conserved microbial pathogen-associated molecular patterns (PAMPs) by germ-line encoded PRRs (Janeway, 1989). Innate immune receptors trigger a variety of responses that depend on the receptor and cell type. Innate receptors might mediate internalization of microbes by phagocytic cells. They might activate antimicrobial killing mechanisms through the production of reactive nitrogen and oxygen. Innate receptors might also stimulate production of inflammatory cytokines that recruit and activate other immune cells and signal the development of adaptive immunity. The proper activation of innate immune response and cooperation between innate receptors play a crucial role in regulating and shaping of immune response for invading pathogens. The innate immunity must be tightly regulated since too little response leaves host susceptible to

the infection and too much response may lead to lethal systemic inflammation or autoimmunity (Underhill, 2003). Microbial pathogens are recognized through multiple, distinct PRRs that can be categorized into three classes: secreted, cytosolic and transmembrane receptors. Secreted PRRs, which include colectins, ficolins, pentraxins, bind to microbial cell surfaces, activate classical and lectin pathways of the complement system, and opsonize pathogens for phagocytosis by macrophages and neutrophils. The cytosolic PRRs include the nucleotide oligomerization domain NOD-like receptors (NLR) and the retinoic acid inducible gene I RIG-like receptors (RLR). The transmembrane PRRs include the Toll-like receptors (TLRs) and members of the C-type lectin family (Iwasaki and Medzhitov, 2010).

2. 1. C-type lectin receptors and DC-SIGN

C-type lectins are PRRs involved in the recognition of pathogen-derived carbohydrates by immune system. Several different C-type lectin receptors have been characterized, such as DC-SIGN, L-SIGN, SIGN-R1, Langerin, Siglecs, LSECtin, Mincle, DCIR, DCAR, BDCA-2, DCAL-1, MICL, Dectin-1, DNGR-1/CLEC9A, MR, DEC-205, MMR, MBL.

Dendritic cell-specific ICAM-3-grabbing non-integrin (DC-SIGN) receptor was discovered by Geijtenbeek *et al.* in 2000 by investigating the binding of intercellular adhesion molecules to DCs and finding that DCs bound the intracellular adhesion molecule-3 (ICAM-3) with very high affinity (Geijtenbeek et al., 2000c). ICAM-3 belongs to the immunoglobulin superfamily (de Fougerolles et al., 1994) and it is expressed mostly in resting T lymphocytes (de Fougerolles and Springer, 1992). ICAM-3 plays a role in the initial adhesion between T lymphocytes and APC and further formation of a functional immunological synapse (Montoya et al., 2002). It was originally described that DCs-expressed β-integrin, leukocyte function associated molecule-1 (LFA-1), was the major ligand for ICAM-3 on T lymphocytes. However, antibodies against LFA-1 failed to abolish T cell-DC clustering, while anti-ICAM-3 antibodies fully abrogated this in-

teraction. Therefore, anti-DC hybridoma supernatants were widely screened to encounter a new DC-expressed molecule with the ability to inhibit ICAM-3 binding. A new C-type lectin was cloned and designated as DC-specific ICAM-3 grabbing non-integrin (DC-SIGN) (Geijtenbeek et al., 2000c). The sequence of DC-SIGN was then found to be identical to a C-type lectin capable of binding HIV envelope glycoprotein gp120 that was cloned in 1992 (Curtis et al., 1992). Subsequent investigation of the group who discovered DC-SIGN showed that this lectin could bind HIV gp120 and retain infectious virus for up to several days. DC-SIGN-bound HIV viral particles could transmit infection to other cells expressing proper HIV receptors and coreceptors in the process described as *trans*-infection (Geijtenbeek et al., 2000b). Similarly to the ligand binding by other C-type lectins, DC-SIGN adhesion to ICAM-3 or HIV can be abrogated by mannose and calcium-chelating agents (Geijtenbeek et al., 2000b; Geijtenbeek et al., 2000c). Over years, consecutive studies were implemented to characterize the biological role of DC-SIGN.

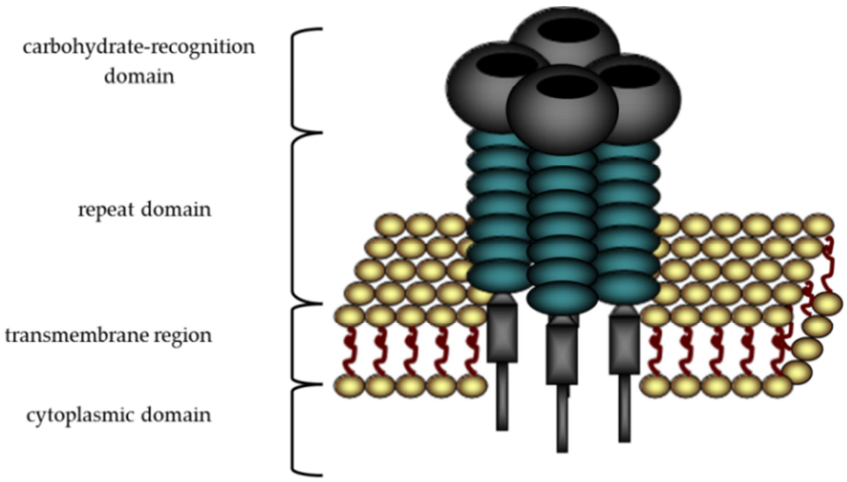

Figure 2. Tetrameric structure of DC-SIGN. Modified from Wu *et al*. (Wu and KewalRamani, 2006).

DC-SIGN is a type II transmembrane C-type lectin that contains a carbohydrate recognition domain (CRD), an extracellular stalk composed of seven complete and one partial tandem repeat, a transmembrane domain and a short cytoplasmic N-terminal do-

main with several intracellular sorting motifs (Fig. 2) (Geijtenbeek et al., 2000c). The neck domain of DC-SIGN, which consists of seven complete and one partial tandem repeat, is required for oligomerization and regulate carbohydrate specificity. The neck domain is followed by a transmembrane region. A cytoplasmic tail of DC-SIGN contains internalization motifs, such as the di-leucine motif (LL), tri-acidic clusters motif (EEE) and an incomplete immunoreceptor tyrosine-based motif (ITAM) (van Kooyk and Geijtenbeek, 2003).

The **CRD of DC-SIGN** is a globular structure, which consists of 12 β-strands, 2 α-helices and 3 disulphide bridges. These elements form a loop on the outer surface of the protein that builds a part of 2 Ca^{2+} -binding sites. One of these Ca^{2+} -binding sites is essential for the conformation of the CRD and the second Ca^{2+} -binding site is fundamental for direct coordination of the carbohydrate structures (van Kooyk and Geijtenbeek, 2003). Four amino acids (Glu347, Asn349, Glu354, Asn365) interact with Ca^{2+} at this site and provide recognition of specific carbohydrate structures. Mutation of these amino acid positions leads to the loss of ligand binding (Geijtenbeek et al., 2002b).

DC-SIGN carbohydrate recognition	
Mannose residues	**Fucose residues**
Man α1→2	α-L-fucose
Man α1→3	Le^x - Galβ1→4[GlcNAcα1→3]Fuc
Man α1→4	Le^y - Fucα1→2[Galβ1→4GlcNAc α1→3]Fuc
Man α1→6	Le^a - Galβ1→3[GlcNAcα1→4]Fuc
Man α1→3[Man α1→6]Man	Le^b- Fucα1→2 [Galβ1→3[GlcNAc α1→4] Fuc
Man α1→3[Man α1→3[Man α1→6] Man α1→6] Man	
GlcNAc β1→2Man α1→3 [GlcNAcβ1→2Man α1→6] Man	
Man_9-$GlcNAc_2$	
Man_5-$GlcNAc_2$	
methyl α-mannoside	
N-acetylmannosamine	

Table 1. Carbohydrate profiling of DC-SIGN recognition.

The CRD of DC-SIGN shows high affinity for mannose and fucose residues (Table 1) (Feinberg et al., 2001; Guo et al., 2004; Mitchell et al., 2001) and it has been demonstrated that DC-SIGN binds with much higher affinity for the fucose-containing carbohydrates than for mannose-containing carbohydrates (Appelmelk et al., 2003; Geijtenbeek and van Kooyk, 2003; Mitchell et al., 2001). DC-SIGN binds also to Lewis blood groups antigens (Le^x, Le^y, Le^a, Le^b), which contain fucose residues in different anomeric linkages. Moreover, it has been shown that DC-SIGN interacts with glucose, methyl α-glucoside, GlcNAc, 2-deoxyglucose, however with much weaker affinity than it interacts with mannose or fucose (Mitchell et al., 2001).

Glycans cover the surface of all mammalian cells. They are added to the protein or lipid backbones during **glycosylation process**. During the biosynthesis of the glycans, these molecules are transported from the ER to the Golgi. Glycosylation is mediated by cell machinery, which involve glycosyltranferases (catalyze the transfer of the sugar from a nucleotide sugar donor or a lipid sugar to a substrate) and glycosidases (catalyze hydrolysis of glycosidic bonds in glycan structures). Genes that are responsible for encoding for the glycosylation process represent >1% of the total genome and there are more than 100 glycosyltranferases and glycosidases described so far (Ohtsubo and Marth, 2006). The glycosylation might give different structural variations to a protein, which results in thousands of variations of potential glycan structures. Within mammalian cell, 3 types of glycosylation have been identified, such as O-linked glycosylation, N-linked glycosylation and glycosaminoglycosylation. N-linked glycans are attached to the nitrogen of asparagine and O-linked glycans are attached to the hydroxy oxygen of serine, threonine, tyrosine, hydroxylysine, or hydroxyproline side-chains.

O-linked glycosylation (Fig. 3) takes place in a later phase during protein folding (Drickamer, 2006). Biosynthesis of the O-linked oligosaccharide begins with transfer of N-acetyl-galactosamine (GalNAc) from UDP-N-acetyl-galactosamine to hydroxyl group of a serine or threonine residue in the protein. This reaction is catalyzed by a GalNAc transferase, which is localized to the ER or the *cis*-Golgi network. Following

the transfer of the protein to the *trans*-Golgi vescicles, a galactose residue is added to the N-acetyl-galactosamine by a specific *trans*-Golgi galactosyltransferase. In most vertebrate cells biosynthesis of O-linked oligosaccharides is completed by addition of two negatively charged N-acetylneuraminic acid (sialic acid) residues in *trans*-Golgi apparatus or *trans*-Golgi network (Lodish, 2000).

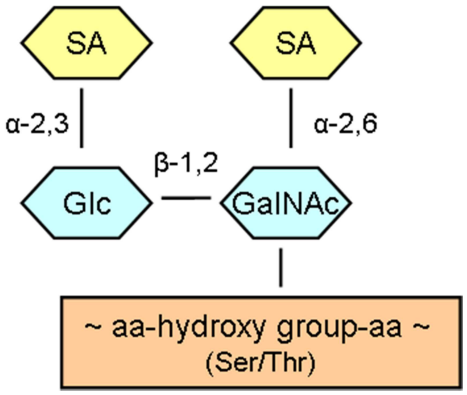

Figure 3. O-linked oligosaccharide structures. aa-any amino acid, GalNAc-N-acetylgalactosamine, Glc-glucose, SA-sialic acid, Ser-serine, Thr-threonine. Modified from Lodish *et al.* (Lodish, 2000).

Biosynthesis of N-linked oligosaccharides begins in the rough ER with the addition of a large oligosaccharide precursor. This oligosaccharide precursor is linked by pyrophosphoryl residue to dolichol, a long-chain (75-95 carbon atoms) polyisoprenoid lipid, which is inserted in the ER membrane and acts as a carrier for the oligosaccharide. The dolichol pyrophosphoryl oligosaccharide is formed on the ER membrane in a complex set of reactions that are catalyzed by enzymes attached to the cytosolic and luminal faces of the ER membrane. The final dolichol pyrophosphoryl oligosaccharide is oriented in the way that the oligosaccharide faces the ER lumen. The structure of this precursor is conserved in plants, animals and single-cell eukaryotes and it contains the oligosaccharide chain of 3 glucoses, 9 mannoses and 2 N-acetylglucosamines. Five residues of this 14-sugar precursor (core) are conserved in all N-linked oligosaccharides. The entire precursor is transferred from the dolichol carrier to asparagine present in tripeptide sequence asparagine-X-serine/threonine (where X can by any amino acid except proline) in the reaction catalyzed by oligosaccharyltransferase. Immediately after, the oligosaccharide is transferred to a nascent polypeptide, 3 glucoses are removed

from the chain and the protein is exported from the ER. The 3 glucose residues appear to act as a signal peptide, informing that the oligosaccharide is complete and ready to be transferred to a protein. The protein is then transported to the Golgi apparatus, where further removal of mannose residues occurs, that leads to the core structure that contains 3 mannose and 2 N-acetylglucosamine residues (Fig. 4). Different enzymes localized in the *cis*-, *medial*- and *trans*-Golgi cisternae catalyze these reactions as a protein moves through Golgi complex. Galactosyltransferases are localized in *trans*-Golgi, sialyltransferases are localized in the *trans*-Golgi and *trans*-Golgi network and mannosidases are localized in *trans*-Golgi (Lodish, 2000).

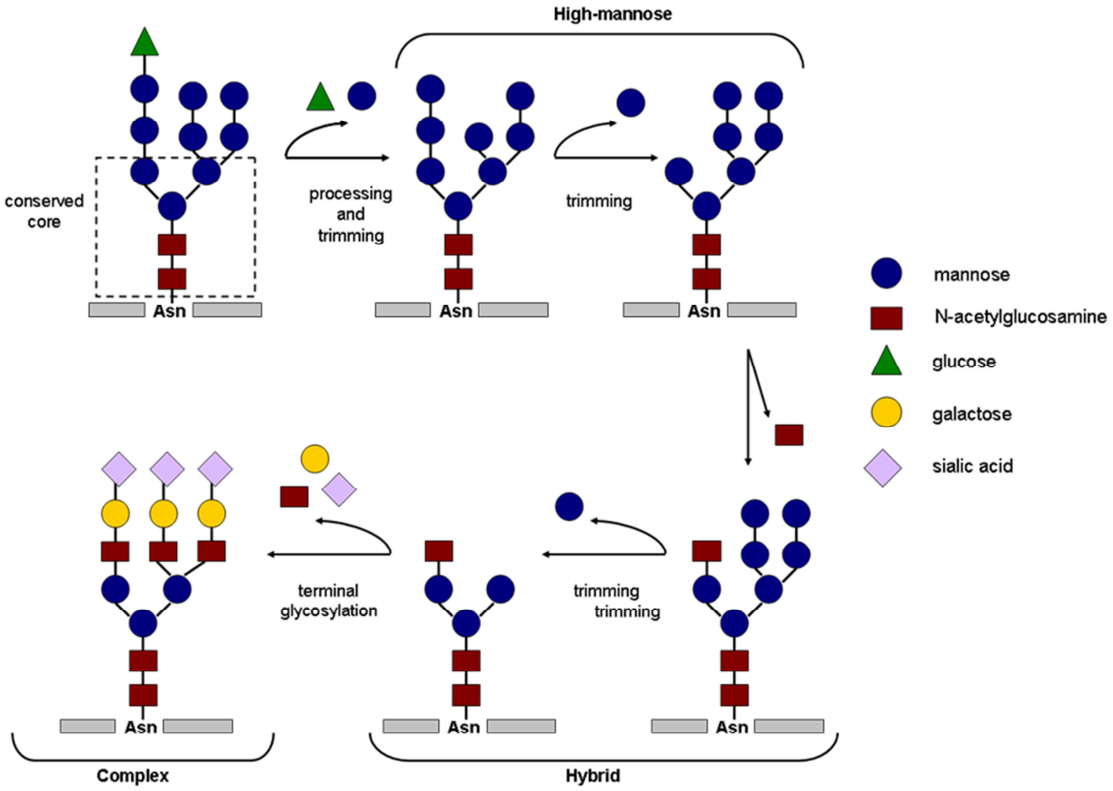

Figure 4. Biosynthetic pathway for the generation of N-linked glycosylation. Processing of N-linked glycans occurs in the ER and Golgi apparatus. Glucose trimming in the ER results in high mannose glycans, which are available for further processing and trimming by glycosidase and mannosidases to yield high-mannose, hybrid and complex glycan structures. Modified from Lodish *et al*. (Lodish, 2000).

Differences in the processing of oligosaccharides within the ER and Golgi result in the variations of N-linked oligosaccharides structures. In some cases, the first reactions of removal of glucose residues may not occur, thus the relevant part of N-linked oligosaccharide is not accessible to the enzymes catalyzing these reactions. The resulted glycoprotein contains thus high-mannose oligosaccharide (Fig. 5C). In most mammalian cells, high-mannose oligosaccharide is further modified by mannosidases. The addition of various monosaccharide residues to oligosaccharide chain results in gaining complexity in terms of residues type, modification and branching, which are called C-glycans (Fig. 5A, 5B). C-glycans are different in size, electric charge and are performing different biological functions (Lodish, 2000).

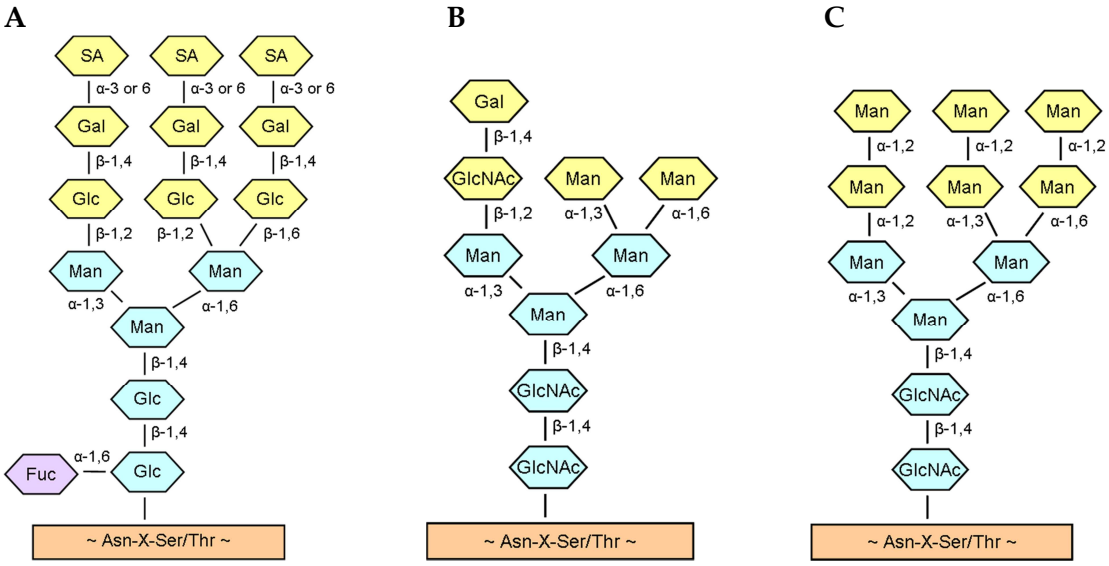

Figure 5. N-linked high mannose structures. **A.** Tri-antennary complex-type N-glycan. **B.** Hybrid-type N-glycan. **C.** High-mannose-type N-glycan. Asn-asparagine, Fuc-fucose, Gal-galactose, GlcNAc-N-acetylglucosamine, Man-mannose, SA-sialic acid, Ser-serine, Thr-threonine, X-any amino acid except proline. Modified from Lodish *et al.* (Lodish, 2000).

It has been shown that **DC-SIGN plays a role in the immune system response**, however the biological importance of its functions have not been clarified yet. The initially described binding of DC-SIGN to ICAM-3 was identified to be important for the initial

DC-T cells interactions (Starling et al., 1995). The intercommunication of T cells with DCs is antigen-dependent and allows scanning of the peptide – MHC class II complex-repertoire by TCRs. This cooperation requires the formation of a specialized immunological synapse that is generated by the recruitment of specific adhesion receptors, which strengthen DC-T cell contact (Dustin and Chan, 2000; Grakoui et al., 1999; Monks et al., 1998). The initial DC-T cell interaction stabilizes DC-T cell membrane contact, enabling efficient TCR engagement. The transient character of this communication allows DCs to interact with a large number of T cells until reaching the productive TCR involvement (Geijtenbeek and van Kooyk, 2003). DC-SIGN regulates also DC migration from blood into tissues for continuous surveillance of immune system. Precursors and immature DCs migrate to peripheral tissues to replenish resident DCs or in a response to inflammatory signals. The way out from blood into tissues is mediated by multiple processes, such as leukocyte rolling, rapid activation of leukocytes, adhesion to endothelial ligands and diapedesis (Vestweber and Blanks, 1999). ICAM-2 is an endothelial ligand, constitutively expressed on the endothelium of blood, lymphatic and vascular cells. DC-SIGN mediates binding and rolling of DC-SIGN$^+$ cells along ICAM-2 expressing surfaces. DC-SIGN therefore is involved in the adhesion of DCs to endothelium and further trans-endothelial migration (Geijtenbeek et al., 2000a). DC-SIGN plays also the role of antigen receptor. Binding of soluble ligands by DC-SIGN induces rapid internalization of this receptor from cell surface and further targeting to late endosomes, where antigens are processed and presented by MHC class II molecules (Engering et al., 2002). It has been also indicated that engagement of DC-SIGN on DCs results in the activation of signal transduction pathways, which can cause wide modulation of immune responses, mostly when co-activated with Toll-like receptors (Gringhuis et al., 2007). DC-SIGN may thus induce of tolerance by immature DCs after recognition of glycosylated self-antigens for homeostatic control (Geijtenbeek et al., 2004).

The second function of **DC-SIGN is its role as a receptor for pathogens**. DC-SIGN recognizes the glycoproteins expressed on the surface of different pathogens that contains a relatively large number of N-linked carbohydrates (HIV, Ebola virus, Cytomeg-

alovirus, Hepatitis C virus, Dengue virus, *Helicobacter pylori*, *Klebsiella pneumoniae*, *Mycobacterium tuberculosis*, *Candida albicans*, Leishmania, *Schistosoma mansoni*) (Alvarez et al., 2002; Appelmelk et al., 2003; Cambi et al., 2003; Colmenares et al., 2002; Curtis et al., 1992; Geijtenbeek et al., 2002b; Geijtenbeek et al., 2003; Halary et al., 2002; Maeda et al., 2003; Navarro-Sanchez et al., 2003; Pohlmann et al., 2003; van Die et al., 2003; van Kooyk and Geijtenbeek, 2003). It has been suggested that DC-SIGN can enhance viral uptake for direct infection in the process referred as *cis*-infection, as well as it can internalize viral particles into cell and storage in non-lysosomal compartments for subsequent transfer to susceptible cells in the process called as *trans*-infection (Alvarez et al., 2002; Geijtenbeek et al., 2000b; Lee et al., 2001). DC-SIGN-bound viral particles were speculated to enter the cell, but escape from degradation by internalization into non-lysosomal organelles and after migration to the lymphoid tissues, recycle back to the cell surface transmitting the infection to susceptible cells (van Kooyk and Geijtenbeek, 2003).

However, all of predicted functions of DC-SIGN are mostly based on multiple *in vitro* studies. To clarify the hypothesized physiological functions of DC-SIGN in coexistence with other lectins the proper *in vivo* model should be set up. It has been shown that human DC-SIGN family consists only of two receptors: DC-SIGN and L-SIGN, whereas the mice have 8 DC-SIGN homologs (Park et al., 2001; Powlesland et al., 2006). The sequence analysis of those homologs and human DC-SIGN indicated that DC-SIGN receptor family suffered considerable diversification, which might be the result of evolution pressure from exposure to different species-specific pathogens. As a result, there is not one member of mice DC-SIGN receptor family capable of performing the same functions as human DC-SIGN. The studies concerning glycan binding showed that the members of mice DC-SIGN family differ substantially in the glycan recognition from the pattern recognized by human DC-SIGN (Park et al., 2001; Powlesland et al., 2006; Takahara et al., 2012). It has been also shown that there are differences in the DC-SIGN-activated cytokine responses and in the signaling pathways activated downstream of ligand binding by DC-SIGN in mice and human (Gringhuis et al., 2009; Kato and Kojima, 2010; Ohtani et al., 2012; Srivastava et al., 2009; Tanne et al., 2009; Wieland

et al., 2007). Additionally, the receptor distribution pattern might be also responsible for divergence between human DC-SIGN and mice receptor SIGNR. The receptor SIGNR1 is expressed on marginal zone macrophages (Geijtenbeek et al., 2002a), SIGNR3 is expressed on a fraction of DCs and/or macrophages in lymph nodes, spleen and dermis (Nagaoka et al., 2010). The most similar pattern of expression to DC-SIGN reveals SIGNR5, however this receptor does not mediate internalization and differ significantly in glycan binding pattern as compared to DC-SIGN (Powlesland et al., 2006).

To overcome the problem of wide variability between human DC-SIGN and mice SIGNR, a transgene encoding for human DC-SIGN was introduced in C57/B16 mice (hSIGN) (Schaefer et al., 2008). Human receptor DC-SIGN was expressed on hSIGN mice under the control of minimal promoter CD11, which allows reproducing a part of the expression pattern of human DC-SIGN. In the study of challenging of hSIGN mice with *Mycobacterium tuberculosis* the results showed that hSIGN mice infected with this pathogen survived longer as compared with wild-type mice, which might results from DC-SIGN functions in limiting the tissue-damaging inflammatory responses (Schaefer et al., 2008). Nevertheless hSIGN model displays also other C-type-mice specific lectins together with human DC-SIGN, which might contribute to the host response for the mannosylated glycans on *Mycobacterium tuberculosis*. Therefore it was suggested that SIGNR receptors showing mannose specificity should be knocked out in future mice models to address DC-SIGN function *in vivo* (Garcia-Vallejo and van Kooyk, 2013). It has been also demonstrated that Rhesus macaque DC-SIGN has a high homology with human DC-SIGN performing therefore similar functions of *trans*-receptor in HIV-1 infection. The primate homologue to DC-SIGN is abundantly expressed in mucosal and lymphoid tissues, which might suggest its involvement in sexual transmission (Baribaud et al., 2001; Geijtenbeek et al., 2001; Schwartz et al., 2002; Yu Kimata et al., 2002). These facts indicate that primate model may be suitable for further dissecting the role of DC-SIGN in the transmission and pathogenesis of HIV-1. However, the difficulty of handling primate models and availability of proper installation for this kind of studies encourage continuing the development of new *in vivo* models for future DC-SIGN investigation. Therefore, although appropriate *in vivo* models will be crucial for

understanding of the physiological role of DC-SIGN, in the meantime, *in vitro* studies on this aspect should be encouraged since it is the most relevant source of information so far.

3. Ebola virus and DC-SIGN

Ebola virus, together with Marburg virus, belongs to the family of *Filoviridae*. Ebola virus was first recognized during two major disease outbreaks, which occurred almost simultaneously in Zaire and Sudan in 1976 (Johnson et al., 1977). At that time over 500 cases were reported, with the mortality rate of 88% in Zaire and of 53% in Sudan. Although the emergence of both strains (EBOZ and EBOS) took place simultaneously, both strains varied significantly taking into account criteria such as sequence analysis and serology. In 1989, a new strain of Ebola virus was isolated from monkeys being held in quarantine in Reston after their transportation from Philippines (Jahrling et al., 1990). The Ebola Reston (EBOR) strain is less virulent in humans than EBOZ and EBOS. The EBOR reappeared in monkeys in Italy in 1992 and in Texas in 1996 (Sanchez et al., 2001). The second outbreak of EBOZ occurred in Zaire in 1995. In 1994 the fourth strain of Ebola virus was described in Ivory Coast (Lozano et al., 1995). This strain was fatal for humans as well as for monkeys. A large outbreak of EBOS reoccurred in Uganda in 2000-2001 (CDC, 2001). A fifth species of Ebola virus was confirmed in an outbreak that took place in 2007 in Bundibugyo in Uganda (Alsop, 2007).

The infection with Ebola virus starts with incubation period of 4-16 days, which often is marked by fever, chills, headache, anorexia, myalgia. These signs are soon followed by nausea, vomiting, sore throat, abdominal pain, and diarrhea. In general when first examined, patients are ill, dehydrated, apathetic, disoriented. Within several days other symptoms appear, such as a characteristic maculopapular rash, mucous membrane hemorrhages, and gastrointestinal bleeding. Shock in patients develops shortly before death, often 6-16 days after onsets of illness (Jahrling, 2003). Although the development of preventive vaccine for Ebola virus in primates has been described, there is no ap-

proved specific Ebola virus therapy for humans available. The highly effective vaccination strategy in non-human primates was based on an immunization with a single plasmid encoding Zaire-strain virion glycoprotein that generated a substantial virus-specific antibody response and conferred protective immunity in guinea pigs (Sullivan et al., 2000).

Ebola virus is an enveloped, non-segmented, negative-strand RNA virus. The viral particles are typically 790-970 nm long and consistently 80 nm in diameter (Geisbert and Jahrling, 1995). The Ebola virus genome consists of 7 genes, which direct the synthesis of 8 proteins.

Figure 6. Organization of Ebola virus genome.

Transcriptional editing of the fourth gene, glycoprotein, leads to the expression of 2 products: a 676-residue transmembrane-linked glycoprotein GP and a 364-residue secreted glycoprotein sGP. The transcriptional editing of glycoprotein gene is due to the overlapping of transcription stop site with transcription start site of the downstream VP30 gene (Sanchez et al., 1996).

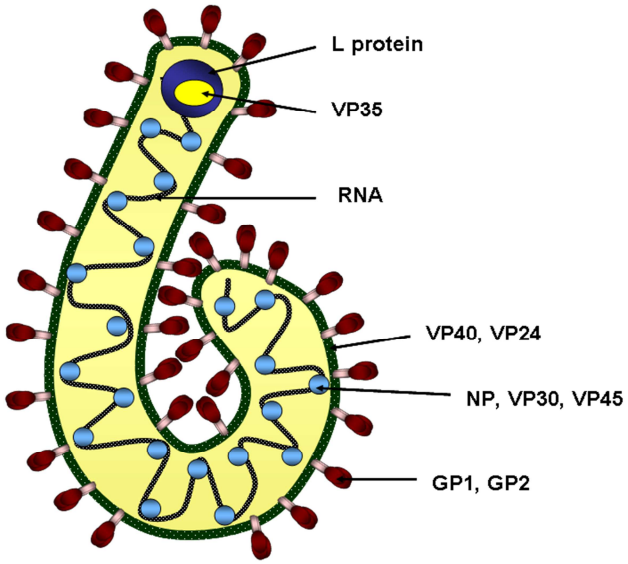

Figure 7. Ebola virus particle.

After entry of Ebola virus into the host cell cytoplasm, the RNA is transcribed to generate a polyadenylated, subgenomic mRNA. The genome shows the following gene order: 3′ leader, nucleoprotein (NP), virion protein 35 (VP35), virion protein 40 (VP40), glycoprotein (GP/sGP), virion protein 30 (VP30), virion protein 24 (VP24), polymerase protein (L), 5′ leader (Fig. 6). The transcription and translation lead to the synthesis of 7 structural polypeptides. Four of produced proteins, NP, VP30, VP35 and L, are associated with the viral RNA in ribonucleoprotein complex. Three structural proteins, GP1/2, VP24, VP40 are membrane associated. VP24 and VP40 are located in the inner site of the membrane (Fig. 7). The NP, VP35 and L proteins are essential for virus transcription and replication. VP40 functions as the matrix protein. Additionally, one nonstructural, secreted glycoprotein (sGP) is expressed (Feldmann and Kiley, 1999).

3. 1. Ebola virus glycoproteins

Ebola virus glycoproteins are encoded by the fourth gene of RNA genome. The primary structure of the editing site is composed of 7 uridine residues in the genomic sequence. Transcriptional editing is performed by the viral RNA-dependent RNA polymerase (L protein). Unedited viral mRNA (about 70-80% of GP-specific mRNA) give rise to the primary product of the forth gene, the secreted, non-structural glycoprotein (sGP). In about 20-25% of GP-specific transcripts, the addition of single adenosine residue at editing site shifts the ORF to -1, which results in the production of transmembrane GP (Cook and Lee, 2013; Sanchez et al., 1996) (Fig. 8). It has been observed that the shift of ORF to -2 might also occur that results in the expression of third nonstructural small secreted protein (Volchkova et al., 1998) (Fig. 8). There are solid evidences that viral envelope glycoproteins of Ebola viruses are modulators of host antiviral defenses (Cook and Lee, 2013). The GP gene product, which is responsible for viral entry, is synthesized in only about 20-25% of transcripts (Cook and Lee, 2013; Sanchez et al., 1996).

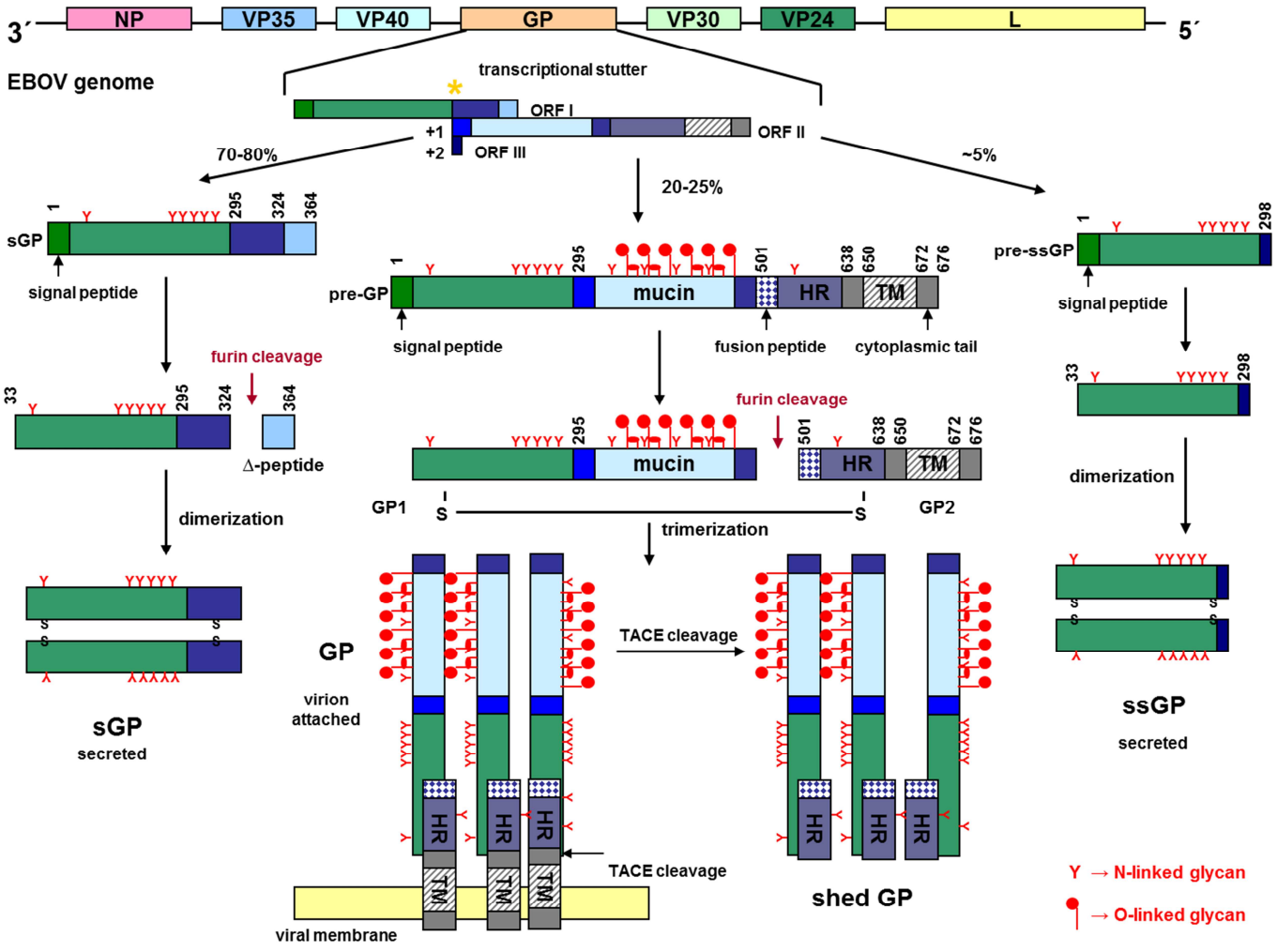

Figure 8. Processing of EBOV glycoproteins. Modified from Cook *et al.* (Cook and Lee, 2013).

The rest of synthesized products are free glycoproteins that act mostly to mislead humoral immune responses. The Ebola-infected cells release into person´s sera secreted glycoprotein sGP and shed GP (Dolnik et al., 2004; Sanchez et al., 1998). Both secreted glycoproteins might compete with virion-attached GP in the antibody-binding as it was shown that most of the antibodies derived from EBOV survivors or macaques were directed against sGP rather than the virion-attached GP (Druar et al., 2005; Ito et al., 2001; Maruyama et al., 1999).

Transcriptional editing based on the insertion of one adenosine residue at editing site of the glycoprotein gene results in the synthesis of **transmembrane glycoprotein GP**. The precursor of Ebola virus glycoprotein (preGP) undergoes a complex of processing events in ER and Golgi that result in the production of mature GP. After the removal of the signal peptide, preGP is N-glycosylated and oligomerized in ER. ER processing is followed by acetylation in pre-Golgi compartment, O-glycosylation and maturation of N-glycans in Golgi apparatus (Feldmann et al., 1991). preGP is then cleaved proteolytically into large amino-terminal GP1 (~130 kDa) and smaller carboxy-terminal GP2 (~24 kDa) subunits in the *trans*-Golgi network by the furin, enzyme belonging to the subtilizin-like protein convertase family. The furin cleavage motif is highly conserved among all filovirus transmembrane glycoprotein sequences and it consists of R-X-K/R-R motif (Volchkov et al., 1998). Mature envelope glycoprotein (150-170 kDa) is anchored in the membrane by a carboxy-terminal hydrophobic domain of GP2. Ebola virus glycoproteins form a trimeric conformation on the viral surface that is composed of 3 covalently attached monomers adopting a chalice-like shape. Each monomer contains two disulphide-linked subunits, GP1 and GP2. GP trimerization is mediated by multiple GP1-GP2 and GP2-GP2 contacts. Three GP1 ectodomains form together a bowl-like structure encircled by helices of three GP2 subunits (Lee et al., 2008). GP1 is responsible for the cell-surface attachment. GP1 is composed of a single domain that can be subdivided into: base, head and the glycan cap regions (Fig. 9). The base subdomain is composed of two sets of β-sheets, which form a semicircular surface that fix the internal fusion loop with a helix of GP2 through the hydrophobic interactions. The base region contains Cys53 that form an intermolecular disulphide bridge to Cys609 of the

GP2 subunit (Jeffers et al., 2002). The head subdomain is located between the base and the glycan cap regions. The head region contains two intramolecular disulphide bonds that stabilize the structure of GP1. The glycan cap subdomain contains 4 predicted N-glycosylation sites and is fully exposed on the outer surface of the chalice (Lee et al., 2008). GP2 is responsible for fusion of viral and host cell membranes since it contains a fusion peptide motif at residues 528-539. GP2 consists also of the internal fusion loop, the immunosuppressive motif at residues 584-600, the heptad regions: HR1, HR2, a transmembrane domain at position 651-670 and a cytoplasmic domain at residues 671-676 (Fig. 9).

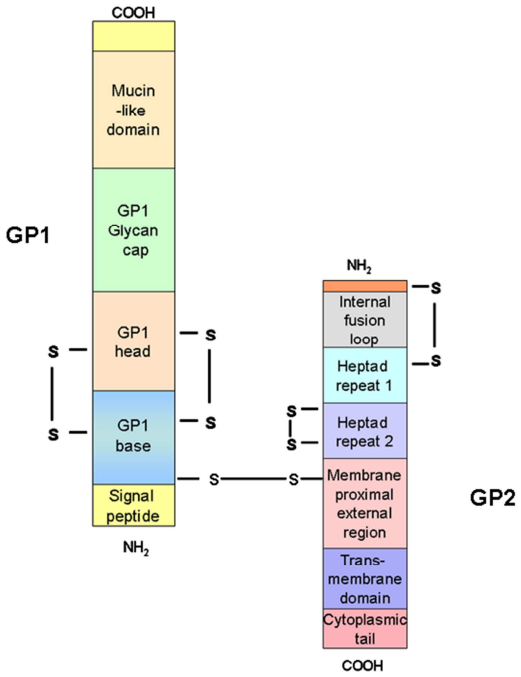

Figure 9. The structure of domains that form GP of Ebola virus. Modified from Lee *et al*. and Sanchez *et al*. (Lee et al., 2008; Sanchez et al., 1998).

The middle region of GP1/GP2 is extremely hydrophobic and contains a bulk of N- and O-linked glycans that account for more than one-third of the molecular mass of the mature protein (Geyer et al., 1992). Most of N-glycans are located in the mucin-like domain and the glycan cap of GP1. The approximate number of total oligosaccharides on the full-length GP is estimated to be 19 (17 on the mucin-like region). Among all attached oligosaccharides, Ebola virus glycoprotein contains 11 high-mannose N-glycosylation sites. The dense clustering of glycans generates an unfavorable condition for the interaction with neutralizing antibodies. The most critical regions responsible for Ebola virus entry such as the receptor-binding site are hidden under layers of glycans and no neutralizing antibodies were identified targeting this site (Wilson et al., 2000). Thus, although the major role of GP1 is receptor binding, it acts also in the pro-

tection of the virion from immune response through extensive glycosylation. GP2 plays a role in assembly of trimer structure, positioning of GP1 for receptor binding and host cell entry (Sanchez et al., 2001).

The **secreted glycoprotein** of EBOZ is a 365 aa in length and shares the amino-terminal 295 aa with the transmembrane glycoprotein GP (Fig. 10).

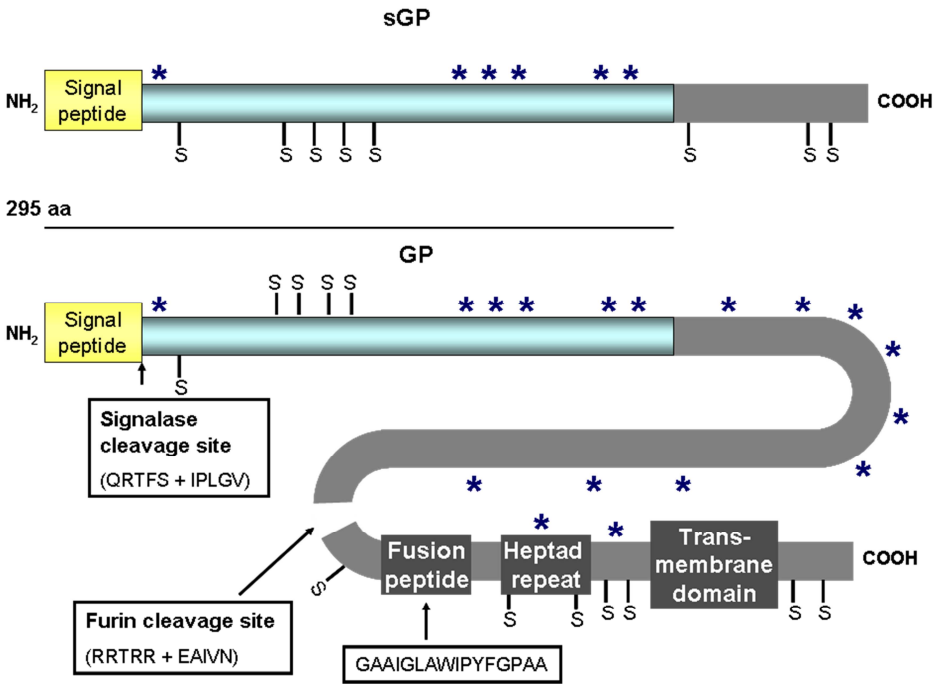

Figure 10. Diagrammatic representation of glycoprotein (GP) and secreted glycoprotein (sGP) of Ebola virus strain Zaire. The N-terminal 295 nt region identical in GP and sGP is shown in blue. The C termini with unique sequences in GP and sGP are shown in grey. The furin cleavage site for GP0 (uncleaved form of GP), the fusion peptide, the heptad region and the transmembrane anchor are shown on the graphics. Additionally, the cysteine residues (S) and the predicted N-glycosylation sites (blue stars) are shown in both GP and sGP. Modified from Sanchez *et al.* (Sanchez et al., 1998).

Pre-sGP undergoes several co- and post-translational processing events, such as signal peptide cleavage, glycosylation, oligomerization and proteolytic cleavage (Volchkova et al., 1998). Post-translational cleavage by furin in the Golgi compartments results in cleavage into sGP (50-70 kDa) and a small peptide termed **Δ-peptide** (Volchkova et al., 1999). Due to the lack of a transmembrane domain, sGP is secreted efficiently from in-

fected cells. sGP forms disulphide bonds between cysteines at the both ends of this molecule, which results in dimer formation. sGP might interact with the immune system at the cellular and humoral level. sGP plays a role in depletion of the immune cells. sGP binds to neutrophils and inhibits their activation, which results in the inflammatory instead of immune response. At the humoral immunity level, sGP prevents from acting of high-affinity antibodies on virion (Sanchez et al., 1996). By-product of sGP processing, Δ-peptide varies in length between 40-48 aa (10-14 kDa).

The **small secreted glycoprotein** (28 kDa) resembles a natural carboxy-terminal truncated variant of sGP. It lacks three carboxy-terminal cysteines, which are responsible for the dimerization of sGP. ssGP is therefore secreted in a monomeric form (Volchkov et al., 1995).

3. 2. Ebola virus receptors

Ebola virus cell entry is mediated by the interaction of a GP1 subunit with the receptors expressed on host cell. A number of molecules have been proposed as the main cellular entry receptors for Ebola virus. It has been identified that a glycophosphatidylinositol-linked protein, a folate receptor α (FRα), serves as a co-factor in Ebola virus cell entry. FRα is highly conserved in mammalian cells and it is expressed in the epithelial and parenchymal cells of a number of organs, but not in liver or endothelial cells (Chan et al., 2001). It has been demonstrated that endosomal membrane protein Niemann-Pick C1 (NPC1) encoding an endolysosomal cholesterol transporter plays an essential function in Ebola virus entry (Carette et al., 2011; Cote et al., 2011). It was shown that cells lacking NPC1 revealed resistance to infection by Ebola and Marburg envelope glycoprotein pseudotyped viruses (Carette et al., 2011). *In vitro* studies demonstrated that treatment of cells with molecules targeting NPC1 potently inhibited viral infection by Ebola GP-pseudotyped viruses (Cote et al., 2011). Binding of Ebola virus GP to different cellular lectins has been also shown to augment virus infection. Lectins might play a role through the concentration of viral particles on the cell surface and

therefore increasing the cell entry and infection level (Alvarez et al., 2002). Essential lectins enhance Ebola virus entry, such as DC-SIGN, L-SIGN (Alvarez et al., 2002), MBL (Ji et al., 2005), a human macrophage galactose (hMGL), N-acetylgalactosamine-specific C-type lectin (Takada et al., 2004), the liver-specific asialoglycoprotein receptor (ASGP-R) (Becker et al., 1995) and LSECtin (Gramberg et al., 2005). The members of tyro3 protease kinase family (Shimojima et al., 2006) and integrin β1 (Takada et al., 2000) play also the role in facilitating Ebola cell entry.

Ebola viruses can lead to the productive infection in a number of systems, such as human, simian and bat (Anonymous, 1978; Bowen et al., 1978; Fisher-Hoch et al., 1992). Wool-Lewis *et al*. has studied the cellular tropism of Ebola virus by using MLV particles pseudotyped with Ebola Zaire glycoprotein. It was shown that Ebola GP-pseudotyped particles displayed a very broad host range of receptors being able to infect different cell lines from various species and tissues, including 293T, HeLa, Vero, BSC-1, Cos-7, NIH 3T3, MDBK, BAEC, PK-15, BHK, CHO, Qt6, CEF, TEF, U87, MDCK, Tb 1 Lu and Pt K1. Remarkably, they discovered that human and murine lymphoid cell lines were resistant to Ebola GP-pseudoparticles infection suggesting that lymphoid lineage cells lack the functional Ebola virus receptors (Wool-Lewis and Bates, 1998; Yang et al., 1998). In the natural course of Ebola virus infection, hepatocytes, DCs, monocytes and macrophages are the preferred target cells of filoviruses and the infection of these cells is important for hemorrhagic manifestations and immune disorders (Davis et al., 1997).

3. 3. DC-SIGN-mediated Ebola virus infection

The potential role of DC-SIGN in Ebola virus infection has been studied in the cellular model based on non-permissive for Ebola virus infection T-lymphocyte-derived Jurkat cells. This study demonstrated that the expression of DC-SIGN molecule on the surface of non-susceptible cells has allowed Ebola GP-pseudotyped retrovirus cell entry (Alvarez et al., 2002). DC-SIGN is not the main receptor for Ebola virus and many dif-

ferent cell lines lacking DC-SIGN has been earlier described as a target of viral infection (Wool-Lewis and Bates, 1998; Yang et al., 1998). It has been shown that the expression of DC-SIGN increases the level of the infection with Ebola virus in susceptible cells. Moreover, DC-SIGN acts as a *trans*-receptor since Ebola particles might be captured by DC-SIGN-expressing monocyte-derived DCs to be further transmitted to recipient cells (Alvarez et al., 2002). Although all predicted *in vitro* DC-SIGN functions have not been confirmed in *in vivo* studies, DC-SIGN was predicted to participate in the dissemination of the virus at the first moments of the infection. Therefore, over the years many different antiviral strategies based on carbohydrate compounds targeting DC-SIGN were used to block Ebola virus-DC-SIGN interaction.

4. Human Immunodeficiency Virus (HIV) and DC-SIGN

4. 1. The discovery of HIV

AIDS was first described as a new clinical syndrome in 1981 when the first five clinical cases of AIDS were published in the *Morbidity and Mortality Weekly report* and subsequently in *the New England Journal of Medicine*. These reports described an epidemic of *Pneumocystis carinii* pneumonia (PCP) combined in most cases with oral rush and chronic ulcerating perianal herpes infection in previously healthy homosexual men (Gottlieb et al., 1981; Masur et al., 1981). The first evidence of the AIDS agent was shown by the group of Luc Montagnier and Françoise Barré-Sinoussi, who isolated a retrovirus from a lymph node of patient with persistent generalized lymphadenopathy showing AIDS symptoms and named it lymphadenopathy-associated virus (LAV) (Barresinoussi et al., 1983). In early 1984, the group of Robert Gallo isolated the lymphotropic retrovirus from the peripheral blood mononuclear cells (PBMCs) of patient with AIDS syndrome and named it HTLV-III (Gallo et al., 1984). At the same time, the group of Levy isolated also the retrovirus infecting $CD4^+$ T cells from patients with AIDS symptoms as well as from asymptomatic patients from the risk groups in San

Francisco and named it ARV (AIDS-associated retrovirus). Finding the ARV in asymptomatic individuals indicated for the first time the healthy carrier for the AIDS agent (Levy et al., 1984). A short time later, it was shown that all three virus variants (LAV, HTLV-III, ARV) corresponded to the same infectious agent that was renamed in 1986 by The International Committee on Taxonomy of Viruses to human immunodeficiency virus type I (HIV-1). In 2008 the French group of Luc Montagnier and Françoise Barré-Sinoussi received the Nobel Prize in Medicine for the discovery of HIV-1.

4. 2. The structure of HIV

HIV-1 particle is 100-120 nm in diameter, with heterogeneous morphological shape (Kuznetsov et al., 2003). Each viral particle is surrounded by lipoprotein membrane with integrated glycoprotein complexes. The glycoprotein complex is composed of trimers of an external glycoprotein gp120 and a transmembrane spanning protein gp41. The number of viral spikes was initially described as 72 (Chan et al., 1997), however electron microscopy studies showed that by the time the virus particle is released from the cell only 7-14 spikes appear to be present on the virion surface (Chertova et al., 2002; Layne et al., 1992). The spikes are arranged on the virion surface as tripod-like structures in the varied number reflected by the reduction in envelope formation rather than envelope shedding (Chertova et al., 2002). The diameter of each spike is about 14 nm and its high is 9-10 nm. Infectious particles contain the three *gag* proteins: matrix (MA, p17), capsid (CA, p24) and nucleocapsid (NC, p7) (Gomez and Hope, 2005). MA forms the inner shell in the viral particle below the viral membrane, CA forms the canonical core enclosing the viral genomic RNA and NC interacts with the viral RNA inside the capsid (Fig. 11). The genomic RNA is a dimer, held together by sequences near its 5' ends of both subunits (Bender and Davidson, 1976). The viral proteins are generated by the viral protease (PR), which processes the HIV-1 p55 *gag* precursor polyprotein into p17, p24, p2, p7, p1 and p6 (Fig. 12). Inside the CA are two identical RNA strands in close contact with the viral RNA-dependent DNA polymerase (reverse tran-

scriptase, RT) and NC proteins (p6 and p9). The inner part of the viral membrane is surrounded by a myristylated p17 core protein (MA) (Gelderblom et al., 1988).

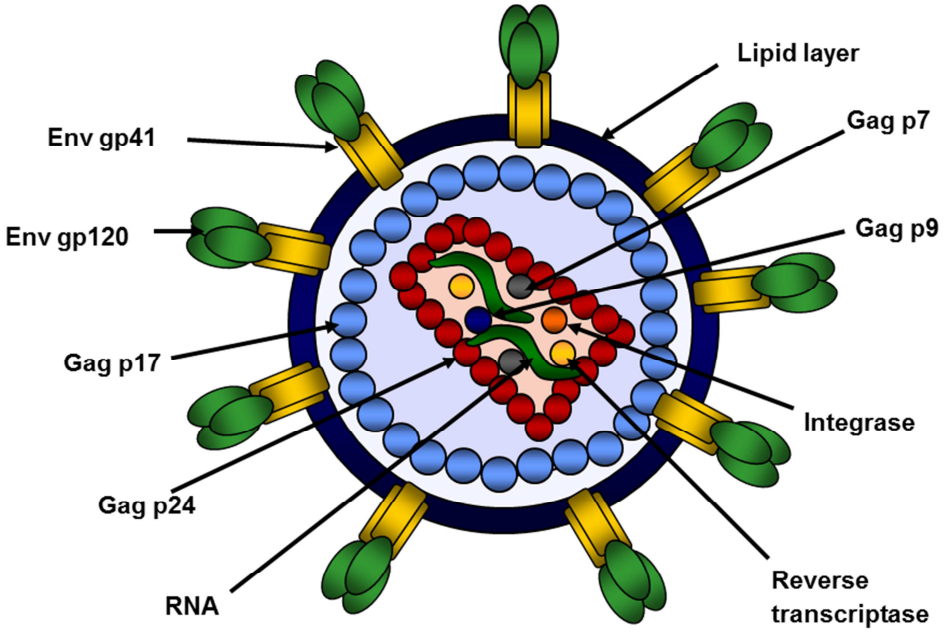

Figure 11. Structure of HIV particle. Modified from Hoffmann *et al.* (Hoffmann and Rockstroh, 2010).

The genomic size of HIV is about 9 kb, with three open reading frames (ORF) coding for several viral proteins. The structural scheme of a retroviral genome is: 5'LTR – gag – pol – env – LTR3' (Fig. 12). The long terminal repeat (LTR) regions represent the terminal parts of the viral genome, which are connected to the host cellular DNA after integration and do not encode for viral proteins. The *gag* genes code for nucleocapsid, capsid and core proteins. The *env* genes encode envelope glycoproteins. The *pol* genes code for viral enzymes (Wong-Staal, 1991). The primary transcript of HIV is full-length viral mRNA, which is translated into the polymerase (*pol*) and group-antigen (*gag*) proteins. The *pol* precursor is autocleaved by its PR region into viral enzymes: RT, PR and integrase (IN). The proteolytic cleavage of *gag* precursor gives rise to p24, p17, p9, p6,

p2 and p1. The *env* precursor gp160 is cleaved by endoprotease furin into superficial gp120 and transmembrane gp41 (Gomez and Hope, 2005).

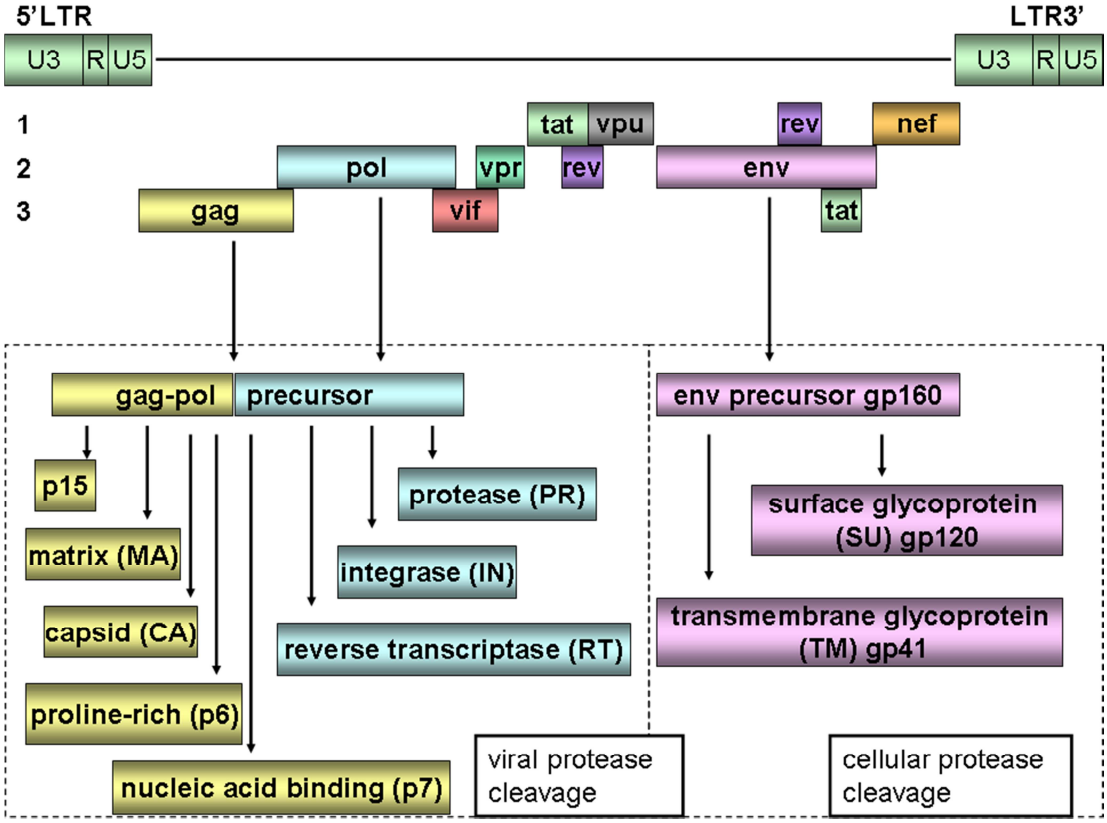

Figure 12. The organization of HIV-1 genome. Modified from Coffin (Coffin et al., 1997).

4. 3. The structure of HIV envelope

The HIV envelope glycoprotein is a type I membrane spanning protein that is synthesized and processed to its mature form by the host cell machinery (McKeating and Willey, 1989). The *env* protein gives rise to surface (SU) and transmembrane (TM) envelope glycoproteins that are derived from a common precursor. The nascent *env* polypeptide binds to a signal recognition particle through its amino-terminal leader segment and becomes associated with the membrane of the ER. Further translation extrudes most of the envelope polypeptide through the membrane into the lumen of ER,

where the process of oligomerization takes place. After cleavage of the leader sequence, *env* is transported by vesicular traffic through the Golgi apparatus to the plasma membrane. During the transport through Golgi apparatus, the *env* protein is glycosylated during N-glycosylation and O-glycosylation process. *Env* is then cleaved in Golgi by a cellular protease, furin, to yield mature SU gp120 and TM gp41 glycoproteins. SU and TM remain attached to each other by non-covalent interactions (Coffin et al., 1997). The glycosylation process of HIV envelope is required for proper folding and conformational stability of the envelope glycoprotein (Fenouillet et al., 1994). The glycosylation mainly involves the attachment of N-linked high-mannose-type oligosaccharides to the protein backbone to the asparagine in Asn-X-Thr or Asn-X-Ser motifs, where X is any aa apart from proline. The number and distribution of N-linked glycosylation sites varies widely between different HIV isolates, being in the range of approximately 18-32 PNGS in gp120 accounting for about 50% of the total molecular weight. As the glycoprotein is transported through the Golgi, accessible glycan moieties are trimmed and modified by various cellular enzymes resulting in the generation of complex-type oligosaccharides. The gp120-gp41 complexes, which remain associated through non-covalent interactions between the gp41 ectodomain and discontinuous structures composed of NH_2- and COOH-terminal gp120 sequences, are initially expressed at the surface of infected cells. During the process of HIV budding, the gp120-gp41 complexes are then incorporated into the virus envelope and displayed on the viral surface as viral spikes (Wyatt and Sodroski, 1998). gp120 is composed of five constant regions (C1-C5) and five variable regions (V1-V5) (Starcich et al., 1986). Intramolecular disulfide bonds in the gp120 glycoprotein result in the incorporation of the first four variable regions into large, loop-like structure (Leonard et al., 1990). gp120 core is composed of 25 β-strands, 5 α-helices and 10 loop segments folded into a heart-shaped globular structure with dimensions of 5 x 5 x 2.5 nm. The core is formed of inner and outer domains that are linked together by a four-stranded sheet called bridging sheet. The inner domain is more conserved than outer domain and is largely devoid of glycans (Kwong et al., 1998). The inner domain of gp120 faces the trimer axis, whereas the outer domain is mostly exposed on the surface of *env* oligomer. The outer domain is largely covered by glycans resulting in lower overall immunogenicity of this domain

(Wyatt et al., 1998). The bridging sheet links the inner and outer domain. The primary HIV-specific receptor is CD4, a 58 kDa monomeric glycoprotein, which is expressed on the surface of T lymphocytes, monocytes, dendritic cells, and brain microglia (Deng et al., 1996). The binding site for CD4 on the ligated gp120 structure is formed by the interface between the inner domain, bridging sheet and outer domain. Most of the CD4 contact residues are situated on the outer domain of the ligand-covered gp120 and form a continuous binding region (Kwong et al., 1998). The majority of gp120 conformational shifts resulting from CD4 binding are located in the portion of gp120 that interacts with gp41. These conformational changes are necessary to lock the coreceptor-binding site (CoRBs) into a fixed conformation resulting in the initiation of the first steps in fusion process (Wyatt and Sodroski, 1998). The region that is important for the interaction with the β-chemokine receptor CCR5 has been mapped to the residues in the bridging sheet located close to the V3 stem. V3 loop plays a major role in determining the coreceptor usage of virus strain. Moreover, certain single amino acid changes within V3 loop can alter cell tropism of HIV-1 (Takeuchi et al., 1991). The isolates using CCR5 coreceptor are named R5-tropic viruses, isolates using CXCR4 coreceptor are named X4-tropic viruses and the isolates able to use both coreceptors are called dual-tropic (DM) (Berger, 1997). The HIV-1 clinical isolates of primary infection use generally the CCR5 coreceptor for its entry (Feng et al., 1996). It has been proven that a single viral particle most often establishes infection (80% of heterosexual transmissions), which results in very homogeneous virus population at the beginning of the infection. After time, viral population diversifies, accumulating mutations to evade HIV-specific immune responses (Abrahams et al., 2009; Keele et al., 2008). The CoRBs is not present on the gp120 until CD4 binding occurs (Rizzuto and Sodroski, 2000). The CoRBs is one of the most conserved surfaces on the gp120 core, even more conserved than the CD4 binding site (CD4Bs) (Rizzuto et al., 1998). The CoRBs is located close to the trimer axis and faces the target cell surface after CD4 ligation to gp120. The rearrangements in gp120 involve a movement of the V1-V2 stem away from the underlying CoRBs, while V3 loop may move towards this binding site. Binding of the coreceptor to gp120 leads to further conformational changes resulting in the gp41 activation into its fusion-active state. gp41 exists in a metastable non-coiled-coil conformation when associated with

gp120. After coreceptor binding, the envelope glycoprotein complex undergoes conformational changes, which lead to the insertion of gp41 fusion peptide into the membrane of the target cell and the formation of a pre-hairpin intermediate, where gp41 protein is both a viral and a cell membrane protein. The pre-hairpin intermediate is followed by a formation of a gp41 coiled-coil structure, which further leads to the apposition of membranes and to the fusion (Wyatt et al., 1995).

The exposure of the primate immunodeficiency virus envelope glycoproteins on the surface of virions or infected cells makes them the major target of neutralizing antibodies (NAbs). NAbs responses against HIV-1 infection *in vivo* is generally limited (Wyatt and Sodroski, 1998). Structures on the viral envelope glycoproteins that are conserved among diverse viral strains are generally poorly exposed to humoral immune system. The conserved gp120 surfaces involved in binding to gp41, CD4 and chemokine receptors, exhibit problems with respect to the elicitation or sensitivity to NAbs. The moieties involved in binding to CD4 or coreceptors are buried in the interior of functional spikes, flanked by variable regions exhibiting high glycosylation pattern (Wyatt et al., 1993). Because most carbohydrates moieties may appear as "self" to the immune systems, this concentrated glycosylation may reduce the potential of a large portion of the gp120 surface to serve as an immunogenic target. The efficacy of the humoral immune response in limiting the spread of virus *in vivo* is compromised by the relative resistance of primary virus isolates to neutralization and the temporal pattern with which NAbs are generated (Wyatt and Sodroski, 1998). The non-covalent nature of the association between gp120 and gp41 contributes to the lability of the functional envelope trimer. During natural infection, disassembled envelope glycoproteins elicit most of the Abs directed to these viral components (Wang et al., 1986). In general, the cognate Abs cannot bind the assembled, functional envelope spikes to exhibit neutralizing activity. Thus, although Abs are detected in the sera of HIV-1-infected individuals by 2-3 weeks after infection, they lack the ability to inhibit virus infection. By the time that NAbs are efficiently elicited, HIV-1 infection is established in the host. Several weeks after infection, NAbs can be detected in sera of HIV-1-infected individuals, however, they often exhibit little or no activity against other strains. Later in the course of infec-

tion, Abs capable of neutralizing wider range of HIV-1 isolates may appear, however they are mostly active against early infection virus variants (Wyatt and Sodroski, 1998).

It has been shown that hypervariable loops of HIV-1 envelope tend to be shorter and to carry fewer PNGS in viruses from early infection as compared with their chronic counterparts (Chohan et al., 2005; Frost et al., 2005). Larger loops mask epitopes recognized by NAbs, thus it is hypothesized that during the time of infection they are acquired under immune pressure. Increased length of VLs may also reduce CD4 receptor and CCR5 coreceptor access (Sagar et al., 2009). Changes in glycosylation pattern play a key role in chronic infection, which may results in immune escape. Although the reduced loops lengths and number of PNGS are characteristic for early viruses, some specific PNGS in outer domain has been shown to be lost in the course of chronic infection. It has been shown that glycans at positions N188, N362, N462, N392, N397, N356 play a role in facilitating of transmission in early infection, and their loss contributes to immune escape in chronic infection (Gnanakaran et al., 2011).

The dense layer of the glycans have an important role in viral transmission through interactions with lectins, particularly the C-type lectin DC-SIGN (de Witte et al., 2008). It has been shown that some glycan changes confer to the increased binding to DC-SIGN. DC-SIGN can facilitate viral infection in *trans* and in *cis*, especially when CD4 and coreceptors levels are limited. The presence of an additional glycan (N158) at the N-terminal base of the V2 loop of SHIVSF162 gp120 compared to the parental strain was responsible for the increasing binding to DC-SIGN (Lue et al., 2002). It has been also shown that R5 viruses emerging during end-stage AIDS disease displayed reduced ability to use DC-SIGN. R5 end-stage viruses lacked PNGS in the gp120 V2 (N160) and V4 (N406) as compared with early infection viruses. N160 was shown to be responsible for more efficient use of DC-SIGN for binding and *trans*-infection. The competition assay reveled that strains containing N160 were selected for *trans*-infection, whereas strains lacking N160 were selected for direct cell infection (Borggren et al., 2008). Hong *et al.* demonstrated also that elimination of PNGS by mutagenesis at

positions N293Q, N382Q, N388Q and N328Q exhibited a significant decrease in binding to DC-SIGN as compared with wild type JR strain (Hong et al., 2007).

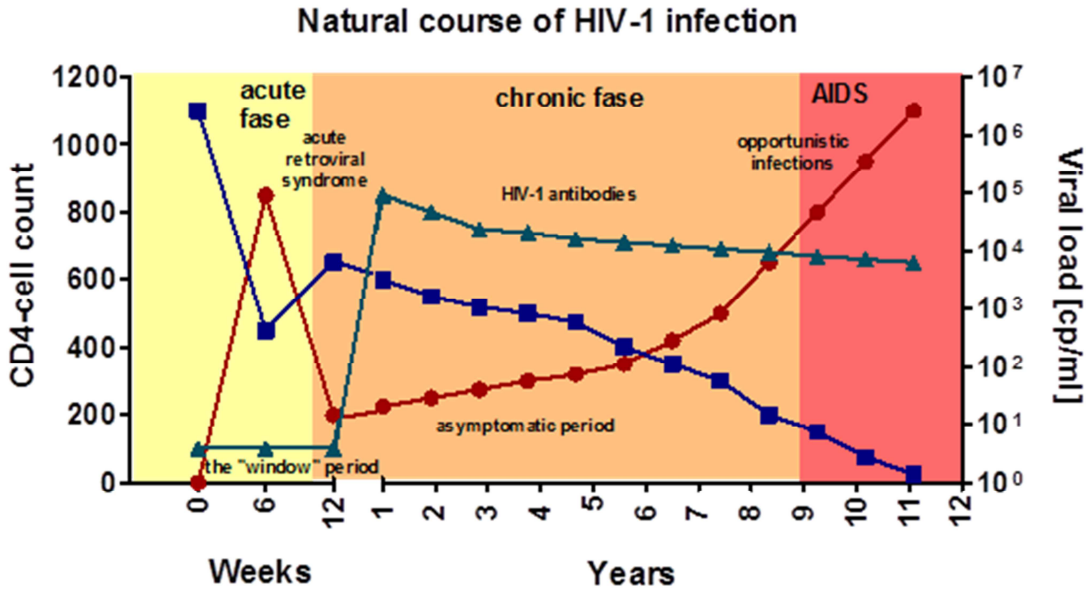

Figure 13. Natural course of HIV-1 infection. Modified from Hoffmann *et al*. (Hoffmann and Rockstroh, 2010).

4. 4. The natural course of HIV infection

Shortly after HIV exposure, the acute retroviral syndrome is observed in some patients. This syndrome is defined by unspecific and variable "flu-like" symptoms that make the diagnosis of HIV-1 more difficult (Schacker et al., 1996; Vanhems et al., 1999). The acute infection phase was characterized in details by Fiebieg *et al.* showing the presence of specific HIV markers in each phase of the acute period (Fiebig et al., 2003). After acute phase, the period of several years of asymptomatic chronic infection takes place in most of the people. Followed asymptomatic phase of HIV-1 infection, the AIDS-defining illness occurs at a median of 8-10 years after infection (Phillips, 1992).

Without antiretroviral therapy (ARV) this phase eventually leads to the death of patients after a variable period of time (Fig. 13).

4. 5. Mechanisms of durable HIV control in the absence of antiretroviral treatment: HIV-1 controllers

Most of HIV-1-infected patients show high plasma viral load and the loss of $CD4^+$ T cells along the course of HIV-1 infection in case of absence of ART (Lassen et al., 2009). The majority of antiretroviral-untreated individuals eventually develops immunodeficiency of immune system and dies from AIDS-related complications in approximately 10-year time after becoming infected. However, a very small percentage of untreated individuals remain clinically and/or immunologically stable for years (Cao et al., 1995; Munoz et al., 1995). The term of "long-term non-progressors (LTNP)" was used in case of people that were able to maintain normal $CD4^+$ T cell counts for prolonged periods (>10 years). According to virological criteria, some of the individuals (less than 1% of infected population) called "elite controllers (EC)" are able to maintain viral loads undetectable (<50 copies HIV RNA/ml) (Deeks and Walker, 2007). According to the International HIV Controller Consortium there are three main criteria for enrolment a patient as EC: 1) being HIV antibody positive as determined by serologic tests, 2) being under no antiretroviral therapy in the last 12 month period, 3) having done at least 3 plasma HIV RNA determinations spanning at least 12 last months that resulted in being below the limit of detection. The International HIV Controller Consortium defined the second group of HIV controllers called viremic controllers (VC). Individuals who belong to VC group have to accomplish 3 following criteria: 1) maintain RNA levels below 2000 copies of viral RNA per ml, 2) not receive antiretroviral therapy for 1 year or longer, 3) episodes of viremia are acceptable as long as they represent the minority of all available determinations (www.eliteconrollers.org).

The factors associated with HIV control *in vivo* have not been fully defined yet, in part due to the fact that HIV controllers form a very heterogeneous population (Lefrere et al., 1997). Individuals destined to become HIV controllers seem to have less symptomatic primary infections as compared with those destined to remain viremic (Madec et al., 2005a), which suggest that complex virus and host interactions leading to prolonged control of viral replication play already an important role during the earliest phases of HIV disease (Altfeld et al., 2006). It has been shown that neither the route of HIV acquisition is associated with the likelihood of controlling HIV infection (Madec et al., 2005b), neither the gender of infected person (Deeks and Walker, 2007; Sterling et al., 1999) nor the race, geographical location, viral subtype (Deeks and Walker, 2007). It has been speculated about the potential role of virus factors or host genetics as an elements associated with virological control.

There is some evidence that pathogenicity of HIV isolates can differ, which was shown in a group of individuals infected through blood transfusion from a common donor harbouring a virus containing deletion in the *nef* gene and who maintained low viremia for years (Deacon et al., 1995). Over the time, many of these individuals eventually have progressed to AIDS (Churchill et al., 2006), which showed that viral attenuation through the *nef* gene did not lead to life-long control of HIV infection *in vivo*. Different small studies or case reports argued that mutations or deletions within the HIV functional and accessory genes (*rev*, *tat*, *vif*, *vpr* and *vpu*) can lead to virus control and/or immunologic non-progression (Alexander et al., 2000; Hassaine et al., 2000; Kirchhoff et al., 1995; Lum et al., 2003; Wang et al., 1996; Yamada and Iwamoto, 2000). Nevertheless, there are difficulties in the interpretation of these studies since they were based on a very low number of infected individuals. The frequency of infectious units per million of resting $CD4^+$ T cells has been estimated as a value of 0.02, which is 1.5 log lower than the value observed during suppressive ART. In some studies virus from HIV controllers showed normal replication kinetics *in vitro* and lacked any genetic insertions or deletions, providing the evidence of rather host and not virus factors being responsible for viral control (Blankson et al., 2007). However, other studies have revealed that HIV envelopes derived from EC demonstrated reduced entry fitness (Casado et al., 2013;

Lassen et al., 2009; Miura et al., 2009). Envelopes from EC interacted with cellular receptors CD4 and CCR5 inefficiently as compared to those from individuals with detectable viral loads. Envelope clones derived from EC required higher levels of receptor and coreceptor for efficient entry. This work has also demonstrated that the HIV envelope clones EC-derived revealed delay in fusion kinetics as compared with acute and chronic envelope clones (average $T_{1/2}$ of 92.1 min versus $T_{1/2}$ of 67.5 min for acute infection clones and $T_{1/2}$ of 58.3 min for chronic infection clones). The HIV clones derived from EC also completed reverse transcription process slower ($T_{1/2}$ =8.89 hours) than acute infection clones ($T_{1/2}$ =7.74 hours) and chronic infection clones ($T_{1/2}$ =7.95 hours) (Lassen et al., 2009). However, lower envelope fitness is likely not sufficient to mediate absolute viral suppression. The envelope sequence diversity of plasma virus obtained from HIV controllers showed low genetic diversity, which might suggest limited viral replication and evolution during the course of the infections. The lack of envelope diversification has raised the suggestion that HIV envelopes in EC may be closely related in genotype and phenotype to the founder virus establishing infection (Bailey et al., 2006a; Casado et al., 2013; Lassen et al., 2009).

The most consistent factor responsible for virological control is a vigorous cellular response. After the acute phase of HIV infection there is an increase in HIV-specific $CD8^+$ T cells, which are able to kill HIV-infected cells. It has been shown that the function of HIV-specific $CD8^+$ T cells is clearly higher in controllers as compared with non-controllers including their ability to proliferate after encounter with HIV antigens, the ability to produce the cytolytic protein perforin (Migueles et al., 2002) and the ability to produce multiple cytokines such as: interferon-γ, MIP-1β, TNF-α and IL-2 (Betts et al., 2006; Zimmerli et al., 2005). The virus-specific cytotoxic T cell response plays the crucial role in the control of HIV/SIV infection (Goulder and Watkins, 2004). HLA molecules detect and present infectious agent peptides to T cells. There is a high level of variability between individuals and populations in both HLA classes (HLA class I: A, B, C and HLA class II: DR, DQ, DP) (Hughes and Yeager, 1998; Parham and Ohta, 1996). Different HLA alleles specify the molecules of infectious agents to be presented on the cell surface, therefore various HIV-1 peptide motifs might be presented influ-

encing in this way the differences in the kinetics of HIV-1 infection in diverse individuals (Barber et al., 1995; Gao et al., 2001; Moore et al., 2002). The presence of several different HLA alleles have been described to be associated with effective HIV control, such as HLA-B57, HLA-B5801, HLA-B27, HLA-B14, HLA-A32 (Gao et al., 2001; Geczy et al., 2000; Hendel et al., 1999; Kaslow et al., 1996; Keet et al., 1999; Magierowska et al., 1999; McNeil et al., 1996; Saah et al., 1998). HLA-B57 allele was consistently shown to be associated with a delay onset to AIDS (Carrington and O'Brien, 2003; O'Brien et al., 2001). HLA-B57 presents the HIV epitope TW10 (TSTLQEQIGW) that corresponds to *gag* residues 240-249. It has been demonstrated that TW10 epitope within p24 gag reveals high conservation between different HIV-1 strains and TW10 escape mutations reduce significantly viral replicative capacity (Martinez-Picado et al., 2006). The presence of allele variants HLA-B5701 and HLA-B27 were found strongly enriched among European and North American cohorts of HIV controllers as compared to non-controllers (Bailey et al., 2006b; Lambotte et al., 2005). The incidence of HLA-B5703 alleles was also found enriched among African populations who were able to maintain low viral loads (Kiepiela et al., 2007). Nevertheless, some other HLA allele variants have been associated with rapid progression to AIDS, including HLA-B35, HLA-A23, HLA-B37, HLA-B49, which seemed to fail at stimulation of cytotoxic T-cell recognition (Carrington et al., 1999; Chen et al., 1997; Gao et al., 2001; Kaslow et al., 1996; Saah et al., 1998). The potential impact of reduced host cell susceptibility to HIV infection has been also studied by verifying the presence of a 32 base pair deletion in LTNP patients. A Δ32 deletion in the coreceptor gene CCR5 is strongly associated with the resistance to HIV infection, however this deletion was described not to be specifically associated with the HIV controllers (Lambotte et al., 2005). In addition, it was also described that individuals, who maintain low viral load in the absence of therapy often lack high-titer neutralizing antibodies (Bailey et al., 2006a; Deeks et al., 2006).

Most recently it has been also shown that some patients might keep viral control after treatment interruption. These individuals were called as “secondary controllers” (Van Gulck et al., 2012) or “post-treatment controllers” (PTC) (Saez-Cirion et al., 2013). The majority of these patients were treated already in the acute phase of infection, therefore

it cannot be excluded that some of these patients could actually evolved to become EC or VC (Vanham et al., 2014). PTC individuals were shown distinct to EC in the meaning of host genetics, including HLA allele profile and cellular response. PTCs revealed a higher viral load and a lower $CD4^+$ T cell count as compared to EC. Moreover, PTC patients demonstrated lower immune activation including lower $CD8^+$ T cell HIV-specific inhibitory activity as compared to EC. Additionally, some of PTC-derived viruses cultivated from $CD4^+$ T cells revealed delayed kinetics or low fitness. Although PTCs are a heterogeneous population, the most consistent factor associated with this group so far has been a very low proviral reservoir. Nevertheless, the characteristics of PTC patients has been based on very small cohorts of individuals, therefore the phenomenon of post-treatment virological control requires further investigation (Lewin and Rouzioux, 2011; Saez-Cirion et al., 2013; Van Gulck et al., 2012; Vanham et al., 2014).

4. 6. Signaling through DC-SIGN

DC-SIGN contains several different motifs in its cytoplasmic tail, which allow for the induction of intracellular signaling pathways. It has been indicated that engagement of DC-SIGN on DCs results in the activation of signal transduction pathways, which can cause a wide modulation of immune response, mostly when co-activated with Toll-like receptors (Gringhuis et al., 2007). It has been suggested that DC-SIGN signaling after binding to HIV leads to modifications of NF-kB activity and the production of immunosuppressive cytokines. The engagement of DC-SIGN by HIV activates Raf-1-dependent signaling, which results in the phosphorylation of p65 subunit of NF-kB p65-p50 dimer. The phosphorylation of serine 276 of the p65 subunit induces acetylation of lysines in p65, which outcomes in prolonged transcriptional activity of NF-kB and prolonged nuclear retention. Increased activity of NF-kB causes the enhanced transcription rate from IL-10 gene. IL-10 inhibits Th-1 response and decreases capacities of antigen presentation by DCs. The phosphorylation of serine in the p65 subunit

of NF-kB allows also the recruitment of the transcription-elongation factor pETF-b to the HIV promoter that phosphorylates RNA polymerase II at serine 2. This phosphorylation increases processivity of the RNA polymerase II, allowing therefore the synthesis of full-length HIV transcripts in DCs (Fig. 14) (Svajger et al., 2010; Tsegaye and Pohlmann, 2010)

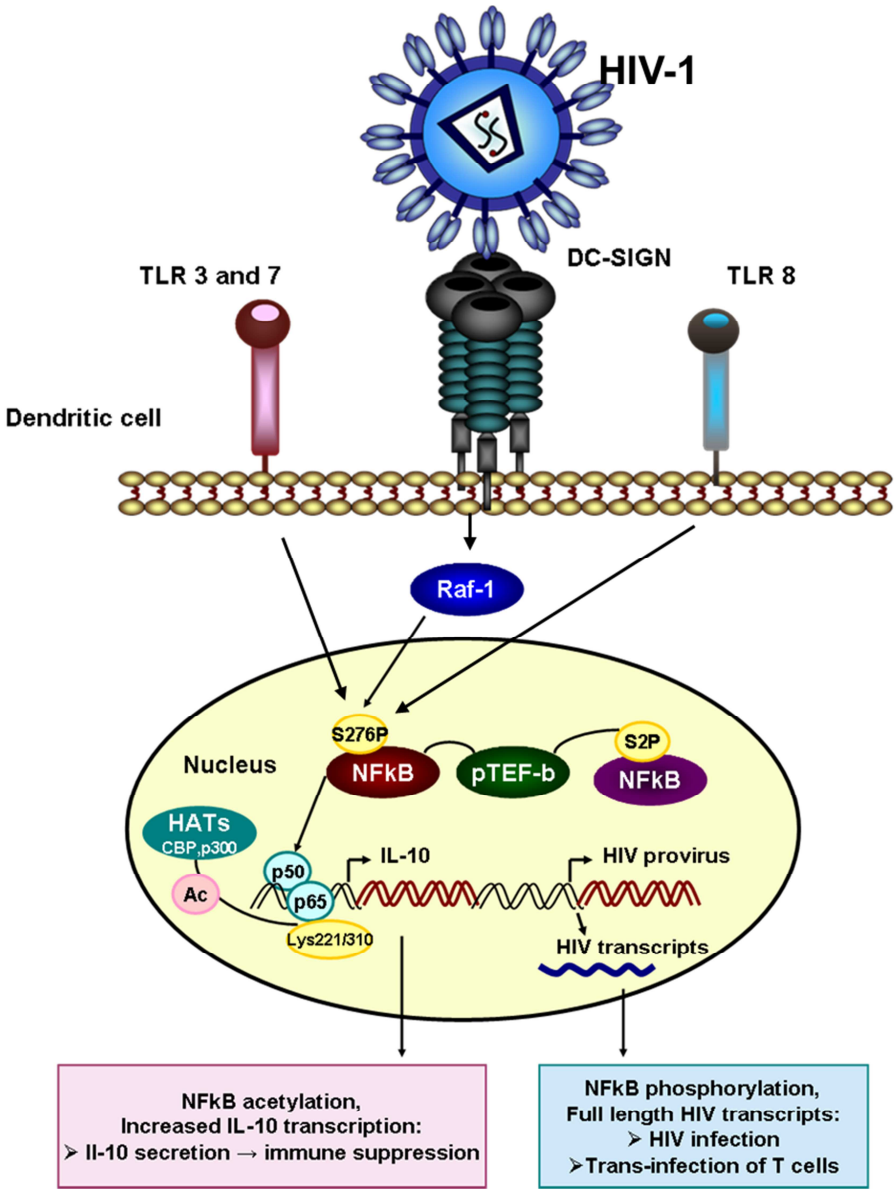

Figure 14. DC-SIGN signaling upon HIV binding promotes DCs infection and production of immunosuppressive cytokines. Modified from Tsegaye *et al.* (Tsegaye and Pohlmann, 2010).

4. 7. Mechanisms of DC-mediated HIV transmission

The sexual transmission has been shown as a primary route of HIV-1 infection nowadays. Several different cells, including DCs and Langerhans cells, have been demonstrated to be present at the mucosal surface during HIV sexual transmission. Different C-type lectins expressed on these cells may play a role in HIV-1 attachment and further virus dissemination (de Witte et al., 2007; Wu and KewalRamani, 2006). Langerin is a lectin expressed exclusively on Langerhans cells, which induces the formation of Birbeck granules that play significant role in antigen processing (Hunger et al., 2004; Valladeau et al., 2000). De Witte *et al.* showed that infection of T cells was significantly inhibited by Langerhans cells as compared with DCs. Moreover, they demonstrated that Raji-Langerin cells could efficiently bind HIV-1 particles, however they could not transfer HIV-1 viruses to T cells. The results obtained in their study proved that Langerin plays a role as a scavenger receptor rather than as *trans*-receptor for HIV-1 dissemination. Langerin acts in capturing of HIV-1 particles and further internalization into Birbeck granules for virus degradation (de Witte et al., 2007). In contrary, DCs are thought to facilitate viral dissemination through HIV-1 capture at mucosal site and transmission to secondary lymphoid tissues (Haase, 2005, 2010; Pope et al., 1994; Shattock and Rosenberg, 2012; Steinman et al., 2003). The DC-mediated HIV infection can occur through several distinct processes taking place concurrently, including *trans*-infection through infectious synapse, *trans*-infection through exosomes or *cis*-infection following *de novo* production of viral particles in DCs (Fig. 15) (Wu and KewalRamani, 2006).

The efficient $CD4^+$ T cell infection through infectious synapse in the process of HIV *trans*-infection requires cell-to-cell contact (Tsunetsugu-Yokota et al., 1997). It has been shown that HIV particles and HIV receptors (including DC-SIGN attachment molecules) are concentrated at the zone of infectious synapse (McDonald et al., 2003). Infectious synapse is therefore responsible for most of rapid and efficient virus transfer between DCs and $CD4^+$ T cells. HIV *trans*-infection might also occur through exosomes. HIV particles captured by immature DCs might be rapidly internalized into endosomal

multivescicular bodies (endocytic bodies enriched in transmembrane proteins, such as tetraspanins). Some of endocytosed HIV particles are released into extracellular milieu associated with endocytic vesicles, which are known as exosomes (Thery et al., 2002; Wiley and Gummuluru, 2006). Those exosomes might subsequently fuse with target cell membrane and deliver infectious virus. The remaining HIV particles in multivescicular bodies in DCs might enter lysosomal pathway and be further degraded (Wiley and Gummuluru, 2006).

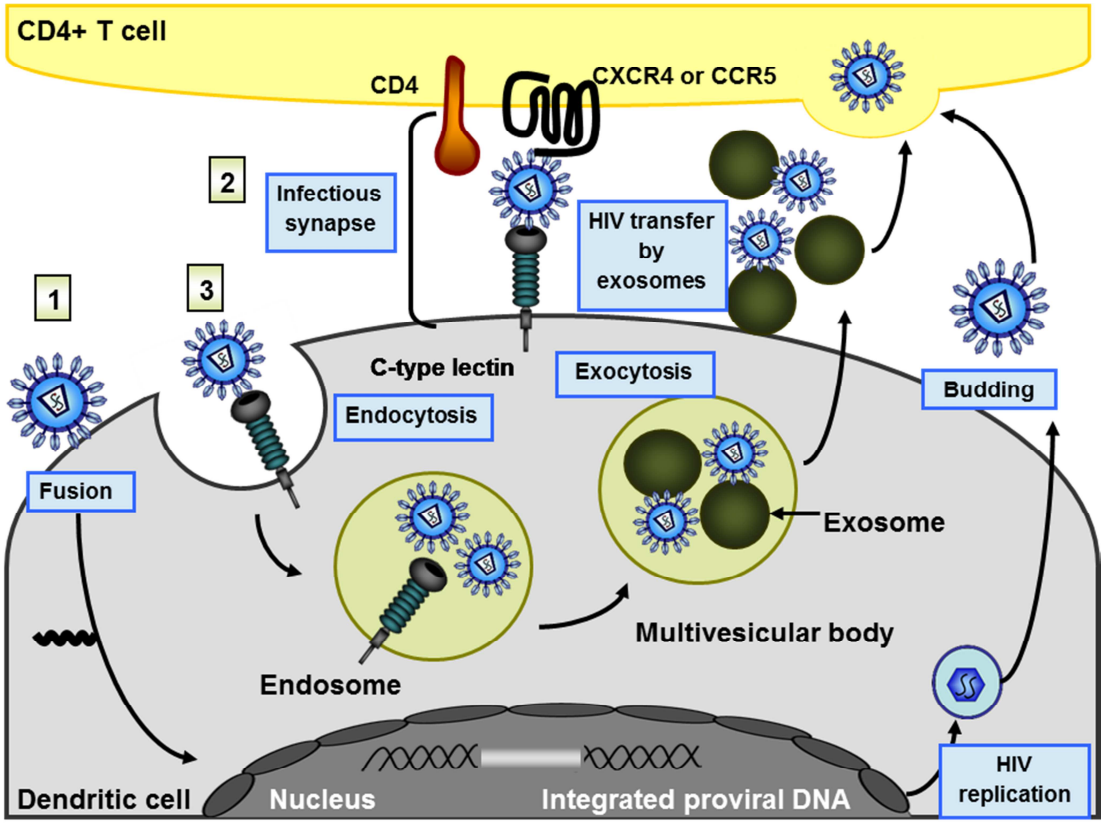

Figure 15. Mechanisms of DC-mediated HIV transmission. 1) HIV infection resulting from *cis*-infection of DCs, production *de novo* of viral particles and transmission of HIV to $CD4^+$ T cells; 2) HIV transmission through infectious synapse between DCs and $CD4^+$ T cell; 3) HIV transmission by an exocytic pathway. Modified from Wu *et al.* (Wu and KewalRamani, 2006).

HIV transmission might also occur through HIV infection in *cis*. It has been reported that immature DCs can retain infectious virus up to 6 days after exposure to HIV

(Trumpfheller et al., 2003). However, it was also suggested that most of incoming viruses are degraded in DCs within 24 hours (Turville et al., 2004). Therefore, after 24 hours, the virus that is transmitted is thought to be the *de novo* produced virus. The first phase (within 24 hours of exposure to HIV) involves trafficking of captured viral particles from the endolysosomal pathway to the DC-T-cell infectious synapse. In the second phase (24-72 hours after exposure to HIV) the virus is replicating *de novo* in DCs providing production of progeny virus able to infect $CD4^+$ T cells (Wu and KewalRamani, 2006). HIV-infected DCs function as viral reservoirs during their migration to the lymphoid organs, helping in spreading of the viral infection. In addition, DC-bound viruses can be internalized and processed for MHC presentation. DC-SIGN engagement triggers also signal transduction that modulates TLR-dependent cytokine production (Fig. 16) (Tsegaye and Pohlmann, 2010).

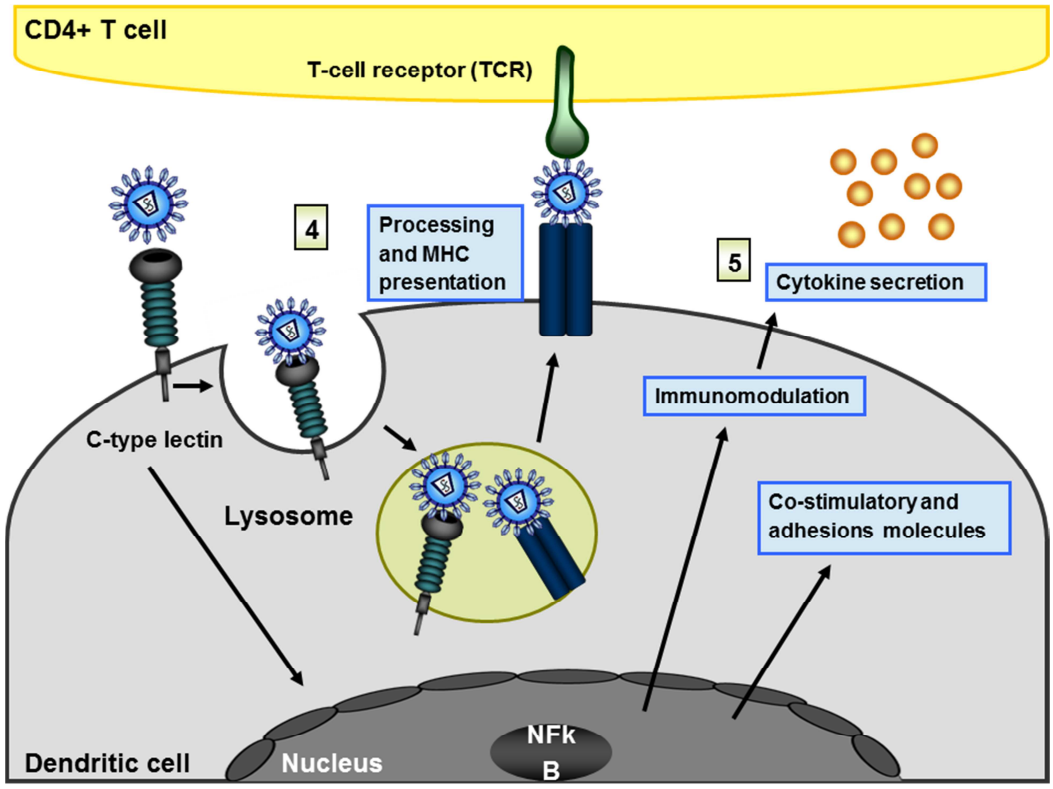

Figure 16. Mechanisms of DC-mediated HIV transmission. 4) DC-SIGN-bound viruses are internalized, processed and presented by MHC molecules; 5) Binding of pathogens to DC-SIGN involve signal transduction and production of cytokines to attract other cells of immune response. Modified from Wu *et al.* and Tsegay *et al.* (Tsegaye and Pohlmann, 2010; Wu and KewalRamani, 2006).

It has been shown that some genetic polymorphisms within DC-SIGN gene might be associated with promoting of HIV-1 capture and transmission to T cells. The study of Martin *et al.* identified single-nucleotide polymorphisms (SNP) in the DC-SIGN promoter that was linked to higher susceptibility to parental infection. Patients with the promoter variant p-336C were more vulnerable than individuals with p-336T DC-SIGN variant for parental acquisition of HIV-1 infection but not for a mucosal route (Martin et al., 2004). Subsequently, Boily-Larouche *et al*. have studied the association between the major haplotypes of DC-SIGN and the risk of mother-to-child transmission (MTCT) among Zimbabwe infants. They found out that the infants carrying H4 and H6 haplotypes of DC-SIGN were under increased risk of intra-uterine HIV-1 infection while the haplotype 2 was described to be related less likely to intra-uterine transmission. Further study of SNP revealed that several variants of DC-SIGN promoter (p-336C and p-201A) and exon 4 (198Q and 242V) have been associated with increased risk of HIV-1 infection during pregnancy (Boily-Larouche et al., 2012). The variant of DC-SIGN promoter p-336C was identified in both study as a polymorphism associated with increased risk for parental HIV-1 acquisition.

Given that unprotected sexual intercourse is the most common global mode of HIV-1 transmission (Royce, 1997), many different interventions have been proposed for slowing the spread of HIV-1 infection worldwide. It has been shown that male circumcision reduces the risk of HIV-1 infection. Randomized, controlled trials in Africa have demonstrated that circumcision could reduce the acquisition of HIV-1 in men by ~60% (Auvert et al., 2005; Bailey et al., 2007; Gray et al., 2007). During sexual intercourse, the foreskin in uncircumcised men is often retracted over the shaft exposing thus the inner mucosa to genital secretions of sexual partner, which very often contain high levels of HIV particles (Butler et al., 2008). It has been shown that favorable moistened environment is generated in the subpreputial penile in uncircumcised med after sexual intercourse while in circumcised men this environment is quite dry. Moreover, the foreskin was demonstrated to be vulnerable to tissue damage and inflammatory conditions during intercourse (Gray et al., 2007). Hirbod *et al.* studied the localization of different HIV-1 target cells and the expression of C-type lectins in the foreskin tissue in a group

of young Kenyan men at high risk of HIV exposure. This study revealed the presence of intraepithelial Langerhans cells, $CD11c^+$ mononuclear phagocytes and DCs as well as the expression of Langerin, DC-SIGN and MR on these cells. It was suggested that male circumcision decrease the number of HIV-1 target cells with proper virus receptors and results therefore in better resistance to HIV-1 particles penetration (Hirbod et al., 2010).

The development of HIV-1 preventive strategies at mucosal site as a first line of contact with pathogens is the prior subject of interest. The attempts to develop an efficient vaccine against chronic viruses have failed so far, mainly due to the immunological escape mechanisms of these viruses or the lack of conserved epitopes of viruses involved in acute infections (Letvin, 2006). Along the time of HIV epidemic a broad range of antiviral drugs become available for the treatment of virus infections. However, the appearance of long-term side effects, emergence of viral resistance under drug pressure very often weakens therapy, making drugs useless and harmful in the long run (Balzarini, 2007). Condom use and behavioral interventions have been only partially successful in slowing the spread of HIV-1 infection worldwide. There is an urgent need for additional interventions to prevent new infections, such as the development of female-controlled topical formulations of anti HIV-1 compounds that could be used as a gel, cream, suppository before sexual intercourse (Elias and Coggins, 1996). Ideally, topical microbicides should be inexpensive, easy to use, colorless, stable under low pH conditions, tasteless, non-irritating to genital mucosal tissue, stable at higher temperatures, compatible with latex, acceptable to all sexual partners. The main role however should be to inactivate a variety of sexually transmitted microbes within genital secretions and/or block relevant HIV-1 receptors on initial target cells (Kawamura et al., 2000).

CHAPTER 1:

A model of viral infection mediated by DC-SIGN

II. CHAPTER 1:

A model of viral infection mediated by DC-SIGN

1. OBJECTIVES

Standardize and evaluate a cellular model of viral infection mediated by DC-SIGN: (a) consistency of the infection model using different cell lines expressing the DC-SIGN receptor, (b) standardization of the DC-SIGN expression level and the infective titre of recombinant retroviruses for infection assays and (c) establish the proper conditions for the DC-SIGN mediated *cis*-infection and *trans*-infection assays.

2. MATERIAL AND METHODS

2. 1. Plasmids

pNL4-3.Luc.R-E- is an envelope-defective HIV-1 genome that contains firefly luciferase gene inserted into the pNL4-3 *nef* gene as a reporter gene. pNL4-3.Luc.R-E- consists of two frameshifts (5′ Env and Vpr aa 26), which render this clone Env^- and Vpr^-. pNL4-3.Luc.R-E- is competent for a single round of replication and it requires co-transfection with envelope expression vector to produce infectious particles (Connor et al., 1995). pNL4-3.Luc.R-E contains: *gag* (790-2292), *pol* (2085-5096), *rev* (5969-8643), *tat* (5830-8414), *env* (6221-8785), *vpu* (6061-6306), *vif* (5041-5619), *nef/luc* (8787-9407), *vpr* (5559-5849), 5´LTR (1-634), 3´LTR (9076-9709).

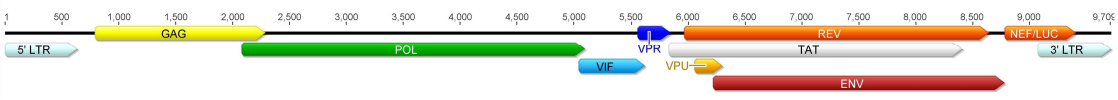

p1012-Ebola GP is a vector containing the full sequence of Ebola envelope glycoprotein strain Zaire *Mayinga* or Ebola strain Reston under the expression of CMV promoter. p1012-Ebola GP contains following genes: human CMV immediate-early promoter (1-675), Ebola virus glycoprotein (1074-3479), polyadenylation signal (3561-3756), kanamycin resistance gene (5083-5885).

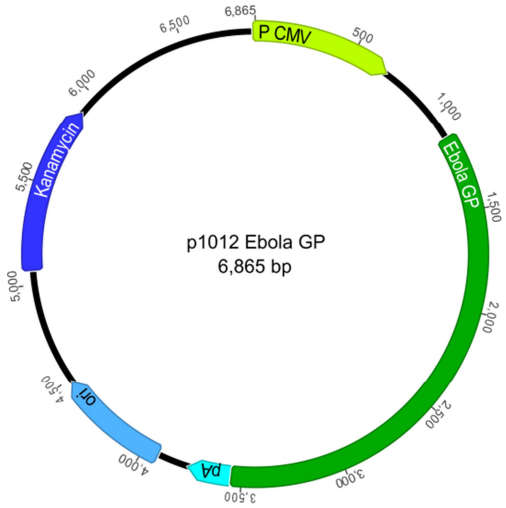

pcDNA3.1/V5-His TOPO TA-HIV-1 env is an expression plasmid containing: human CMV immediate-early promoter (209-863), T7 promoter/priming binding site (863-882), MCS (902-1019), TOPO cloning site (953-954), HIV-1 envelope gene (1020-3551), V5 epitope (3552-3593), polyhistidine tag (3603-3620), BGH reverse priming site (3660-3643), BGH polyadenylation signal (3642-3856), f1 origin of replication (3919-4332), SV40 promoter and origin (4397-4722), neomycin resistance gene (4758-5552), SV40 polyadenylation signal (5571-5809), pUC origin (6914-6241), ampicillin resistance gene (7059-7919).

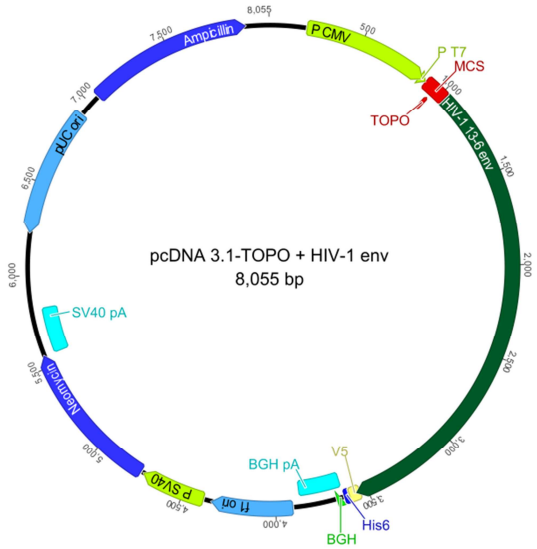

pNGLV-3-VSV contains the gene of complete glycoprotein of Vesicular Stomatitis virus (VSV-G) envelope under the expression of CMV promoter. pNGLV-3-VSV includes: human CMV immediate-early promoter (1-675), intron A (676-1067), VSV glycoprotein (1071-2606), rabbit β-globin polyadenylation site (2691-2886), *ori* replication origin (3068-3603), kanamycin resistance (4213-5015).

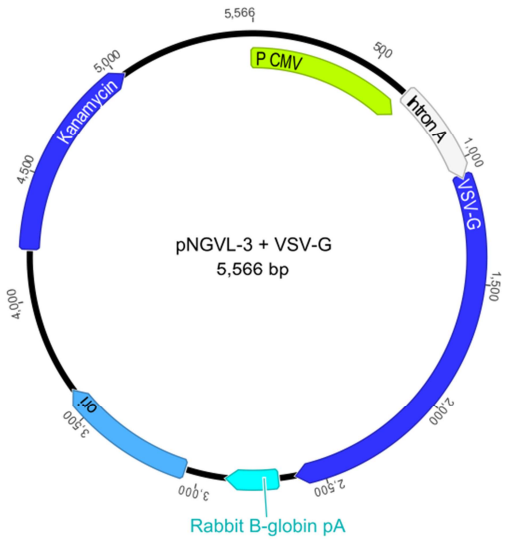

2. 2. Cell lines used in this study

Human Embryonic Kidney 293 cell line (HEK 293T) is derived from human embryonic kidney cells. HEK was generated in the early 70s by the transformation of human embryonic kidney cultures with adenovirus 5 DNA in the laboratory of Alex van der Eb in Leiden (The Netherlands). The human embryonic kidney cells were obtained from a healthy aborted fetus and transformed subsequently with adenovirus by Frank Graham (Graham et al., 1977). E1A adenovirus gene is expressed in these cells and participates in trans-activation of some viral promoters, allowing these cells to produce very high levels of protein. The widespread use of this cell line is due to its extreme transfectability by various techniques, including calcium phosphate method, achieving efficiencies approaching 100%. An important variant of this cell line is the 293T cell line, which contains additionally the SV40 Large T-antigen that allows for episomal replication of transfected plasmids containing the SV40 origin of replication. This enables amplification of transfected plasmids and extended temporal expression of the desired gene products.

Human cervical epithelial carcinoma cell line (HeLa) was the first human cell line, which functioned successfully *in vitro*, providing therefore great achievement for scientific research (Rahbari et al., 2009). HeLa cells were derived from cervical cancer cells taken from Henrietta Lacks shortly before she died of her cancer in 1951 and propagated by George Otto Gey (Watts, 2010). At the beginning the cells were donated by Gey to any scientists that requested them and later they were commercialized. HeLa cells contain human papillomavirus 18 (HPV18) that was integrated to its genome by horizontal gene transfer. HeLa cell line is widely used in cancer research, AIDS research, gene mapping, studies of the effects of radiation and toxic substances (Silberman, 2010).

Human astroglioma cell line (U87) is an epithelial cell line obtained from human astroglioma cells (Ponten and Macintyre, 1968).

U87-CD4-CXCR4 – Parental U87 cells were stably transduced with the MV7neo-T4 retroviral vector and selected for the resistance to G418 antibiotic. Cells were subsequently transduced with pBABE-puro-CXCR4 and selected for the resistance to puromycin antibiotic. Human CD4 and CXCR4 expression is directed by the MV7 vector and pBABE vector, both driven by MLV LTR promoter. U87-CD4-CXCR4 is suitable for the infection experiments with HIV and SIV pseudotyped viruses (Bjorndal et al., 1997).

U87-CD4-CCR5 - Parental U87 cells were stably transduced with the MV7neo-T4 retroviral vector and selected for the resistance to G418 antibiotic. Cells were subsequently transduced with pBABE-puro-CCR5 and selected for the resistance to puromycin antibiotic. Human CD4 and CCR5 expression is directed by the MV7 vector and pBABE vector, both driven by MLV LTR promoter. U87-CD4-CCR5 is suitable for the infection experiments with HIV and SIV pseudotyped viruses (Bjorndal et al., 1997).

Human T cell leukemia cell line (Jurkat) is immortalized line of T lymphocytes, which was established in the late 1970s from the peripheral blood of a 14 year old boy suffering from T cell leukemia (Schneider et al., 1977). Jurkat cells express CD4 on its surface and after induction might secrete interferon-γ. Jurkat cell line is widely used in the studies of acute T cell leukemia, T cell signalling, expression of various chemokine receptors that permit virus cell entry, determination of differential susceptibility of cancer to drugs and radiation (Weiss et al., 1984).

Jurkat DC-SIGN-GFP is a "home-prepared" cell line that was transduced with recombinant retrovirus construction (pNGVL-VSV-G – encoding the sequence of VSV envelope, pNGVL-MLV-gag-pol – codifying the proteins of capsid and matrix of MLV, LZR-DC-SIGN-CITE-GFP – encoding the sequence of DC-SIGN) to express protein DC-SIGN on its surface. The expression of DC-SIGN was quantified by direct measure of fluorescence by FACS.

Human B lymphocyte Burkitt´s lymphoma cell line (Raji) is the first continuous human cell line from hematopoietic origin that is categorized as lymphoblast-like (Karpova et al., 2005). Raji cells were established by R. J. V. Pulvertaft in 1963 from a Burkitt´s lymphoma of the left maxilla of an 11-year-old black male (Pulvertaft, 1964). This cell line is EBNA positive and produces unusual strain of Epstein-Barr virus, which can transform blood lymphocytes and induce early antigens in Raji cells. The Raji cells are partially resistant to poliovirus and Vesicular Stomatitis virus. Raji cells are widely used for: studying hematopoietic malignancies, transfection or detection of immune complex (Epstein and Barr, 1965; Ohsugi et al., 1980).

Raji cell line is Epstein Barr Virus–positive Burkitt´s lymphoma line obtained from the ATCC (Wu et al., 2004).

Raji DC-SIGN$^+$ cell line is derived from Raji cells, an EBV-positive Burkitt´s lymphoma cells. Parental Raji cells were transduced with the MLV vector MX-DC-SIGN and sorted by FACS as a population for high levels of DC-SIGN ex-

pression. The MX-DC-SIGN vector encodes no drug-selectable marker gene (Wu et al., 2004).

2. 3. Production of recombinant viruses

Recombinant viruses were produced in 293 T cells. The viral construction was pseudotyped with virus envelope (Ebola virus envelope glycoprotein, HIV-1 envelope glycoprotein, VSV envelope glycoprotein) and expressed luciferase as a reporter of the infection (Yang et al., 1999). The recombinant pseudoviruses are composed of expression plasmid with the sequence of desired pathogen envelope and of pNL4-3.LUC.R-E- (obtained through the NIH AIDS Research and Reference Reagent Program, Division of AIDS, NIAID, NIH: pNL4-3.Luc.R–E– from Dr. Nathaniel Landau) (Connor et al., 1995).

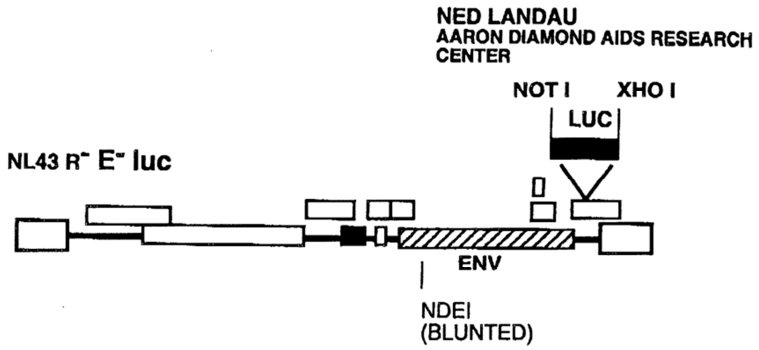

Fiure 17. pNL4-3.LUC.R-E- vector structure (NIH AIDS Research and Reference Reagent Program, Division of AIDS, NIAID).

pNL4-3.LUC.R-E- (Fig. 17) is a backbone plasmid containing whole HIV-1 genome with two frameshifts at 5'envelope gene and at aa26 of *vpr* gene (both mutations render this clone *env-* and *vpr-).* Additionally, the firefly luciferase gene is inserted into pNL4.3 *nef* gene. For the production of viral particles it is necessary to co-transfect with an *env*$^{+}$ expression plasmid (driven by intermediate-early CMV promoter). Pseudopar-

ticles are able to infect but due to the absence of complete genome are unable to produce infectious progeny. Produced pseudoparticles are capable of 1 cycle of infection and 1 round of viral genes expression but unable to propagate a spreading infection. Due to those mutations, the HIV genome cannot be retrotranscribed in subsequent cycles of replication.

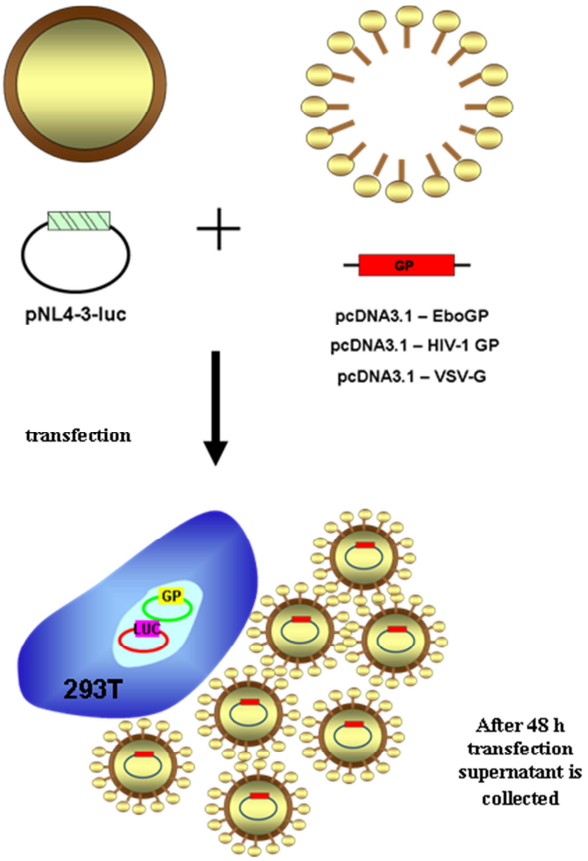

Figure 18. Production of recombinant viruses.

One day (18-24 h) before transfection, 5 x 10^6 293T were seeded onto 10 cm plates. Cells were cultured in DMEM medium supplemented with 10% heat-inactivated FBS, 25 mg Gentamycin, 2 mM L-glutamine. Few minutes before transfection, the medium on transfection plates was changed to 9 ml DMEM and chloroquine was added to 25 µM final concentration. Transfection reaction with all reagents at room temperature (RT) was prepared in 15 ml tubes: 183 µl of 2M $CaCl_2$, virus envelope (500 ng of Ebola virus

envelope, 9 µg of HIV-1 envelope, 6 µg of VSV envelope), 21 µg of pNL4-3 luc and 1350 µl of H_2O. Next, 1.5 ml of 2xHBS (Hepes Buffer Saline) pH 7.00 was added quickly to the tubes and bubbled for 30 sec. HBS/DNA solution was dropped gently onto medium. After 8 h of incubation at 37º C with 5% CO_2, medium on transfection plates was changed to 10 ml DMEM and once again one day after transfection to 7 ml DMEM. Transfection supernatants were harvested after 48 h, centrifuged at 1200 rpm for 10 min at RT to remove cell debris, and stored frozen at -80° C (Fig. 18).

2. 4. Infection in *cis* assay with Ebola GP-pseudotyped retroviruses

Infection in *cis* was performed on Jurkat cells expressing receptor DC-SIGN (Fig. 19). Since Ebola virus does not infect T-lymphocytes, its entry to Jurkat cells is absolutely dependent on the interaction with DC-SIGN. Jurkat DC-SIGN$^+$ (2.5–5 x 10^5) were challenged with 5000-10000 TCID of recombinant viruses. After 48 h of incubation, cells were washed twice with PBS and lysed with 100 µl of 1x Lysis Buffer (Promega) for luciferase assay. Control experiment of infection in *cis* was performed with VSV-G (DC-SIGN independent) pseudoviruses in the same conditions.

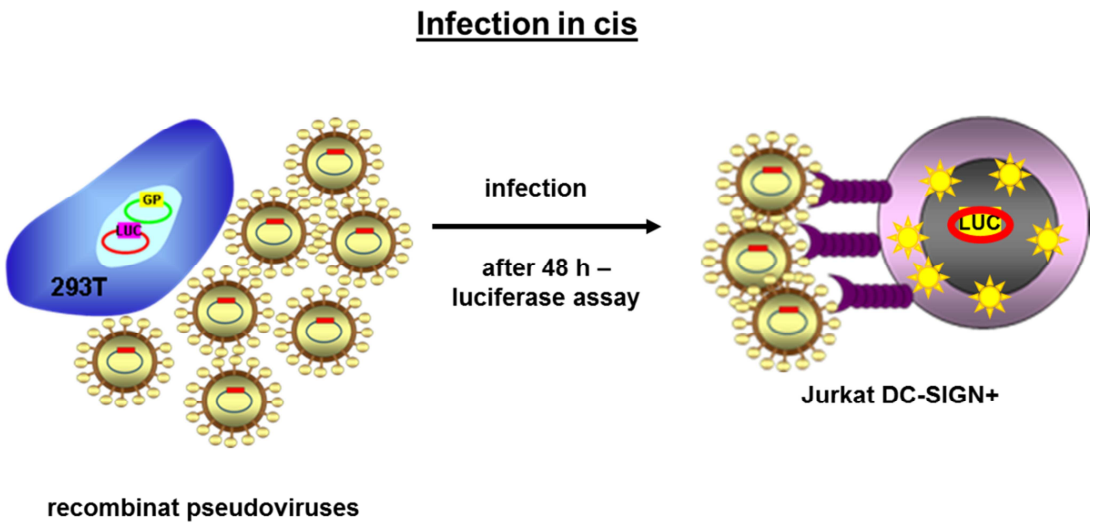

Figure 19. Infection in *cis* with recombinant Ebola GP-pseudotyped retroviruses in cellular model Jurkat DC-SIGN$^+$.

2. 5. Infection in *trans* assay with Ebola GP-pseudotyped retroviruses

Jurkat DC-SIGN$^+$ cells (2.5-5 x 10^5) were challenged with 5000-10000 TCID of recombinant viruses and incubated for 2 h at RT with rotation. After 2 h, cells were centrifuged at 1000 rpm for 5 min and washed twice with 1 ml of PBS supplemented with 0.5% BSA and 1mM $CaCl_2$. Jurkat DC-SIGN$^+$ were resuspended in 500 µl of RPMI medium and co-cultivated with adherent HeLa cells (10^5 cells/ well) on 24-well plate (Fig. 20). After 48 h, the supernatant was removed and monolayer of HeLa was washed twice with 1 ml of PBS and lysed with 100 µl of 1x Lysis Buffer (Promega) for luciferase assay. As a control, *trans*-infection experiment with DC-SIGN independent VSV-G pseudoviruses was performed.

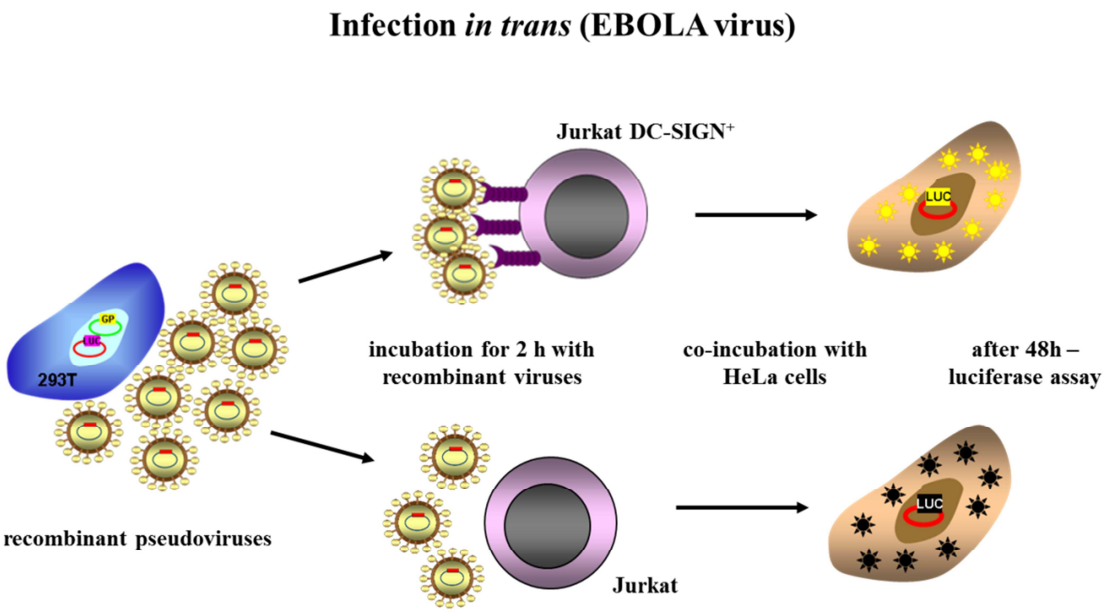

Figure 20. Infection in *trans* with recombinant Ebola GP-pseudotyped retroviruses. Jurkat DC-SIGN$^+$/ Jurkat are challenged with recombinant viruses and further co-cultivated with susceptible HeLa cells.

2. 6. Infection in *trans* assay with HIV-1 GP-pseudotyped retroviruses

Infection in *trans* was performed on Jurkat DC-SIGN$^+$ or Raji DC-SIGN$^+$ (5 x 10^5), which can capture and transmit HIV-1 virus to susceptible cells. Cells were pulsing with HIV-1 pseudoviruses for 3 h at 37º C. After 3 h, cells were centrifuged at 1000 rpm for 5 min and washed twice with 1 ml of PBS (supplemented with 0.5% BSA and 1mM $CaCl_2$) to remove unspecifically bound viruses. Next, Jurkat/ Raji DC-SIGN$^+$ were co-cultivated with susceptible U87-R5/X4 cells (Fig. 21). After 48 h, the supernatant was removed and monolayer of U87-R5/X4 was washed twice with 1 ml of PBS and lysed with 100 µl of 1x Lysis Buffer (Promega) for luciferase assay.

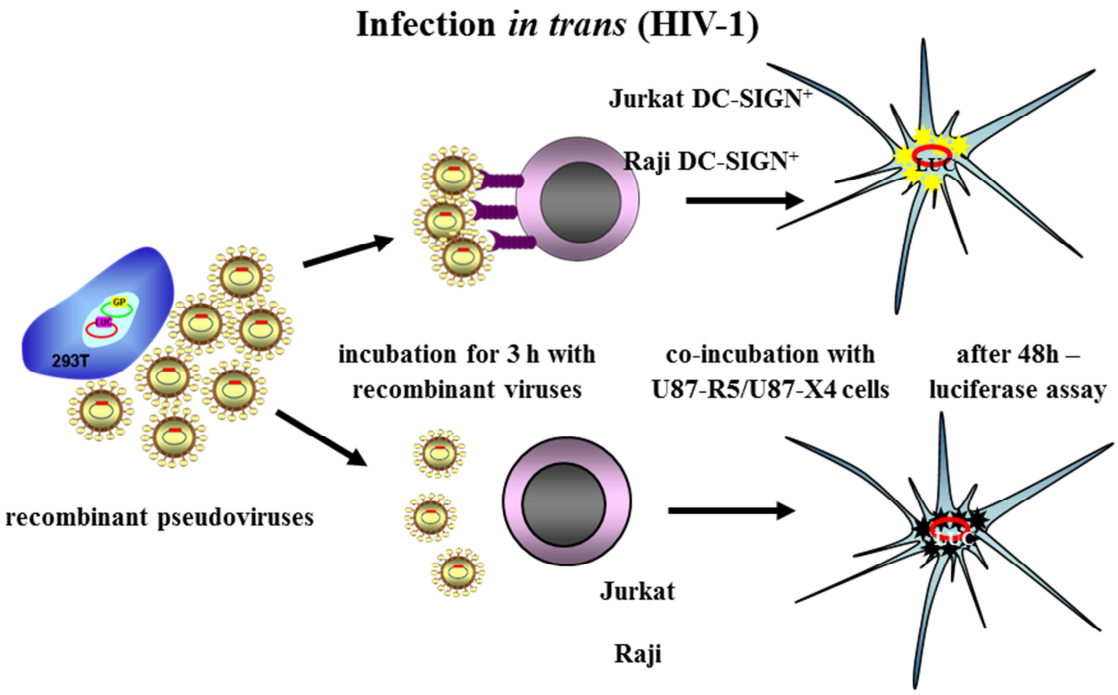

Figure 21. Infection in *trans with r*ecombinant HIV-1 GP-pseudotyped retroviruses, which are captured by Raji DC-SIGN$^+$/Jurkat DC-SIGN$^+$ and further transmitted to U87-CD4-CCR5/CXCR4 cells.

3. RESULTS

3. 1. DC-SIGN model validation

3. 1. 1. Impact of DC-SIGN expression level on the *trans*-infection ratio

The impact of the DC-SIGN expression level on the *trans*-infection ratio was verified in the *trans*-infection experiment, in which cells expressing different level of DC-SIGN were challenged with 10000 TCID of recombinant viruses pseudotyped with HIV-1 envelope 13-6. The experiment was performed in triplicate using 100%, 75%, 50%, 25%, 10%, 5%, 1% and 0% Jurkat DC-SIGN$^+$ cells. The results obtained in this experiment clearly showed that he cellular infection model based on DC-SIGN is very straightforward and the infection depends exclusively on the presence of DC-SIGN on the cell surface. This infection model showed that *trans*-infection ratio was doses-dependent on the expression level of DC-SIGN (Fig. 22).

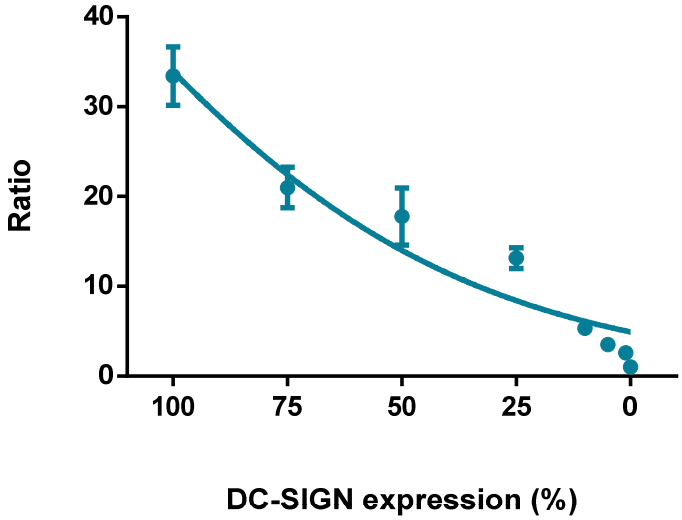

Figure 22. *Trans*-infection experiment with HIV-1 GP-pseudotyped retroviruses in the cellular model Jurkat DC-SIGN$^+$/ U87-CD4-CCR5 showing the dependency of *trans*-infection phenomenon on DC-SIGN expression level. The symbols on the graph represent mean with SEM error bars of 3 independent experiments.

The ratio obtained in case of all tested lower DC-SIGN expression levels was statistically significant as compared to the cellular population that expressed 100% of DC-SIGN (75% p=0.0352, 50% p=0.0266, 25% p=0.0042, 10% p=0.0010, 5% p=0.0009, 1% p=0.0007) (Fig. 22). Given that the infection in the cellular model based on Jurkat DC-SIGN$^+$ is not dependent on any other variable, it can be useful in the studies of the entry as well as the entry inhibition by antiviral strategies targeting this receptor.

3. 1. 2. Impact of virus titer on *trans*-infection studies

The impact of the virus titer on the *trans*-infection ratio was verified in the experiment of *trans*-infection, where cells were challenged with different titers (range: 100–25000 TCID) of recombinant retroviruses pseudotyped with 6 HIV-1 envelopes: 8-13, 13-6, 15-7, 20-1, 37-2 and 40-2. In case of most of the envelopes used in the experiment, the notable variation in the ratio was seen when using titers below 5000 TCID. The recombinant virus titers above 5000 TCID did not show any statistically significant influence on the *trans*-infection ratio thus 5000-10000 TCID was chosen as an optimal for further experiments (Fig. 23).

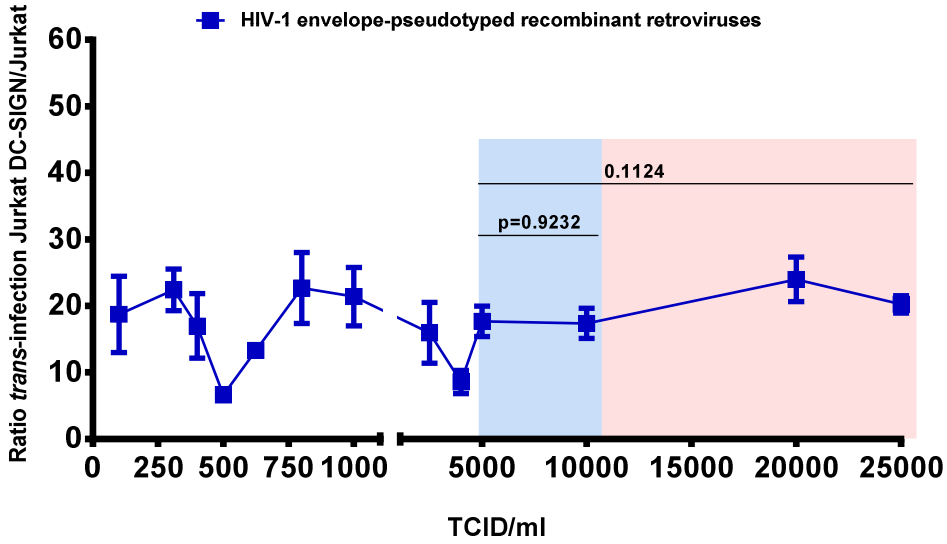

Figure 23. *Trans*-infection experiment with 6 HIV-1 GP-pseudotyped viruses in the cellular model Jurkat DC-SIGN$^+$/U87-CD4-CCR5. The *trans*-infection ratio was defined for the range of virus titers: 100-25000 TCID. The symbols on the graph represent mean with SEM error bars of 3-12 independent experiments.

3. 2. Model of the infection in *cis*

The infection in *cis* model is based on cells expressing receptor DC-SIGN on its surface. The experiment of *cis*-infection was performed by challenging control cells and cells expressing DC-SIGN with recombinant Ebola retroviruses. This infection system is very efficient since infection *in vitro* of cells, distinguished only in the expression of DC-SIGN, by Ebola virus is absolutely dependent on the presence of receptor DC-SIGN on cell surface (Fig. 24). Cells, which do not express DC-SIGN, were used as a negative control of infectivity. VSV-G pseudotyped retrovirus was used as a control virus for infection experiment based on the interaction with DC-SIGN. VSV is an enveloped, non-segmented, negative-strand RNA virus that belongs to the family of Rhabdoviruses (Matlin et al., 1982). Although VSV express 2 highly N-glycosylated structures on its surface, it fails to interact with DC-SIGN, what indicates some specificity in DC-SIGN binding (Kwon et al., 2002).

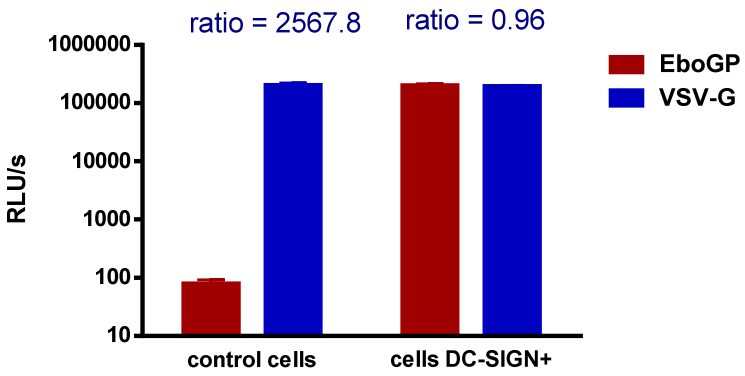

Figure 24. *Cis*-infection with the recombinant Ebola GP (red) and VSV-G (blue) pseudotyped viruses in the cellular model Jurkat DC-SIGN$^+$ cells/ Jurkat control cells. The bars represent mean with SEM error bars of 3 independent experiments.

3. 3. Model of the infection in *trans*

During *trans*-infection process more complex events take place, such as internalization and presentation of the viral particles to susceptible cells. The *trans*-infection experi-

ment was performed on DC-SIGN$^+$ cells, which bind and transfer viral particles. Cells expressing DC-SIGN$^+$ were incubated with recombinant pseudoviruses for 2 h, washed and co-cultivated with adherent susceptible cells. The *trans*-infection assay was performed by, either: 1) challenging DC-SIGN$^+$ cells with recombinant Ebola retroviruses and further infection of HeLa cells, or 2) challenging DC-SIGN$^+$ cells with recombinant HIV-1 retroviruses and infection of U87-CD4-CCR5/ U87-CD4-CXCR4 cells. Both recombinant retroviruses use DC-SIGN receptor for capturing and transferring its particles to susceptible cells expressing all receptors necessary for efficient infection. Cells that do not express DC-SIGN were used as a negative control of transmitted *trans*-infection. VSV-G-pseudotyped recombinant retroviruses are DC-SIGN-independent and can infect control cells and DC-SIGN$^+$ cells (Fig. 25).

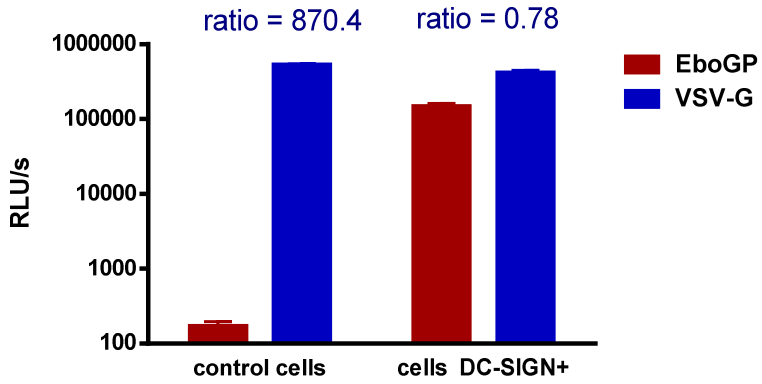

Figure 25. *Trans*- infection with the recombinant Ebola GP (red) and VSV-G (blue) pseudotyped viruses, which are captured by Jurkat DC-SIGN$^+$ cells or Jurkat control cells for further transmission to susceptible HeLa cells. The bars represent mean with SEM error bars of 3 independent experiments.

3. 4. Comparison of two infection models based on Raji DC-SIGN$^+$/Raji cells and Jurkat DC-SIGN$^+$/Jurkat cells

The *trans*-infection process was studied in two different cellular models to verify the efficiency of DC-SIGN usage by recombinant viruses when using Jurkat DC-SIGN$^+$ and Raji DC-SIGN$^+$ cells in comparison to control cells. The assay was performed by using HIV-1 recombinant retroviruses pseudotyped with 4 different HIV-1 envelopes (Fig.

26). The level of DC-SIGN usage by both cell lines showed similar tendency when using certain HIV-1 envelopes. The level of DC-SIGN-mediated infection by Raji DC-SIGN$^+$ was generally slightly higher than the level mediated by Jurkat DC-SIGN$^+$ cells. Nevertheless, both cellular models clearly showed the importance of DC-SIGN receptor in capturing and transmitting viral particles to susceptible cells as compared with control cells that did not express DC-SIGN on its surface.

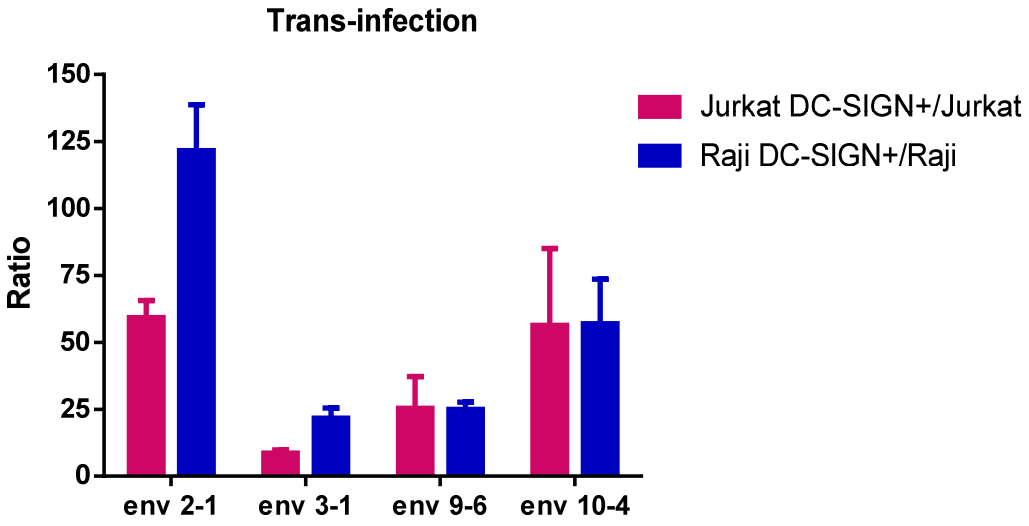

Figure 26. *Trans*-infection experiment using two cellular models: 1) Jurkat DC-SIGN$^+$/Jurkat cells (pink) and 2) Raji DC-SIGN$^+$/Raji cells (blue) for transmission to U87-CD4-CCR5/CXCR4 cells of recombinant viruses pseudotyped with 4 HIV-1 envelopes: 2-1, 3-1, 9-6, 10-4. The bars represent mean with SEM error bars of 3-7 independent experiments.

4. DISCUSSION

It has been previously shown that DC-SIGN *in vitro* plays multiple functions in different aspects of immune system as well as it can mediate efficient virus infection, both in *cis* and in *trans* of cells expressing appropriate entry receptors (Alvarez et al., 2002; Geijtenbeek et al., 2000b; Lee et al., 2001). The expression of DC-SIGN receptor might enable the direct infection by some viruses, such as Ebola, of cells previously non-permissive for those viruses.

The DC-SIGN *trans*-infection model was validated by studying the impact of DC-SIGN expression level and the titer of recombinant pseudoviruses. It was clearly shown that the *trans*-infection ratio in Jurkat DC-SIGN$^+$/Jurkat cellular model depends exclusively on the presence of DC-SIGN on the cell surface (Fig. 22). Since it is the only variable having impact on the infection in this cellular system, it can be considered as a useful model to study viral entry and to test antiviral strategies targeting DC-SIGN. The impact of the virus titer on the *trans*-infection ratio was also verified and revealed no significant differences between 5000 and higher TCID in case of most HIV-1 envelopes used in the experiment. When using low virus titers, the notable variations in the *trans*-infection ratio were observed therefore the titer 5000-10000 TCID was chosen as an optimal for further infection experiments (Fig. 23).

The model of infection in *cis* based on Jurkat DC-SIGN$^+$/Jurkat cells clearly showed dependence of the Ebola virus cell entry on DC-SIGN presence (ratio 2567.8) (Fig. 24). The *cis*-infection of both cell lines by DC-SIGN independent VSV-G-pseudotyped retroviruses was at very similar level (ratio 0.96) (Fig. 24). The model of *trans*-infection confirmed the results obtained in the *cis*-infection experiment, revealing higher transmission of Ebola infection to susceptible cells by Jurkat DC-SIGN$^+$ as compared with negative cells (ratio 870.4) (Fig. 25). The *trans*-infection obtained with VSV-G-pseudotyped viruses was comparable between both cell lines (Fig. 25). The *trans*-infection model was also verified in the cellular model of Raji DC-SIGN$^+$ and Raji control cells. Raji is a B-cell line that has been extensively used in DC-SIGN *trans*-infection experiments (Chung et al., 2010; Geijtenbeek et al., 2000b; Trumpfheller et al., 2003). The results obtained in the experiment of *trans*-infection with 4 recombinant retroviruses pseudotyped with 4 different HIV-1 envelopes supported the consistency of the presented model showing the high usage of DC-SIGN receptor by viral particles in the transmission of the infection (Fig. 26).

5. CONCLUSIONS

The infection model based on cell lines expressing DC-SIGN is a consistent platform to study direct viral entry (Ebola virus) and the *trans*-infection phenomenon (Ebola virus and HIV) since the infection events depend almost exclusively on DC-SIGN-viral interaction.

CHAPTER 2:

A screening platform of antiviral strategies targeting DC-SIGN

III. CHAPTER 2:

A screening platform of antiviral strategies targeting DC-SIGN

1. OBJECTIVES

Study the utility of the DC-SIGN infection model as a screening platform of antiviral strategies targeting DC-SIGN. Analyze the potential antiviral effect of synthetic designed compounds: glycodendritic structures, tetravalent dendrons, dendrimers-based compounds, glycofullerenes and glycodendrinanoparticles.

2. MATERIAL AND METHODS

2. 1. Plasmids: p1012-Ebola GP, pNGLV-3-VSV, pNL4-3.Luc.R-E- (See Chaper I. 2. 1.)

2. 2. Glycodendritic structures

Glycodendritic structures were kindly provided by Dr. Javier Rojo from Glycosystems Laboratory, Instituto de Investigaciones Químicas (CSIC; Seville, Spain). Compound RR114 and compound RR115 are two new glycodendritic structures based on carbohydrate moiety, a pseudo-1,2-mannobioside, presenting high enzymatic stability and good affinity for DC-SIGN (Reina et al., 2007). This ligand was conjugated to the scaffolds based on the pentaerythritol and *bis*-pentaerythritol presenting 4 and 6 terminal alkyne groups. The attachment of the ligands to the multivalent scaffold was performed by the coupling reaction, which results in the synthesis of compound RR114 containing 4 copies of pseudo-1,2-mannobiosides (Fig. 27B) and compound RR115 containing 6 copies of pseudo-1,2-mannobiosides (Fig. 27A).

A. **B.**

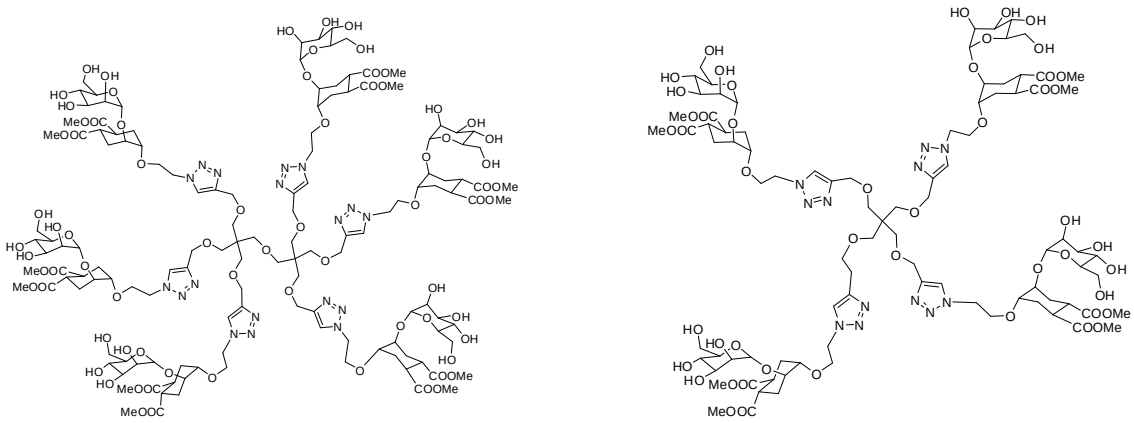

Figure 27. **A.** Structure of compound RR115. **B.** Structure of compound RR114.

2. 3. Tetravalent dendrons

Tetravalent dendrons were kindly provided by Dr. Anna Bernardi from Università degli Studi di Milano (Milan, Italy). Compound 12 and compound 14 are tetravalent dendrons (compound 12 is tetravalent pseudo-diMannose, compound 14 is tetravalent pseudo-triMannose) (Fig. 28 and Fig. 29). These tetravalent compounds are based on a scaffold composed of 2, 2′-bis (hydroxymethyl) propionic acid that was used for presentation of multiple copies of selected ligands (Fig. 29). The ligands in the production of compounds 12 and 14 (Fig. 28) were attached by applying chemistry presented in the figure 29.

A. **B.**

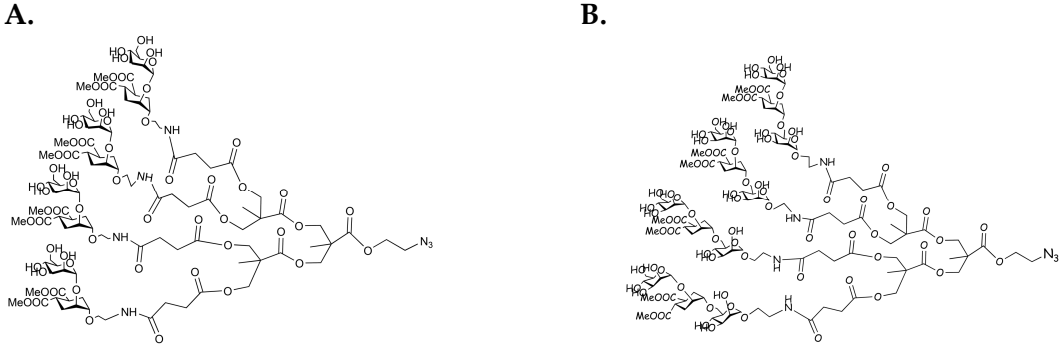

Figure 28. Ligands presented on tetravalent dendrons: **A.** compound 12 and **B.** compound 14.

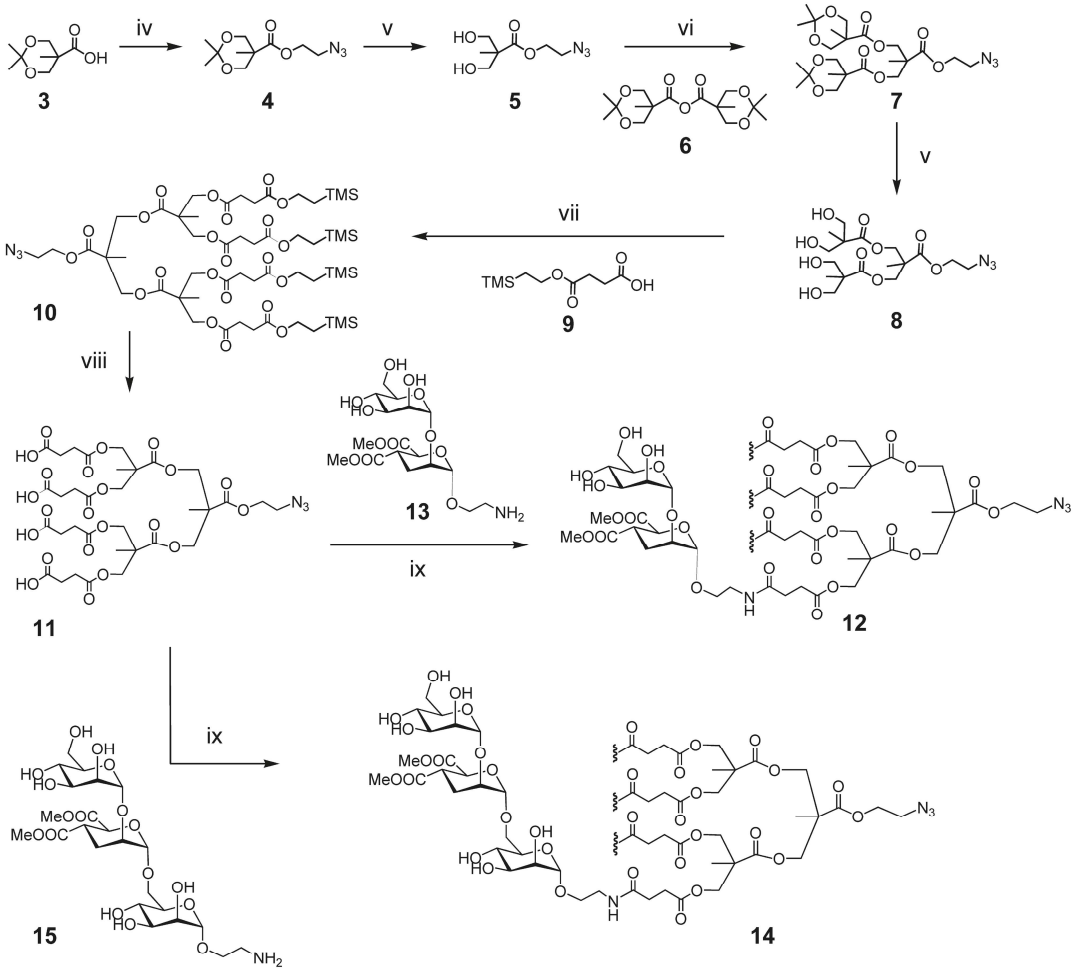

Figure 29. Synthesis of compounds: 12 and 14.

2. 4. Dendrimer-based compounds

Dendrimer-based compounds were kindly provided by Dr. Anna Bernardi from Università degli Studi di Milano (Milan, Italy). Compound G3(pseudodi)$_{32}$ and compound G3(pseudotri)$_{32}$ are 3rd Generation Boltorn type (Fig. 30) dendrimer-based compounds. The preparation of a Boltorn-type polyester dendrimers in a monodisperse manner was approached by using a strategy based on the anhydride 1 as a building block monomer and pentaerythriol as a central core. The set of reactions used in the produc-

tion of compounds G3(pseudodi)$_{32}$ and G3(pseudotri)$_{32}$ is presented in the figure 30 (Luczkowiak et al., 2011).

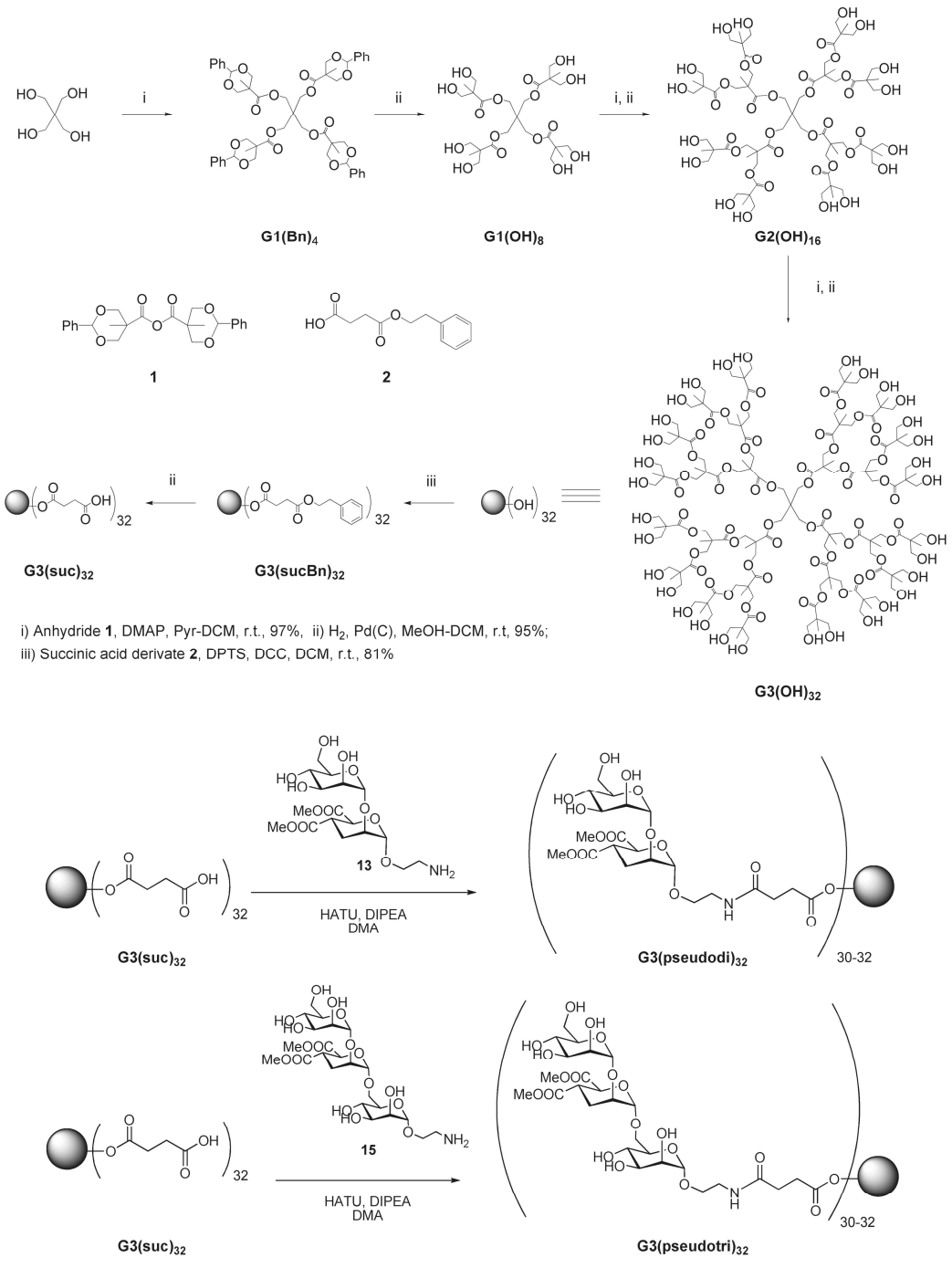

Figure 30. Synthesis of G3(pseudodi)$_{32}$ and G3(pseudotri)$_{32}$.

2. 5. Glycofullerenes

Glycofullerenes were kindly provided by Dr. Nazario Martín, Universidad Complutense (Madrid, Spain). Fullerenes are molecules composed of carbon in the form of a hollow sphere resembling "the balls used in association football". Fullerene C_{60} is a truncated icosahedron made of 20 hexagons and 12 pentagons with a carbon atom at the verticals of each polygon and a bond along each polygon edge. The van der Waals diameter of a C_{60} molecule is about 1.1 nm with the nucleus diameter of 0.71 nm (Qiao et al., 2007). Fullerenes can be considered as very attractive spherical scaffolds for a multivalent presentation of carbohydrates in a globular shape. Many synthetic methods for functionalization of fullerenes have been well established during past decades. Nowadays, fullerene hexa-bingle adducts can be obtained in a very straightforward approach in good yields. This strategy permits the introduction of substituents in the positions corresponding to octahedral vertexes resulting in the complete coverage by ligands showing a globular presentation.

Glycofullerenes (sugar balls) are soluble in water due to the presence of non-protected carbohydrates that surround completely the fullerene molecule. Additionally, these compounds show good stability and low toxicity, which confirm the appropriate features to be used in cellular assays. Glycofullerene 3 with 12 copies of mannoses was prepared using a straightforward strategy based on click chemistry conjugation of sugars onto a hexa-bingle adduct fullerene (Fig. 31A). Since DC-SIGN is not able to recognize galactose, a fullerene with 12 copies of galactoses (glycofullerene 4) has been prepared as negative control for experiment involving DC-SIGN as a target molecule (Fig. 31B).

Glycofullerenes 1 and 2 bearing 36 copies of mannoses have been prepared based on a convergent strategy using a small glycodendron 6 or 10 and the hexa-bingle adduct 5 (Fig. 32 and Fig. 33). Glycodendron 6 used for the synthesis of glycofullerene 1 presenting a short linker at the focal position has been previously prepared by using a functionalized mannose with an azido group providing a building block to create highly

multivalent species. The glycofullerene 1 with 36 mannoses was prepared by conjugation of the glycodendron 6 with the hexa-bingle 5 (Fig. 33). The glycofullerene 2 was synthesized using the same strategy. This compound contains a larger spacer between the carbohydrate ligands and the fullerene scaffold (conjugation of the glycodendron 10 with the hexa-bingle 5). The introduction of a larger spacer provided increase in the flexibility of the carbohydrate ligands on the fullerene surface allowing a better accessibility and availability of ligands for the receptor recognition (Fig. 33) (Luczkowiak et al., 2013).

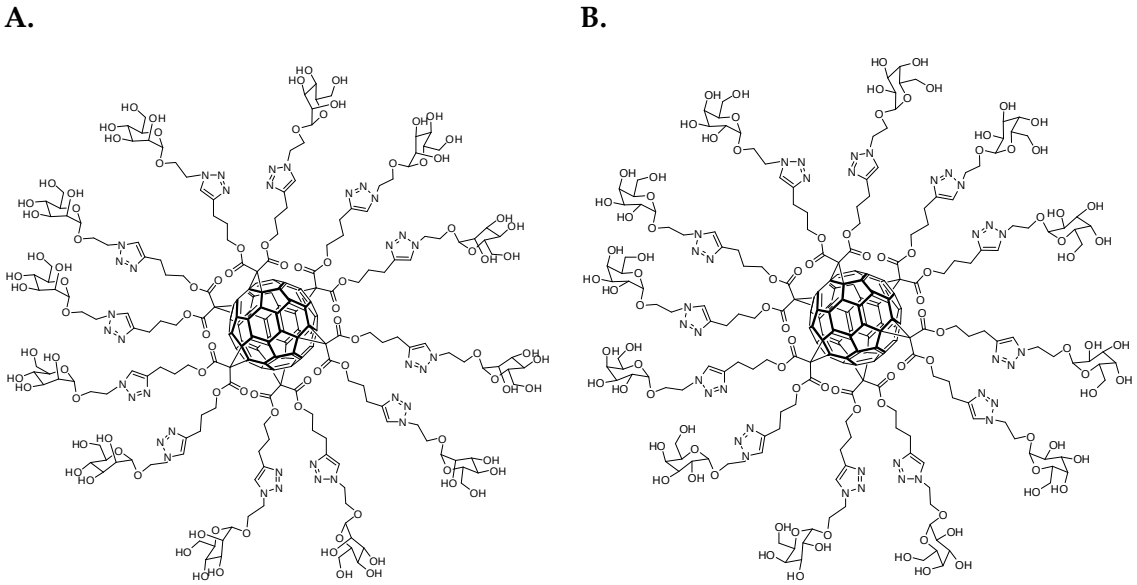

Figure 31. Structure of: **A.** glycofullerene 3 presenting 12 mannoses, **B.** glycofullerene 4 presenting 12 galactoses.

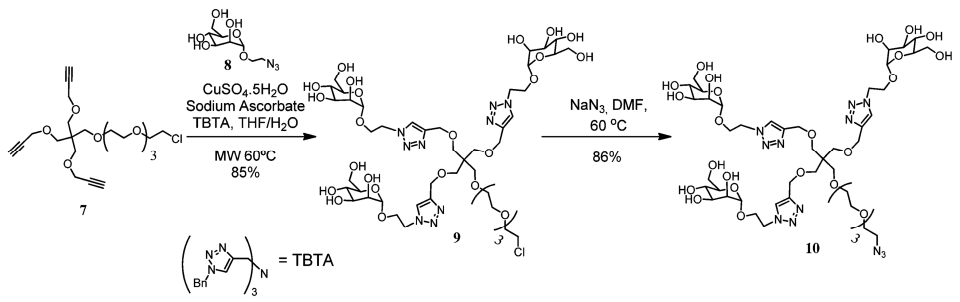

Figure 32. Synthesis of glycodendron 10.

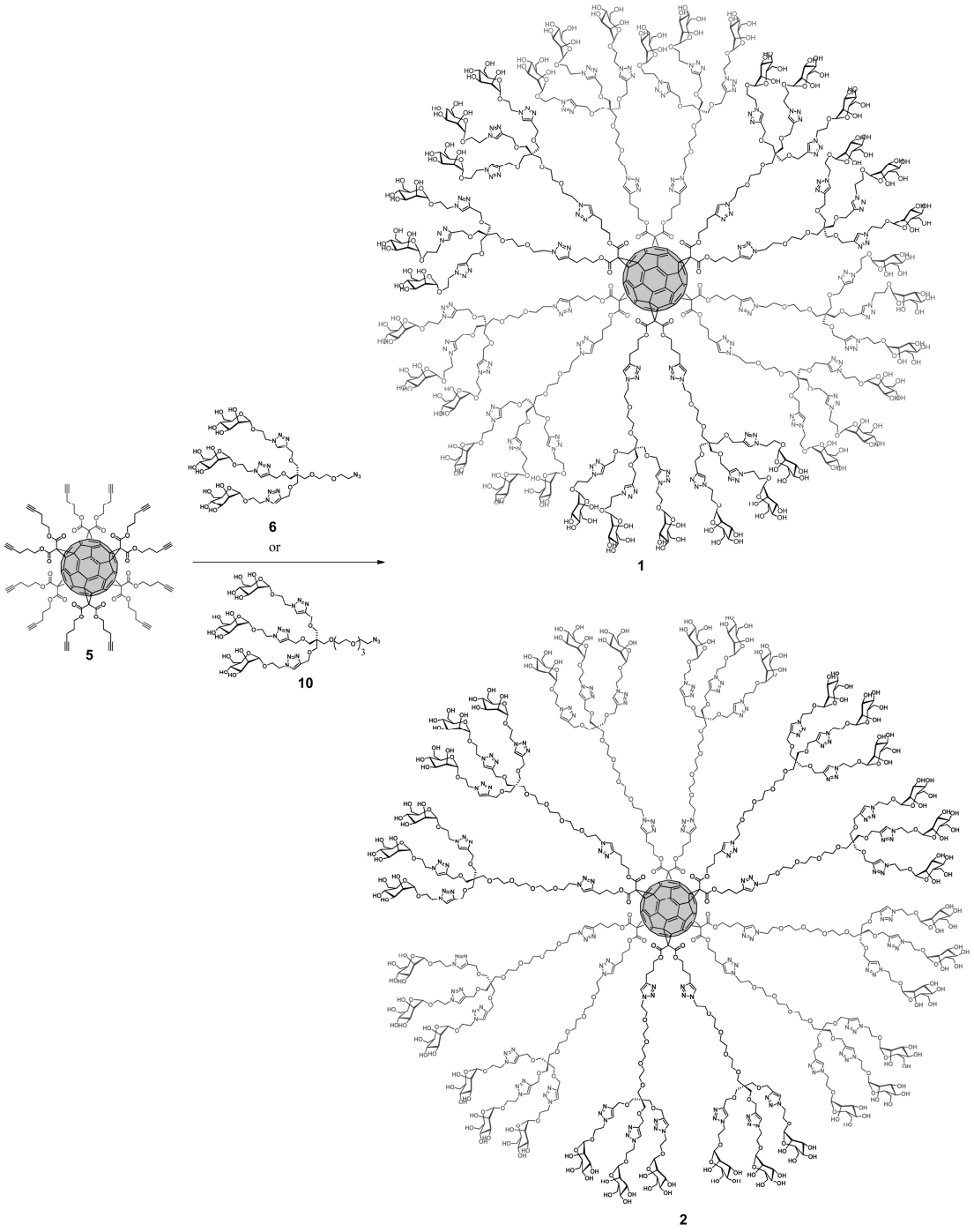

Figure 33. Synthesis of glycofullerenes: 1 and 2.

2. 6. Glycodendrinanoparticles

Glycodendrinanoparticles were kindly provided by Dr. Benjamin G. Davis from University of Oxford (Oxford, The United Kingdom). The glycodendrinanoparticles are based on the structure obtained from bacteriophage Qbeta. The monomeric proteins of Qbeta are of about 30 nm in diameter and of a 14 kDa molecular weight. Monomers Qbeta were conjugated together to form a 180-copy multivalent scaffold resembling "virus-like" particle (Fig. 34). The assembly of entities with higher dimensions might provide the mimic displayed in target pathogens. A non-natural amino-acid tag was selectively introduced to a protein scaffold Qbeta for further attachment of the selected glycodendrons, appropriately functionalized, at the focal position. Moieties of α-D-mannoses were then introduced onto the dendritic scaffolds prepared by Cu(I)-catalysed modification of the Huisgen cycloaddition to serve as relevant ligands for the DC-SIGN recognition (Ribeiro-Viana et al., 2012) (Fig. 35).

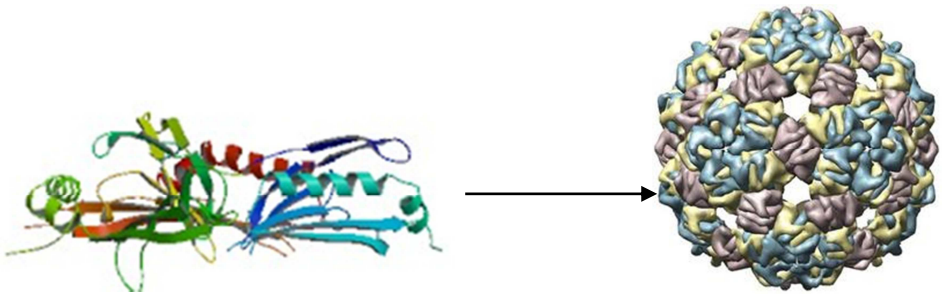

Figure 34. Schematic representation of virus-like glycodendrinanoparticles assembly. Glycodendrons are created through multivalent assembly and then attached to multiple tags, each in a monomer protein.

Compound Qbeta (MW = 2538900) did not contain any carbohydrate moiety attached to the scaffold and was therefore used as a control compound of this virus-like scaffold in the *cis*-infection experiment. Compound Qbeta-$(Mann_3)_{180}$ (MW = 2738880) contained

540 mannose residues conjugated to the Qbeta scaffold. Compound Qbeta-(Mann$_9$)$_{180}$ (MW = 3220020) displayed 1620 mannose residues attached to the Qbeta scaffold.

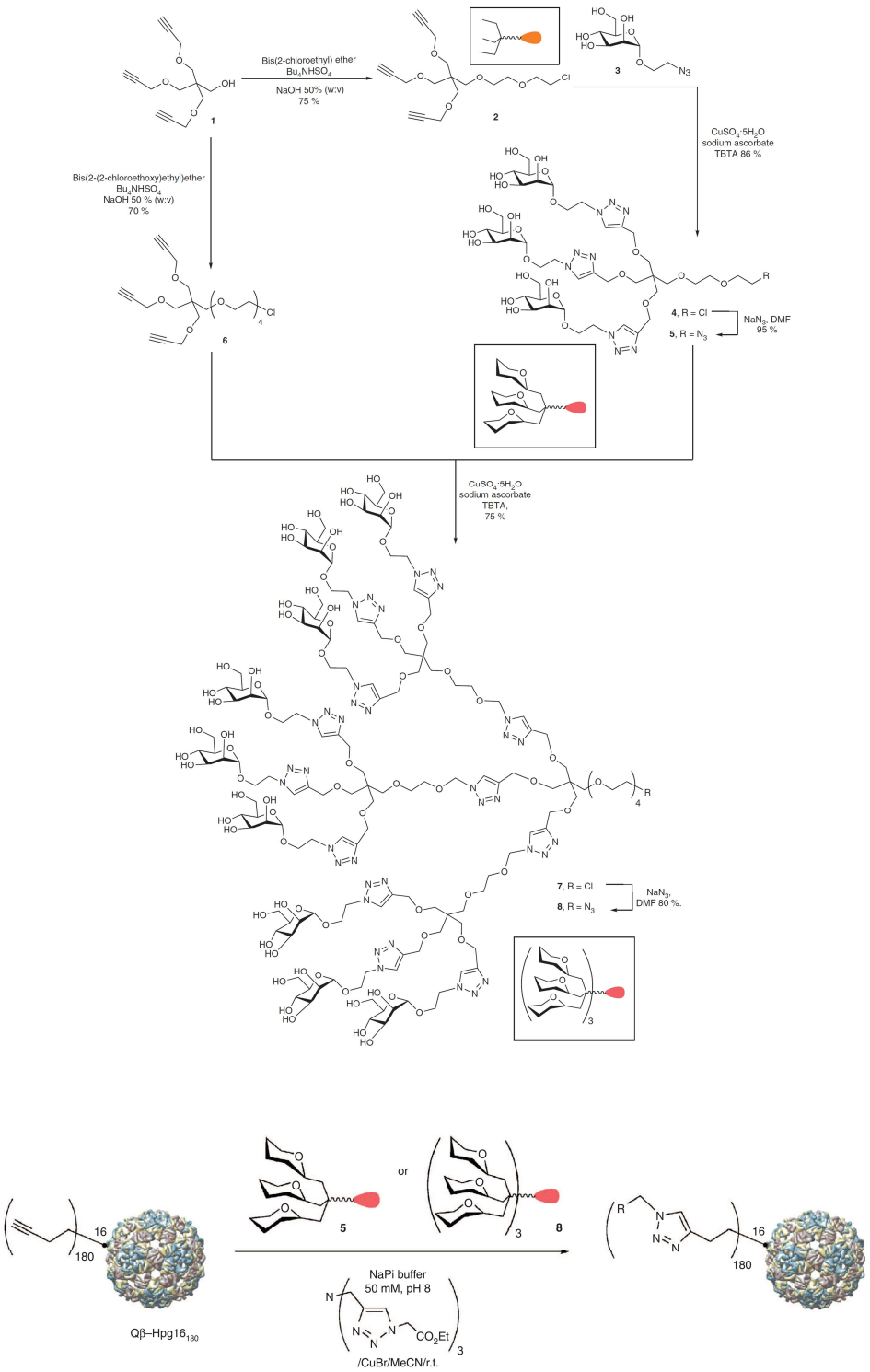

Figure 35. Synthesis of polyvalent virus-like glycodendrinanoparticles using a tag-and-modify strategy.

2. 7. Isolation of Peripheral Blood Mononuclear Cells (PBMCs) and generation of monocyte-derived Dendritic Cells (DCs)

PBMCs were isolated from buffy coats from healthy donors (Hospital 12 de Octubre, Madrid, Spain) by Ficoll-Paque (Pharmacia, Uppsala, Sweden) density-gradient centrifugation. Following the centrifugation of 40 ml of whole blood samples on Ficoll-Paque at 1800 rpm for 40 min, the cells from interface were collected and washed 3 times with PBS at 1200 rpm for 10 min at RT. PBMCs were then resuspended in RPMI medium (supplemented with 10% heat-inactivated FBS, 25 mg Gentamycin, 2 mM L-glutamine) at concentration 2 x 10^6 cells per cm^2 and placed onto 24-well plate for 1 h at 37º C with 5% CO_2. The adherent monolayer of monocytes were then washed twice with PBS and resuspended in RPMI medium supplemented with cytokines GM-CSF (200 ng/ml) (MACS, Miltenyi Biotec) and IL-4 (10 ng/ml) (MACS, Miltenyi Biotec). For the proper differentiation of immature monocyte-derived DCs, cells were incubated at 37º C with 5% CO_2 for 7 days and subsequently activated with cytokines on a day 2 and 5.

2. 8. Inhibition of the infection in *cis* of immature monocyte-derived DCs by DC-SIGN targeting compounds

Immature DCs (2 x 10^4 cells) were incubated at RT for 20 min with the carbohydrate-based compounds and then challenged with 5000 TCID of EBOV-GP recombinant pseudoviruses. After 48 h of incubation, cells were washed twice with PBS and lysed for luciferase assay. As a control, experiment of inhibition of infection of EBOV-GP was performed in the presence of monoclonal antibody anti-DC-SIGN (R&D Systems) and mannan at concentration of 25 μg/ml.

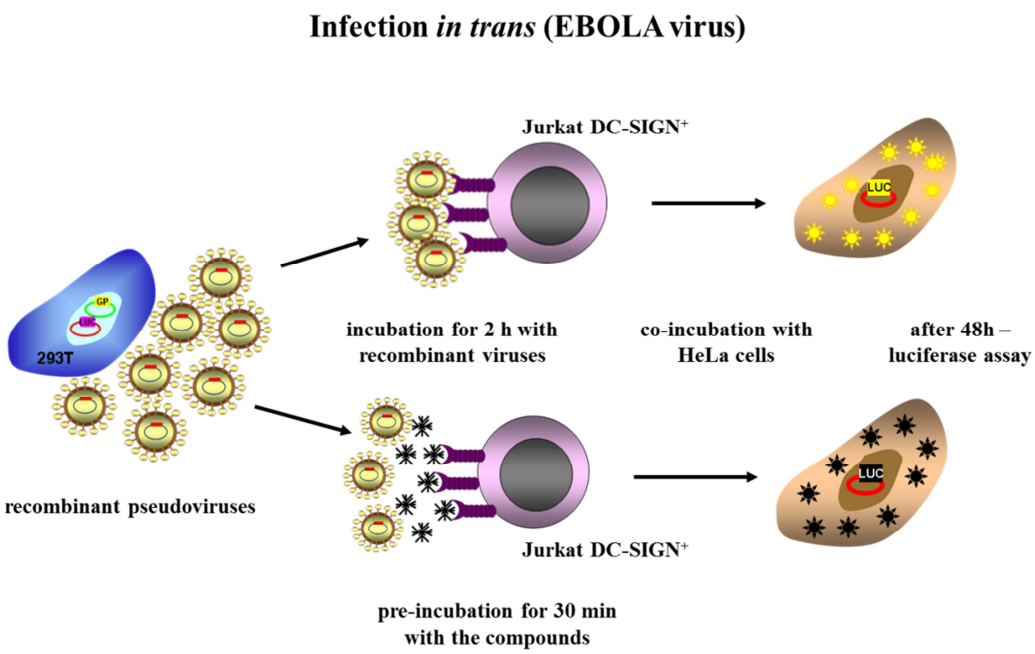

Figure 36. Infection in *trans* with recombinant Ebola GP-pseudotyped retroviruses in cellular model Jurkat DC-SIGN+/ HeLa cells. Jurkat DC-SIGN+ and Jurkat control cells were pre-incubated with compounds targeting DC-SIGN, challenged with recombinant viruses and after intensive washing co-cultivated with susceptible HeLa cells.

2. 9. Inhibition of the infection in *trans* of Ebola pseudoparticles by DC-SIGN targeting compounds

Jurkat DC-SIGN+ cells (2.5-5 x 10^5) were pre-incubated for 20 min at RT with carbohydrate compounds. Then, the cells were challenged with 5000-10000 TCID of recombinant viruses and incubated for 2 h at RT with rotation. After 2 h, cells were centrifuged at 1000 rpm for 5 min and washed twice with 1 ml of PBS supplemented with 0.5% BSA and 1mM $CaCl_2$. Jurkat DC-SIGN+ were resuspended in 500 µl of RPMI medium and co-cultivated with adherent HeLa cells (10^5 cells/ well) on 24-well plate. After 48 h, the supernatant was removed and monolayer of HeLa was washed twice with 1 ml of PBS and lysed with 100 µl of 1x Lysis Buffer (Promega) for luciferase assay (Fig. 36). As a control, *trans*-infection experiment with DC-SIGN independent VSV-G pseudoviruses was performed.

3. RESULTS

DC-SIGN molecule is not the only receptor responsible for the entrance and binding of Ebola and HIV-1 envelopes. Although DC-SIGN is not the main receptor in case of both Ebola and HIV-1 viruses, it plays a significant role in the cell entrance and/or *trans*-infection process of these two infectious agents. Therefore, DC-SIGN can function as a good model of studying the first steps of pathogenesis of those viruses and screening the antiviral strategies based on DC-SIGN targeting compounds for vaccination and treatment purposes. The antiviral activity of carbohydrate compounds was tested using pseudotyped viral particles presenting Ebola virus glycoproteins. The possibility of blocking DC-SIGN receptor was examined in the experiments of *cis*-infection and *trans*-infection in the presence of carbohydrate-based compounds at different final concentrations. All compounds were checked at least in 3 independent experiments. During the infection in *cis* experiment, Jurkat DC-SIGN$^+$ were challenged with recombinant retroviruses in the presence or absence of compounds. In the *trans*-infection experiment Jurkat DC-SIGN$^+$ were incubated with recombinant pseudoviruses for 2 h in the presence or absence of carbohydrate-based compounds, washed and co-cultivated with adherent HeLa cells.

The results of blocking DC-SIGN receptor by different compounds were shown as a function of concentration. The 50% of inhibition of the infection was calculated with the 95% confidence intervals. As a control, infection with VSV-G pseudotyped retroviruses was performed in the same conditions.

3. 1. Glycodendritic structures

The results obtained in the infection in *cis* experiment did not show any difference in the potency of those compounds in blocking of EBOV GP pseudotyped particles. The IC_{50} were of the same order of magnitude. The IC_{50} of compound RR114 was 3.6 μM

(95%CI=1.2–10.9 μM) (Fig. 37A). The IC_{50} for compound RR115 was 2.8 μM (95%CI=670.6 nM–12.1 μM) (Fig. 37B).

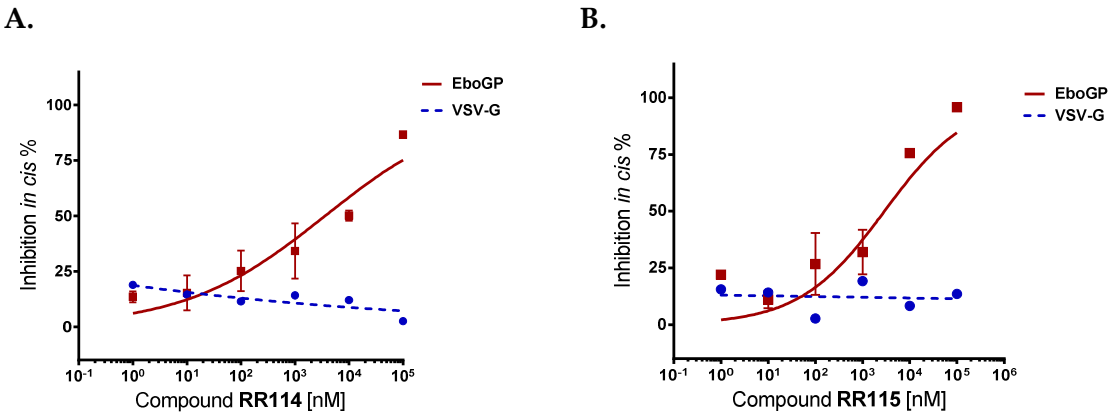

Figure 37. Inhibition of *cis*-infection by pseudotyped Ebola viruses of Jurkat DC-SIGN+ cells using: **A.** Compound RR114, **B.** Compound RR115

Although both compounds showed similar efficiency in the infection in *cis*, in the experiment of infection in *trans* compound RR115 was more potent than compound RR114. The IC_{50} for compound RR114 was 52.4 μM (24.4–112.6 μM) (Fig. 38A). The highest concentration of compound RR114 used in the experiment (100 μM) was able to block infection in the median percentage of 40% (range of 23-85%).The IC_{50} obtained for compound RR115 was 7 μM (4.6–10.7 μM) (Fig. 38B).

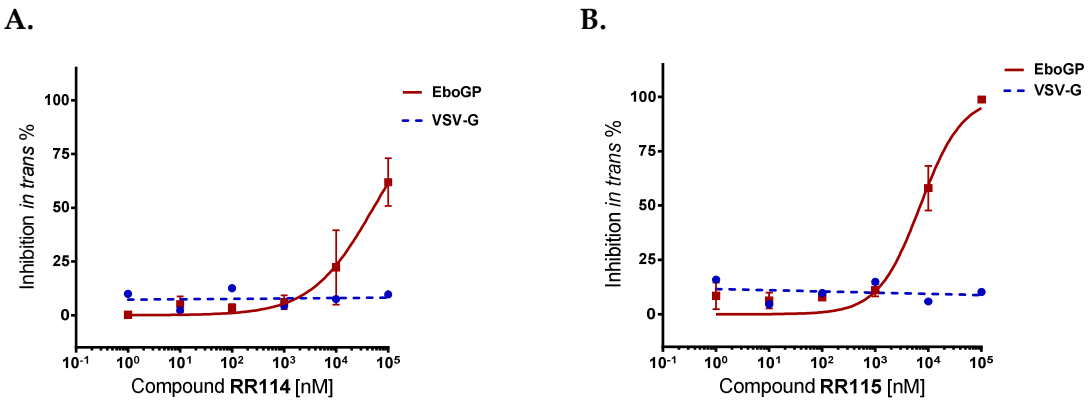

Figure 38. Inhibition of *trans*-infection by pseudotyped Ebola viruses of Jurkat DC-SIGN+ cells using: **A.** Compound RR114, **B**. Compound RR115.

3. 2. Tetravalent dendrons

The results obtained in the *cis* infection experiment revealed that the tetravalent systems presenting four copies of pseudomannotrioside (compound 14) showed a potency of 1 order of magnitude higher than the tetravalent systems presenting four copies of linear pseudomannobiosides (compound 12). The IC_{50} of compound 14 was 106.5 nM (95%CI=24.07–470.9 nM) and the IC_{50} of compound 12 was 1.4 μM (95%CI =404.2 nM–5.166 μM) (Fig. 39).

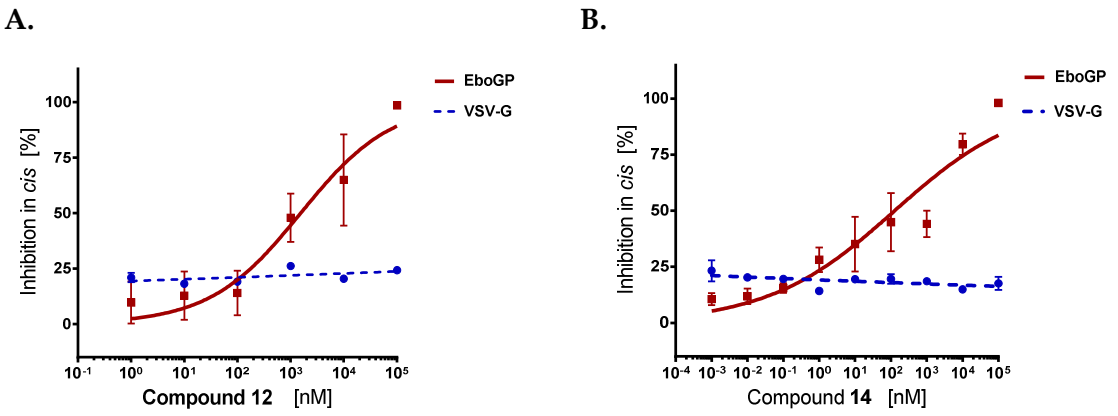

Figure 39. Inhibition of *cis*-infection by pseudotyped Ebola viruses of Jurkat DC-SIGN+ cells using: **A.** Compound 12, **B.** Compound 14.

The results obtained in the *trans*-infection experiment were similar to the results of the infection in *cis*. The tetravalent dendron 14 with 4 copies of pseudomannotrioside showed an IC_{50} of 203 nM (95%CI=73.84–562.5 nM) (Fig. 40B). The tetravalent dendron 12 with 4 copies of pseudomannobioside was 1 order of magnitude less potent with an IC_{50} of 1.22 μM (95%CI=475.5 nM–3.17 μM) (Fig. 40A).

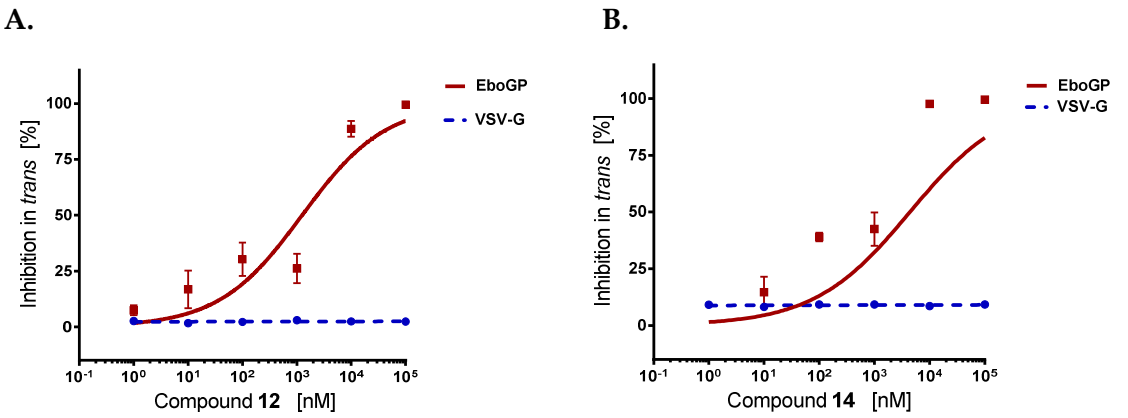

Figure 40. Inhibition of *trans*-infection by pseudotyped Ebola viruses of Jurkat DC-SIGN⁺ cells using: **A**. Compound 12, **B**. Compound 14.

3. 3. Dendrimer-based compounds

Dendrimer-based compounds are multivalent systems presenting an average of 30-32 glycomimetic ligands. In case of multivalent systems bearing 30-32 pseudomannotrioside (G3(pseudotri)$_{32}$) or 30-32 pseudomannobiosides (G3(pseudo-di)$_{32}$) no difference was found in their potency of inhibition of EBOV GP pseudotyped particles cell entry. The IC_{50} value of compound G3(pseudotri)$_{32}$ was 17.12 nM (95% CI=5.946 nM–49.30 nM) and the IC_{50} value of compound G3(pseudodi)$_{32}$ was 27.21 nM (95% CI =16.53 nM–44.78 nM) (Fig. 41).

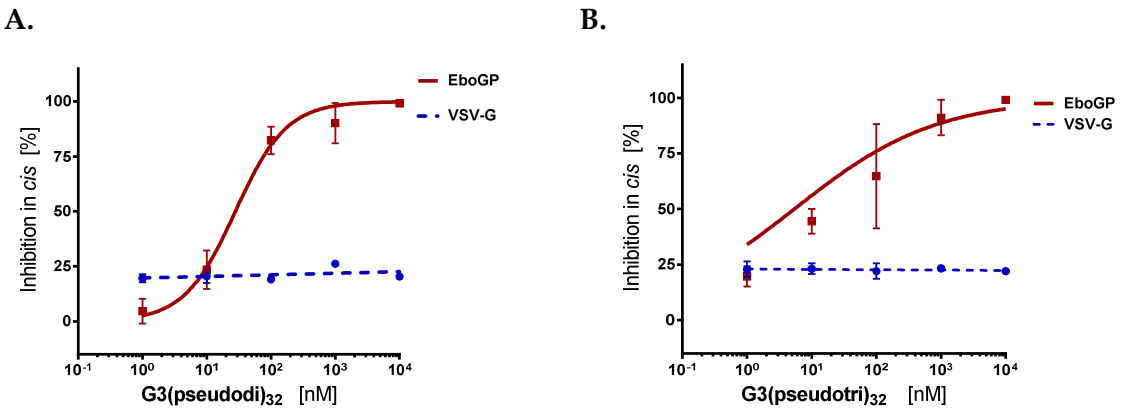

Figure 41. Inhibition of *cis*-infection by pseudotyped Ebola viruses of Jurkat DC-SIGN⁺ cells using: **A.** Compound G3(pseudodi)$_{32}$, **B.** Compound G3(pseudotri)$_{32}$.

The results obtained in the *trans*-infection experiment were similar to the results of the infection in *cis*. The IC_{50} values of 32-valent systems were of the same order of magnitude. The IC_{50} of multivalent pseudomannobioside was 62 nM (95%CI=43.53 nM–89.1 nM) (Fig. 42A). The IC_{50} of multivalent pseudomannotrioside was 31.51 nM (95%CI=13.89 nM–71.48 nM) (Fig. 42B).

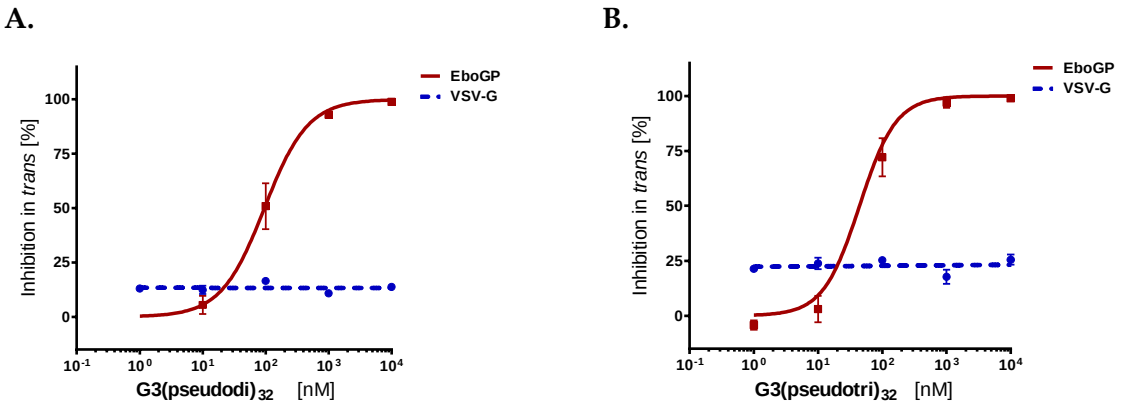

Figure 42. Inhibition of *trans*-infection by pseudotyped Ebola viruses of Jurkat DC-SIGN⁺ cells using: **A.** Compound G3(pseudodi)$_{32}$, **B**. Compound G3(pseudotri)$_{32}$.

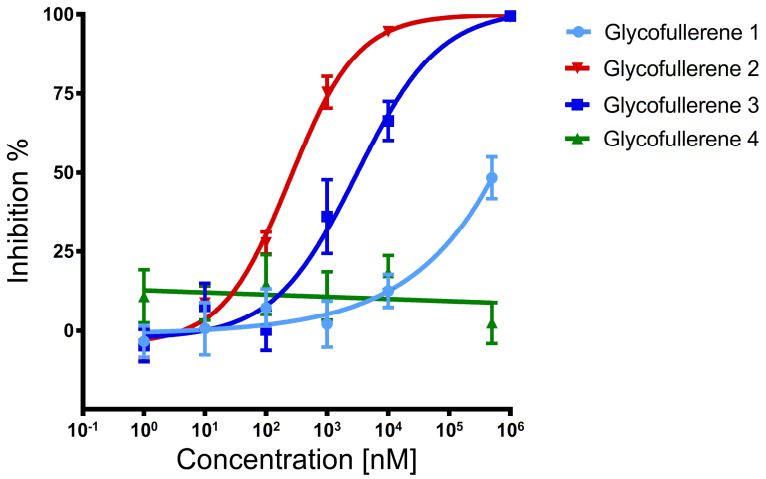

Figure 43. Inhibition of infection by pseudotyped Ebola virus infection of Jurkat DC-SIGN⁺ cells using mannosylated glycofullerenes 1, 2, 3 and negative control galactosyl glycofullerene 4.

3. 4. Glycofullerenes

The results obtained in the infection in *cis* experiment revealed the dependence of the inhibition effect on mannoses (Fig. 43). Galactosyl fullerene 4, as expected, was not able to inhibit the infection process mediated by DC-SIGN. The comparison of the fullerene 1 (presenting 36 mannoses) and fullerene 3 (displaying 12 mannoses) showed an important decrease of activity with the increase of valency. Glycofullerene 3 with 12 mannoses showed the IC_{50} of 2 μM (95%CI=859.8 nM–3 μM). The IC_{50} for the fullerene 1 was 68 μM (34 fold less active than fullerene presenting 12 mannoses). The introduction of a longer spacer in glycofullerene 2 had a very important effect on recovering the activity of this compound with the IC_{50} of 286.4 nM (more than 200 fold increase in comparison with glycofullerene 1 presenting the same valency).

3. 5. Glycodendrinanoparticles

Compound Qbeta was used in the experiment as a control of the impact of this new type of structures on the results in the infection in *cis*. The highest concentration of compound Qbeta (25 nM) used in the experiment could block infection in ~30-40%. The same concentration (25 nM) of compound Qbeta-$(Man_3)_{180}$ could block infection in 50-60%. The concentration of 25 nM of compound Qbeta-$(Man_9)_{180}$ could efficiently block infection in ~90-100%. The values presented on the graphs correspond to means of 6 experiments with error bars representing standard errors of the mean (Fig 44). The IC_{50}s were estimated using GraphPad Prism v4.0 with a 95% CI (7.7 nM–24.3 nM for Qβ-$(Man_3)_{180}$ and 404.2 pM–4.1 nM for Qβ-$(Man_9)_{180}$) and settings for normalize dose-response curves (Fig. 45).

The inhibitory effect of glycodendrinanoparticles were then studied in the direct infection of DCs, which were generated from isolated human peripheral blood mononuclear cells (PBMCs) and displayed multiple C-type lectins. Compounds Qbeta and Qbeta-$(Man_9)_{180}$ were tested at concentrations of 25 nM, 5 nM and 1 nM. The values presented

on the graph corresponded to the mean of 2 experiments with range shown above each bar. As a control, inhibition of infection of EBOV-GP pseudovirus was verified in the presence of antibody anti-DC-SIGN and mannan at concentration of 25 μg/ml. Compound Qbeta-$(Man_9)_{180}$ displayed potent activity, inhibiting infection by >80% at 5 nM and >95% at 25 nM (estimated IC_{50} ~ 2 nM) (Fig. 46).

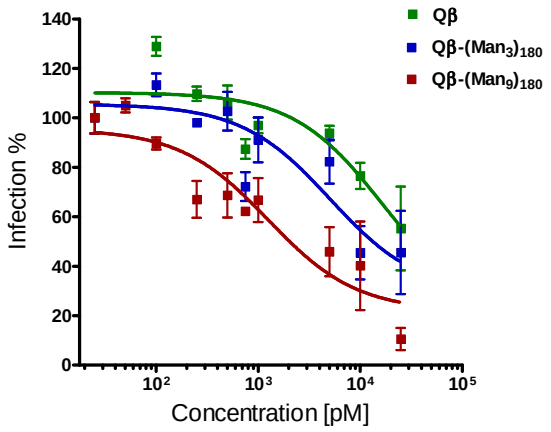

Figure 44. Results of infection in *cis* experiment using compounds: Qbeta, Qbeta-$(Man_3)_{180}$, Qbeta-$(Man_9)_{180}$.

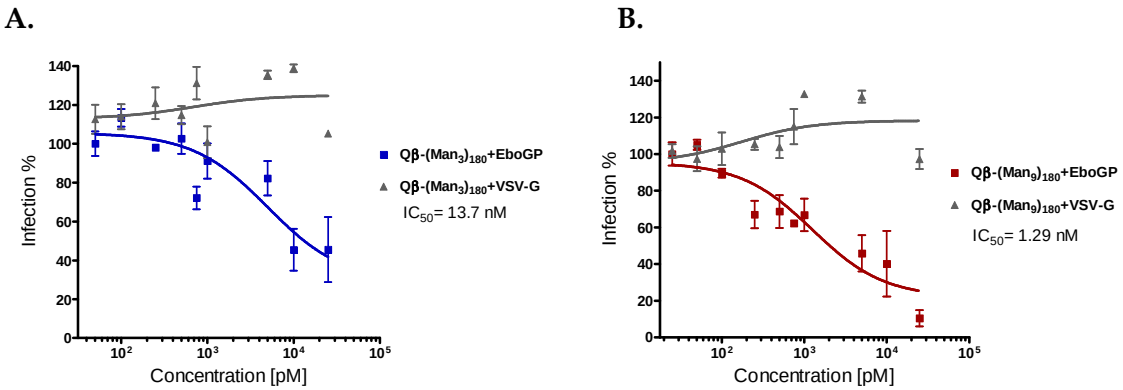

Figure 45. *Cis*-infection by pseudotyped Ebola viruses of Jurkat DC-SIGN$^+$ cells using: **A.** Compound Qbeta-$(Man_3)_{180}$, **B.** Compound Qbeta-$(Man_9)_{180}$.

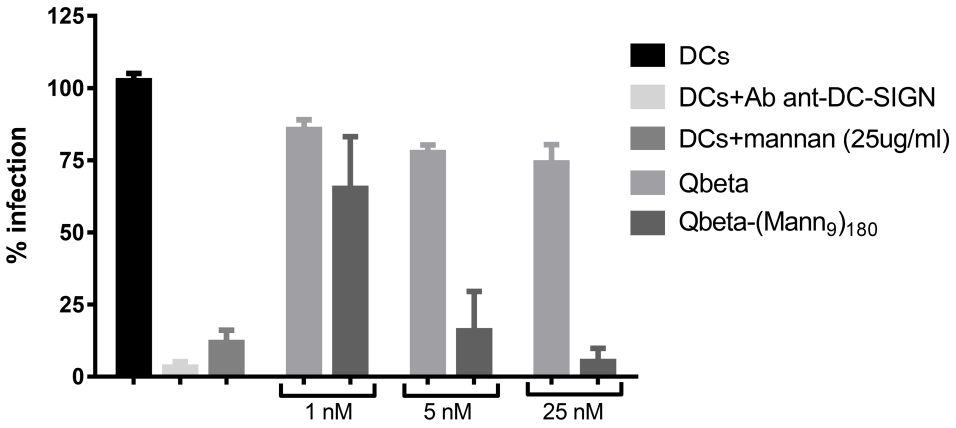

Figure 46. Infection of primary DCs by EBOZ pseudotyped viruses.

4. DISCUSSION

Although *in vitro* DC-SIGN models are not sufficient for understanding the physiological role of DC-SIGN, the cellular model based on DC-SIGN$^+$ cells might function as a useful model of antiviral screening platform of compounds targeting this receptor. DC-SIGN recognizes mannosylated and fucosylated oligosaccharides presented in a multivalent manner on the surface of several pathogens. Therefore, the preparation of multivalent carbohydrate systems is necessary for the efficient interaction with this receptor as well as for the effective competition with the natural ligands. However, there is not sufficient information about the adequate orientation of the ligands thus many different strategies of the synthesis has been tested so far, such as: gold-nanoparticles (de La Fuente et al., 2001), polymers (Roy, 1996), liposomes (Stewart and Boggs, 1993), dendrimers (de La Fuente et al., 2001; Imberty et al., 2008), multivalent glycoconjugates (Luczkowiak et al., 2013; Luczkowiak et al., 2011; Ribeiro-Viana et al., 2012; Rojo and Delgado, 2004). Multivalent carbohydrate systems based on dendrimers or dendritic polymers have been shown to be promising candidates as antiviral agents. These dendrimers are able to form stable complexes with cell receptors or viral structures, which results in disruption of infection process by abolishing virus-cell interaction. A multi-

valent scaffold based on Boltorn polymer functionalized with monosaccharide mannose has been shown to inhibit DC-SIGN-mediated Ebola virus infection at nanomolar concentrations (IC_{50}=337 nM). However, these glycodendritic structures are recognized and degraded by mannosyl glycosylases thus the synthesis strategy should be performed by usage of mimic carbohydrates that are not recognized by hydrolytic enzymes (Rojo and Delgado, 2004). The carbohydrate mimics, such as pseudomannobioside, demonstrated higher antiviral activity than mannose in the inhibition of HIV-1 infection. This new carbohydrate-based compounds were considered as proper candidates for further clinical use since they were more stable against enzymatic degradation (Reina et al., 2007; Sattin et al., 2010).

In the CARMUSYS programme interdisciplinary group of scientists (biologist, virologists, synthetic chemists, computational chemists, biochemists, immunologists) aimed at designing and synthesizing carbohydrate multivalent systems to be used as inhibitors for pathogen attachment and penetration into target cells that present the receptor DC-SIGN. In this collaboration we have planned to use these multivalent systems as tools to get information about the molecular basis of the recognition process between pathogen glycoproteins and DC-SIGN with the aim to rationalize the design and synthesis of new drugs. The development of compounds with strong affinity for the receptor DC-SIGN is a topic of remarkable interest due to the role of this lectin in pathogen infection processes. DC-SIGN is a tetravalent calcium-dependent lectin, expressed on DCs, that specifically recognizes highly glycosylated structures present at the surface of several pathogens such as viruses, bacteria, yeast and parasites (Geijtenbeek et al., 2000c). DC-SIGN recognizes mannosylated and fucosylated oligosaccharides presented in multivalent manner. Therefore, the multivalent carbohydrate systems are required to interact in an efficient manner with this receptor and compete with the natural ligands (Lasala et al., 2003; Luczkowiak et al., 2011; Rojo and Delgado, 2004). The main carbohydrate ligand recognized by DC-SIGN is the high mannose glycan, $(Man)_9$,$(GlcNAc)_2$, a branched oligosaccharide displayed in multiple copies on several pathogen glycoproteins (gp120, GP1). Thus, the structural analogues of Man_9 would compete with binding of virus glycoprotein to DC-SIGN. It has been reported that the

pseudo-dimannoside, mimicking the natural disaccharide Manα1-2Man, binds to DC-SIGN and exhibits anti-infective activity in an Ebola pseudovirus infection model (Reina et al., 2007). The additional results showed that 2-C-substituted branched D-mannose analogues bind to DC-SIGN with higher affinity than mannose (Mitchell et al., 2007). Multivalent oligomannosides, which display complex oligomannose dendrons in high density, were also described to block DC-SIGN receptor (Wang et al., 2008). The gold nanoparticles presenting various linear and branched mannosyl oligosaccharides (Manno-GNPs) might behave as potent inhibitors of HIV-1 *trans*-infection at the cellular level (Martinez-Avila et al., 2009). It has been demonstrated that multivalent carbohydrate systems based on dendrimers and dendritic polymers are promising candidates as antiviral drugs. Dendrimers are able to form stable complexes with receptors or viral structures at the cell surface, which results in disruption of the virus-cell interaction during the process of the virus infection. The functionalization with negatively charged molecules of dendrimers based on polyamidoamine (PAMAM) support generation of polyanion structures that are able to interact with viral envelope glycoproteins, preventing therefore the binding of viruses such as HIV-1 or herpes simplex virus (HSV) (Bourne et al., 2000; Witvrouw et al., 2000). Glycodendrimers, presenting at their surface numerous moieties of carbohydrates, were described as excellent tools to address carbohydrate-protein interactions. Hyperbranched glycodendritic polymers were shown to block the binding of pathogen glycoproteins to DC-SIGN. Glycodendritic structures, based on Boltorn polymer of second and third generations, are easy to prepare, non-toxic, soluble in physiological conditions and able to block the cell receptor DC-SIGN (Rojo and Delgado, 2004). The commercially available hyperbranched BoltornH30 (Perstrop Speciality Chemicals), that was modified to present 32 mannose units linked through succinyl spacer (BH30sucMan), was shown to inhibit DC-SIGN-mediated Ebola GP-pseudotyped retroviruses during Jurkat DC-SIGN$^+$ cells infection in *cis* and in *trans* with the IC_{50} of 0.3 μM (Lasala et al., 2003). Combining dendritic platforms with glycomimetic compounds to obtain novel DC-SIGN antagonists could provide stronger binding affinity to block DC-SIGN and inhibit the HIV infection process. The pseudo-trisaccharide mimic of the linear mannotriose Manα1-2 Manα1-6 Manα produced by replacing the central mannose units with a carbocyclic

diol, could inhibit HIV infection of $CD4^+$ T lymphocytes at low micromolar concentration. This tetravalent construct presenting 4 copies of the pseudo-trimannoside on Boltorn-type dendron at 50 μM concentration reduced the *trans*-infection of $CD4^+$ T lymphocytes by over 90% (Sattin et al., 2010).

The results obtained in the experiments performed within this thesis, could contribute in a very fast and effective way in the first studies of antiviral screening based on different strategies: tetravalent dendrons, dendrimer-based compounds, glycofullerenes and glycodendrinanoparticles. Tetravalent dendrons and dendrimers-based compounds are the combination of new pseudomannoside carbohydrate mimic and the potency of multivalent presentation. The importance of the valency was evaluated by the presentation of the same pseudosaccharide ligands on the tetravalent system presenting 4 copies of the ligand and on the multivalent scaffolds displaying 30-32 of selected ligands (Luczkowiak et al., 2011). The synthesis of glycofullerenes provided the achievement of even higher valency (36 mannoses). These compounds were synthesized by combining glycodendrons with a hexakisadduct [60] fullerene allowing thus globular presentation of carbohydrates (Luczkowiak et al., 2013). Nevertheless, the highest valency constructs were gained in case of glycodendrinanoparticles. This design was based on the multivalent assembly of protein monomers (glycodendriproteins) carrying polyvalent glycan motifs (glycodendrons). In this way these constructs displayed many glycans in a precise manner and created well-defined single entities of up to 32 nm in diameter (Ribeiro-Viana et al., 2012).

4. 1. Tetravalent systems

The tetravalent systems presenting four copies of pseudomannobiosides (compound 12) or pseudomannotrioside (compound 14) were tested *in vitro* in the experiments of *cis*- and *trans*-infection as antiviral compounds. The results obtained in the experiments showed inhibition of the infection by blocking of DC-SIGN receptor. In the infection in *cis* experiment, the tetravalent pseudomannotrioside was more than 10 times more active than tetravalent pseudomannobioside (the IC_{50} of 106 nM vs 1.4 μM) (Fig. 39). The

results obtained in the *trans*-infection experiment confirmed previously obtained results in the *cis*-infection assay. The tetravalent dendron 14 showed an IC_{50} of 203 nM and the tetravalent dendron 12 was 1 order of magnitude less potent with an IC_{50} of 1.22 μM (Fig. 40). Our results confirmed that these systems could be considered as a very potent inhibitors to be tested in further experiments as ligands for multivalent presentation (Luczkowiak et al., 2011).

4. 2. Dendrimer-based compounds

The synthesis of multivalent systems was based on the commercially available third generation of a Boltorn dendritic polymer that serves as a very convenient platform for a multivalent presentation of carbohydrates (Arce et al., 2003). These polydisperse dendritic polymers bear 30-32 copies of selected ligands. In the case of pseudodimultivalent and pseudotrimultivalent systems, no significant differences were found as a function of the pseudosaccharide presented. The IC_{50} values obtained for the multivalent systems were around 20 nM (17.12 nM for G3(pseudotri)$_{32}$ and 27.21 nM for G3(pseudodi)$_{32}$), which shows that their inhibitory potency is between 1 to 2 orders of magnitude higher than that of corresponding tetravalent systems (Fig. 41). Similar results were gained in the *trans*-infection experiment. The IC_{50} of 32-valent system bearing pseudomannobioside was 62 nM and bearing pseudomannotrioside was 31.5 nM (Fig. 42). In the same way like in *cis*-infection assay, in the *trans*-infection relatively small differences were observed between the two selected monovalent ligands presented in the multivalent scaffold. Both multivalent systems G3(pseudosugar)$_{32}$ showed very strong inhibition effect in the low nanomolecular range in both assays. The results acquired in performed experiments confirmed pseudoglycosylated multivalent systems as very promising antiviral drugs with strong DC-SIGN blocking activities (Luczkowiak et al., 2011).

4. 3. Glycofullerenes

The mannosylated fullerenes containing several copies of carbohydrates in a globular presentation are water-soluble and show a low cytotoxicity of several cell lines. Our experiments have demonstrated for the first time the potential biological function of glycodendrofullerenes in preventing viral infection. The fullerene displaying 12 mannoses showed a low micromolar IC_{50} in the infection model using Ebola glycoprotein-pseudotyped viruses. The increase of valency in glycofullerene 1 from 12 to 36 mannoses induced a negative effect, probably due to steric congestion of sugars at the surface of the fullerene. This result has highlighted the importance to combine an adequate scaffold to achieve the multivalency (the spherical fullerene) with the right ligand accessibility and flexibility. The introduction of a longer spacer in glycofullerene displaying 36 mannoses had a very important effect on its antiviral functions. Longer spacer enabled recovering the activity of this compound and showed potent DC-SIGN blocking effect with the IC_{50} of 286.4 nM (Fig. 43). The valency of the compound is an important factor to obtain good affinities in a carbohydrate-lectin interaction but as it has been shown in these experiments that it is not the only factor to be taken into account. Nevertheless, we can consider fullerenes as very attractive scaffolds for a globular multivalent presentation of sugars (Luczkowiak et al., 2013).

4. 4. Glycodendrinanoparticles

The main problem in the preparation of synthetic carbohydrate systems that are able to prevent DC-SIGN-mediated infection is reaching adequate size and multivalency while maintaining control of shape and structure (Sanchez-Navarro and Rojo, 2010). These features are very important in effective mimic of natural systems such as viruses or bacteria. It has been previously shown that ligand valences above 32 have not had a full control (Greatrex et al., 2009; Lasala et al., 2003). Glycodendrinanoparticles were prepared under the control design for highly polyvalent proteins that displayed sugar moieties in polyvalent manner (structure Qbeta). Therefore the inhibitory properties of

each mannoside monomer were considerably more potent when displayed on Qbeta (Qb) structures as compared with monosaccharide presentation (~250-fold when displayed on $Qb(Man3)_{180}$ and ~860- fold when on $Qb(Man9)_{180}$). These well-defined polyvalent glycoproteins presented on their surface up to 1620 copies of glycan, a considerably higher valency than has never been obtained before using a fully controlled strategy. The efficiency of this system was gained by the effect of a high number of displayed ligands as well as proper size and geometry. It has been reported that no homogeneous polyvalent systems that can generate such a large surface area have been described before. The constructs tested in our experiments were composed of nested glycan polyvalency, which allows the display of many varying polyvalent combinations, playing therefore different biological functions. Glycodendrinanoparticles are therefore not 'balls of sugar' but homogenous constructs exhibiting different polyvalent glycans. Thus it might be suggested that the most relevant features can be the topology of glycan presentation, its relation to the inter-domain distances in the DC-SIGN tetramer (Tabarani et al., 2009) and the constructs organization on cell surface (de Bakker et al., 2007) rather than just average glycan-to-glycan distance (Tabarani et al., 2009). The results obtained in performed experiments showed a potent antiviral activity of glycodendrinanoparticles in the Ebola DC-SIGN-mediated infection model. The glycodendrinanoparticles presenting 1620 glycan moieties showed antiviral activity in the picomolar to low nanomolar to range (Fig. 44-46). These results revealed the efficiency of these systems to interact with DC-SIGN and to compete with pathogens during their entry into target cells. However, the functions of these glycodendrinanoparticles *in vivo* remain to be tested. The high activity, high surface area and morphology of these new glycoconjugates provides them as promising candidates for the development of new antiviral agents (Ribeiro-Viana et al., 2012).

5. CONCLUSIONS

1) The DC-SIGN infection model is a useful model of an antiviral screening platform to test carbohydrates strategies targeting DC-SIGN.

2) The inhibition of DC-SIGN-mediated infection by carbohydrate-based compounds depends strongly on the multivalency of glycan presentation.

3) The most potent antiviral activity was obtained by glycodendrinanoparticles showing an effective antiviral activity in the picomolar to low nanomolar concentration range. Multivalency depends on the presentation of 1620 glycan moieties generating a large surface of interaction (30 nm in diameter).

CHAPTER 3:

DC-SIGN in EBOLA virus pathogenesis:

DC-SIGN-mediated *trans*-infection in pathogenic and non-pathogenic strains of Ebola virus

IV. CHAPTER 3:

DC-SIGN in EBOLA virus pathogenesis: DC-SIGN-mediated *trans*-infection in pathogenic and non-pathogenic strains of Ebola virus

1. OBJECTIVES

Evaluate DC-SIGN-mediated *trans*-infection by the pathogenic and non-pathogenic Zaire and Reston strains of Ebola virus.

2. MATERIAL AND METHODS

2. 1. Plasmids: p1012-Ebola Zaire GP, p1012-Ebola Reston GP, pNL4-3.Luc.R-E- (see Chapter I: 2.1.)

2. 2. Isolation of PBMCs and generation of monocyte-derived DCs (see Chapter II: 2.6.)

2. 3. Infection in *cis* of immature monocyte-derived DCs

Immature DCs (2 x 10^4 cells) were challenged with 5000 TCID of recombinant viruses pseudotyped with: a) EBOZ or b) EBOR envelope glycoproteins. After 48 h of incubation, cells were washed twice with PBS and lysed for luciferase assay. As a control, experiment of inhibition of infection of EBOV-GP was performed in the presence of monoclonal antibody anti-DC-SIGN (R&D Systems) and mannan at concentration of 25 μg/ml.

2. 4. Infection in *trans* assay with Ebola GP-pseudotyped retroviruses (see Chapter I: 2.5)

2. 5. Statistical analysis

2. 5. 1. The t Student test

The t Student test compares the means of two groups. It is used to determine if two sets of data are significantly different from each other. It is most commonly applied when the statistic test follows a normal distribution.

2. 5. 2. The two-tailed test

The two-tailed test is a statistical test used in inference, in which a given statistical hypothesis, H_0 (the null hypothesis), will be rejected when the value of the test statistic is either sufficiently small or sufficiently large. The statistical results of the two-tailed test were calculated by GraphPad Prism 4. The two-tailed test assumes that samples follow a Gaussian bell-shaped distribution. If the values of the test statistic fell into tail of its sampling distribution, the null hypothesis would be rejected. The p value of the two-tailed test was calculated.

3. RESULTS

3. 1. Analysis of the sequences of envelope glycoproteins of EBOZ and EBOR

The glycoproteins of Ebola viruses are considered to be the major determinants in virus pathogenesis, responsible for the binding of virus to the cell receptors and virus entry into the cell cytoplasm (Feldmann et al., 1993). Ebola virus glycoproteins are highly glycosylated by both N-linked and O-linked carbohydrates, which contributes to 30-50% of their total molecular weight (Geyer et al., 1992). The Ebola group of filoviruses comprises five subtypes: Zaire, Sudan, Reston, Cote dÍvoire, Bundibugyo, among which Ebola Zaire strain shows the highest mortality rate (50-90%), whereas Ebola Reston has never been associated with human disease (Usami et al., 2011). The main

envelope gene product, secreted glycoprotein (sGP), is slightly longer in Ebola virus strain Reston (368 aa) than sGP of Ebola virus strain Zaire (365 aa), however both contain 6 N-linked glycans. The second glycoprotein product resulting from transcriptional editing of the glycoprotein ORF, transmembrane GP, is similar in length in both strains (Ebola Zaire = 677 aa and Ebola Reston = 678 aa). The transmembrane glycoprotein contains 11 N-linked glycans in both strains, located mostly in the mucin-like domain and the glycan cap. Although the sequences of those regions show relatively low level of similarity (23.7% of pairwise identity in mucin-like domain, 52.3% of pairwise identity in the glycan cap), the number of N-linked glycans is quite conserved in both Ebola strains (Lee et al., 2008). The mucin-like domain is a region of 151 aa containing 5 N-glycans in Ebola Zaire (N317, N333, N346, N386, N436) and 4 N-linked glycans in Ebola Reston (N317, N318, N339, N420). The N-glycosylation pattern in the glycan cap is conserved in both strains. The glycan cap is 86 aa long and contains 4 N-linked glycans (EBOZ: N228, N238, N257, N268; EBOR: N229, N239, N258, N269) in both Ebola strains. The shift of one aa in the PNGS position results from the length of signal peptide of GP since in EBOR is 34 aa long and in EBOZ is 33 aa long. N-linked glycosylation sites for Ebola Zaire and Reston were predicted by the NetNGlyc (Gupta et al., 2004).

3. 2. DC-SIGN-mediated *trans*-infection of EBOZ and EBOR in the cellular system Jurkat DC-SIGN$^+$/Jurkat

Recombinant retroviruses pseudotyped with envelope glycoproteins of Ebola Zaire and Ebola Reston were produced by transfection of 293T by using standard Calcium Chloride protocol. The *trans*-infection experiment with retroviral particles pseudotyped with EBOZ or EBOR GP was performed to study the differences in DC-SIGN-mediated infection by both strains. Infection in *trans* was performed on Jurkat DC-SIGN$^+$, which could capture and transmit Ebola virus to susceptible cells. As a control, Jurkat cells which did not express DC-SIGN on its surface were used. The ratio be-

tween *trans*-infection Jurkat DC-SIGN$^+$ and Jurkat cells for Ebola Zaire and Ebola Reston glycoprotein was calculated as an average from 9 independent experiments.

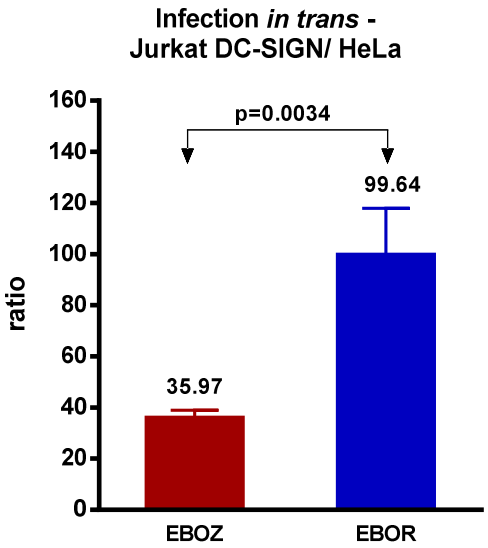

Figure 47. *Trans*-infection with EBOZ (red) and EBOR (blue) in Jurkat DC-SIGN$^+$/Jurkat system. The bars represent mean with SEM error bars of 9 independent experiments. The statistical analysis was performed by two-tailed Student t test.

The statistical significance of differences between the ratios of EBOZ and EBOR pseudoparticles obtained in 9 independent experiments of *trans*-infection was analyzed by Student t test. The two-tailed p value was calculated by GraphPad Prism V4. The difference in the mean ratio in the *trans*-infection experiment between EBOZ and EBOR was statistically significant (p=0.0034) (Fig. 47). Additionally, the mean (35.97 vs 99.64), 95% CI of mean (28.97-42.97 vs 57.56-141.7), SEM (3.035 vs 18.25), SD (9.106 vs 54.74) were calculated by using GraphPad Prism V4.

3. 3. DC-SIGN-mediated *cis*-infection of primary DCs by EBOZ and EBOR

Dendritic cells used in the infection experiment were generated from isolated human peripheral blood mononuclear cells (PBMCs) and displayed multiple C-type lectins providing a route for infection of pseudotyped Ebola retroviruses. The difference in

using DC-SIGN receptor by EBOZ and EBOR pseudoviruses was verified in direct infection assay of immature DCs cells. The infection levels were adjusted by the results of direct infection with the same amount of recombinant Ebola Zaire and Reston pseudoviruses of HeLa cells. As a control, immature DCs were pre-incubated with the monoclonal antibody anti-DC-SIGN and then challenged with recombinant EBOZ and EBOR pseudoviruses.

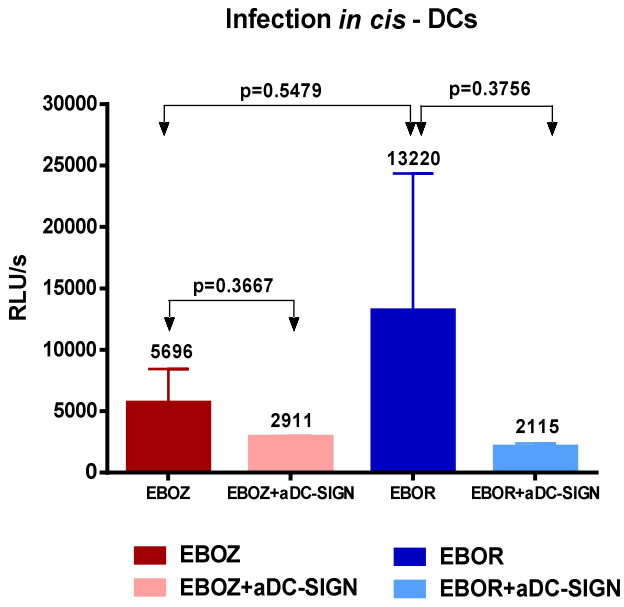

Figure 48. DC-SIGN-mediated *cis*-infection of primary DCs by EBOZ (red) and EBOR (blue). The inhibition of the infection with monoclonal antibody anti-DC-SIGN was performed for both, EBOZ (pink) and EBOR (light blue). The bars represent mean with SEM error bars of 3 independent experiments. The statistical analysis was performed by two-tailed Student t test.

The statistical significance of differences between the infection levels of Ebola Zaire and Ebola Reston pseudoparticles in immature DCs obtained in 3 independent experiments of infection in *cis* was analyzed by Student t test. The two-tailed p value was calculated by GraphPad Prism V4. The difference in the mean infection level in the *cis*-infection experiments between Ebola strain Zaire and Ebola strain Reston was not statistically significant (p=0.5479) (Fig. 48). Moreover, the mean (5696.53 vs 13219.67), SEM (2738.13 vs 11144.68), SD (4742.58 vs 19303.15) were calculated by using GraphPad Prism V4.

3. 4. DC-SIGN-mediated *trans*-infection of EBOZ and EBOR in the cellular system: primary DCs/HeLa cells

The relevance of the differences in DC-SIGN receptor involvement in the *trans*-infection process in immune system was verified by using immature DCs. Immature DCs were incubated with recombinant EBOZ and EBOR and after intensive washing, they were co-cultured with susceptible HeLa cells. The infection levels were adjusted by the results of direct infection with the same amount of recombinant EBOZ and EBOR viruses of HeLa cells. The ratio between DCs-mediated *trans*-infection for EBOZ and EBOR glycoprotein was calculated as an average from 3 independent experiments. As a control, immature DCs were pre-incubated with the monoclonal antibody anti-DC-SIGN and then challenged with recombinant EBOZ and EBOR. The statistical significance of differences between the transmitted infection by Ebola Zaire and Ebola Reston pseudoparticles to susceptible HeLa cells obtained in 3 independent experiments of *trans*-infection was analyzed by Student t test. The two-tailed p value was calculated by GraphPad Prism V4. The difference in the mean of transmitted infection in the *trans*-infection experiments between Ebola strain Zaire and Ebola strain Reston was statistically significant (p=0.0084) (Fig. 49). In addition, the mean (24426.67 vs 38781.88), SEM (533.67 vs 2921.65), SD (924.35 vs 50606.45) were calculated by using GraphPad Prism V4.

4. DISCUSSION

Ebola viruses cause a severe, often fatal disease consisting in a highly lethal hemorrhagic fever syndrome (Peters et al., 1996). Ebola virus strain Zaire is the virus variant with the highest mortality rate being in the range 50-90%. In contrast to the Zaire strain, Ebola virus strain Reston does not cause a disease in humans despite a number of documented infections during animal epizootics (Barrette et al., 2009; Miranda et al., 1999). The molecular basis for this difference in their pathogenesis remains unclear.

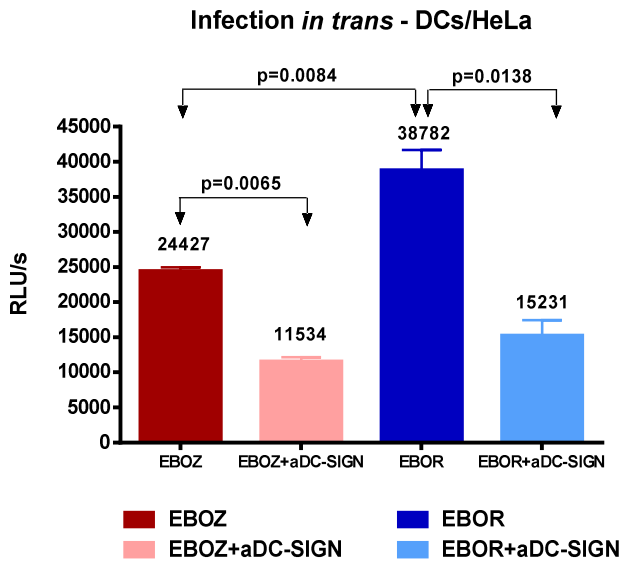

Figure 49. DC-SIGN-mediated *trans*-infection of EBOZ (red) and EBOR (blue) in the cellular system: primary DCs/HeLa cells. The inhibition of the *trans*-infection with monoclonal antibody anti-DC-SIGN was performed for both, EBOZ (pink) and EBOR (light blue). The bars represent mean with SEM error bars of 3 independent experiments. The statistical analysis was performed by two-tailed Student t test.

It has been speculated about the important role of viral glycoprotein in this phenomenon. This hypothesis was raised after a number of *in vitro* studies, which analyzed the possible role of immunosuppressive motifs (Becker, 1995; Volchkov et al., 1992; Yaddanapudi et al., 2006), efficiency of cleavage by furin (Neumann et al., 2002; Neumann et al., 2007) or cytotoxicity (Alazard-Dany et al., 2006; Volchkov et al., 2001; Yang et al., 2000). However, there is no confirmed evidence for these speculations *in vivo*. The sequence analysis of Ebola Zaire and Reston envelope glycoproteins revealed similarity in overall length and PNGS number of envelope gene products, however, important divergence was seen in the sequence of mucin-like domain and glycan-cap. Glycan-cap subdomain contains 4 predicted PNGS in both strains (EBOZ: N228, N238, N257, N268; EBOR: N229, N239, N258, N269). This region does not form any monomer-monomer contacts within the trimeric GP but is fully exposed on the outer side of the glycoprotein (Lee et al., 2008). Although the PNGS number in this region is conserved in both strains, the sequence similarity is relatively low (52.3% of pairwise identity). Mucin-like domain is the high molecular mass region of about 75 kDA, where

most of PNGS are concentrated. The crystal structure presented by Lee *et al*. demonstrated that the mucin-like domain is associated with the side of each monomer of glycoprotein trimer and may function in building up the walls of the chalice. The mucin-like domain of Ebola Zaire contains 5 PNGS (N317, N333, N346, N386, N436) and of Ebola Reston has 4 PNGS (N317, N333, N346, N386, N436). The sequence similarity is very low as comparing both strains showing 23.7% of pairwise identity. The mucin-like domain and glycan-cap are located together as an external domain playing the role in the immune evasion (Lee et al., 2008). The main envelope gene product, secreted glycoprotein (sGP), of both Ebola strains is of similar length (slightly longer in case of EBOR 368 aa vs 365 aa of EBOZ) and contains the same number of PNGS. The second glycoprotein product resulting from transcriptional editing of the glycoprotein ORF, transmembrane GP, is very similar in length in both strains (EBOZ: 677 aa, EBOR: 678 aa) and have 11 N-linked glycans in both strains, located mostly in the mucin-like domain and the glycan cap (Fig. 50).

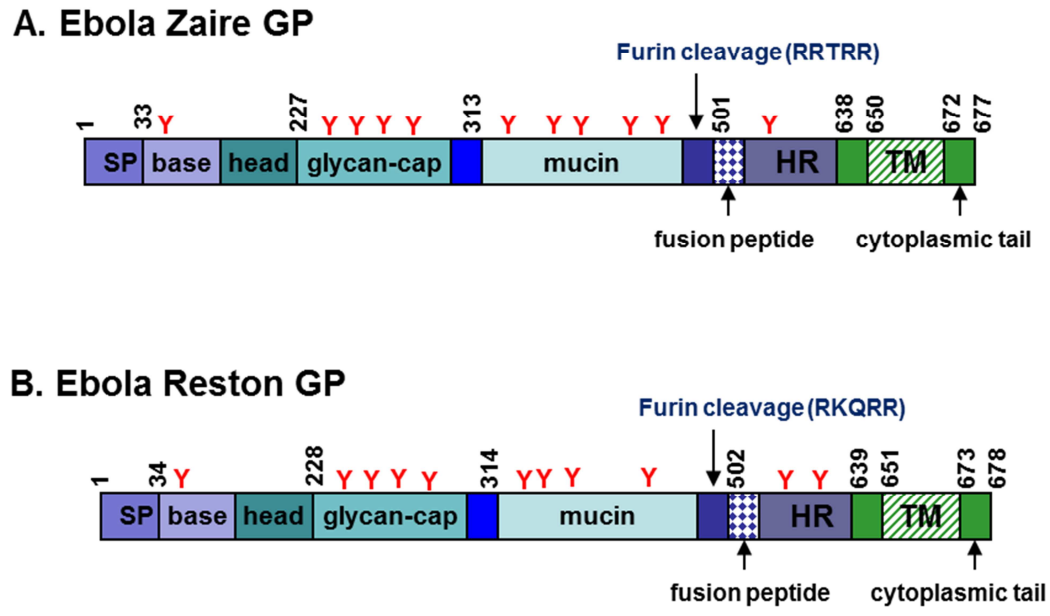

Figure 50. Structure of Ebola virus glycoprotein. **A.** Ebola Zaire GP. **B.** Ebola Reston GP. Predicted N-linked glycans are represented by red Y-shaped symbols. SP – signal peptide, HR – heptad repeat, TM – transmembrane domain. Modified from Cook *et al*. (Cook and Lee, 2013).

Yang *et al.* identified the Ebola virus glycoprotein as the main viral determinant of Ebola virus pathogenicity (Yang et al., 2000). It has been shown that the process of transfection of retrovirus producer cells with GP of Ebola virus had a considerable effect on alteration of the cells phenotype. After 24 hours cells were rounded and detached, and by the time of 2-4 days post-transfection the cell death was observable. In this study, they mapped the region of GP responsible for cytotoxic effect by using deletion mutations and checking the functional activity of created mutants. It has been then discovered that GP proteins with internal deletion in serine-threonine-rich mucin-like domain did not cause morphological changes of cells or cellular cytotoxicity. The effect of wild-type and mutant GP on endothelial cells was then studied by the comparison of the outcome elicited by adenovirus vectors encoding wild-type GP (ADV-GP) or mucin-region-deleted GP (ADV-GPΔmuc). They observed that endothelial cells infected with ADV-GP exhibited altered cell morphology with cells rounding and detachment after 12-16 h, whereas cells transfected with ADV-GPΔmuc were unchanged. Therefore, they suggested the mucin-like domain as being responsible for the GP cytotoxicity to endothelial cells *in vitro* since the deletion of this region abrogated its toxic effect without affecting the cell surface expression. Further, they studied the contribution of other viral genes to the cytotoxicity of Ebola virus, however, none of genes studied showed cytotoxic activity. It was also shown that cytotoxic effect required the intracellular synthesis and/or transport of GP gene product to the cell surface since it was blocked by an inhibitor of protein synthesis and the exposure to extracellular sGP protein fused downstream with mucin-like domain of GP had no effect on cell morphology or viability. Subsequently, they tried to analyze the effect of GP on endothelial cells in blood vessels by using adenovirus vectors to infect porcine or human saphenous vein explants. It has been demonstrated that ADV-GP, unlike ADV-GPΔmuc, increased the permeability of cells of both models resulting from damage and loss of endothelial cells. To identify the potential relevance of GP *in vivo*, Yang *et al*. examined also the effects of Ebola Zaire and Reston GP expression in vascular cells of nonhuman primates and in men. They showed that ADV-GP Zaire caused endothelial damage in both human and monkey vessels explants, while ADV-GP Reston demonstrated this effect only in nonhuman primate model. Moreover, they confirmed the crucial role of mucin-

like domain of Zaire strain in the cytotoxic effect by inserting this region into an analogous region of another viral envelope (MLV) and observing more cell rounding and detachment as compared with a wild-type envelope. The trials of inserting of Ebola Zaire mucin-like domain into Reston GP yielded a protein that was not expressed on the cell surface thus the determination of the effect of this domain on the cytotoxicity could not be studied in this model (Yang et al., 2000).

Nevertheless, the study of Groseth *et al.* about the contribution of Ebola virus glycoprotein for virulence *in vivo*, did not confirm the data obtained when using adenovirus vectors. The approach to understand the role of GP in pathogenesis was performed in the model of Ebola virus chimeras, where the glycoproteins of these two strains were exchanged and examined in the full-length clone system (recombinant REBOV, recombinant REBOV expressing ZEBOV GP, recombinant ZEBOV and recombinant ZEBOV expressing REBOV GP). The study indicated that exchange of the GP ORF is well tolerated in terms of basic viral functions including entry, replication and budding enabling the successful growth *in vitro*. Although no significant differences could be identified between the parental and wild-type viruses, the 2-3 log differences were observed between REBOV-based viruses as compared with ZEBOV-based viruses. The chimeric envelopes were examined in the $IFNAR^{-/-}$ model (severe combined immunodeficiency (SCID) and STAT1 knock-out ($STAT^{-/-}$) mouse model), the only rodent model that recapitulate difference in virulence between ZEBOV and REBOV in humans (Bray, 2001). The infection with rREBOV did not exhibit lethal disease while infection with rZEBOV showed uniform lethality with animals displaying decrease in activity, weight loss, ruffled fur and hunched posture. This mice model revealed information about significant changes in the ability of the chimeric rZEBOV-RGP to reduce lethality and prolong the time to death as compared with rZEBOV. However, REBOV and REBOV-ZGP-infected $IFNAR^{-/-}$ mice did not cause any signs of disease. The introduction of Ebola Zaire GP to full-length Ebola Reston led to a slight decrease in the virulence of this envelope chimera, which indicated that GP alone is not a sufficient determinant of EBOV virulence in this model. Despite the observed differences in the mortality caused by infection with ZEBOV and ZEBOV-RGP, no important changes in viral load in any or-

gans/tissues were observed. Comparison of the pathology from REBOV-based or ZEBOV-based recombinant viruses showed continuously higher levels of inflammation and necrosis in case of animals infected with ZEBOV or ZEBOV-RGP, as compared to REBOV and REBOV-ZGP. The findings of their work could possibly reflect fundamental difference between ZEBOV and REBOV in their *in vivo* growth and spread in this model. The data obtained in this study clearly supported the conclusion that while GP is a relevant element of filovirus pathology, alone is not sufficient for Ebola virulence (Groseth et al., 2012).

Binding of Ebola virus GP to different cellular lectins has been shown to augment virus infection. Although DC-SIGN is not the main receptor for Ebola cell entry, it has been demonstrated that the presence of DC-SIGN on non-permissive cells enable the virus entry. In case of Ebola virus, DC-SIGN receptor acts as a cell entry receptor as well as *trans*-infection receptor responsible for binding of viral particles and further transmission to susceptible cells (Alvarez et al., 2002).

In our study, we have used recombinant particles expressing two Ebola virus envelope glycoproteins (Ebola Reston and Ebola Zaire) to evaluate the role of DC-SIGN in the cell entry and dissemination mediated by both Ebola variants. The DC-SIGN-mediated infection was verified in the experiments of *trans*-infection Jurkat DC-SIGN$^+$/Jurkat, *cis*-infection of primary DCs and *trans*-infection DCs/HeLa cells.

The first experiment of the *trans*-infection in cellular model Jurkat DC-SIGN$^+$/Jurkat showed the significant differences in the mean ratio of the *trans*-infection experiments between Ebola Zaire and Ebola Reston ($p=0.0034$). The mean ratio of EBOR was about three times higher than the ratio of EBOZ (35.97 vs 99.64) (Fig. 43). The relevance of the differences in DC-SIGN receptor usage in the *trans*-infection process was then verified by using immature DCs. These cells were incubated with EBOZ/EBOR and after intensive washing they were co-cultured with susceptible HeLa cells. The results obtained in the experiment based on human immune cells (DCs) have confirmed the results of *trans*-infection in cell line system. The difference between the transmitted infection by

Ebola Zaire and Ebola Reston pseudoparticles to susceptible HeLa cells was statistically significant (p=0.0084) (Fig. 45). Both of performed experiments demonstrated statistical significance of higher EBOR DC-SIGN-mediated *trans*-infection as compared with EBOZ. Despite significant differences in DC-SIGN usage by EBOZ/EBOR in the *trans*-infection experiment, the direct infection of immature DCs did not give any significant result (Fig. 44).

Our results found the association between the Ebola Reston and a higher *trans*-infection ratio mediated by DC-SIGN. This finding might raise a hypothesis that although DC-SIGN receptor participates effectively in the cell entrance, *in vivo* it could play apparently more important role in the proper immune system activation. DC-SIGN may be responsible for virus capture, destruction and further presentation of its antigens to cells causing effective immunological control. DC-SIGN therefore, although able to capture effectively Ebola virus particles, might serve more as a host defence factor rather than pathogen escape receptor. Therefore the higher level of DC-SIGN-mediated entry of Ebola Reston might suggest that overall DC-SIGN might be more implicated in antiviral responses. The results obtained in performed experiments somehow resemble the results from the Schaefer *et al.* study, in which mice expressing human DC-SIGN survived longer than wild-type mice after infection with *Mycobacterium tuberculosis,* suggesting the role of DC-SIGN in the proper immune system activation by the antigen presentation and limiting of tissue-damaging inflammatory responses (Schaefer et al., 2008).

5. CONCLUSIONS

Despite the role of DC-SIGN in Ebola virus entry and potential initial dissemination, we found significantly higher DC-SIGN *trans*-infection by the non-pathogenic Ebola Reston strain. This finding could indicate that in Ebola virus infection DC-SIGN is involved in a more efficient immune control.

CHAPTER 4:

DC-SIGN in HIV-1 pathogenesis:

Implication of DC-SIGN-mediated *trans*-infection in HIV-1 virological control

V. CHAPTER 4:

DC-SIGN in HIV-1 pathogenesis: Implication of DC-SIGN-mediated *trans*-infection in HIV-1 virological control

1. OBJECTIVES

Evaluate the implication of DC-SIGN *trans*-infection in HIV-1 virological control through the study of a group of clinical isolates of virological controllers and non-controllers.

2. MATERIAL AND METHODS

2. 1. Patients and samples

All biological samples included in this thesis were obtained from patients from La Unidad VIH-1 del Hospital Universitario 12 de Octubre de Madrid under active follow-up by Dr. Rafael Rubio and Dr. Federico Pulido and from the Hospital La Paz, Madrid, Spain. Each sample was accessed upon informed consent under an internal review board approved protocol and were then stored in the Biobank of Laboratory of Microbiology. Some HIV-1 envelopes from HIV-1 controllers and patients with chronic HIV-1 infection included in this thesis were kindly provided by Cecilio Lopez Galindez (Centro Nacional de Microbiología, Madrid, Spain) and by Miguel Thomson (Centro Nacional de Microbiología, Madrid, Spain).

2. 2. Plasmids: pcDNA3.1/V5-His TOPO TA-HIV-1 env, pNL4-3.Luc.R-E- (See Chapter I. 2. 1)

2. 3. Isolation of whole blood DNA (*QIAamp DNA Mini Kit*, Qiagen)

Isolation of whole blood DNA was performed by using of *QIAamp DNA Mini Kit* (Qiagen). Proteinase K (Qiagen) in volume of 40 μl was pipetted into the bottom of a 1.5 ml microcentrifuge tube. The 400 μl of sample was added to the tube followed by 400 μl of Buffer AL. The sample was mixed by pulse-vortexing for 15 sec and incubated at 56º C for 10 min. After incubation, the tubes were centrifuged briefly to remove drops from the inside of the lid. Next, 400 μl of ethanol (96-100%) was added to the sample and mixed again by pulse-vortexing for 15 sec. After mixing, the microcentrifuge tubes were centrifuged briefly. The mixture was carefully applied to the QIAamp Spin Column (in a 2 ml collection tube) without wetting the rim, the cap was closed and the columns were centrifuged at 6000 g (8000 rpm) for 1 min. The QIAamp Spin Column was placed in a clean 2 ml collection tube and the filtrate was discarded. Then 500 μl of Buffer AW1 was added and the tubes were centrifuged at 6000 g (8000 rpm) for 1 min. The QIAamp Spin Column was again placed in a clean 2 ml collection tube and the filtrate was discarded. The 500 μl of Buffer AW2 was added and the tubes were centrifuged at full speed (20000 g; 14000 rpm) for 3 min. The QIAamp Spin Column was again placed in a new 2 ml collection tube and the filtrate was discarded. Next, the tubes were centrifuged at 20000 g (14000rpm) for 1 min. The QIAamp Spin Column was placed in a clean 1.5 ml microcentrifuge tube and the collection tube containing the filtrate was discarded. Then, 100 μl of Buffer AE or distilled water was added. The tubes were incubated at RT for 5 min and centrifuged at 6000 g (8000 rpm) for 1 min.

2. 4. Purification of viral RNA (*QIAamp RNA Mini Kit*, Qiagen)

Purification of viral RNA was performed by using of *QIAamp RNA Mini Kit* (Qiagen). Buffer AVL containing carrier RNA was pipetted in a volume of 560 μl into the bottom of a 1.5 ml microcentrifuge tube. The 140 μl of plasma sample was added to the Buffer AVL-carrier RNA and mixed by pulse-vortexing for 15 sec. The sample was incubated at RT for 10 min to lyse completely viral particles. After incubation, the tubes were cen-

trifuged briefly to remove drops from the inside of the lid. Next, 560 µl of ethanol (96-100%) was added to the sample and mixed by pulse-vortexing for 15 sec. After mixing, the microcentrifuge tubes were again centrifuged briefly. The 630 µl of the solution was carefully applied to the QIAamp Mini Spin Column (in a 2 ml collection tube) without wetting the rim, the cap was closed and the columns were centrifuged at 6000 g (8000 rpm) for 1 min. The QIAamp Mini Spin Column was placed in a clean 2 ml collection tube and the filtrate was discarded. Then, the rest of the solution was applied to the column and centrifuged at 6000 g (8000 rpm) for 1 min. The 500 µl of Buffer AW1 was added to the tubes, the caps were closed and the microcentrifuge tubes were centrifuged at 6000 g (8000 rpm) for 1 min. The QIAamp Mini Spin Column was again placed in a clean 2 ml collection tube and the filtrate was discarded. The 500 µl of Buffer AW2 was added and the tubes were centrifuged at full speed (20000 g; 14000 rpm) for 3 min. The QIAamp Mini Spin Column was again placed in a new 2 ml collection tube and the filtrate was discarded. Next, the tubes were centrifuged at 20000 g (14000rpm) for 1 min to eliminate residual AW2 Buffer. The QIAamp Mini Spin Column was placed in a clean 1.5 ml microcentrifuge tube and the collection tube containing the filtrate was discarded. Then, 40 µl of Buffer AVE was added. The tubes were incubated at room temperature for 5 min and centrifuged at 6000 g (8000 rpm) for 1 min.

2. 5. Synthesis of HIV-1 cDNA

The viral cDNA was synthesized by using SuperScriptIII System (Invitrogen). Each sample was synthesized by using envelope-specific outer reverse primer OAS.

OAS: 5′ TTGCTACTTGTGATTGCTCCATGT 3′

Each cDNA reaction was performed in a final volume of 40 µl using 500 ng – 1 µg of total RNA for reaction. The following components: 2 pmol of gene-specific OAS primer, 10 mM of each dNTPs, 500 ng – 1 µg of total RNA in a total volume of 26 µl were added to a nuclease-free microcentrifuge tube, heated at 65º C for 10 min and then in-

cubated on ice for 2 min. Next, the 14 µl of reaction mixture containing 1X First-Strand Buffer, 5 mM DTT, 80 units of RNaseOUT™ Recombinant RNase Inhibitor, 400 units of SuperScriptIII was added into each reaction tube. The reaction mixture was mixed by pipetting gently up and down. RT-PCR cycle for the generating cDNA was: 25° C for 10 min, followed by incubation at 50° C for 40 min and inactivation at 70° C for 15 min. The synthesized cDNA was then used as a template for the amplification by PCR.

2. 6. Amplification of HIV-1 envelope sequences by PCR

The envelope sequence of HIV-1 was amplified by using Expand High Fidelity PCR System (Roche) in Thermo Cycler 2720 (Applied Biosystems). Each sample was amplified by nested PCR using a set of outer primers OS/OAS and a set of inner primers IS/IAS.

OS: 5′ TAGAGCCCTGGAAGCATCCAGGAAG 3′

OAS: 5′ TTGCTACTTGTGATTGCTCCATGT 3′

IS: 5′ GATC**AAGCTT**TAGGCATCTCCTATGGCAGGAAGAAG 3′

HindIII restriction site

IAS: 5′ AGCT**GGATCC**GTCTCGAGATACTGCTCCCACCC 3′

BamHI restriction site

Each first-round PCR reaction was performed in a final volume of 50 µl using 750 ng – 1 µg of total cellular DNA or 7.5 µl of cDNA for reaction. Reactions were performed as follows: 1X Expand High Fidelity Buffer (with 15 mM $MgCl_2$), 0.25 mM $MgCl_2$, 0.2 mM dNTP, 0.5 µM of each primer and 1 unit of Expand High Fidelity Polymerase (Roche). PCR cycle for the first-round PCR was: 94° C for 3 min as initial denaturation, followed by 94° C for 15 sec, 50° C for 30 sec and 72° C for 5 min. After 10 cycles, the step of extension was modified by adding 5 sec to each subsequent cycle (5 min + 5 sec/cycle).

The PCR reaction was run for 20 more cycles followed by final extension at 72° C for 10 min. For the second-round PCR, the amplification was performed in a final volume of 50 μl using 3-5 μl of first-round PCR product. The conditions of second-round PCR were as follows: 1X Expand High Fidelity Buffer (with 15 mM $MgCl_2$), 0.25 mM $MgCl_2$, 0.2 mM dNTP, 0.5 μM of each primer and 1 unit of Expand High Fidelity Polymerase (Roche). The second-round PCR cycle was: 3 min at 94° C followed by 15 sec at 94° C, 30 sec at 60° C, 2.5 min at 72° C. After 10 cycles, the step of extension was modified by adding 5 sec to each subsequent cycle (5 min + 5 sec/cycle). The PCR reaction was run for 20 cycles followed by final extension at 72° C for 10 min. PCR amplicons were visualized on a 0.8% agarose gel stained with ethidium bromide. The second-round PCR using primers IS/IAS results in a product of approximately 2.8-3 kb.

2. 7. Cloning of HIV-1 envelopes into pcDNA3.1/V5-His TOPO by ligation and transformation of competent bacteria TOP10-F (*Invitrogen*)

Each HIV-1 envelope obtained by nested PCR was cloned into pcDNA3.1/V5-His TOPO (Invitrogen). The cloning reaction was as follows: 2 μl of PCR product, 1 μl of Salt Solution, 2 μl of H_2O, 1 μl of TOPO vector. The reaction was mixed gently and incubated at RT (22-23º C) for 30 min. Next, the ligation reaction was added into a tube with competent bacteria cells and mixed gently. The transformation reaction was incubated on ice for 30 min. Next, the heat-shock was performed on competent bacteria cells for 30 sec at 42º C without shaking. After heat-shock, the tubes were immediately transferred on ice. Following 10 min of incubation on ice, 250 μl of RT SOC medium was added into the tubes. The tubes were capped and incubated for 1 h at 37º C with shaking 200-250 rpm. Next, the tubes were centrifuged at 1000 rpm for 5 min and half of medium was removed. The rest of each transformation was resuspended, spread on the selective plates (LB^+) and incubated up-side-down overnight at 37º C. The next day, the plate was analyzed, the colonies were picked up and cultured for further isolation of plasmid DNA.

2. 8. Isolation of plasmid DNA (*QIAprep Spin MiniPrep Kit,* Qiagen)

One day before isolation, 3 ml of LB (supplemented with proper antibiotic) were inoculated with 30 μl of bacteria carrying desired plasmid or 1 single colony picked from LB^+ agar plates and cultured overnight with shaking (250 rpm) at 37º C. The following day, the bacteria culture was pelleted by centrifugation at 6500 rpm for 10 min at RT and the isolation of plasmid DNA was performed by using *QIAprep Spin MiniPrep Kit* (Qiagen). The pelleted bacteria were resuspended in 250 μl of Buffer P1 and transferred into microcentrifuge tubes. Next, 250 μl of Buffer P2 was added and tubes were mixed thoroughly by inverting 6 times until the solution become clear. After 5 min of incubation, 350 μl of Buffer N3 was added and the tubes were mixed immediately thoroughly by inverting 6 times. The tubes were centrifuged for 10 min at 13000 rpm. Then, the supernatant after centrifugation was applied into QIAprep spin column by pipetting. The columns were centrifuged for 1 min at 13000 rpm and the flow-through was discarded. Next, 0.5 ml of Buffer PB was added, the columns were centrifuged for 1 min at 13000 rpm and the flow-through was discarded. Then, QIAprep spin columns were washed by centrifugation for 1 min at 13000 rpm with 0.75 ml of Buffer PE. The flow-through was discarded and the columns were centrifuged for an additional 1 min to remove residual wash buffer. The QIAprep spin column were placed into a clean 1.5 ml microcentrifuge tubes. To elute DNA, 50 μl of Buffer EB was added into column, incubated for 5 min and centrifuged for 1 min at 13000 rpm.

2. 9. Isolation of plasmid DNA (*PureLink HiPure Plasmid Filter MaxiPrep*, Invitrogen)

One day before isolation, 150 ml of LB (supplemented with proper antibiotic) were inoculated with 75-150 μl of bacteria carrying desired plasmid and cultured overnight with shaking (250 rpm) at 37º C. The next day, the bacteria culture was harvested by centrifugation at 4000 rpm for 30 min at 4º C and the plasmid DNA was isolated by using *PureLink HiPure Plasmid Filter MaxiPrep* (Invitrogen). The supernatant was removed

and harvested bacteria were resuspended in 10 ml of Resuspension Buffer (R3) with RNase A. Next, 10 ml of Lysis Buffer (L7) was added and bottles were mixed gently by inverting until the lysate mixture was homogeneous. After 5 min of incubation, 10 ml of Precipitation Buffer (N3) was added and the bottles were mixed again by inverting. Immediately after this step, the precipitated lysate was transferred into equilibrated (with 30 ml of Equilibrating Bufer EQ1) HiPure Filter Maxi Column. The lysate was let to run through the filter by gravity flow until the flow stops or becomes very slow (<1 drop per 10 sec). The flow-through was discarded and the HiPure Filter Maxi Column was additionally washed with 10 ml of Wash Buffer (W8) to increase final DNA yield. Immediately after the HiPure Filter Maxi Column has stopped dripping, the Filtration Cartridge from the column was removed. The column was then washed with 50 ml of Wash Buffer (W8) allowing the solution to flow by gravity flow. The flow-through was discarded and the column was placed into new 50 ml tube. The DNA was eluted by 15 ml of Elution Buffer (E4). The solution was let to drain by gravity flow. The HiPure Filter Maxi Column was discarded and the flow-through was precipitated by adding 10.5 ml of isopropanol and centrifugation at 12000 g for 45 min at 4º C. After centrifugation, the supernatant was carefully discarded and 5 ml of cold 70% ethanol was added. The tubes were again centrifuged at 12000 g for 30 min at 4º C. The supernatant was then removed and the pellet was let to air-dry for 10 min. The DNA pellet was resuspended in 300 μl of TE Buffer (TE) and the DNA concentration was subsequently measured. The purified DNA was stored at -20º C.

2. 10. Screening of cloned envelopes by restriction digestion

After isolation of plasmid DNA, the cloning efficiency and the orientation of the insert (cloning into pcDNA3.1/V5-His TOPO is bi-directional) were verified by restriction digestion. The reaction mix of total volume 20 μl was composed of: 500 ng of DNA, 1X of Restriction Buffer, 1X of BSA, 1U of BamHI. The reaction was then incubated for 2 h at 37º C and visualized on a 0.8% agarose gel stained with ethidium bromide to check the orientation of the HIV-1 envelope cloned into pcDNA3.1/V5-His TOPO.

2. 11. Sequencing of HIV-1 envelopes

PCR-sequencing reaction was performed by using of *ABI PRISM BigDye Terminator v3.1 Cycle Sequencing* (Applied Biosystems). The PCR products were first purified with 2 μl of the ExoI/SAP-IT (2 μl of the ExoI/SAP-IT per 5 μl of PCR product) by incubation at 37º C for 15 min. After PCR clean-up treatment, ExoI/SAP-IT was inactivated by heating at 80º C for 15 min. ExoI/SAP-IT (USB) is composed of two hydrolytic enzymes, Exonuclease I and Shrimp Alkaline Phosphatase. Exonuclease I degrades residual single-stranded primers and single-stranded DNA produced by PCR. The Shrimp Alkaline Phosphatase hydrolyses remaining dNTPs from PCR mixture, which would interfere with sequencing reaction.

For the each well of 96-well plate the reaction mix of final volume 10 μl was prepared as follows: 1 μl of the reaction mix BigDye, 1 μl of primer at the concentration of 4 μM, 2 μl of BigDye Reaction buffer and DNA (30–90 ng of HIV-1 envelope PCR product or 200-500 ng of plasmid pcDNA3.1/V5-His TOPO-HIV-1 envelope). Each sequencing reaction was amplified in the termocycler 2720 (Applied Biosystems). The PCR cycle was: initial denaturation of 1 min at 96º C, denaturation of 10 sec at 96º C, annealing of 5 sec at 50º C and extension of 4 min at 60º C. The cycle was repeated 25 times and the PCR product was left to cool at 4º C.

Primers used for sequencing of HIV-1 envelopes:

- **gp120:**

AV304 5′ ACATGTGGAAAAATGACATGGT 3′ (HxB2: 6501-6522)

AV305 5′ GAGTGGGGTTAATTTTACACATGG 3′ (HxB2: 6572-6595)

AV306 5′ TGTCAGCACAGTACAATGTACACA 3′ (HxB2: 6937-6960)

AV307 5′ TCTTCTTCTGCTAGACTGCCAT 3′ (HxB2: 6999-7020)

AV308 5′ TCCTCAGGAGGGGACCCAGAAATT 3′ (HxB2: 7304-7327)

AV309 5′ CARTAGAAAAATTCYCCTCYACA 3′ (HxB2: 7346-7368)

AV313 5′ TCCYTCATATYTCCTCCTCCAGGTC 3′ (HxB2: 7620-7644)

- **gp41:**

AV322 5′ AAGCAATGTATGCCCCTCC 3′ (HxB2: 7509-7527)

AV323 5′ CTGCTCCYAAGAACCCAA 3′ (HxB2: 7771-7790)

AV324 5′ GGCAAAGAGAAGAGTGGT 3′ (HxB2: 7714-7731)

AV326 5′ TTGGGGYTGCTCTGGAAAAC 3′ (HxB2: 7999-8018)

AV327 5′ TTTTATATACCACAGCCA 3′ (HxB2: 8246-8263)

AV328 5′ ATAATGATAGTAGGAGG 3′ (HxB2: 8270-8286)

AV329 5′ GTCCCAGAAGTTCCACA 3′ (HxB2: 8557-8573)

AV330 5′ GGARCCTGTGCCTCTTCA 3′ (HxB2:8496-8513)

AV331 5′ TCTCATTCTTTCCCTTA 3′ (HxB2: 8833-8849)

2. 12. Automatic sequencing

The sequencing was performed in automatic ABI PRISM 3100-Avant Genetic Analyzer (Applied Biosystems). The PCR products, amplified previously by BigDye chemistry, were resuspended in 20 µl of formamide at RT. Before placing in the sequencer, the 96-well plate with all PCR products was vortexed for 15 sec and centrifuged at 2000 g for 1 min.

2. 13. Analysis of sequences

The sequences were obtained from automatic sequencer ABI PRISM 3100 in a form of chromatograms. The chromatograms were analyzed, assembled with the reference sequence to form the full length fragment (contig) of desired product and edited by Geneious Bioinformatics Software.

2. 14. Genotypic prediction of HIV-1 coreceptor usage

The nucleotide sequences corresponding to the region V3 of the HIV-1 gp120 were analyzed and utilized for genotypic prediction of HIV-1 tropism, that is determined by usage of coreceptors: either CCR5 (R5 tropic viruses) or CXCR4 (X4 tropic viruses), by using geno2pheno algorithm (www.geno2pheno.org) at the 5.75% false positive rate.

2. 15. Production of recombinant viruses (See Chapter I. 2. 3.)

2. 16. Infection in *trans* experiment with HIV-1 GP-pseudotyped retroviruses (See Chapter 1. 2. 5)

3. RESULTS

3. 1. Analysis of HIV-1 envelope sequences from clinical isolates

The HIV-1 envelopes were obtained by RT-PCR, cloned and sequenced. The sequences of 30 HIV-1 envelopes (elite controllers–6, viremic controllers–8, patients with chronic infection–16) were analyzed by using Geneious Bioinformatics Software V6.1. The length and the number of N-glycosylation sites (PNGS) were determined in each variable loop (VL) (Table 2 and Table 3). The length of V1 was 24-40 aa and the number of N-glycosylation sites was 3–6 PNGS (Fig. 51A). The length of V2 was 37-53 aa and the

number of PNGS was 1-5 PNGS (Fig. 51B). The total length of V1V2 varied significantly in all envelopes and was in the range 61-83 aa and the number of PNGS was 4-9 PNGS. The region of V3 is the most conserved in all envelopes since it is responsible for the interaction with the proper coreceptor on the host cell surface. The length of V3 was 34-36 aa. The number of PNGS in all envelopes was 1 (Fig. 52A). The length of V4 varied in 30 HIV-1 envelopes from 27 to 40 aa and the number of PNGS was 3-6 PNGS (Fig. 52B). The V5 region is the shortest VL of HIV-1 envelope. The length of V5 was 10-18 aa and the number of PNGS was 0-3 PNGS (Fig. 52C). The total length of VL in 30 HIV-1 envelopes was 139-164 aa and the number of PNGS was 9–16. The full gp160 length was in range 843-874 aa and the number of PNGS was 26-36. The gp120 length was 498-524 aa and the number of PNGS was 22-32. The length of gp41 was in range 344-353 aa. The number of N-glycans in gp41 was 4-7 PNGS (Table 2 and Table 3).

3. 2. Genotypic prediction of HIV-1 clinical isolates coreceptor usage

The tropism of each HIV-1 variant was predicted by geno2pheno statistical tool at the significance level of 2% and 5.75% that are optimized cut offs based on analysis of clinical data from MOTIVATE clinical trial (McGovern et al., 2010). The significance level (false positives rate = FPR) is the probability of classifying an R5-virus falsely as X4. The evaluation of the results by geno2pheno is based on publically available data of 1100 V3 sequences (769 R5, 210 X4, 131 R5X4) from 332 patients (mainly from the HIV sequence database in Los Alamos, but also from scientific publications that have not been included in the Los Alamos database so far). The classification of the tropism and the FPR value for each HIV-1 envelope was determined (Table 4). The analysis of V3 region of gp120 in the group of patients showed that 28 out of 30 sequences were classified as R5 by geno2pheno tool. The envelope HIV-1 9-6 and 13-6 were predicted to be X4 tropic (FPR of 0.5% and 5.3% respectively).

	env	V1 aa	V1 N	V2 aa	V2 N	V1V2 aa	V1V2 N	V3 aa	V3 N	V4 aa	V4 N	V5 aa	V5 N
1	**3-1**	27	3	53	5	79	8	35	1	34	6	14	1
2	**9-6**	32	3	38	2	69	5	36	1	34	5	12	1
3	**12-2**	26	3	40	2	65	5	35	1	33	5	11	1
4	**15-7**	26	3	40	2	65	5	35	1	30	3	12	1
5	**19-10**	40	6	42	2	81	8	35	1	30	4	13	2
6	**36-4**	26	3	40	2	65	5	35	1	32	4	12	1
7	**37-2**	25	3	40	1	64	4	35	1	28	4	12	0
8	**40-2**	37	5	43	1	79	6	35	1	31	5	13	1
9	**88-1**	30	4	46	2	75	6	35	1	30	4	11	2
10	**84-35***	27	4	41	3	67	7	35	1	32	5	11	2
11	**65-4***	32	4	40	2	61	6	35	1	36	5	10	1
12	**2-1***	31	4	40	2	70	6	34	1	29	4	17	2
13	**10-4***	26	3	46	3	71	6	35	1	33	4	14	2
14	**13-6***	24	3	39	2	62	5	35	1	27	5	13	1
media Controllers		**29,2**	**3,6**	**42**	**2,2**	**69,5**	**5,8**	**35**	**1**	**31,4**	**4,5**	**12,5**	**1,3**
15	**8-13**	33	6	39	2	72	8	35	1	31	5	15	2
16	**16-4**	26	3	48	3	73	6	35	1	28	5	13	1
17	**17-10**	31	4	42	3	72	7	35	1	31	5	15	2
18	**18-4**	35	4	49	3	83	7	35	1	33	4	13	2
19	**22-78**	29	5	40	2	68	7	35	1	31	5	12	1
20	**22-52**	28	4	39	2	66	6	35	1	33	5	13	2
21	**26-56**	31	4	47	3	77	7	34	1	28	4	16	2
22	**26-88**	25	4	42	2	66	6	35	1	29	3	14	2
23	**28-80**	25	3	44	3	68	6	35	1	32	4	13	1
24	**29-01**	29	6	42	1	70	7	35	1	29	3	14	2
25	**29-14**	27	4	37	2	63	6	35	1	31	5	12	2
26	**26-87**	26	3	40	2	65	5	35	1	31	5	17	2
27	**27-54**	25	4	40	1	64	5	35	1	31	4	15	1
28	**28-46**	32	6	45	3	76	9	35	1	33	5	18	3
29	**23-13**	36	5	38	2	73	7	34	1	31	4	14	2
30	**20-41**	26	3	47	3	72	6	35	1	40	4	12	2
media IC		**29**	**4,2**	**42,4**	**2,3**	**70,5**	**6,56**	**34,9**	**1**	**31,4**	**4,4**	**14,1**	**1,8**

Table 2. Comparison of the length and PNGS number in 30 HIV-1 clinical isolates (14 HIV-1 controllers and 16 chronically infected patients, IC).

	env	HIV-1 stage	DC-SIGN ratio (J)	DC-SIGN ratio (R)	Tropism	FPR (%)	Net charge	VL length	VL PNGS	gp120 length	gp120 PNGS	gp41 length	gp41 PNGS	gp160 length	gp160 PNGS
1	**3-1**	EC	8,57	21,62	R5	57,1	19,516	162	16	522	29	345	4	867	33
2	**9-6**	VC	25,33	25,01	X4	0,5	23,516	151	12	514	25	345	7	859	32
3	**12-2**	VC		53,83	R5	55,3	20,516	144	12	505	24	345	5	850	29
4	**15-7**	EC	13,06	49,71	R5	30,1	17,516	142	10	503	22	345	5	848	27
5	**19-10**	VC	8,99	5,61	R5	21	14,102	159	15	521	29	344	5	865	34
6	**36-4**	EC	86,35	16,31	R5	24,7	23,516	144	11	505	22	345	5	850	27
7	**37-2**	EC	21,58	38,33	R5	96,5	16,516	139	9	501	22	345	4	846	26
8	**40-2**	EC	22,66	11,85	R5	12,1	15,102	158	13	521	25	345	5	866	30
9	**88-1**	EC		46,45	R5	28,8	19,223	151	13	514	28	346	5	860	33
10	**84-35***	VC		41,03	R5	78,8	16,516	145	15	507	28	346	5	853	33
11	**65-4***	VC		39,61	R5	32,4	15,809	142	13	515	28	346	4	861	32
12	**2-1***	VC	59,28	121,58	R5	14,8	25,102	150	13	514	26	345	5	859	31
13	**10-4***	VC	56,29	56,92	R5	35,6	20,688	153	13	512	27	345	4	857	31
14	**13-6***	VC	53,74	92,85	X4	5,3	18,516	139	12	498	24	345	5	843	29
media EC+VC			**32,84**	**45,49**		**35,21**	**19,01**	**148,50**	**12,64**	**510,86**	**25,64**	**345,14**	**4,86**	**856,00**	**30,50**
15	**8-13**	CI	20,84	26,23	R5	63,1	17,516	152	16	516	32	345	4	861	36
16	**16-4**	CI	13,77	7,96	R5	35,3	16,688	149	13	510	26	346	4	855	30
17	**17-10**	CI	25,41	13,32	R5	21,2	13,516	153	15	514	27	345	4	860	31
18	**18-4**	CI	18,68	17,64	R5	79,5	17,809	164	15	524	28	345	4	869	32
19	**22-78**	CI		22,20	R5	91,9	24,637	146	14	506	27	346	5	852	32
20	**22-52**	CI		13,47	R5	29,5	19,223	147	14	508	25	353	5	861	30
21	**26-56**	CI		33,50	R5	10,2	20,223	155	14	512	27	344	5	856	32
22	**26-88**	CI		46,46	R5	8,1	19,102	144	12	505	23	345	5	850	28
23	**28-80**	CI		27,72	R5	13	14,223	148	16	509	26	344	4	853	30
24	**29-01**	CI		28,36	R5	48,9	16,102	148	13	507	28	346	5	853	33
25	**29-14**	CI		5,32	R5	27,1	21,102	141	14	500	29	344	5	844	33
26	**26-87**	CI		23,82	R5	30,1	19,809	148	13	507	25	345	5	852	30
27	**27-54**	CI		14,82	R5	6	20,516	145	11	503	23	345	5	848	28
28	**28-46**	CI		10,42	R5	34,6	19,102	162	18	522	30	345	4	867	34
29	**23-13**	CI		9,60	R5	78,8	23,102	152	14	512	26	345	5	857	31
30	**20-41**	CI		5,86	R5	12,5	17,102	159	16	522	24	346	4	868	28
media IC			**17,4**	**20,42**		**36,86**	**18,74**	**150,81**	**14,25**	**511,06**	**26,63**	**345,56**	**4,56**	**856,63**	**31,13**

Table 3. Characteristics of 30 HIV-1 clinical isolates including: patient information, sequence analysis and DC-SIGN-mediated *trans*-infection.

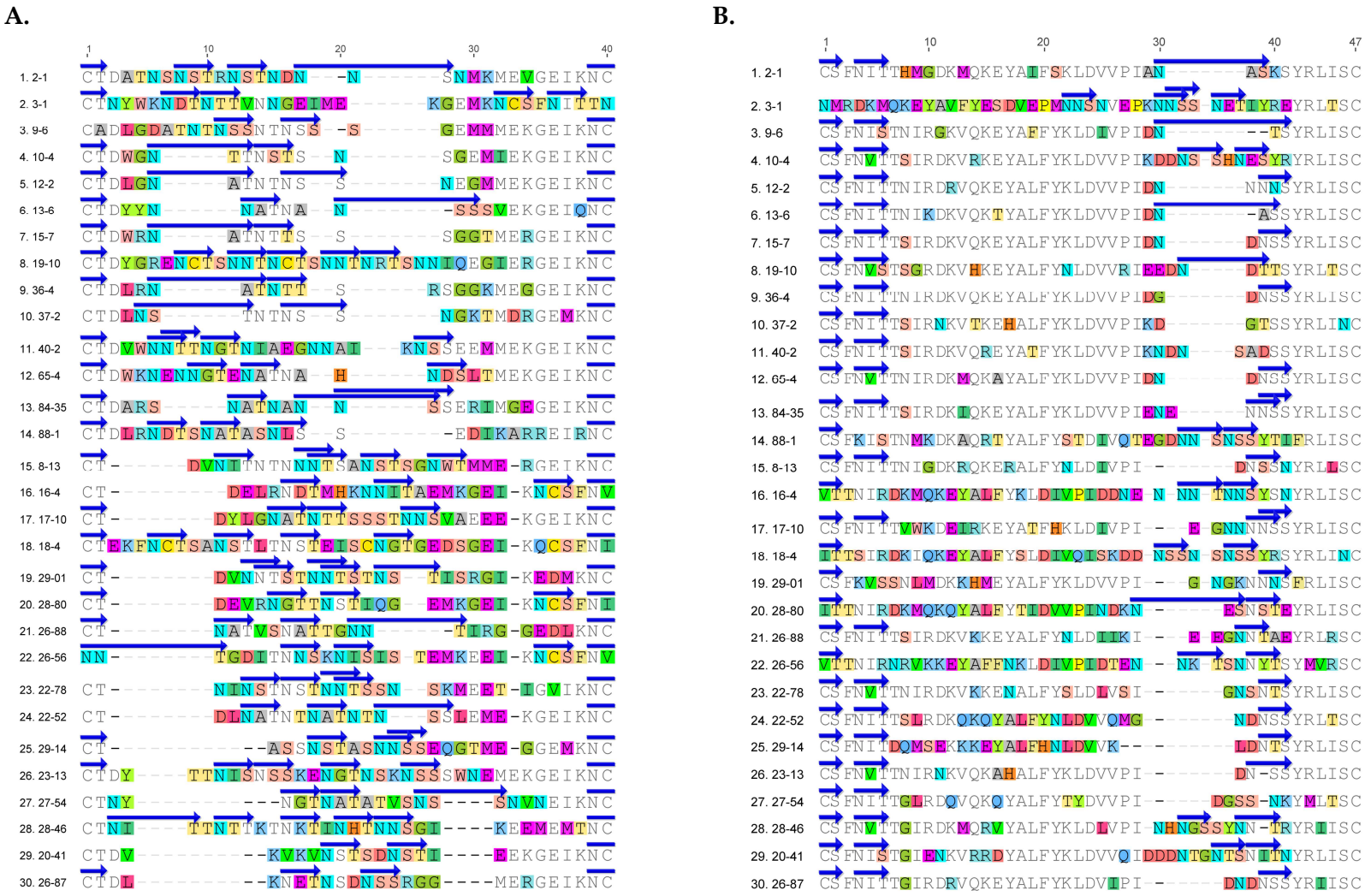

Figure 51. Alignment of 30 HIV-1 envelopes representing: **A.** V1 loop. **B.** V2 loop.

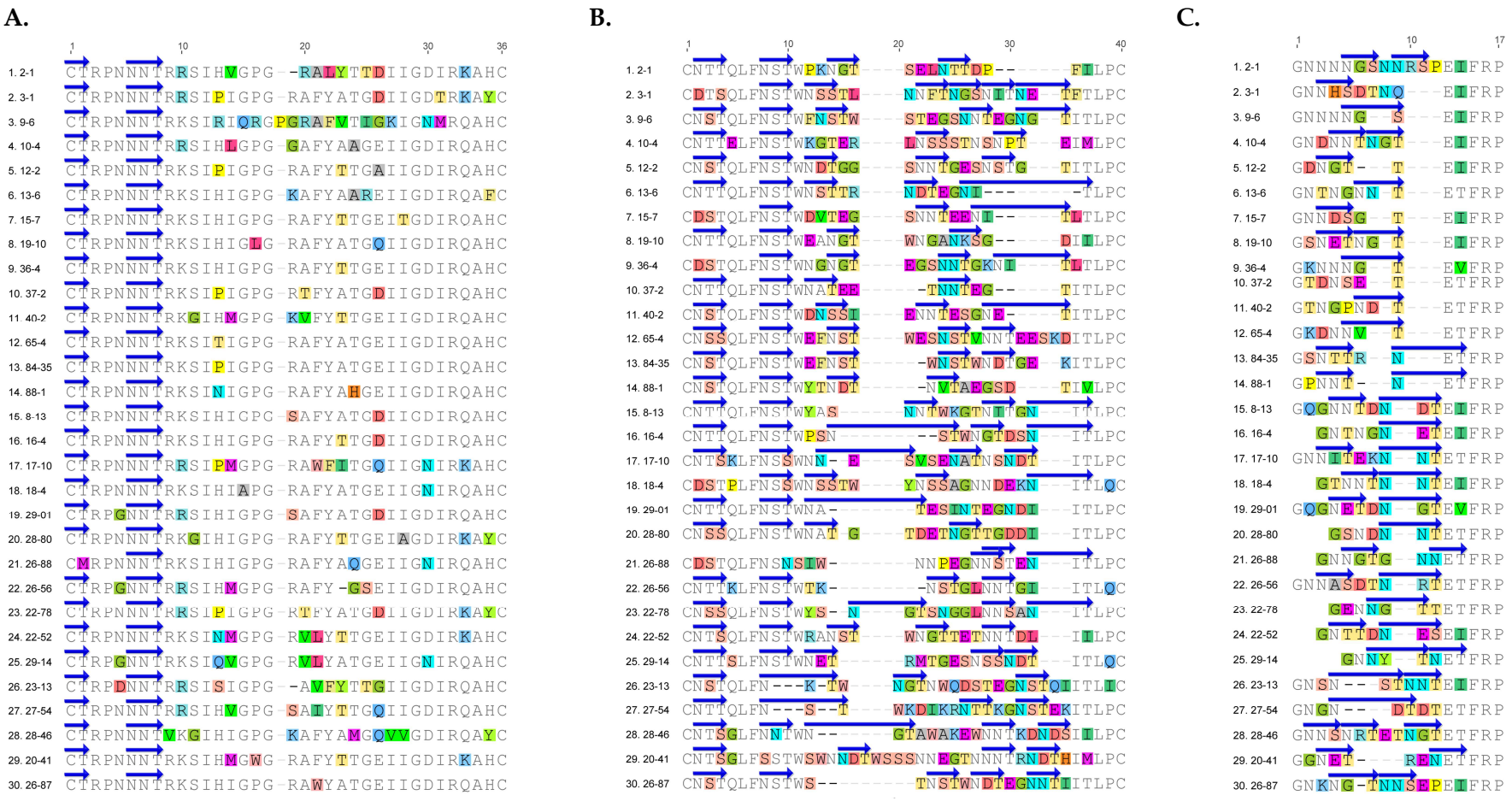

Figure 52. Alignment of 30 HIV-1 envelopes representing: **A.** V3 loop. **B.** V4 loop. **C.** V5 loop.

	envelope	subtype	tropism	FPR (%)
1	**3-1**	B	R5	57.1
2	**9-6**	B	X4	0.5
3	**12-2**	B	R5	55.3
4	**15-7**	B	R5	30.1
5	**19-10**	B	R5	21
6	**36-4**	B	R5	24.7
7	**37-2**	B	R5	96.5
8	**40-2**	B	R5	12.1
9	**88-1**	B	R5	28.8
10	**84-35***	B	R5	78.8
11	**65-4***	B	R5	32.4
12	**2-1***	B	R5	14.8
13	**10-4***	B	R5	35.6
14	**13-6***	B	X4	5.3
15	**8-13**	B	R5	63.1
16	**16-4**	B	R5	35.3
17	**17-10**	B	R5	21.2
18	**18-4**	B	R5	79.5
19	**22-78**	B	R5	91.9
20	**22-52**	CRF_14-BG	R5	29.5
21	**26-56**	B	R5	10.2
22	**26-88**	B	R5	8.1
23	**28-80**	B	R5	13
24	**29-01**	B	R5	48.9
25	**29-14**	B	R5	27.1
26	**26-87**	B	R5	30.1
27	**27-54**	B	R5	6
28	**28-46**	B	R5	34.6
29	**23-13**	B	R5	78.8
30	**20-41**	B	R5	12.5

Table 4. Coreceptor usage and the tropism prediction for 30 HIV-1 clinical isolates.

3. 3. Phenotypic prediction of HIV-1 clinical isolates coreceptor usage

The phenotypic assay to confirm the coreceptor usage of HIV-1 clinical isolates was performed in U87-R5 and U87-X4 cells. Cells were challenged in the infection in *cis* assay with recombinant retroviruses pseudotyped with each HIV-1 envelope variant. The results of the phenotypic assay confirmed the results obtained by bioinformatics tool geno2pheno and showed the usage of CCR5 coreceptor in 29 out of 30 HIV-1 envelopes and the usage of CXCR4 in only one envelope 9-6. Although genotypic test predicted

the X4 tropism for HIV-1 envelope 13-6 (FPR=5.3%), the phenotypic assay clearly revealed the usage of CCR5 receptor for this HIV-1 envelope (Fig. 53).

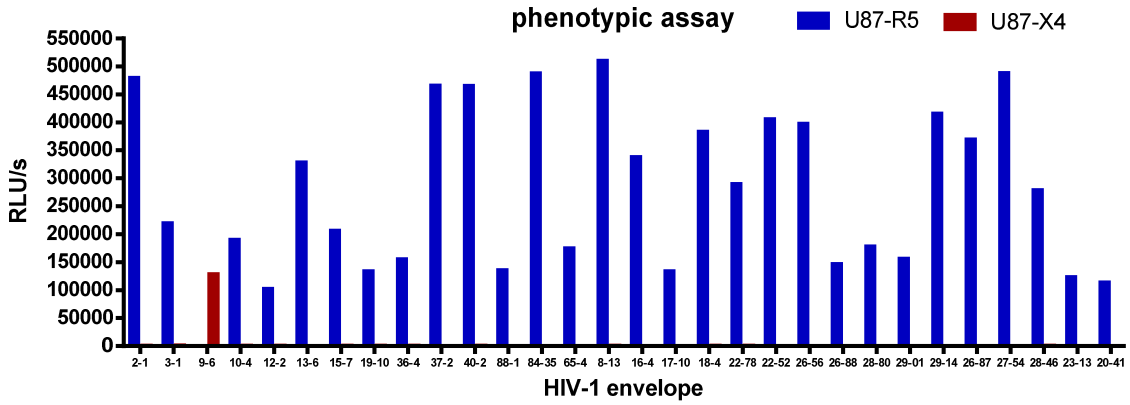

Figure 53. Phenotypic assay of the coreceptor usage of 30 HIV-1 clinical isolates. The tropism of the virus was studied in the infection in *cis* experiment, where U87-R5 (blue bars) and U87-X4 (red bars) cells were challenged with HIV-1 pseudotyped retroviruses.

3. 4. *Trans*-infection experiment with HIV-1 clinical isolates

The *trans*-infection experiment with 30 HIV-1 envelopes was performed to study the differences in DC-SIGN-mediated infection (EC-6, VC-8 and CI-16). A substantial group of EC HIV-1 envelopes (10 out of 16) could not be tested in the *trans*-infection experiments. All of 10 HIV-1 envelopes were confirmed as not defective by sequencing, however in cellular assay 4 out of 10 were observed non-functional and 6 out of 10 showed the infectivity continuously below dynamic range required for the infection experiments thus they were excluded from our analysis.

Infection in *trans* was performed on Raji DC-SIGN$^+$, which could capture and transmit HIV-1 pseudotyped retroviruses to susceptible cells. As a control, Raji cells, which did not express DC-SIGN on its surface, were used. The ratio between *trans*-infection Raji

DC-SIGN+ and Raji cells for 30 different HIV-1 envelopes was calculated as an average from at least 3-9 independent experiments. The results of the *trans*-infection ratio varied significantly among all HIV-1 envelopes, being in the range 121.58-5.32 in the Raji system (Fig. 54).

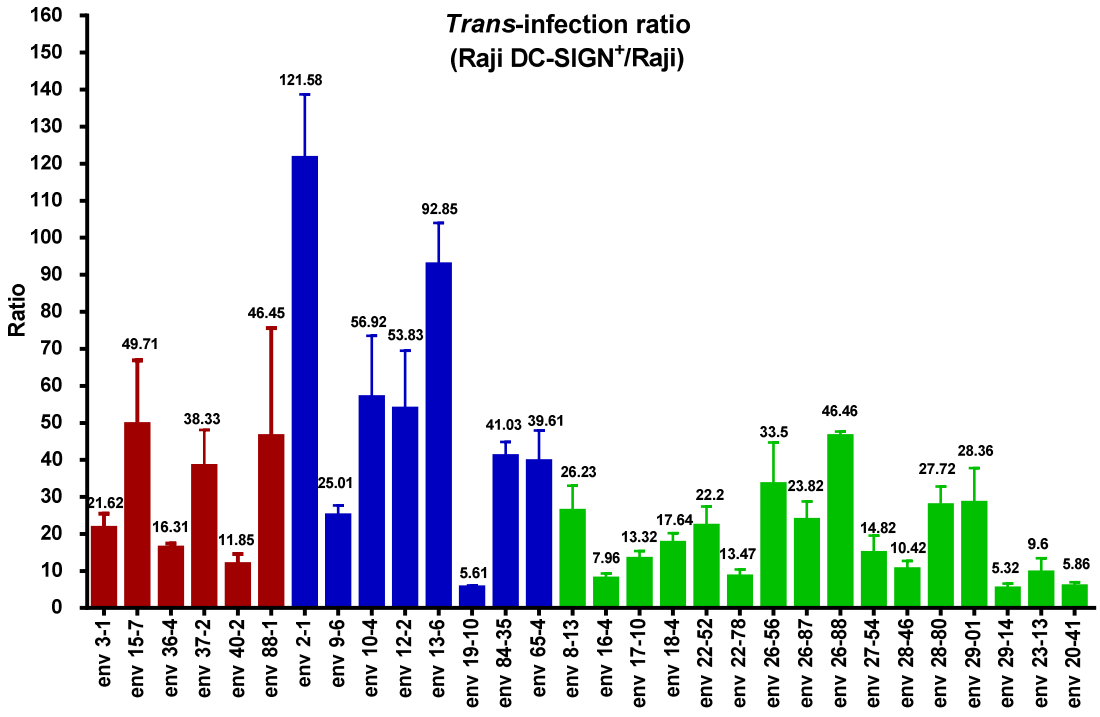

Figure 54. *Trans*-infection experiment in a group of EC (red), VC (blue) and patients with chronic HIV-1 infection (green) using Raji DC-SIGN+/Raji cellular system. The bars on the graph represent mean of the ratio with SEM error bars of 3-9 independent experiments.

3. 5. Analysis of *trans*-infection ratios in the groups of patients: Elite Controllers, Viremic Controllers and patients with chronic HIV-1 infection

The results of the *trans*-infection experiments were compared between different groups of patients to verify if the virological control might have any association with the ratio of *trans*-infection. The results obtained in the Raji DC-SIGN+/Raji system included 24 results from 6 HIV-1 envelopes of elite controllers, 30 results from 8 HIV-1 envelopes of viremic controllers and 72 results from 16 HIV-1 envelopes of patients with chronic HIV-1 infection. The statistical analysis of differences between the groups of patients

was performed by using Mann-Whitney test (GraphPad Prism V4). The results obtained in the analysis showed statistically significant differences between HIV-1 controllers and patients with chronic HIV-1 infection with the mean controllers=45.49 vs CI=20.42 (<p=0.0001) (Fig. 55).

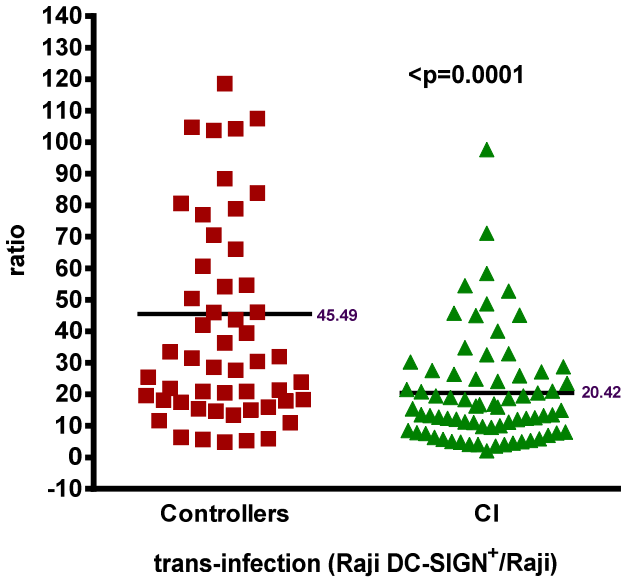

Figure 55. *Trans*-infection ratios of HIV-1 controllers (red) and of patients with chronic HIV-1 infection (green) using Raji DC-SIGN$^+$/Raji system. The statistical analysis was performed by using Mann-Whitney test.

These differences were further verified separately between the subgroups of HIV-1 controllers (elite and viremic controllers) to determine if the type of virological control could have influence DC-SIGN-mediated *trans*-infection result. The data obtained in this study clearly showed that the group of patients that was associated with higher DC-SIGN *trans*-infection was the subgroup of viremic controllers, patients at the limit of virological control. Significantly higher *trans*-infection ratio was observed in case of viremic controllers as compared with chronically infected patients (VC=56.6 vs CI=20.42, <p=0.0001) (Fig. 56). Interestingly, there was also a statistically significant difference in *trans*-infection ratio between VC and EC with the mean VC=56.6 vs EC=28.02 (p=0.0007) (Fig. 56). When analysing EC and CI patients no statistically significant vari-

ations were found, however there was a trend towards higher DC-SIGN-mediated *trans*-infection in EC individuals (EC=28.02 vs CI=20.42, p=0.1331) (Fig. 56).

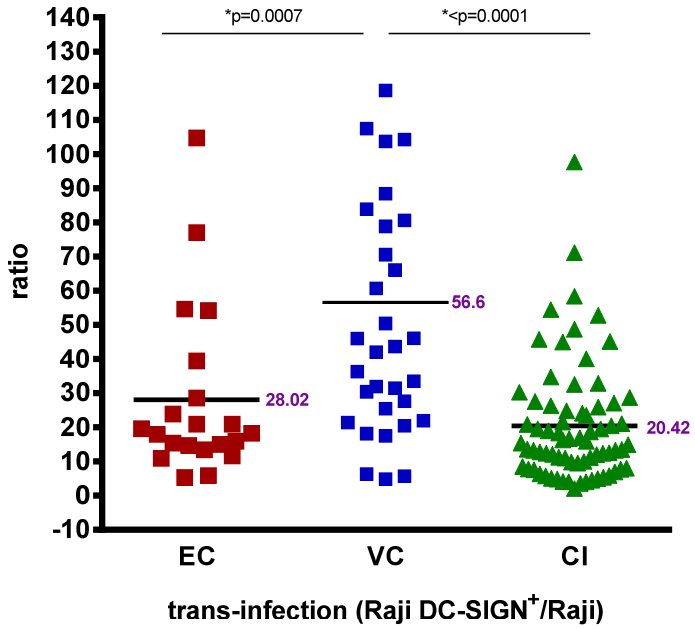

Figure 56. *Trans*-infection ratios of EC (red), VC (blue) and chronically infected patients (green) obtained in Raji DC-SIGN$^+$/Raji system. The statistical analysis was performed by using Mann-Whitney test.

3. 6. Analysis of differences in HIV-1 envelope sequence and *trans*-infection ratio between elite controllers, viremic controllers and patients with chronic HIV-1 infection

For the identification of factors responsible for the differences in the ratio of *trans*-infection, the length and PNGS in: gp160, gp120, gp40, V1-V5 were analyzed between EC, VC and CI (Table 2 and 3). No significant differences were found in V1-V4 regions with the exception of V5 (Fig. 57). The length of V5 was significantly shorter in the group of HIV-1 EC as compared with CI (EC=12.33 vs CI=14.13aa, p=0.0325). The group of VC also demonstrated a trend towards shorter V5 loop (VC=12.63 aa vs CI=14.13 aa,

p=0.0858). The number of PNGS in V5 was higher in the group of patients with chronic HIV-1 infection (EC=1 PNGS, VC=1.5 PNGS and CI=1.813, EC vs CI p=0.0072).

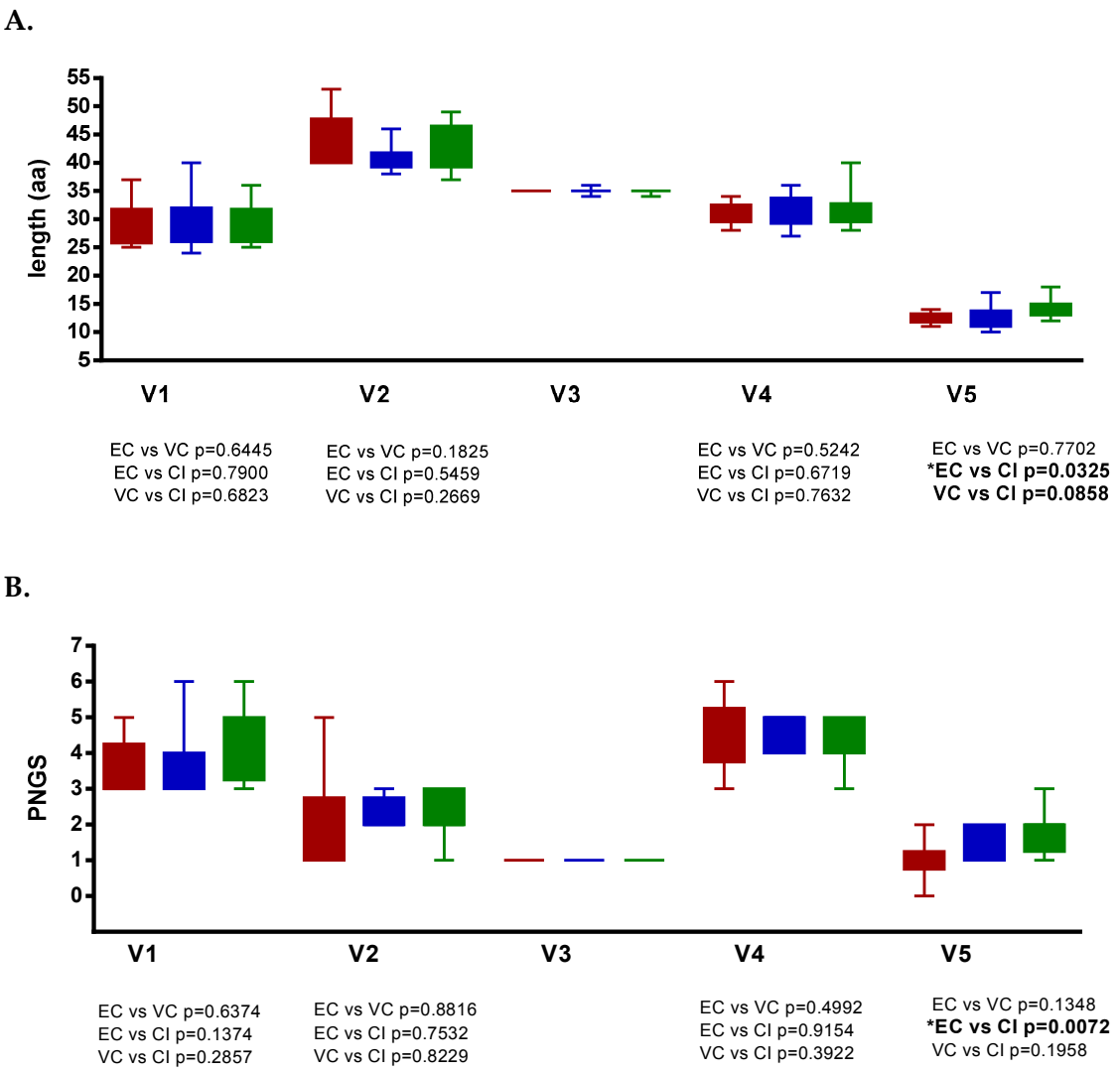

Figure 57. Comparison of: **A**. Length of each VL; **B.** PNGS in each VL; in EC (red), VC (blue) and patients with chronic HIV-1 infection (green). The statistical analysis was performed by using Mann-Whitney test.

Although the analysis of the HIV-1 envelope sequences between the patients showed statistically significant differences in V5 loop, there was no correlation found between the *trans*-infection ratio and the length of V5 (r=0.0925, p=0.6267) or the number of PNGS in V5 (r= -0.0895, p=0.6382) (Fig. 58).

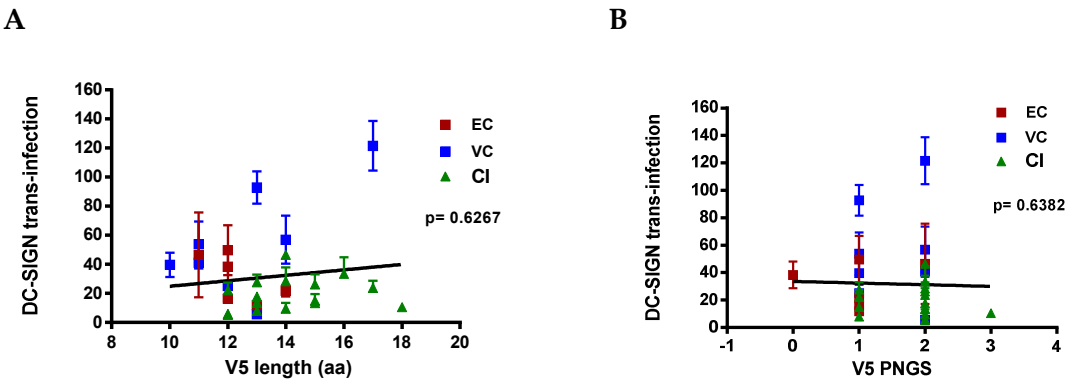

Figure 58. Correlation analysis between DC-SIGN *trans*-infection and: **A**. Length of V5. **B.** PNGS in V5. p values, estimated by using two-tailed t test, are shown on each graph.

4. DISCUSSION

The receptor DC-SIGN was initially cloned and characterized as a receptor for the HIV envelope glycoprotein gp120. In fact, it was precisely shown that gp120 affinity for DC-SIGN is even higher than for CD4 receptor, a classical HIV-1 entry receptor (Curtis et al., 1992). Years before the discovery of DC-SIGN, studies of Cameron *et al*. and Pope *et al.* showed that DC pulsed with HIV-1 endorsed infection of co-cultivated T cells (Cameron et al., 1992; Pope et al., 1994). Shortly after the identification of DC-SIGN, Geijtenbeek *et al.* defined this phenomenon as HIV-1 *trans*-infection (Geijtenbeek et al., 2000b). It has been clearly shown that DC-SIGN binds carbohydrate structures, such as mannose-containing glycoconjugates, expressed on the surface of different pathogens (den Dunnen et al., 2010). The envelope of HIV-1 is one of the most highly glycosylated proteins in nature, containing 22-32 PNGS in gp120. Therefore, many different *in vitro* studies evidently have shown the high affinity of HIV-1 envelopes to cells expressing DC-SIGN receptor. DC-SIGN does not function as a direct HIV-1 receptor but it works efficiently in the viral transmission from periphery to secondary lymphoid tissues. It has been demonstrated that HIV-1 particles bound to DC-SIGN are remarkably stable and retain infective for prolonged periods (Geijtenbeek et al., 2000b). Despite of all

proposed roles of DC-SIGN based on *in vitro* models, the confirmation of the physiological behaviour of DC-SIGN *in vivo* should be further clarified.

The changes in the length and the number of N-glycosylation sites over the time of HIV-1 epidemic might be explained by the adaptation of HIV-1 envelopes to human immune response. During HIV-1 infection many antibodies are generated, however most of them are non-neutralizing (Weiss et al., 1985). The humoral immune response to HIV-1 infection is usually characterized by rather low levels of NAbs. It has been shown that several functionally conserved regions of HIV-1 envelope might serve as potential targets for NAbs, such as the CD4-binding site, coreceptor-binding site and the regions of gp120 and gp41 responsible for the fusion to target cells (Li et al., 2006; Migueles et al., 2000). However, the restricted accessibility of these conserved domains leads to difficulties in efficient eliciting of NAbs. It has been also shown that HIV-1 envelope uses many different mechanisms to escape from antibody neutralization, such as amino acid substitutions, insertions in the variable loops of gp120 (Bunnik et al., 2008; Rong et al., 2007; Sagar et al., 2006) or increasing the number of glycans on its outer surface (Bunnik et al., 2008; Chackerian et al., 1997; Wei et al., 2003). It has been demonstrated that VLs of HIV-1 envelope tend to be shorter and contain fewer PNGS in viruses from early infection as compared to chronic isolates (Chohan et al., 2005; Frost et al., 2005). HIV-1-infected individuals develop neutralizing antibodies against HIV-1 envelope glycoprotein, which strongly drive the selection of antibody escape variants (Richman et al., 2003). Thus larger loops might mask epitopes recognized by those NAbs (Sagar et al., 2009). To date, several NAbs were described as having a broad potency to recognize and neutralize diverse HIV-1 isolates. Nevertheless, typically there is a long gap in the appearance of NAbs in the hosts. Over the time of infection escape mutants are selected mainly due to high levels of ongoing replication, thus by the time that NAbs are produced in the infected individuals, the newly produced viral particles are already resistant to neutralization (Richman et al., 2003; Wei et al., 2003). NAbs are developed against earlier viral isolates and reveal very low neutralizing activity against contemporary viruses (Skrabal et al., 2005; Tremblay and Wainberg, 1990). It was claimed that antibody response for HIV-1 infection appears to

be going constantly after moving target (Montefiori et al., 1996). Although shorter VLs with fewer PNGS are characteristic for early viruses, the loss of some specific PNGS has been shown to be associated with chronic infection. Gnanakaran *et al.* demonstrated that glycans at positions N188, N362, N462, N392, N397 and N356 plays a role in early stages of HIV-1 infection and are lost over the course of disease (Gnanakaran et al., 2011). N188 is involved in the interactions with CD4 and CCR5 (Ly and Stamatatos, 2000), N362 enhances fusogenicity at the moment of transmission (Sterjovski et al., 2007), glycans N392, N397 and N356 were shown to be part of "silent face" of gp120 responsible for binding to DC-SIGN enhancing therefore HIV-1 transmission (Geijtenbeek et al., 2000b; McCaffrey et al., 2004; Wyatt et al., 1998). N392 additionally was revealed to be to critical component of the epitope of the NAbs 2G12, thus the loss of this glycan site makes chronic isolates to be unrecognizable by this NAbs (Sanders et al., 2002).

In addition to humoral response, the cellular immunity has been also demonstrated to play a role in HIV-1 infection. DCs are known as the most potent inducers of specific immune responses and essential for the initiation of primary antigen-specific immune reactions. DCs are able to activate antigen-specific T cell responses being thus crucial in adaptive immunity (Lu et al., 2004). The stimulation of $CD8^+$ T lymphocytes and the formation of antigen-specific cytotoxic T cells depends on the peptide presentation together with MHC class I antigens. Cytotoxic T cells are able to recognize and eliminate virus-infected cells thus it was suggested that the initial HIV-specific CTL response contributes efficiently to better control of viremia during acute infection (Goonetilleke et al., 2009). $CD8^+$ T cells recognize specific antigens in the context with HLA class I molecules on APC, while $CD4^+$ T cells require the antigen presentation in the context with HLA class II molecules. The generation of HIV-specific immune response is dependent on the individual HLA pattern, therefore APC might bind different HIV peptides and activate $CD8^+$ T cells in moderate way in each patient. The ability of DCs to activate T cells depends also on the presence of secretory cytokines, which might cause differentiation of $CD4^+$ T cells into Th1 and Th2. $CD4^+$ Th1 release IL-2 and INF-γ supporting the effector functions of the immune system and $CD4^+$ Th2 produce IL-4, IL-10,

IL-5 and IL-6 playing role in development of a humoral response (Clerici et al., 1992). The close contact between $CD4^+$ T cells and APC, the presence of infectious virions on the surface of DCs and production of pro-inflammatory cytokines: IL-1, Il-6 or TNF-α, promotes the induction of viral replication in infected cells (Stacey et al., 2009).

Although the majority of antiretroviral-untreated individuals develops immunodeficiency of immune system and dies from AIDS-related complications in approximately 10-year time after becoming infected, a very small percentage of untreated individuals remain clinically and/or immunologically stable for years (Cao et al., 1995; Munoz et al., 1995). The factors associated with HIV control *in vivo* have not been fully defined yet. It has been proposed that infection by attenuated or defective viruses might be responsible for virus control and/or immunologic non-progression (Alexander et al., 2000; Hassaine et al., 2000; Kirchhoff et al., 1995; Lum et al., 2003; Wang et al., 1996; Yamada and Iwamoto, 2000). Less symptomatic primary infections were described more often in case of HIV controllers as compared with those destined to remain viremic (Madec et al., 2005a). However, the most consistent host factor that might be associated with virus control is the strong cellular response. The function of $CD8^+$ T cells have been shown higher in controllers as compared with non-controllers (Migueles et al., 2002). The presence of several different HLA alleles in infected patients, which detect and present HIV-1 antigens, have been described to be associated with effective HIV control, such as HLA-B57, HLA-B5801, HLA-B27, HLA-B14, HLA-A32 (Gao et al., 2001; Geczy et al., 2000; Hendel et al., 1999; Kaslow et al., 1996; Keet et al., 1999; Magierowska et al., 1999; McNeil et al., 1996; Saah et al., 1998). Among protective HLA alleles, HLA-B57 allele was consistently shown to be associated with a delay onset to AIDS (Carrington and O'Brien, 2003; O'Brien et al., 2001). It seems clear that although a number of factors have been associated with control of HIV-1, none of these features alone might predict virus control (Deeks and Walker, 2007; Walker, 2007).

In our study, we analyzed the sequences from 6 HIV-1 elite controllers, 8 HIV-1 viremic controllers and 16 HIV-1 chronic infections for DC-SIGN-mediated *trans*-infection.

The ratio of the *trans*-infection varied significantly among all HIV-1 envelopes showing correlation of DC-SIGN ratio with virological control in case of both cellular systems tested (Raji DC-SIGN$^+$/Raji and Jurkat DC-SIGN$^+$/Jurkat). The analysis of the results obtained from Raji DC-SIGN$^+$/Raji system revealed overall significant difference in the ratio of DC-SIGN-mediated *trans*-infection between HIV-1 controllers and patients with chronic HIV-1 infection (Controllers=45.49 vs CI=20.42, $p<0.0001$) (Fig. 55). Interestingly, the subgroup of HIV-1 viremic controllers demonstrated the highest DC-SIGN-mediated *trans*-infection as compared with EC (VC=56.6 vs EC=28.02, $p=0.0007$) and CI (VC=56.6 vs CI=20.42, $p<0.0001$) (Fig. 56). EC showed a trend towards more efficient *trans*-infection as compared with CI ($p=0.1331$), however much less efficient when compared with VC (Fig. 56). The overall result of the *trans*-infection experiment was subsequently confirmed by *trans*-infection experiment in Jurkat DC-SIGN$^+$/Jurkat cellular system showing significantly higher DC-SIGN-mediated *trans*-infection as compared with chronically HIV-1 infected patients (Controllers=32.84 vs CI=17.4, $p=0.0233$). The low association between EC and efficient DC-SIGN-mediated *trans*-infection might suggest that other factors, such as reduced viral fitness (Casado et al., 2013; Lassen et al., 2009; Miura et al., 2009) or extremely vigorous CD8$^+$ T cell response (Goulder and Watkins, 2004; Migueles et al., 2002) account for virological control in this subgroup of patients. Our results have confirmed the frequent low fitness linked to EC envelopes. In our study, a considerable group of EC HIV-1 envelopes (10 out of 16) could not be tested in the *trans*-infection experiments. All of 10 HIV-1 envelopes were confirmed as not defective by sequencing, however in cellular assay 4 out of 10 were observed nonfuntional and 6 out of 10 had the infectivity continuously below dynamic range required for the infection experiments thus they were excluded from our analysis. Although extremely strong CD8$^+$ T cellular response has been frequently suggested as a factor associated with virological control in EC, other studies have demonstrated that the phenomenon of elevated CD8$^+$ T cell activity in these patients was related to chronic inflammation that eventually leads to progressive immunodeficiency. It was observed that higher T cell activation was related to lower CD4$^+$ T counts supporting the hypothesis that cellular response activation leads to disease progression independently of viral replication (Hunt et al., 2008). It was also suggested that sustained prolong very

low level of viral replication in EC individuals can be involved directly in endothelial damage (Torriani et al., 2008) as well as it can lead to continuous T cells and monocyte activation that can contribute to increased arterial inflammation (Pereyra et al., 2012). The higher atherosclerosis incidence in HIV-1 controllers was confirmed in study of Hsue *et al.*, where EC in the absence of ART showed augmented chronic inflammation that accounted for atherosclerosis (Hsue et al., 2009). In the absence of ART, HIV-1 infection has been associated with increased levels of IL-6, a pro-inflammatory cytokine that is strongly linked to cardiovascular problems and mortality in untreated HIV-1 patients, including HIV-1 controllers (Kuller et al., 2008). Moreover, it has observed that EC were hospitalized significantly more frequently that treated individuals, mostly for pulmonary or cardiovascular causes (Katsnelson, 2014). The first study of ART initiation in the group of HIV-1 controller was conducted by Hatano *et al*. to determine the virological and immunological effect of the treatment. This study revealed that controllers had statistically decreased ultrasensitive plasma and rectal HIV RNA levels. Furthermore, the markers of T cell activation and T cell dysfunction in blood and gut mucosa were reduced substantially in EC on ART (Hatano et al., 2013). Virological control in the subgroup of HIV-1 viremic controllers is less well understood. It might be possible that this subgroup of patients have stronger innate immune response, which can influence virological control. VC have used DC-SIGN more efficiently as compared to other groups of patients, therefore it might be hypothesized that DC-SIGN in these patients play a potential role in antigen capture and further presentation for the proper immune system activation.

To access the information about the basis of these differences in DC-SIGN-mediated *trans*-infection, the HIV-1 envelope length and PNGS number were compared between EC, VC and CI. Although it has been demonstrated that the envelope glycoprotein from HIV controllers is shorter and contains fewer PNGS (Bailey et al., 2006a), in our small study the virus sequences of HIV-1 controllers and patients with chronic infection were of similar length and containing comparable number of PNGS in most of gp160 regions with the only exception of V5 loop (Fig. 57). However, further analysis has shown that V5 length and V5 PNGS did not have any association with DC-SIGN

trans-infection ratio (Fig. 58). Thus it could be suggested that these changes occurred in the natural course of HIV-1 infection, possibly in the response to the pressure caused by NAbs. It has been previously shown that HIV-1 envelope length and glycan numbers have a tendency to increase over the course of HIV-1 epidemic (Bunnik et al., 2010; Bunnik et al., 2008). Our analysis of the data obtained from HIV Los Alamos Data base confirmed those studies showing the apparent evolution of the HIV-1 envelope glycoproteins towards longer and containing more PNGS (Supplementary material 1). Therefore the change in V5 towards longer loop containing more N-glycans and the increase in overall PNGS number in all variable loops could be explained by the HIV evolution pattern and did not have association with more efficient usage of DC-SIGN in the *trans*-infection experiment.

The results of this study might contribute to better understanding of DC-SIGN receptor role in HIV-1 pathogenesis. We indicated the substantial usage of DC-SIGN receptor in the *trans*-infection experiment by HIV-1 controllers, especially in the subgroup of VC. Those results were verified in two cellular systems and both showed the association of higher *trans*-infection ratio with virological control. The HIV-1 envelopes of VC have used DC-SIGN more efficiently as compared with EC and patients with chronic HIV-1 infection. It is possible that virological control in the group of EC results from reduced viral fitness or more effective adaptive cellular response rather than the role of DC-SIGN in the first steps of virus infection. However, in the group of VC it might be possible that more robust involvement of this receptor is associated with antigen presentation and more effective immune system response rather than virus dissemination leading to better cellular control of the infection resulting in more efficient virological control. The HIV-1 virological control is characterized by maintaining low viral loads in the absence of antiretroviral therapy. Thus the low viral load and the lack of active replication determine that envelope sequences in HIV controllers have small loop and few number of N-glycans (Bailey et al., 2006a). Although DC-SIGN shows strong affinity for mannose-containing moieties, our study has confirmed that the number of PNGS is not the fundamental factor associated with stronger DC-SIGN bindings. The comparison of N-glycosylation pattern did not show any statistically significant differences be-

tween the number of glycans in VC as compared with EC and CI, therefore higher DC-SIGN-mediated *trans*-infection in the subgroup of VC could not be explained by the quantitative occurrence of N-glycosylation. It might be thus suggested that DC-SIGN binding involves complex pattern of specific N-glycosylation and not the amount of glycans on the envelope surface. Our data demonstrated that HIV-1 envelopes of controllers although containing generally lower number of glycans on the virus surface, use DC-SIGN more effectively than HIV-1 chronic isolates. In this respect a viral evolution towards less use of DC-SIGN has been reported to occur during clinical follow up, specially between acute vs late-stage strains within the same individuals suggesting a negative DC-SIGN selection along the time of infection (Borggren et al., 2008).

5. CONCLUSIONS

1) The envelope glycoproteins of HIV-1 virological controllers use DC-SIGN more efficiently in the *trans*-infection experiment as compared with patients with chronic HIV-1 infection.

2) DC-SIGN-mediated *trans*-infection is not associated with the amount of N-glycan residues in HIV-1 envelope glycoprotein. Probably a more complex pattern of specific N-glycosylation is responsible for this mechanism.

3) In the group of VC, the observed significantly higher *trans*-infection could indicate that DC-SIGN participates in viral detection, presentation and immune control more than dissemination as in the case of observation of more efficient DC-SIGN-mediated *trans*-infection by Ebola Reston.

4) The EC group did not show the same DC-SIGN *trans*-infection use as observed in VC. In this group of patients virological control could be more associated with factors such as viral fitness or vigorous CTL response.

CONCLUSIONS/ CONCLUSIONES

VI. CONCLUSIONS

1) The infection model based on cell lines expressing DC-SIGN is a consistent platform to study direct viral entry (Ebola virus) and the *trans*-infection phenomenon (Ebola virus and HIV) since the infection events depend almost exclusively on DC-SIGN-viral interaction.

1) El modelo de infección basado en las líneas celulares que expresan DC- SIGN es una plataforma consistente para estudiar la entrada viral directa (virus del Ébola) y el fenómeno de *trans*-infección (virus Ebola y VIH) debido a que la interacción virus-DC-SIGN en este sistema depende casi exclusivamente de la presencia DC–SIGN.

2) The DC-SIGN infection model is a useful model of an antiviral screening platform to test carbohydrates strategies targeting DC-SIGN.

2) El modelo de infección DC-SIGN es un modelo útil para estudiar estrategias antivirales dirigidas a DC-SIGN.

3) The inhibition of DC-SIGN-mediated infection by carbohydrate-based compounds depends strongly on the multivalency of glycan presentation.

3) La inhibición de la infección mediada por DC-SIGN mediada por los compuestos basados en hidratos de carbono depende en gran medida de la multivalencia de presentación de los glicanos.

4) The most potent antiviral activity was obtained by glycodendrinanoparticles showing an effective antiviral activity in the picomolar to low nanomolar concentration range. Multivalency depends on the presentation of 1620 glycan moieties generating a large surface of interaction (30 nm in diameter).

4) La actividad antiviral más potente se obtuvo en caso de las glicodendrinanoparticulas que muestran una actividad antiviral eficaz en el rango de concentración picomolar -nanomolar. Multivalencia depende de la presentación de los 1620 glicanos generando una gran superficie de interacción (30 nm de diámetro).

5) Despite the role of DC-SIGN in Ebola virus entry and potential initial dissemination, we found significantly higher DC-SIGN *trans*-infection by the non-pathogenic Ebola Reston strain. This finding could indicate that in Ebola virus infection DC-SIGN is involved in a more efficient immune control.

5) A pesar del papel del DC-SIGN en la entrada del virus del Ébola y la difusión inicial del virus, en nuestro estudio encontramos significativamente mayor uso de DC-SIGN por la cepa no patógena de Ébola Reston. Este hallazgo podría indicar que DC-SIGN en caso de Ébola Reston está involucrado en un control inmunitario más eficiente.

6) The envelope glycoproteins of HIV-1 virological controllers use DC-SIGN more efficiently in the *trans*-infection experiment as compared with patients with chronic HIV-1 infection.

6) Las glicoproteínas de la envoltura del VIH- 1 de los controladores virológicos utilizan DC-SIGN más eficiente en el experimento de *trans*-infección en comparación con los pacientes con enfermedad crónica.

7) DC-SIGN-mediated *trans*-infection is not associated with the amount of N-glycan residues in HIV-1 envelope glycoprotein. Probably a more complex pattern of specific N-glycosylation is responsible for this mechanism.

7) La *trans*-infección mediada por DC-SIGN no está asociada con la cantidad de los N- glicanos en la glicoproteína de la envuelta de VIH-1. Probablemente un patrón más complejo de N- glicosilación específica es responsable de este mecanismo.

8) In the group of VC, the observed significantly higher *trans*-infection could indicate that DC-SIGN participates in viral detection, presentation and immune control more than dissemination as in the case of observation of more efficient DC-SIGN-mediated *trans*-infection by Ebola Reston.

8) En el grupo de VC, la significativamente mayor *trans*-infección observada podría indicar que DC-SIGN participa en la detección viral, presentación y control inmunológico más que en la difusión viral, como en el caso de *trans*-infección por Ébola Reston.

9) The EC group did not show the same DC-SIGN *trans*-infection use as observed in VC. In this group of patients virological control could be more associated with factors such as viral fitness or vigorous CTL response.

9) El grupo de EC no demostró la misma *trans*-infección que los VC. El control virológico en el grupo de los EC puede resultar de la reducción de la replicación viral o extremadamente vigorosa respuesta de las células T $CD8^+$.

THESIS SUMMARY (ENG)

DC-SIGN as a model of pathogen recognition receptor: interaction with the envelope glycoproteins of HIV-1 and Ebola virus and the role in viral pathogenesis

1. Introduction

The mammalian immune system is composed of two types of immunity that are used to protect the host from infections: innate and adaptive immunity (Medzhitov and Janeway, 1999). The innate immune system is the first line of host defense against pathogens. It is immediate and genetically programmed to detect features of invading microbes. Adaptive immunity is highly specific and it is responsible for the elimination of pathogens in the late phase of infection and for the generation of immunological memory (Akira et al., 2006). The key role in translating innate information into adaptive immunity plays the members of the dendritic cell family (Reis e Sousa, 2001). Immature DCs can express receptors that mediate adsorptive endocytosis, including C-type lectin receptors and Toll-like receptors (TLRs). DC-SIGN is a type II C-type lectin, which belongs to the transmembrane PRR family. DC-SIGN plays a role in immune response through control of DC migration, T cell priming, antigen capture and presentation. The receptor DC-SIGN was initially identified as an attachment factor for HIV, which binds to viral envelope and augments virus infection (Curtis et al., 1992; Geijtenbeek et al., 2000c). DC-SIGN contains a carbohydrate recognition domain (CRD), an extracellular stalk composed of seven complete and one partial tandem repeat, a transmembrane domain and a short cytoplasmic N-terminal domain with several intracellular sorting motifs (Geijtenbeek et al., 2000c). The CRD of DC-SIGN shows high affinity for mannose and fucose residues (van Kooyk and Geijtenbeek, 2003). DC-SIGN recognizes the glycoproteins that contain a relatively high number of N-linked carbohydrates present on the surface of different pathogens (Geijtenbeek and van Kooyk, 2003). DC-SIGN binds to HIV, Ebola virus, Cytomegalovirus, Hepatitis C virus, Dengue virus, *Helicobacter pylori*, *Klebsiella pneumoniae*, *Mycobacterium tuberculosis*, *Candida albicans*, Leishmania, *Schistosoma mansoni*.

DC-SIGN is not the main receptor for Ebola virus and many different cell lines lacking DC-SIGN has been earlier described as a target of viral infection (Wool-Lewis and Bates, 1998; Yang et al., 1998). It has been shown that the expression of DC-SIGN increases the level of the infection with Ebola virus in susceptible cells. Moreover, DC-

SIGN acts as a *trans*-receptor since Ebola particles might be captured by DC-SIGN-expressing monocyte-derived DCs to be further transmitted to recipient cells (Alvarez et al., 2002). Although all predicted *in vitro* DC-SIGN functions have not been confirmed in *in vivo* studies, DC-SIGN was predicted to participate in the dissemination of the virus at the first moments of the infection. Therefore, over the years many different antiviral strategies based on carbohydrate compounds targeting DC-SIGN were used to block Ebola virus-DC-SIGN interaction. Ebola group of filoviruses comprises five subtypes: Zaire, Sudan, Reston, Cote dÍvoire, Bundibugyo, among which Ebola Zaire strain shows the highest mortality rate (50-90%), whereas Ebola Reston has never been associated with human disease (Usami et al., 2011). The phenomenon of Ebola Reston being non-fatal to humans has not been fully clarified yet. It has been speculated that envelope glycoproteins of both strains might be responsible for these differences in viral pathogenesis. This hypothesis was raised after a number of *in vitro* studies, which analyzed the possible role of immunosuppressive motifs (Becker, 1995; Volchkov et al., 1992; Yaddanapudi et al., 2006), efficiency of cleavage by furin (Neumann et al., 2002; Neumann et al., 2007) or cytotoxicity (Alazard-Dany et al., 2006; Volchkov et al., 2001; Yang et al., 2000). However, these speculations have not been confirmed yet in a proper *in vivo* model.

The human immunodeficiency virus (HIV) is a lentivirus that belongs to the family of retroviruses. HIV is responsible for causing acquired immunodeficiency syndrome (AIDS) that is characterized by progressive failure of the immune system and appearance of life-threatening opportunistic infections (Coffin, 1992; Coffin et al., 1997; Douek et al., 2009; Weiss, 1993). HIV infection is characterized by diminished counts of $CD4^+$ T cells, an increase in $CD8^+$ T cells and reduced mitogen-induced proliferative capacity of lymphocytes (Gottlieb et al., 1981; Masur et al., 1981). Most of HIV-1-infected patients show high plasma viral load and the loss of $CD4^+$ T cells along the course of HIV-1 infection in case of absence of antiretroviral therapy (Lassen et al., 2009). The majority of antiretroviral-untreated individuals eventually develops immunodeficiency of immune system and dies from AIDS-related complications in approximately 10-year time after becoming infected. However, a very small percentage of untreated individuals remain

clinically and/or immunologically stable for years (Cao et al., 1995; Munoz et al., 1995). The term of "long-term non-progressors (LTNP)" was used in case of people that were able to maintain normal $CD4^+$ T cell counts for prolonged periods (>10 years). By virological criteria, a small subset of individuals (less than 1% of infected population) called "elite controllers (EC)" are able to maintain viral loads undetectable (<50 copies HIV RNA/ml) (Deeks and Walker, 2007). The International HIV Controller Consortium defined the second group of HIV controllers called viremic controllers (VC), individuals who maintain RNA levels below 2000 copies of viral RNA per ml in the absence of ART. The factors associated with HIV control *in vivo* have not been fully defined yet, in part due to the fact that HIV controllers form a very heterogeneous population (Lefrere et al., 1997). Individuals destined to become HIV controllers seem to have less symptomatic primary infections as compared with those destined to remain viremic (Madec et al., 2005a), which suggest that complex virus and host interactions leading to prolonged control of viral replication play already an important role during the earliest phases of HIV disease (Altfeld et al., 2006). It has been suggested that infection with attenuated or defective virus may lead to no progression (Deacon et al., 1995). Several studies have shown that HIV envelopes derived from EC demonstrated reduced entry fitness (Casado et al., 2013; Lassen et al., 2009; Miura et al., 2009). Nevertheless, the most consistent factor responsible for virological control is a vigorous cellular response. It has been shown that the function of cytotoxic $CD8^+$ T cells is clearly higher in controllers as compared with non-controllers (Migueles et al., 2002). HLA molecules are involved in immune system recognition of virally infected cells and the presence of several different HLA alleles have been described to be associated with effective HIV control, such as HLA-B57, HLA-B5801, HLA-B27, HLA-B14, HLA-A32 (Gao et al., 2001; Geczy et al., 2000; Hendel et al., 1999; Kaslow et al., 1996; Keet et al., 1999; Magierowska et al., 1999; McNeil et al., 1996; Saah et al., 1998). Although, elite control of HIV infection has been associated with a number of factors, none of these features alone might predict elite control (Walker, 2007).

DC-SIGN captures HIV-1 particles through its high-affinity interactions with HIV-1 envelope glycoprotein. DCs are thought to facilitate viral dissemination through HIV-1

capture at mucosal site and transmission to secondary lymphoid tissues (Haase, 2005, 2010; Pope et al., 1994; Shattock and Rosenberg, 2012; Steinman et al., 2003). The DC-mediated HIV infection can occur through several distinct processes taking place concurrently, including *trans*-infection through infectious synapse, *trans*-infection through exosomes or *cis*-infection following *de novo* production of viral particles in DCs (Wu and KewalRamani, 2006). Unprotected sexual intercourse is the most common global mode of HIV-1 transmission (Royce, 1997) therefore the development of HIV-1 preventive strategies at mucosal site as a first line of contact with pathogens is the prior subject of interest. The attempts to develop an efficient vaccine against chronic viruses have failed so far, mainly due to the immunological escape mechanisms of these viruses or the lack of conserved epitopes of viruses involved in acute infections (Letvin, 2006). Condom use and behavioral interventions have been only partially successful in slowing the spread of HIV-1 infection worldwide. There is an urgent need for additional interventions to prevent new infections, such as the development of female-controlled topical formulations of anti HIV-1 compounds that could be used as a gel, cream, suppository before sexual intercourse (Elias and Coggins, 1996).

2. Objectives

The aim of our study was to standardize and evaluate a cellular model of viral infection mediated by DC-SIGN: (a) consistency of the infection model using different cell lines expressing the DC-SIGN receptor, (b) standardization of the DC-SIGN expression level and the infective titre of recombinant retroviruses for infection assays and (c) establish the proper conditions for the DC-SIGN mediated *cis*-infection and *trans*-infection assays. We wanted to study the utility of the DC-SIGN infection model as a screening platform of antiviral strategies targeting DC-SIGN and analyze the potential antiviral effect of compounds such as glycodendritic structures, tetravalent dendrons, dendrimers-based compounds, glycofullerenes and glycodendrinanoparticles. We also evaluated the DC-SIGN-mediated *trans*-infection by the pathogenic and non-pathogenic Zaire and Reston strains of Ebola virus as well as the implication of DC-SIGN trans-infection in HIV-1 virological control.

3. Material and Methods

3. 1. Cloning of HIV-1 envelopes

The viral cDNA was synthesized by using SuperScriptIII System. The envelope sequence of HIV-1 was amplified by nested PCR using Expand High Fidelity PCR System and further cloned into pcDNA3.1/V5-His TOPO. Sequencing of HIV-1 envelopes was performed by using of BigDye Terminator v3.1 chemistry and the sequences were analyzed by *Geneious* Bioinformatics Software.

3. 2. Isolation of Peripheral Blood Mononuclear Cells (PBMCs) and generation of monocyte-derived Dendritic Cells (DCs)

PBMCs were isolated from buffy coats from healthy donors by Ficoll-Paque density-gradient centrifugation. The monocytes were then cultured in RPMI medium supplemented with cytokines GM-CSF (200 ng/ml) and IL-4 (10 ng/ml). For the proper differentiation of immature monocyte-derived DCs, cells were incubated for 7 days and subsequently activated with cytokines on a day 2 and 5.

3. 3. Production of recombinant viruses

Recombinant viruses were produced in 293 T cells by standard Calcium Chloride transfection protocol. The viral construction was pseudotyped with virus envelope (Ebola, HIV-1, VSV) and expressed luciferase as a reporter of the infection (Yang et al., 1999).

3. 4. Infection in *cis* assay

Infection in *cis* was performed on Jurkat cells expressing receptor DC-SIGN. Jurkat DC-SIGN$^+$ (2.5–5 x 10^5) were incubated with carbohydrate compounds in 96-well suspension plates for 30 min at RT and then challenged with 5000-10000 TCID of recombinant viruses for 48 h.

3. 5. Infection in *trans* assay (Ebola virus)

Jurkat DC-SIGN$^+$ cells (2.5-5 x 10^5) were pre-incubated for 20 min at RT with carbohydrate compounds. Then, the cells were challenged with 5000-10000 TCID of recombinant viruses for 2 h at RT with rotation. After pulsing with pseudoviruses, cells were intensively washed and co-cultivated with adherent HeLa cells (10^5 cells/ well) for 48 h.

3. 6. Infection in *trans* assay (HIV-1)

Infection in *trans* was performed on Jurkat DC-SIGN$^+$ or Raji DC-SIGN$^+$ (5 x 10^5), which can capture and transmit HIV-1 virus to susceptible cells. Cells were pulsing with HIV-1 pseudoviruses for 3 h at 37º C. After challenging with recombinant viruses, cells were washed and co-cultivated with susceptible U87-R5/X4 cells for 48 h.

3. 7. Carbohydrate-based compounds tested in the experiments of infection in *cis* and infection in *trans*The blocking effect of the following antivirals was studied: glycodendritic structures, tetravalent dendrons, dendrimers-based compounds, glycofullerenes and glycodendrinanoparticles.

4. Results

4. 1. DC-SIGN infection model

The model of infection in *cis*, based on Jurkat DC-SIGN$^+$/Jurkat cells, clearly showed dependence of the Ebola virus cell entry on DC-SIGN presence (ratio 2567.8). The *cis*-infection of both cell lines by DC-SIGN independent VSV-G-pseudotyped retroviruses was at very similar level (ratio 0.96). The model of *trans*-infection confirmed the results obtained in the *cis*-infection experiment, revealing higher transmission of Ebola infection to susceptible cells by Jurkat DC-SIGN$^+$ as compared with negative cells (ratio 870.4). The *trans*-infection obtained with VSV-G-pseudotyped viruses was comparable between both cell lines.

4. 2. DC-SIGN as a model of antiviral screening strategies

The antiviral activity of carbohydrate compounds was tested using recombinant viral particles presenting Ebola virus GP. The possibility of blocking DC-SIGN receptor was examined in the experiments of *cis*-infection and *trans*-infection in the presence of carbohydrate-based compounds at different final concentrations.

Glycodendritic structures

The IC_{50} of compound RR114 was 3.6 μM and the IC_{50} for compound RR115 was 2.8 μM. Although both compounds showed similar efficacy in the infection in *cis*, in the experiment of infection in *trans* compound RR115 was more potent than compound RR114 (IC_{50} of 7 μM vs IC_{50} of 52.4 μM).

Tetravalent dendrons

The results obtained in the *cis* infection experiment revealed that the tetravalent systems presenting four copies of pseudomannotrioside (compound 14) showed a potency of 1 order of magnitude higher than the tetravalent systems presenting four copies of linear pseudomannobioside (compound 12). The IC_{50} of compound 14 was 106.5 nM and the IC_{50} of compound 12 was 1.4 μM. The results obtained in the *trans*-infection experiment were similar to the results from infection in *cis*. The tetravalent dendron 14 with 4 copies of pseudomannotrioside showed an IC_{50} of 203 nM. The tetravalent dendron 12 with 4 copies of pseudomannobioside was 1 order of magnitude less potent with an IC_{50} of 1.22 μM.

Dendrimer-based compounds

Dendrimer-based compounds bearing 30-32 pseudomannotriosides (G3(pseudotri)$_{32}$) or 30-32 pseudomannobiosides (G3(pseudodi)$_{32}$) showed no difference in their potency of inhibition of EBOV GP pseudotyped particles cell entry. The IC_{50} value of compound G3(pseudotri)$_{32}$ was 17.12 nM and the IC_{50} value of compound G3(pseudodi)$_{32}$ was 27.21 nM. The results obtained in the *trans*-infection experiment were similar to the results from infection in *cis* showing the IC_{50} values of the same order of magnitude. The IC_{50} of multivalent pseudomannobioside was 62 nM. The IC_{50} of multivalent pseudomannotriose was 31.51 nM.

Glycofullerenes

Glycofullerene displaying with 12 mannoses showed the IC_{50} of 2 μM. The IC_{50} for the fullerene presenting 36 mannoses was 68 μM. The introduction of a longer spacer in glycofullerene with 36 mannoses had a very important effect on recovering the activity of this compound with the IC_{50} of 286.4 nM. Galactosyl fullerene, as expected, was not able to inhibit the infection process mediated by DC-SIGN.

Glycodendrinanoparticles

Compound Qβ was used in the experiment as a control of the impact of this new type of structures on the results in the infection in *cis*. The highest concentration of com-

pound Qβ (25 nM) used in the experiment could block infection in ~30-40%. The same concentration (25 nM) of compound Qβ-$(Man_3)_{180}$ could block infection in 50-60%. The concentration of 25 nM of compound Qβ-$(Man_9)_{180}$ could efficiently block infection in ~90-100%. IC_{50}s values were estimated with a 95% CI (7.7-24.3 nM for Qβ-$(Man_3)_{180}$ and 404.2 pM–4.1 nM for Qβ-$(Man_9)_{180}$). Compounds Qβ and Qβ-$(Man_9)_{180}$ were tested at concentrations of 25 nM, 5 nM, 1 nM in the infection in *cis* experiment of DCs. Compound Qβ-$(Man_9)_{180}$ displayed potent activity, inhibiting infection by >80% at 5 nM and >95% at 25 nM (estimated IC_{50}~2 nM).

4. 3.The role of DC-SIGN in Ebola pathogenesis

The differences in DC-SIGN-mediated infection by Ebola Zaire and Ebola Reston were first studied in the *trans*-infection experiment in Jurkat DC-SIGN$^+$/Jurkat cellular system. The difference in the mean ratio in the *trans*-infection experiment between EBOZ and EBOR was statistically significant (p=0.0034). The differences between the infection levels of EBOZ and EBOR pseudoparticles were then studied in the DC-SIGN-mediated *trans*-infection by primary DCs to HeLa cells. Results obtained in the experiment revealed statistically significant differences between EBOZ and EBOR (p=0.0084). The *cis*-infection of immature DCs did not confirm results of both *trans*-infection experiments (p=0.5479).

4. 4. The role of DC-SIGN in HIV-1 pathogenesis

Analysis of *trans*-infection ratios in the groups of patients: EC, VC and patients with chronic HIV-1 infection

The results of the *trans*-infection experiments were compared between different groups of patients to verify if the virological control might have any association with the ratio of *trans*-infection. The results obtained in the analysis showed statistically significant differences between HIV-1 controllers and patients with chronic HIV-1 infection with the mean controllers=45.49 vs CI=20.42 (<p=0.0001). These differences were further verified separately between the subgroups of HIV-1 controllers (EC and VC) to determine

if the type of virological control could have influence DC-SIGN-mediated *trans*-infection result. The data obtained in this study clearly showed that the group of patients that was associated with higher DC-SIGN *trans*-infection was the subgroup of VC. Significantly higher *trans*-infection ratio was observed in case of viremic controllers as compared with chronically infected patients (VC=56.6 vs CI=20.42, <p=0.0001). Interestingly, there was also a statistically significant difference in *trans*-infection ratio between VC and EC with the mean VC=56.6 vs EC=28.02 (p=0.0007).

Analysis of differences in HIV-1 envelope sequence and trans-infection ratio between elite controllers, viremic controllers and patients with chronic HIV-1 infection

For the identification of factors responsible for the differences in the ratio of *trans*-infection, the length and PNGS in: gp160, gp120, gp40, V1-V5 were analyzed between EC, VC and CI. No significant differences were found in V1-V4 regions with the exception of V5 (Fig. 57). The length of V5 was significantly shorter in the group of HIV-1 EC as compared with CI (EC=12.33 vs CI=14.13aa, p=0.0325). The group of VC also demonstrated a trend towards shorter V5 loop (VC=12.63 aa vs CI=14.13 aa, p=0.0858). The number of PNGS in V5 was higher in the group of patients with chronic HIV-1 infection (EC=1 PNGS, VC=1.5 PNGS and CI=1.813, EC vs CI p=0.0072). Although the analysis of the HIV-1 envelope sequences between the patients showed statistically significant differences in V5 loop, there was no correlation found between the *trans*-infection ratio and the length of V5 (r=0.0925, p=0.6267) or the number of PNGS in V5 (r= -0.0895, p=0.6382)

5. Discussion

5. 1. DC-SIGN as a model of antiviral screening strategies

Although *in vitro* DC-SIGN models are not sufficient for understanding the physiological role of DC-SIGN, the cellular model based on DC-SIGN$^+$ cells might function as a useful model of antiviral screening platform. Infection by Ebola virus in cellular lines is dependent of the presence of DC-SIGN on the cell surface. The cellular model used in

this study for antiviral screening was based on Jurkat DC-SIGN$^+$ cells, the human T cell lymphoblast-like cell line. Since Ebola virus does not infect T-lymphocytes, its entry to Jurkat cells is absolutely dependent on the interaction with DC-SIGN.

The presented above cellular system might serve as an antiviral screening platform to test different carbohydrates strategies targeting DC-SIGN. This receptor recognizes mannosylated and fucosylated oligosaccharides presented in a multivalent manner on the surface of several pathogens. Therefore, the synthesis of multivalent carbohydrate systems is necessary for the efficient interaction with this receptor as well as for the effective competition with the natural ligands. The results obtained in the experiments performed within this thesis, could contribute in a very fast and effective way in the first studies of antiviral screening based on different strategies: tetravalent dendrons, dendrimer-based compounds, glycofullerenes and glycodendrinanoparticles. Tetravalent dendrons and dendrimers-based compounds are the combination of new pseudomannoside carbohydrate mimic and the potency of multivalent presentation. The importance of the valency was evaluated by the presentation of the same pseudosaccharide ligands on the tetravalent system presenting 4 copies of the ligand and on the multivalent scaffolds displaying 30-32 of selected ligands. The IC_{50} values obtained for the multivalent systems were around 20 nM, which showed that their inhibitory potency was between 1 to 2 orders of magnitude higher than that of corresponding tetravalent systems (Luczkowiak et al., 2011). The synthesis of glycofullerenes provided the achievement of even higher valency of 36 mannoses. These compounds were synthesized by combining glycodendrons with a fullerene allowing thus globular presentation of carbohydrates. The results obtained in the infection in *cis* experiment highlighted the importance of combination of an adequate scaffold to achieve the multivalency with the right ligand accessibility and flexibility. The inhibitory effect of glycofullerene presenting 36 mannoses was decreased as compared with glycofullerene displaying 12 mannoses, however the subsequent introduction of longer spacer to this glycofullerene recovered inhibitory potency showing IC_{50} of 286.4 nM (10 times more potent than glycofullerene with 12 mannoses and 340 times more potent than glycofullerene with 36 mannoses containing short linker) (Luczkowiak et al., 2013). The highest valency con-

structs were achieved in case of glycodendrinanoparticles. This design was based on the multivalent assembly of protein monomers (glycodendriproteins) carrying polyvalent glycan motifs (glycodendrons). In this way these constructs displayed many glycans in a precise manner and created well-defined single entities of up to 32 nm in diameter. Glycodendrinanoparticles showed antiviral activity in the low nanomolar to picomolar range (Ribeiro-Viana et al., 2012).

5. 2. DC-SIGN in Ebola virus pathogenesis: DC-SIGN-mediated *trans*-infection in pathogenic and non-pathogenic strains of Ebola virus

Ebola viruses cause a severe, often fatal disease consisting in a highly lethal hemorrhagic fever syndrome (Peters et al., 1996). Ebola virus strain Zaire is the virus variant with the highest mortality rate being in the range 50-90%. In contrast to the Zaire strain, Ebola Reston does not cause a disease in humans despite a number of documented infections during animal epizootics (Barrette et al., 2009; Miranda et al., 1999). The molecular basis for this difference in their pathogenesis remains unclear. Binding of Ebola virus GP to different cellular lectins has been previously shown to augment virus infection, both in *cis* and in *trans* (Alvarez et al., 2002). In our study, we have used recombinant particles expressing two Ebola virus envelope glycoproteins (EBOZ and EBOR) to study the potential role of DC-SIGN in the pathogenesis of both Ebola variants. The DC-SIGN-mediated infection was verified in the experiments of *trans*-infection Jurkat DC-SIGN$^+$/Jurkat, *cis*-infection of primary DCs and *trans*-infection DCs/HeLa cells. The first experiment of the *trans*-infection in cellular model Jurkat DC-SIGN$^+$/Jurkat revealed the significant differences in the mean ratio of the *trans*-infection experiment between Ebola Zaire and Ebola Reston ($p=0.0034$). The mean ratio of EBOR was about three times higher than the ratio of EBOZ (35.97 vs 99.64). The results obtained in the *trans*-infection experiment based on human immune cells (DCs) have confirmed the results of *trans*-infection in the cell line system. The difference between the transmitted infection by Ebola Zaire and Ebola Reston pseudoparticles to susceptible HeLa cells was statistically significant ($p=0.0084$). Both of performed experiments demonstrated statistical significance of higher DC-SIGN-mediated *trans*-infection of

EBOR as compared with EBOZ. Despite significant differences in EBOZ/EBOR usage of DC-SIGN in the *trans*-infection experiment, the direct infection of immature DCs did not give any significant result. Our results found the association between the Ebola Reston and a higher *trans*-infection ratio mediated by DC-SIGN. This finding might raise a hypothesis that although DC-SIGN receptor participates effectively in the cell entrance, *in vivo* it plays apparently more important role in the proper immune system activation. DC-SIGN may be responsible for virus capture, destruction and further presentation of its antigens to cells causing effective immunological control. DC-SIGN therefore, although able to capture effectively Ebola virus particles, might serve more as a host defence factor rather than pathogen escape receptor. Therefore the higher level of DC-SIGN-mediated entry of Ebola Reston might suggest that overall DC-SIGN might be more implicated in antiviral responses. The results obtained in performed experiments somehow resemble the results from the Schaefer *et al.* study, in which mice expressing human DC-SIGN survived longer than wild-type mice after the infection with *Mycobacterium tuberculosis* (Schaefer et al., 2008).

5. 3. DC-SIGN in HIV-1 pathogenesis: Implication of DC-SIGN-mediated *trans*-infection in HIV-1 virological control

The receptor DC-SIGN was initially cloned and characterized as a receptor for the HIV envelope glycoprotein gp120. In fact, it was precisely shown that gp120 affinity for DC-SIGN is even higher than for CD4 receptor, a classical HIV-1 entry receptor (Curtis et al., 1992). Years before the discovery of DC-SIGN, studies of Cameron *et al*. and Pope *et al.* showed that DC pulsed with HIV-1 endorsed infection of co-cultivated T cells (Cameron et al., 1992; Pope et al., 1994). Shortly after the identification of DC-SIGN, Geijtenbeek *et al.* defined this phenomenon as HIV-1 *trans*-infection (Geijtenbeek et al., 2000b). It has been clearly shown that DC-SIGN binds carbohydrate structures, such as mannose-containing glycoconjugates, expressed on the surface of different pathogens (den Dunnen et al., 2010). The envelope of HIV-1 is one of the most highly glycosylated proteins in nature, containing 18-32 PNGS in gp120. Therefore, many different *in vitro* studies evidently have shown the high affinity of HIV-1 envelopes to cells expressing

DC-SIGN receptor. DC-SIGN does not function as a direct HIV-1 receptor but it works efficiently in the viral transmission from periphery to secondary lymphoid tissues. It has been demonstrated that HIV-1 particles bound to DC-SIGN are remarkably stable and retain infective for prolonged periods (Geijtenbeek et al., 2000b). Despite of all proposed roles of DC-SIGN based on *in vitro* models, the confirmation of the physiological behaviour of DC-SIGN *in vivo* should be further clarified.

In our study, we analyzed the sequences from 6 HIV-1 elite controllers, 8 HIV-1 viremic controllers and 16 HIV-1 chronic infections for DC-SIGN-mediated *trans*-infection. The ratio of the *trans*-infection varied significantly among all HIV-1 envelopes showing correlation of DC-SIGN ratio with virological control in case of both cellular systems tested (Raji DC-SIGN$^+$/Raji and Jurkat DC-SIGN$^+$/Jurkat). The analysis of the results obtained from Raji DC-SIGN$^+$/Raji system revealed overall significant difference in the ratio of DC-SIGN-mediated *trans*-infection between HIV-1 controllers and patients with chronic HIV-1 infection (Controllers=45.49 vs CI=20.42, $p<0.0001$) (Fig. 55). Interestingly, the subgroup of HIV-1 viremic controllers demonstrated the highest DC-SIGN-mediated *trans*-infection as compared with EC (VC=56.6 vs EC=28.02, $p=0.0007$) and CI (VC=56.6 vs CI=20.42, $p<0.0001$) (Fig. 56). EC showed a trend towards more efficient *trans*-infection as compared with CI ($p=0.1331$), however much less efficient when compared with VC (Fig. 56). The overall result of the *trans*-infection experiment was subsequently confirmed by *trans*-infection experiment in Jurkat DC-SIGN$^+$/Jurkat cellular system showing significantly higher DC-SIGN-mediated *trans*-infection as compared with chronically HIV-1 infected patients (Controllers=32.84 vs CI=17.4, $p=0.0233$). The low association between EC and efficient DC-SIGN-mediated *trans*-infection might suggest that other factors, such as reduced viral fitness (Casado et al., 2013; Lassen et al., 2009; Miura et al., 2009) or extremely vigorous CD8$^+$ T cell response (Goulder and Watkins, 2004; Migueles et al., 2002) account for virological control in this subgroup of patients. Our results have confirmed the frequent low fitness linked to EC envelopes. In our study, a considerable group of EC HIV-1 envelopes (10 out of 16) could not be tested in the *trans*-infection experiments. All of 10 HIV-1 envelopes were confirmed as not defective by sequencing, however in cellular assay 4 out of 10 were observed non-

funtional and 6 out of 10 had the infectivity continuously below dynamic range required for the infection experiments thus they were excluded from our analysis. Virological control in the subgroup of HIV-1 viremic controllers is less well understood. It might be possible that this subgroup of patients have stronger innate immune response, which can influence virological control. VC have used DC-SIGN more efficiently as compared to other groups of patients, therefore it might be hypothesized that DC-SIGN in these patients play a potential role in antigen capture and further presentation for the proper immune system activation.

To access the information about the basis of these differences in DC-SIGN-mediated *trans*-infection, the HIV-1 envelope length and PNGS number were compared between EC, VC and CI. Although it has been demonstrated that the envelope glycoprotein from HIV controllers is shorter and contains fewer PNGS (Bailey et al., 2006a), in our small study the virus sequences of HIV-1 controllers and patients with chronic infection were of similar length and containing comparable number of PNGS in most of gp160 regions with the only exception of V5 loop (Fig. 57). However, further analysis has shown that V5 length and V5 PNGS did not have any association with DC-SIGN *trans*-infection ratio (Fig. 58). Thus it could be suggested that these changes occurred in the natural course of HIV-1 infection, possibly in the response to the pressure caused by NAbs. It has been previously shown that HIV-1 envelope length and glycan numbers have a tendency to increase over the course of HIV-1 epidemic (Bunnik et al., 2010; Bunnik et al., 2008). Our analysis of the data obtained from HIV Los Alamos Data base confirmed those studies showing the apparent evolution of the HIV-1 envelope glycoproteins towards longer and containing more PNGS (Supplementary material 1). Therefore the change in V5 towards longer loop containing more N-glycans and the increase in overall PNGS number in all variable loops could be explained by the HIV evolution pattern and did not have association with more efficient usage of DC-SIGN in the *trans*-infection experiment.

The results of this study might contribute to better understanding of DC-SIGN receptor role in HIV-1 pathogenesis. We indicated the substantial usage of DC-SIGN receptor in

the *trans*-infection experiment by HIV-1 controllers, especially in the subgroup of VC. Those results were verified in two cellular systems and both showed the association of higher *trans*-infection ratio with virological control. The HIV-1 envelopes of VC have used DC-SIGN more efficiently as compared with EC and patients with chronic HIV-1 infection. It is possible that virological control in the group of EC results from reduced viral fitness or more effective adaptive cellular response rather than the role of DC-SIGN in the first steps of virus infection. However, in the group of VC it might be possible that more robust involvement of this receptor is associated with antigen presentation and more effective immune system response rather than virus dissemination leading to better cellular control of the infection resulting in more efficient virological control. The HIV-1 virological control is characterized by maintaining low viral loads in the absence of antiretroviral therapy. Thus the low viral load and the lack of active replication determine that envelope sequences in HIV controllers have small loop and few number of N-glycans (Bailey et al., 2006a). Although DC-SIGN shows strong affinity for mannose-containing moieties, our study has confirmed that the number of PNGS is not the fundamental factor associated with stronger DC-SIGN bindings. The comparison of N-glycosylation pattern did not show any statistically significant differences between the number of glycans in VC as compared with EC and CI, therefore higher DC-SIGN-mediated *trans*-infection in the subgroup of VC could not be explained by the quantitative occurrence of N-glycosylation. It might be thus suggested that DC-SIGN binding involves complex pattern of specific N-glycosylation and not the amount of glycans on the envelope surface. Our data demonstrated that HIV-1 envelopes of controllers although containing generally lower number of glycans on the virus surface, use DC-SIGN more effectively than HIV-1 chronic isolates. In this respect a viral evolution towards less use of DC-SIGN has been reported to occur during clinical follow up, specially between acute vs late-stage strains within the same individuals suggesting a negative DC-SIGN selection along the time of infection (Borggren et al., 2008).

6. Conclusions

1) The infection model based on cell lines expressing DC-SIGN is a consistent platform to study direct viral entry (Ebola virus) and the *trans*-infection phenomenon (Ebola virus and HIV) since the infection events depend almost exclusively on DC-SIGN-viral interaction.

2) The DC-SIGN infection model is a useful model of an antiviral screening platform to test carbohydrates strategies targeting DC-SIGN.

3) The inhibition of DC-SIGN-mediated infection by carbohydrate-based compounds depends strongly on the multivalency of glycan presentation.

4) The most potent antiviral activity was obtained by glycodendrinanoparticles showing an effective antiviral activity in the picomolar to low nanomolar concentration range. Multivalency depends on the presentation of 1620 glycan moieties generating a large surface of interaction (30 nm in diameter).

5) Despite the role of DC-SIGN in Ebola virus entry and potential initial dissemination, we found significantly higher DC-SIGN *trans*-infection by the non-pathogenic Ebola Reston strain. This finding could indicate that in Ebola virus infection DC-SIGN is involved in a more efficient immune control.

6) The envelope glycoproteins of HIV-1 virological controllers use DC-SIGN more efficiently in the *trans*-infection experiment as compared with patients with chronic HIV-1 infection.

7) DC-SIGN-mediated *trans*-infection is not associated with the amount of N-glycan residues in HIV-1 envelope glycoprotein. Probably a more complex pattern of specific N-glycosylation is responsible for this mechanism.

8) In the group of VC, the observed significantly higher *trans*-infection could indicate that DC-SIGN participates in viral detection, presentation and immune control more than dissemination as in the case of observation of more efficient DC-SIGN-mediated *trans*-infection by Ebola Reston.

9) The EC group did not show the same DC-SIGN *trans*-infection use as observed in VC. In this group of patients virological control could be more associated with factors such as viral fitness or vigorous CTL response.

THESIS SUMMARY (ES)/ EL RESUMEN DE LA TESIS

DC-SIGN como modelo de receptor de reconocimiento de patógenos: interacción con las glicoproteínas de la envoltura de los virus VIH-1 y Ébola y su papel en la patogénesis viral

1. Introducción

El sistema inmune de los mamíferos se compone de dos tipos de inmunidad que se utilizan como protección ante las infecciones: inmunidad innata y adaptativa (Medzhitov and Janeway, 1999). La respuesta del sistema inmune innato es la primera línea de defensa del organismo contra los patógenos, es inmediata y está genéticamente programada para detectar las características de los microorganismos invasores. Con respecto a la inmunidad adaptativa: esta es muy específica y es responsable de la eliminación de los agentes patógenos en la fase tardía de la infección así como de la generación de memoria inmunológica (Akira et al., 2006). Los miembros de la familia de las células dendríticas (DCs) tienen un papel crucial en la traducción de la información innata en inmunidad adaptativa (Reis e Sousa, 2001). Las DCs inmaduras expresan los receptores que median endocitosis de adsorción, incluyendo los receptores tipo Toll y las lectinas tipo C. DC-SIGN es un receptor tipo II de las lectinas tipo C, que pertenece a la familia de los receptores transmembrana. DC-SIGN juega un papel importante en la inmunidad a través de regulación de la migración de las DCs, activación de las células T, la captura y presentación de los antígenos (Geijtenbeek et al., 2000c). El receptor DC-SIGN fue identificado inicialmente como factor de la unión del VIH-1, que capturaba la envoltura viral y facilitaba la infección (Curtis et al., 1992; Geijtenbeek et al., 2000c). DC-SIGN contiene un dominio de reconocimiento de carbohidratos (CRD), un tallo extracelular, un dominio transmembrana y un dominio N-terminal citoplasmático (Geijtenbeek et al., 2000c). El CRD del DC-SIGN muestra una alta afinidad por las moléculas de manosa y fucosa (van Kooyk and Geijtenbeek, 2003). DC-SIGN reconoce las glicoproteínas que contienen un número relativamente alto de los N-carbohidratos presentes en la superficie de diferentes patógenos (Geijtenbeek and van Kooyk, 2003). DC-SIGN se une al VIH-1, virus del Ébola, citomegalovirus, virus de la hepatitis c, virus del dengue, *Helicobacter pylori*, *Klebsiella pneumoniae*, *Mycobacterium tuberculosis*, *Candida albicans*, Leishmania, *Schistosoma mansoni*.

DC-SIGN no es el receptor principal del virus de Ébola porque se ha descrito anteriormente que muchas diferentes líneas celulares que carecen de DC-SIGN se pudieron

infectar con este virus (Wool-Lewis and Bates, 1998; Yang et al., 1998). Se ha demostrado que la expresión de DC-SIGN aumenta el nivel de la infección con el virus de Ébola en células susceptibles. Por otra parte, DC-SIGN actúa como un receptor en *trans*, un fenómeno que consiste que las partículas del virus Ébola pueden ser capturadas por las DCs que expresan DC-SIGN y transmitidas a las células receptoras (Alvarez et al., 2002). Los ensayos *in vitro* sugerían que DC-SIGN participa en la difusión del virus en los primeros momentos de la infección, por lo tanto, en los últimos años se diseñaron diferentes estrategias antivirales basados en compuestos de carbohidratos para bloquear la interacción del Ébola con DC-SIGN. Se ha descrito que el grupo de filovirus del Ébola comprende cinco subtipos: Zaire, Sudán, Reston, Costa de Marfil, Bundibugyo, entre los cuales la cepa del Ébola Zaire muestra la tasa de mortalidad más alta (50-90%), mientras que la del Ébola Reston nunca ha sido asociada con la enfermedad humana (Usami et al., 2011). El fenómeno de las diferencias en la patogénesis del EBOZ y EBOR no ha sido completamente aclarado todavía. Se ha especulado que las glicoproteínas de la envuelta de las dos cepas pueden ser responsables de estas diferencias en la patogénesis. Esta hipótesis surgió después de la realización de una serie de estudios *in vitro*, donde se investigó el posible papel de los elementos inmunosupresores (Becker, 1995; Volchkov et al., 1992; Yaddanapudi et al., 2006), la eficiencia de escisión por furina (Neumann et al., 2002; Neumann et al., 2007) y la citotoxicidad (Alazard-Dany et al., 2006; Volchkov et al., 2001; Yang et al., 2000). Sin embargo, estas especulaciones no han sido confirmados aún en un modelo *in vivo*.

El virus de la inmunodeficiencia humana (VIH) es un lentivirus que pertenece a la familia de los retrovirus. El VIH es responsable de la causa del síndrome de inmunodeficiencia adquirida (SIDA) caracterizado por un fallo progresivo del sistema inmunitario que resulta en infecciones oportunistas y tumores (Coffin, 1992; Coffin et al., 1997; Douek et al., 2009; Weiss, 1993). El VIH fue descubierto por el grupo de Luc Montagnier y Françoise Barré-Sinoussi en 1983 (Barresinoussi et al., 1983), quienes en 2008 recibieron el Premio Nobel de Medicina por este descubrimiento. La infección por VIH se caracteriza por la disminución de células T $CD4^+$, un aumento en las células T $CD8^+$ y una reducción de la capacidad proliferativa inducida por mitógenos de los linfocitos

(Gottlieb et al., 1981; Masur et al., 1981). La mayoría de los pacientes infectados por el VIH-1 muestran una alta carga viral en plasma y la pérdida de células T $CD4^+$ a lo largo del curso de la infección por VIH-1 en caso de ausencia de la terapia antirretroviral (Lassen et al., 2009). Gran parte de los pacientes no tratados desarrollan la inmunodeficiencia del sistema inmunológico y mueren a causa de las complicaciones relacionadas con el SIDA en un tiempo aproximado de 10 años tras haberse infectado. Sin embargo, un porcentaje muy pequeño de individuos no tratados permanecen clínicamente y/o inmunológicamente estables durante años (Cao et al., 1995; Munoz et al., 1995). El término de no-progresadores a largo plazo (LTNP) se utiliza en el caso de las personas que fueron capaces de mantener el recuento de células T $CD4^+$ normales por períodos prolongados (>10 años). Un pequeño subgrupo de los individuos (menos del 1% de la población infectada) denominados "controladores de élite (EC)" son capaces de mantener una carga viral indetectable (<50 copias de ARN del VIH/ml) (Deeks and Walker, 2007). El Consorcio Internacional de los Controladores del VIH definió el segundo grupo llamados “controladores virémicos (VC)”, que pueden mantener los niveles de ARN por debajo de 2000 copias de virus por ml en ausencia de ART. Los factores responsables del control virológico *in vivo* no han sido aún bien definidos. Los individuos destinados a ser controladores del VIH parecen tener infecciones primarias menos sintomáticas en comparación con los pacientes destinados a padecer viremia (Madec et al., 2005b), lo que sugiere que las interacciones complejas entre el virus y el organismo anfitrión juegan un importante papel ya durante las primeras fases de la enfermedad del VIH (Altfeld and Allen, 2006). Se ha sugerido que la infección por el virus atenuado o defectuoso puede estar asociado con la no progresión de la enfermedad (Deacon et al., 1995). Varios estudios demostraron también el peor fitness de la entrada de las envueltas del VIH-1 derivadas de los EC (Casado et al., 2013; Lassen et al., 2009; Miura et al., 2009). El factor más consistente que podría estar asociado con el control del virus es una respuesta celular vigorosa. Se ha demostrado que la función de las células T citotóxicas $CD8^+$ es claramente superior en los controladores en comparación con los no-controladores (Migueles et al., 2002). Las moléculas HLA están implicadas en el reconocimiento del sistema inmune de las células infectadas por virus y la presencia de diferentes alelos HLA se ha asociado con el control eficaz del VIH, tales como: HLA-B57,

HLA-B27, HLA-B5801, HLA-B14, HLA-A32 (Gao et al., 2001; Geczy et al., 2000; Hendel et al., 1999; Kaslow et al., 1996; Keet et al., 1999; Magierowska et al., 1999; McNeil et al., 1996; Saah et al., 1998). Aunque, el control de élite de la infección por VIH-1 se ha asociado con una serie de diferentes factores, ninguna de estas características puede por sí sola predecir el control virológico (Walker, 2007).

DC-SIGN captura las partículas del VIH-1 a través de sus interacciones de alta afinidad con la glicoproteína de la envoltura. Las DCs pueden facilitar la difusión de la infección viral mediante la captura del VIH-1 en la mucosa y la transmisión a los tejidos linfoides secundarios (Haase, 2005, 2010; Klenk and Garten, 1994; Pope et al., 1994; Shattock and Rosenberg, 2012; Steinman et al., 2003). La infección mediada por DCs puede producirse a través de varios procesos distintos que tienen lugar al mismo tiempo, incluyendo *trans*-infección a través de las sinapsis infecciosas, *trans*-infección por los exosomas o *cis*-infección mediante la producción *de novo* de las partículas virales por los DCs (Wu and KewalRamani, 2006). Tener relaciones sexuales sin protección es el modo más común de transmisión del VIH-1 (Royce, 1997). Por lo tanto el desarrollo de las estrategias antivirales preventivas en los sitios de mucosa como la primera línea de contacto con los virus es la prioridad. Los intentos de desarrollar una vacuna eficaz contra los virus crónicos han fallado hasta ahora, debido principalmente a los mecanismos de escape inmunológicos de estos virus o la falta de epítopos conservados de virus implicados en las infecciones agudas (Letvin, 2006). El uso de preservativos y las intervenciones conductuales han sido sólo un éxito parcial para frenar la propagación de la infección VIH-1 en todo el mundo. Existe una urgente necesidad de intervenciones adicionales para prevenir nuevas infecciones, tales como el desarrollo de formulaciones tópicas de compuestos anti-VIH-1 para las mujeres, que se podrían utilizar en formato de gel, crema o supositorio antes de la relación sexual (Elias and Coggins, 1996).

2. Objetivos

El objetivo de nuestro estudio fue estandarizar y evaluar el modelo celular de la infección por el virus mediada por DC-SIGN. Queríamos estudiar la utilidad del modelo de

infección mediada por DC-SIGN como una plataforma de monitorización de las estrategias antivirales destinadas frente DC-SIGN: las estructuras glicodendríticas, los dendrones tetravalentes, los compuestos basados en dendrímeros, los glicofullerenos y lasglicodendrinanoparticulas. Por otra parte, hemos tratado de evaluar la implicación del receptor DC-SIGN en la *trans*-infección por las cepas Zaire y Reston del virus de Ébola. Por último, hemos investigado el proceso de *trans*-infección del VIH-1 y su correlación con control virológico.

3. Material y Métodos

3. 1. Clonación de las envueltas del VIH-1

El ADNc viral se sintetizó usando el Sistema SuperScriptIII. La secuencia de la envoltura completa del VIH-1 se amplificó por PCR usando el Expand High Fidelity PCR System y se clonó en pcDNA3.1/V5-His TOPO. La secuenciación de las envueltas del VIH-1 se realizó mediante el uso de BigDye Terminator Cycle Sequencing v3.1 y las secuencias fueron analizadas por el programa bioinformático Geneious.

3. 2. Aislamiento de las células mononucleares de sangre periférica (PBMCs) y la generación de las células dendríticas derivadas de monocitos (DCs)

PBMCs fueron aisladas de la capa leucocitaria de donantes sanos usando la centrifugación en gradiente de densidad Ficoll-Histopaque. Los monocitos se cultivaron en medio RPMI suplementado con las citoquinas GM-CSF (200 ng/ml) y la IL-4 (10 ng/ml). Para la diferenciación correcta de las DCs inmaduras derivadas de monocitos, las células se incubaron durante 7 días y posteriormente se activaron con las citoquinas en los días 2 y 5.

3. 3. Producción de virus recombinantes

Los virus recombinantes se produjeron en las células 293T por el protocolo estándar de la transfección de Cloruro de Calcio. La construcción viral fue pseudotipada con la envoltura del virus (Ébola, VIH-1 y VSV) y expresaba la luciferasa como un reportero de la infección (Yang et al., 1999).

3. 4. El ensayo de la infección en *cis*

La infección en *cis* se realizó en las células Jurkat que expresaban el receptor DC-SIGN. Jurkat DC-SIGN$^+$ (2.5-5x 10^5) se incubaron con compuestos de carbohidratos en placas de suspensión de 96 pocillos durante 30 min en temperatura ambiente (TA) y luego se infectaron con 5000-10000 TCID de virus recombinantes durante 48 h.

3. 5. El ensayo de la infección en *trans* (Ébola)

Las células (2.5-5x10^5) Jurkat DC-SIGN$^+$ se pre-incubaron durante 20 min a TA con compuestos de carbohidratos. Posteriormente las células se infectaron con 5000-10000 TCID de virus recombinantes durante 2 h a TA con la rotación. Después de 2 h, las células se lavaron intensamente y co-cultivaron con las células HeLa (10^5 células/pocillo) durante 48 h.

3. 6. El ensayo de la infección en *trans* (VIH-1)

La infección en *trans* se realizó con Jurkat DC-SIGN$^+$ o Raji DC-SIGN$^+$ (5x10^5), debido a que pueden capturar y transmitir el virus VIH-1 a las células susceptibles. Las células fueron incubadas con las pseudopartículas del VIH-1 durante 3 h a 37ºC. Después, las células se lavaron y se co-cultivaron con las células U87-R5/X4 durante 48 h.

4. Resultados

4. 1. El modelo de infección mediada por DC-SIGN

El modelo de infección en *cis* mediada por DC-SIGN en el sistema celular Jurkat DC-SIGN$^+$/Jurkat mostró claramente que la entrada del virus de Ébola a la célula es dependiente de la presencia de DC-SIGN (el ratio de *trans*-infección fue 2567.8). La infección en *cis* de las dos líneas celulares por las partículas recombinantes de un virus independiente de DC-SIGN (VSV-G) tuvo un nivel muy similar (el ratio de *trans*-infección fue 0.96). El modelo de *trans*-infección confirmó los resultados obtenidos en el experimento de *cis*-infección, revelando una mayor transmisión de la infección por Ébola en las células susceptibles a través de las células Jurkat DC-SIGN$^+$ en comparación con las células negativas (el ratio de *trans*-infección fue 870.4). La *trans*-infección con el virus recombinante VSV-G fue equivalente entre las dos líneas celulares.

4. 2. DC-SIGN como un modelo de estudiar diferentes estrategias antivirales

La actividad antiviral de los compuestos basados en carbohidratos fue estudiada en los ensayos de inhibición de infección usando partículas virales pseudotipadas con la glicoproteína del virus de Ébola. La posibilidad de bloqueo del receptor DC-SIGN se examinó en los experimentos de *cis* y *trans*-infección en la presencia de compuestos basados en carbohidratos con diferentes concentraciones finales.

Estructuras glicodendríticas

La IC_{50} del compuesto RR114 fue 3.6 μM y la IC_{50} para el compuesto RR115 fue de 2.8 μM. Aunque ambos compuestos mostraron una eficacia similar en la infección en *cis*, el experimento de infección en *trans* mostró más potencia en el compuesto RR115 que el compuesto RR114 (IC_{50} de 7 μM vs IC_{50} de 52.4 μM).

Dendrones tetravalentes

Los resultados obtenidos en el experimento de la infección en *cis* revelaron que los sistemas tetravalentes que presentan cuatro copias de pseudomanotriosidas (compuesto 14) mostraron una potencia de 1 orden de magnitud mayor que los sistemas tetravalentes que presentan cuatro copias de pseudomanobiosidas lineales (compuesto 12). La IC_{50} del compuesto 14 fue 106.5 nM y la IC_{50} del compuesto 12 fue 1.4 μM. Los resultados obtenidos en el experimento de *trans*-infección fueron similares a los resultados de la infección en *cis*. El dendron tetravalente 14 con 4 copias de pseudomanotriosidas mostró una IC_{50} de 203 nM. El dendron tetravalente 12 con 4 copias de pseudomanobiosidas fue de 1 orden de magnitud menos potente con una IC_{50} de 1.22 μM.

Compuestos basados en dendrímeros

Los compuestos basados en dendrímeros que presentan 30-32 pseudomanotriosidas (G3(pseudotri)$_{32}$) o 30-32 pseudomanobiosidas (G3(pseudodi)$_{32}$) no mostraron diferencias en su potencia de inhibición de la entrada de las partículas pseudotipadas con EBOV-GP a la célula. El valor de IC_{50} de compuesto G3(pseudotri)$_{32}$ fue 17.12 nM y el valor de IC_{50} de compuesto G3(pseudodi)$_{32}$G3 fue 27.21 nM. Los resultados obtenidos en el experimento de *trans*-infección fueron similares a los resultados de la infección en *cis* y mostraron valores de IC_{50} del mismo orden de magnitud. La IC_{50} de G3(pseudodi)$_{32}$ fue de 62 nM y la IC_{50} de G3(pseudotri)$_{32}$ fue 31.51 nM.

Glicofullerenos

El glicofullereno cubierto con 12 manosas mostró la IC_{50} de 2 μM.. La IC_{50} para el fullereno que presentaba 36 manosas fue de 68 μM (34 veces menos activo que el fullereno presentando 12 manosas). La introducción de un espaciador más largo en el glicofulle-

reno con 36 manosas tuvo un efecto muy importante en la recuperación de la actividad de este compuesto con una IC_{50} de 286.4 nM. El fullereno cubierto con galactosas no fue capaz de inhibir el proceso de infección mediada por DC-SIGN.

Glicodendrinanopartículas

El compuesto Qbeta se utilizó en el experimento como control de los efectos de este nuevo tipo de estructuras en los resultados de la infección en *cis*. La mayor concentración de compuesto Qbeta (25 nM) utilizada en el experimento fue capaz de bloquear la infección en ~ 30-40%. La misma concentración (25 nM) de compuesto Qbeta-$(Man_3)_{180}$ pudo bloquear la infección en el 50-60%. La concentración de 25 nM de compuesto Qbeta-$(Man_9)_{180}$ fue capaz de bloquear en manera eficaz la infección en ~ 90-100%. Los valores de IC_{50} se calcularon con un CI del 95% (7.7 nM - 24,3 nM para Qβ-$(Man_3)_{180}$ y 404.2 pM – 4.1 nM para Qβ-$(Man_9)_{180}$). Los compuestos Qbeta y Qbeta-$(Man_9)_{180}$ se estudiaron en concentraciones de 25 nM, 5 nM, 1 nM en el experimento de la infección en *cis* de las DCs. El compuesto Qbeta-$(Man_9)_{180}$ mostró una potente actividad inhibiendo la infección por encima del 80% con una concentración de 5 nM, sobrepasando el 95% cuando la concentración era de 25 nM (IC_{50} estimada ~ 2 nM).

4. 3. El papel de DC -SIGN en la patogénesis del virus del Ébola

Las diferencias en la infección mediada por el DC-SIGN por las dos cepas del Ébola fueron estudiadas primero en el experimento de *trans*-infección en el sistema celular Jurkat DC-SIGN$^+$/Jurkat. La diferencia en el ratio de *trans*-infección mediada por DC-SIGN entre EBOZ y EBOR fue estadísticamente significativa (p=0.0034). La significación estadística de las diferencias entre los niveles de infección de EBOZ y EBOR se estudió a continuación en la *trans*-infección mediada por las DCs primarias DCs a las células HeLa. Los resultados obtenidos en el experimento revelaron unas diferencias estadísticamente significativas entre EBOZ y EBOR (p=0.0084). En cambio, la *cis*-infección de células dendríticas inmaduras no resultó en diferencias significativas (p=0.5479).

4. 4. El papel del receptor DC-SIGN en la patogénesis del VIH-1

Análisis de los ratios de la *trans*-infección mediada del VIH-1 por DC-SIGN en grupos de pacientes: EC, VC y los pacientes con infección crónica

Los resultados de los experimentos de *trans*-infección se compararon entre diferentes grupos de pacientes para verificar si el control virológico podría tener alguna asociación con el ratio de *trans*-infección. Los resultados obtenidos en el análisis mostraron diferencias estadísticamente significativas entre ambos grupos de pacientes con la media EC+VC=45.49 vs CI=21.06 ($p<0,0001$). Estas diferencias se verificaron también en los subgrupos de los controladores: EC y VC para determinar si el tipo de control virológico podría tener influencia en el resultado de *trans*-infección. Se observó que el ratio de *trans*-infección fue significativamente mayor en el subgrupo de los VC en comparación con las personas con infección crónica (VC=56.6 vs CI 20.42, $p<0.0001$). Curiosamente, también hubo una diferencia estadísticamente significativa en la *trans*-infección entre VC y EC (EC=56.6 vs EC=28.02, $p=0.0007$).

El análisis de las secuencias de las envueltas y el ratio de *trans*-infección entre los EC, VC y los pacientes con infección crónica

Para la identificación de los factores responsables de las diferencias en el ratio de *trans*-infección se estudiaron las variable como la longitud y el número de PNGS en: gp160, gp120, gp41 y V1-V5 las envueltas del VIH-1 entre EC, VC y CI. No se encontraron diferencias significativas a excepción de la región de V5. La longitud de la V5 fue significativamente mayor en el grupo de pacientes con infección crónica en comparación con los EC y no con los VC (EC=12.33 aa vs CI=14.13aa, $p=0.0325$). El número de PNGS en la V5 mostró un tendencia hacía el mayor número de los glicanos en los aislados crónicos del VIH-1 (EC= 1 PNGS, VC=1.5 PNGS y CI=1.813 PNGS, EC vs CI $p=0.0072$). El análisis posterior demostró que no había correlación entre el ratio de *trans*-infección y la longitud de V5 ($r=0.0925$, $p=0.6267$) o el número de PNGS en la V5 ($r= -0.0895$, $p=0.6382$).

5. Discusión

5. 1. DC-SIGN como un modelo de estudiar las estrategias antivirales

Aunque los modelos *in vitro* de la infección no son suficientes para comprender el papel fisiológico de DC-SIGN, el modelo celular basado en las células que expresan DC-SIGN$^+$ podría funcionar como un modelo de estudio eficaz de estrategias antivirales. La infección por el virus del Ébola en líneas celulares es dependiente de la presencia de DC-SIGN en la superficie celular. El modelo celular utilizado en este estudio para la investigación de los antivirales se basó en las células de la línea celular de linfocitos T CD4$^+$ humanos, Jurkat DC-SIGN$^+$. Dado que el virus del Ébola no infecta a los linfocitos T, su entrada a las células Jurkat es absolutamente dependiente de la interacción con DC-SIGN.

El sistema celular Jurkat DC-SIGN$^+$/Jurkat podría servir como una plataforma de monitorización de diferentes estrategias antivirales dirigidas a DC-SIGN. El receptor DC-SIGN reconoce oligosacáridos fucosilados y manosilados, presentados de una manera multivalente en la superficie de varios agentes patógenos. Por lo tanto, la síntesis de los sistemas de carbohidratos multivalentes es necesaria para la interacción eficiente con este receptor, así como para la competición eficaz con los ligandos naturales. Los resultados obtenidos en los experimentos realizados en esta tesis podrían contribuir de una manera muy rápida y eficaz en los primeros estudios de los antivirales basados en diferentes estrategias: dendrones tetravalentes, compuestos basados en dendrímeros, glicofullerenos y glicodendrinanopartículas. Los dendrones tetravalentes y los compuestos basados en dendrímeros presentan en la manera multivalente los nuevos imitadores de carbohidratos denominados como pseudomanosidas. La importancia de la valencia se evaluó mediante la presentación de los mismos ligandos de pseudosacáridos en el sistema tetravalente presentando 4 copias del ligando, y en los sistemas multivalentes que muestran de 30 a 32 ligandos seleccionados. Los valores de IC_{50} obtenidos para los sistemas multivalentes fueron alrededor de 20 nM, mostrando una potencia inhibidora de 1 a 2 órdenes de magnitud superior que la de los sistemas de tetravalentes correspondientes (Luczkowiak et al., 2011). La síntesis de glicofullerenos permitió alcanzar una

mayor valencia de 36 manosas. Estos compuestos se sintetizaron mediante la combinación de glicodendrones con un fullereno que permite presentar los carbohidratos de un modo globular. Los resultados obtenidos en el experimento de infección en *cis* demostraron la importancia de la combinación de una estructura adecuada para lograr la multivalencia con la accesibilidad y flexibilidad del ligando. El efecto inhibidor del fullereno con 36 manosas era menor en comparación con el glicofullereno que mostró 12 manosas, sin embargo, la posterior introducción del espaciador más largo a este glicofullereno recuperó su potencia inhibidora y mostró una IC_{50} de 286.4 nM (10 veces más potente que el glicofullereno con 12 manosas y 340 veces más potente que el glicofullereno con 36 manosas que contenía el espaciador corto) (Luczkowiak et al., 2013). La mayor valencia de presentación de los ligandos se generó en el caso de las glicodendrinanopartículas. Este diseño se basó en el conjunto multivalente de monómeros de proteínas (glicodendriproteínas) que llevan componentes de glicanos polivalentes (glicodendrones). De esta manera, estas construcciones muestran un número elevado de glicanos de manera precisa y crean entidades individuales bien definidas de hasta 32 nm de diámetro. Las glicodendrinanopartículas mostraron una actividad antiviral en el rango de picomolar a bajo nanomolar (Ribeiro-Viana et al., 2012).

5. 2. La función del DC- SIGN en la patogénesis del virus de Ébola: la *trans*-infección mediada por DC-SIGN de diferentes cepas de virus del Ébola

El virus del Ébola causa una enfermedad grave, a menudo fatal que consiste en un síndrome de fiebre hemorrágica altamente letal (Peters et al., 1996). La cepa Zaire es la variante del virus con la mayor tasa de mortalidad en un intervalo del 50 al 90%. En contraste con la cepa Zaire, el Ébola Reston no causa enfermedad en los humanos a pesar de una serie de infecciones documentadas durante las epizootias animales (Barrette et al., 2009; Miranda et al., 1999). La base molecular de esta diferencia en su patogénesis no está bien definida. La unión del virus del Ébola GP a diferentes lectinas celulares ha sido demostrada previamente con el fin de aumentar la infección del virus, tanto en *cis* como en *trans* (Alvarez et al., 2002). En nuestro estudio, hemos utilizado partículas recombinantes que expresan dos glicoproteínas de la envoltura del virus del Ébola (EBOZ y EBOR) para estudiar el posible papel del DC -SIGN en la patogénesis de las

dos variantes del Ébola. La infección mediada por DC-SIGN de las dos cepas se verificó en los experimentos de *trans*-infección en el sistema Jurkat DC-SIGN$^+$/Jurkat, *cis*-infección de las DCs primarias y *trans*-infección DCs/HeLa. El primer experimento de *trans*-infección en el modelo celular Jurkat DC-SIGN$^+$/Jurkat reveló diferencias significativas en el ratio de *trans*-infección entre la cepa del Ébola Zaire y la cepa del Ébola Reston ($p=0.0034$). El ratio de t*rans*-infeccion del EBOR era alrededor de tres veces superior en comparación con el del EBOZ (35.97 vs 99.64). La relevancia de las diferencias en el uso del receptor DC-SIGN en el proceso de *trans*-infección también se verificó en el sistema inmunológico mediante el uso de las células dendríticas inmaduras. Las DCs inmaduras se incubaron con EBOZ/EBOR y tras la realización de dos lavados intensivos, fueron co-cultivadas con las células susceptibles HeLa. Los resultados obtenidos en el experimento de *trans*-infección basado en las células inmunes humanas (DC) han confirmado los resultados de *trans*-infección en el sistema de línea celular. La diferencia entre la infección transmitida por las pseudopartículas del Ébola Zaire y del Ébola Reston a las células HeLa fue estadísticamente significativa ($p=0.0084$). Ambos experimentos realizados demostraron significación estadística de mayor uso de DC-SIGN en la *trans*-infección de EBOR en comparación con EBOZ. A pesar de las diferencias significativas en el uso de DC–SIGN por EBOZ/EBOR en los experimentos de *trans*-infección, la infección directa de las DCs inmaduras no ofreció ningún resultado significativo. Nuestros resultados encontraron la asociación entre la cepa del Ébola Reston y un mayor ratio de t*rans*-infección mediada por DC-SIGN. Este descubrimiento podría plantear la hipótesis de que a pesar de que DC-SIGN participa efectivamente en la entrada de virus a las células, *in vivo* este receptor juega aparentemente el papel más importante en la activación adecuada del sistema inmune. DC-SIGN puede ser responsable de la captura del virus, su destrucción y de una presentación más eficaz de los antígenos de los patógenos a las células causando un buen rendimiento de control inmunológico. El DC-SIGN, por lo tanto, aunque es capaz de captar con eficacia las partículas del virus del Ébola, podría servir mejor como factor de defensa del organismo anfitrión en lugar de receptor de escape de patógenos. Por tanto, el nivel más alto del uso de DC-SIGN por el Ébola Reston podría sugerir que el DC-SIGN en general podría estar más implicado en las respuestas antivirales. Los resultados obtenidos en los experi-

mentos realizados se pueden relacionar a los resultados de estudio de Schaefer *et al*., en el que los ratones que expresan el receptor humano DC-SIGN sobrevivieron más tiempo que los ratones de tipo salvaje después de la infección con *Mycobacterium tuberculosis* (Schaefer et al., 2008).

5. 3. La función del DC- SIGN en la patogénesis del virus del VIH-1: implicación de la *trans*-infección mediada por DC-SIGN en el control virológico

El receptor DC-SIGN se clonó y se clasificó inicialmente como un receptor para la glicoproteína de la envuelta del VIH-1 gp120. De hecho, precisamente se ha demostrado que la afinidad de la gp120 para DC-SIGN es incluso mayor que para el receptor CD4 (Curtis et al., 1992). Años antes del descubrimiento de DC-SIGN, los estudios de Cameron *et al*. y Pope *et al*. mostraron que los DCs incubados con el VIH-1 causaron la infección de las células T co-cultivadas (Cameron et al., 1992; Pope et al., 1994). Poco después de la identificación del DC-SIGN, Geijtenbeek *et al*. definió este fenómeno como la *trans*-infección del VIH-1 (Geijtenbeek et al., 2000b). Se ha demostrado claramente que DC-SIGN se une a las estructuras de carbohidratos, tales como glicoconjugados que contienen manosa, expresadas en la superficie de diferentes patógenos (den Dunnen et al., 2010). La envuelta del VIH-1 es una de las proteínas más glicosiladas en la naturaleza, que contiene de 18-32 PNGS en la gp120. Por lo tanto, numerosos estudios *in vitro* han demostrado la alta afinidad de la envuelta del VIH-1 a las células que expresan el receptor DC-SIGN. El receptor DC-SIGN no funciona como un receptor directo del VIH-1 pero transmite de manera eficiente el virus de la periferia a los tejidos linfoides secundarios. Se ha demostrado que las partículas del VIH-1 unidas a DC-SIGN son notablemente más estables y retienen la infectividad durante períodos prolongados (Geijtenbeek et al., 2000b). A pesar de todas las funciones propuestas de DC-SIGN basado en modelos *in vitro*, la confirmación del comportamiento fisiológico de DC-SIGN *in vivo* debe seguir siendo estudiado.

En nuestro estudio hemos analizado la glicoproteína de la envuelta de 30 aislamientos clínicos (6 de EC, 8 de VC y 16 de CI) en el ensayo de la *trans*-infección mediada por DC-SIGN. El experimento de *trans*-infección se realizó con 30 envueltas del VIH-1 para

estudiar la correlación del ratio la *trans*-infección y el control virológico en los dos sistemas celulares (Jurkat DC-SIGN$^+$/Jurkat y Raji DC-SIGN$^+$/Raji). El análisis de los resultados obtenidos en el sistema Raji DC-SIGN$^+$/Raji reveló diferencias significativas en la proporción del uso del DC-SIGN entre los controladores del VIH-1 y los pacientes cion infección crónica. Llamatívamente, el subgrupo de los VC demostró el ratio más alto de trans-infección en comparación con los EC ($p=0.0007$) y los CI ($p<0.0001$). Los EC mostraron una tendencia hacía una mayor eficiencia de trans-infección en comparación con los CI ($p=0.1331$), sin embargo mucho menos eficaz en comparación con los VC. El resultado global fueron posteriormente confirmados por el experimento de *trans*-infección con el sistema Jurkat DC-SIGN$^+$/Jurkat (EC+VC=32.84 vs CI=17.4, $p=0.0233$). La baja asociación entre los EC y eficiente *trans*-infección mediada por DC-SIGN podría sugerir que otros factores, incluyendo el bajo fitness viral (Casado et al., 2013; Lassen et al., 2009; Miura et al., 2009) o la respuesta de las células T CD8$^+$ extremadamente vigorosa (Goulder and Watkins, 2004; Migueles et al., 2002), cuentan para el control virológico en este subgrupo de pacientes. Nuestros resultados han confirmado el bajo fitness de las envueltas derivadas de los EC. Una proporción considerable de las envueltas (10 de las 16) no podría ser comprobada en los experimentos de la *trans*-infección. Todas las envueltas fueran secuenciadas y no mostraron ningún defecto en la secuencia. Sin embargo, en los ensayos celulares 4 de ellas se mostraron no funcionales y 6 de ellas tenían la infectividad por debajo del rango dinámico requerido para los experimentos de infección. Control virológico en el subgrupo de los VC es menos conocido. Podría ser posible que en este subgrupo de pacientes, la respuesta inmune innata tuviese una mayor participación lo que puede influir el control virológico. Los VC utilizan DC-SIGN en manera más eficiente en comparación con otros grupos de los pacientes, por lo tanto se podría proponer el hipótesis que el DC-SIGN en este subgrupo de individuos juega el papel importante en la captura de los antígenos virales y la presentación posterior para la activación adecuada del sistema inmune.

Para acceder a la información sobre la base de estas diferencias, la longitud de la secuencia y el número de PNGS en las glicoproteínas de la envoltura se compararon entre ambos grupos de pacientes. Aunque se ha demostrado que la glicoproteína de la

envoltura de los controladores del VIH es más corta y contiene menos PNGS (Bailey et al., 2006a), en nuestro pequeño estudio las secuencias de los virus del VIH-1 de los controladores y de los pacientes con infección crónica eran de longitud análoga y contenían un número similar de PNGS en la mayoría de las regiones de la gp160 con la única excepción de la región V5. Sin embargo, no se encontró ninguna correlación entre la longitud de la V5 o el número de PNGS en la V5 y el ratio de *trans*-infección. Se podría especular que estos cambios se produjeron en el curso natural de la infección por VIH-1, posiblemente en la respuesta causada por los NAbs. Se ha demostrado previamente que el número de PNGS y la longitud de las envueltas del VIH-1 tienen una tendencia de aumentar en la epidemia del VIH-1 (Bunnik et al., 2010; Bunnik et al., 2008). Nuestro análisis de los datos de la Base de datos de VIH de Los Alamos confirmó estos estudios indicando la aparente evolución de la pandemia del VIH-1 hacía las glicoproteínas más largas y más glicosiladas. Por lo tanto el cambio en V5 y V1-V5 hacía el número más elevado de los PNGS podría ser explicado por el patrón la evolución del VIH-1 y no por la *trans*-infección más eficaz. Los resultados de este estudio podrían contribuir a una mejor comprensión de la función del receptor DC-SIGN en la patogénesis del VIH-1. Este trabajo muestra el uso sustancial del receptor DC-SIGN en el experimento de *trans*-infección por los controladores del VIH-1, especialmente por los VC. Esos resultados fueron verificados en dos sistemas celulares y ambos mostraron la asociación entre un mayor ratio de *trans*-infección y el control virológico. Las envueltas del VIH-1 de los VC han utilizado DC-SIGN de forma más eficiente en comparación con los EC y los pacientes con infección crónica VIH-1. Es posible que el control virológico en el subgrupo de los EC resulte de la reducción de la replicación viral o respuesta celular adaptativa más eficaz. Sin embargo, en el grupo de los VC podría ser posible que la fuerte implicación de DC-SIGN estuviera más conectada con la presentación del antígeno y una respuesta más eficaz del sistema inmune, en lugar de la difusión del virus. El control virológico del VIH-1 se caracteriza por mantener cargas virales bajas en ausencia de terapia antirretroviral. Por lo tanto, la carga viral baja y la falta de replicación activa determinan que las secuencias de las envueltas en los controladores del VIH tengan las regiones variables más cortas y números más bajos de N-glicanos (Bailey et al., 2006a). Aunque el DC-SIGN muestra una fuerte afinidad por las moléculas que contienen ma-

nosas, nuestro estudio ha confirmado que el número de PNGS no es un factor fundamental relacionado con uniones más fuertes al DC-SIGN. La comparación del patrón de N-glicosilación no mostró diferencias estadísticamente significativas entre los VC y los EC/CI, por lo tanto el mayor uso de DC-SIGN en la trans-infección por los VC no puede ser explicada por la presencia aumentada de los glicanos. Podría ser posible que la unión a DC-SIGN implique el patrón más complejo de N-glicosilación y no la cantidad de los glicanos en la superficie. Nuestros datos demuestran que las envueltas del VIH-1 de los controladores aunque contienen generalmente menor número de los glicanos en la superficie del virus, utilizan DC-SIGN más eficazmente que los aislados crónicos.

6. Conclusiones

1) El modelo de infección basado en las líneas celulares que expresan DC- SIGN es una plataforma consistente para estudiar la entrada viral directa (virus del Ébola) y el fenómeno de *trans*-infección (virus Ebola y VIH) debido a que la interacción virus-DC-SIGN en este sistema depende casi exclusivamente de la presencia DC–SIGN.

2) El modelo de infección DC-SIGN es un modelo útil para estudiar estategias antivirales dirigidas a DC-SIGN.

3) La inhibición de la infección mediada por DC-SIGN mediada por los compuestos basados en hidratos de carbono depende en gran medida de la multivalencia de presentación de los glicanos.

4) La actividad antiviral más potente se obtuvo en caso de las glicodendrinanopartículas que muestran una actividad antiviral eficaz en el rango de concentración picomolar -nanomolar. Multivalencia depende de la presentación de los 1620 glicanos generando una gran superficie de interacción (30 nm de diámetro).

5) A pesar del papel del DC-SIGN en la entrada del virus del Ébola y la difusión inicial del virus, en nuestro estudio encontramos significativamente mayor uso de DC-SIGN por la cepa no patógena de Ébola Reston. Este hallazgo podría indicar que DC-SIGN en caso de Ébola Reston está involucrado en un control inmunitario más eficiente.

6) Las glicoproteínas de la envoltura del VIH- 1 de los controladores virológicos utilizan DC-SIGN más eficiente en el experimento de *trans*-infección en comparación con los pacientes con enfermedad crónica.

7) La *trans*-infección mediada por DC-SIGN no está asociada con la cantidad de los N-glicanos en la glicoproteína de la envuelta de VIH-1. Probablemente un patrón más complejo de N- glicosilación específica es responsable de este mecanismo.

8) En el grupo de VC, la significativamente mayor *trans*-infección observada podría indicar que DC-SIGN participa en la detección viral, presentación y control inmunológico más que en la difusión viral, como en el caso de *trans*-infección por Ébola Reston.

9) El grupo de EC no demostró la misma *trans*-infección que los VC. El control virológico en el grupo de los EC puede resultar de la reducción de la replicación viral o extremadamente vigorosa respuesta de las células T $CD8^+$.

ABBREVIATIONS

IX. ABBREVIATIONS

aa – amino acid

Ab – antibody

Ag – antigen

AIDS – acquired immunodeficiency syndrome

APC – antigen-presenting cell

APOBEC3G – apolipoprotein B mRNA editing enzyme catalytic polypeptide-like 3G

ART – antiretroviral therapy

ARV – AIDS-associated retrovirus

ASGP-R – liver-specific asialoglycoprotein receptor

BamHI – Bacillus amyloliquefaciens H 1 gene

BCR – B-cell receptor

BDCA-2 – blood DC antigen-2

BG – Birbeck granule

BGH – bovine growth factor

BSA – bovine serum albumin

CA – capsid

CARD – caspase-recruitment domain

CCR5 – C-C chemokine receptor type 5

CD4 – cluster of differentiation 4

CD8 – cluster of differentiation 8

CD4Bs – CD4 binding site

CDC – Centers for Disease Control and Prevention

cDNA – complementary DNA

Cl – chloride

CMV – cytomegalovirus

CoRBs – coreceptor-binding site

CRD – carbohydrate recognition domain

CTL – cytotoxic T cell

CXCR4 – C-X-C chemokine receptor type 4

DAMPs – damage-associated molecular patterns

DC – dendritic cell

DCAL-1 – DC-associated lectin-1

DCAR – DC immunoactivating receptor

DCIR – DC immunoreceptor

DC-SIGN – dendritic cell-specific intracellular adhesion molecule (ICAM)-3 grabbing non-integrin

DEC-205 – lymphocyte antigen 75

Dectin-1 – DC-associated C-type lectin-1

DM – dual tropic

DMEM – Dulbecco´s Modified Eagle´s Medium

DMF –dimethylformamide

DMSO – dimethyl sulfoxide

DNGR-1/CLEC9A – DC, NK lectin group receptor 1

dNTP –deoxynucleotide

dsDNA – double-stranded DNA

dsRNA – double-stranded RNA

EBNA-1 – Epstein-Barr virus nuclear antigen 1

EBV – Epstein-Barr virus

EC – elite controller

EcoRI – Escherichia coli R 1 gene

EEE – tri-acidic clusters motif

ELISA – enzyme-linked immunosorbent assay

ER – endoplasmic reticulum

Fab – fragment antigen-binding

FACS – fluorescence-activated cell sorting

Fc – fragment crystallisable region

FDC – follicular dendritic cell

FRα – folate receptor α

Gal – galactose

GalNAc – N-acetyl-galactosamine

GFP – green fluorescent protein

Glc – glucose

GlcNac - N-acetyl-glucosamine

GM-CSF – granulocyte-macrophage colony-stimulating factor

GP – glycoprotein

gp120 – glycoprotein 120

gp160 – glycoprotein 160

gp41 – glycoprotein 41

h – hour

HAART – highly active antiretroviral therapy

HBS – hepes buffer saline

HEK 293T – human embryonic kidney 293 cell line

HeLa – human cervical epithelial carcinoma cell line

HindIII – Haemophilus influenzae Rd III gene

HIV – human immunodeficiency virus

HLA - human leukocyte antigen

hMGL – human macrophage galactose lectin

HPV18 – human papillomavirus 18

HR – heptad region

HTLV-I – human T-lymphotropic virus I

HTLV-III – human T-lymphotropic virus III

IAS – inner antisense

ICAM-1 – intercellular adhesion molecule 1

ICAM-2 – intercellular adhesion molecule 2

ICAM-3 – intercellular adhesion molecule 3

IgG – immunoglobulin G

IL-1 – interleukin 1

IL-4 – interleukin 4

IL-6 – interleukin 6

IL-10 – interleukin 10

IL-12 – interleukin 12

IL-1R – interleukin 1 receptor

IN – integrase

INF – interferon

IS – inner sense

ITAM – immunoreceptor tyrosine-based activation motif

ITIM – immune receptor tyrosine-based inhibition motif

Langerin – Langerhans cell specific C-type lectin

LAV – lymphadenopathy-associated virus

LB – Luria-Bertani medium

LC – Langerhans cell

LGP2 – laboratory of genetics and physiology-2

LL – di-leucine motif

LRR – leucine-rich-repeat

LSECtin –liver and lymph node sinusoidal endothelial cell C-type lectin

L-SIGN – liver/lymph node intracellular adhesion molecule (ICAM-3) grabbing non-integrin

LTNP – long term non-progressor

LTR – long terminal repeat

M – molar

MA – matrix

Man – mannose

MBL – mannose binding lectin

MCS – multiple cloning site

MDA5 - melanoma differentiation-associated gene 5

MDCs – myeloid DCs

MfeI – Mycoplasma fermentas I gene

Mg – magnesium

mg – milligram

MHC – major histocompatibility complex

MICL – myeloid inhibitory C-type lectin

min – minute

Mincle – macrophage-inducible C-type lectin

MIP-1β – macrophage inflammatory protein-1β

ml – milliliter

MLV – murine leukaemia virus

mM – millimolar

MMR – macrophage mannose receptor

MR – mannose receptor

mRNA – messenger RNA

MTCT – mother-to-child transmission

MW – molecular weight

MyD88 – myeloid differentiation factor

NAb – neutralizing antibody

NaOAc – sodium acetate

NBD – nucleotide-binding domain

NC – nucleocapsid

NF-kB – nuclear factor kB

ng – nanogram

NK – natural killer cell

NLR – nucleotide oligomerization domain NOD-like receptor

nM – nanomolar

NOD – nucleotide oligomerization domain

NotI – Nocardia otitidis-caviarum 1 gene

OAS – outer antisense

ORF – open reading frame

OS – outer sense

PAMPs –pathogen-associated molecular patterns

PBMCs – Peripheral Blood Mononuclear Cells

PBS – phosphate buffer saline

PBS – primer-binding site

PCP – Pneumocystis carinii pneumonia

PCR – polymerase chain reaction

pDC – plasmacytoid dendritic cell

pETF-b – transcription-elongation factor

PGK-1 – phosphoglycerate kinase 1

pol – polymerase

pM – picomolar

pmol – picomole

PR – protease

preGP – precursor GP

PRRs- pattern recognition receptors

RD – repressor domain

RIG-I – retinoic acid inducible gene I

RLR - retinoic acid inducible gene I (RIG-I) like receptors

rpm – revolutions per minute

RRE – rev response elements

RT – room temperature

RT – reverse transcriptase

SA – sialic acid

sec – second

sGP – secreted glycoprotein

ssGP – small soluble glycoprotein

Siglecs – sialic-acid-binding Immunoglobulin-like lectins

SIGNR1 – specific intracellular adhesion molecule-grabbing non-integrin receptor 1

SIV – simian immunodeficiency virus

SNP – single-nucleotide polymorphism

ssDNA – single stranded DNA

ssRNA – single stranded RNA

SU – surface

SV40 – simian virus 40

T-20 – Tween 20

TAR – transactivation-response element

TCID – tissue culture infectious dose

TCR – T-cell receptor

TEMED – tetramethylethylenediamine

Th – T-helper cell

TIR – Toll/IL-1R homology (TIR) domain

TLR - Toll-like receptor

TM – transmembrane

TNF – tumor necrosis factor

TRIM5α – tripartite motif protein isoform 5 alpha

tRNA – transfer RNA

TZM-bl – Human cervical epithelial carcinoma cell line expressing human CD4, CCR5, CXCR4 and containing HIV-1 Tat-regulated reporter genes for firefly luciferase and ß-galactosidase

U87 – human gastroglioma cell line

µg - microgram

µl – microliter

µM – micromolar

V1 – variable loop 1

V2 – variable loop 2

V3 – variable loop 3

V4 – variable loop 4

V5 – variable loop 5

VC – viremic controller

VL – viral load

VLs – variable loops

VP – virion protein

VSV – Vesicular Stomatitis virus

WB –Western Blot

wt – wild-type

BIBLIOGRAPHY

X. BIBLIOGRAPHY

Abrahams, M.R., Anderson, J.A., Giorgi, E.E., Seoighe, C., Mlisana, K., Ping, L.H., Athreya, G.S., Treurnicht, F.K., Keele, B.F., Wood, N., *et al.* (2009). Quantitating the Multiplicity of Infection with Human Immunodeficiency Virus Type 1 Subtype C Reveals a Non-Poisson Distribution of Transmitted Variants. J Virol *83*, 3556-3567.

Akira, S., Uematsu, S., and Takeuchi, O. (2006). Pathogen recognition and innate immunity. Cell *124*, 783-801.

Alazard-Dany, N., Volchkova, V., Reynard, O., Carbonnelle, C., Dolnik, O., Ottmann, M., Khromykh, A., and Volchkov, V.E. (2006). Ebola virus glycoprotein GP is not cytotoxic when expressed constitutively at a moderate level. J Gen Virol *87*, 1247-1257.

Alexander, L., Weiskopf, E., Greenough, T.C., Gaddis, N.C., Auerbach, M.R., Malim, M.H., O'Brien, S.J., Walker, B.D., Sullivan, J.L., and Desrosiers, R.C. (2000). Unusual polymorphisms in human immunodeficiency virus type 1 associated with nonprogressive infection. J Virol *74*, 4361-4376.

Alsop, Z. (2007). Ebola outbreak in Uganda "atypical", say experts. Lancet *370*, 2085-2085.

Altfeld, M., and Allen, T.M. (2006). Hitting HIV where it hurts: an alternative approach to HIV vaccine design. Trends Immunol *27*, 504-510.

Altfeld, M., Kalife, E.T., Qi, Y., Streeck, H., Lichterfeld, M., Johnston, M.N., Burgett, N., Swartz, M.E., Yang, A., Alter, G., *et al.* (2006). HLA alleles associated with delayed progression to AIDS contribute strongly to the initial CD8(+) T cell response against HIV-1. PLoS Med *3*, 1851-1864.

Alvarez, C.P., Lasala, F., Carrillo, J., Muniz, O., Corbi, A.L., and Delgado, R. (2002). C-type lectins DC-SIGN and L-SIGN mediate cellular entry by Ebola virus in cis and in trans. J Virol *76*, 6841-6844.

Anonymous (1978). Ebola haemorrhagic fever in Zaire, 1976. Bull World Health Organ *56*, 271-293.

Appelmelk, B.J., van Die, I., van Vliet, S.J., Vandenbroucke-Grauls, C.M., Geijtenbeek, T.B., and van Kooyk, Y. (2003). Cutting edge: carbohydrate profiling identifies new pathogens that interact with dendritic cell-specific ICAM-3-grabbing nonintegrin on dendritic cells. J Immunol *170*, 1635-1639.

Arce, E., Nieto, P.M., Diaz, V., Castro, R.G., Bernad, A., and Rojo, J. (2003). Glycodendritic structures based on Boltorn hyperbranched polymers and their interactions with Lens culinaris lectin. Bioconjug Chem *14*, 817-823.

Arina, A., Murillo, O., Dubrot, J., Azpilikueta, A., Alfaro, C., Perez-Gracia, J.L., Bendandi, M., Palencia, B., Hervas-Stubbs, S., and Melero, I. (2007). Cellular liaisons of natural killer lymphocytes in immunology and immunotherapy of cancer. Expert Opin Biol Ther *7*, 599-615.

Auvert, B., Taljaard, D., Lagarde, E., Sobngwi-Tambekou, J., Sitta, R., and Puren, A. (2005). Randomized, controlled intervention trial of male circumcision for reduction of HIV infection risk: the ANRS 1265 Trial. PLoS Med *2*, e298.

Bailey, J.R., Lassen, K.G., Yang, H.C., Quinn, T.C., Ray, S.C., Blankson, J.N., and Siliciano, R.F. (2006a). Neutralizing antibodies do not mediate suppression of human immunodeficiency virus type 1 in elite suppressors or selection of plasma virus variants in patients on highly active antiretroviral therapy. J Virol *80*, 4758-4770.

Bailey, J.R., Williams, T.M., Siliciano, R.F., and Blankson, J.N. (2006b). Maintenance of viral suppression in HIV-1-infected HLA-B*57(+) elite suppressors despite CTL escape mutations. J Exp Med *203*, 1357-1369.

Bailey, R.C., Moses, S., Parker, C.B., Agot, K., Maclean, I., Krieger, J.N., Williams, C.F., Campbell, R.T., and Ndinya-Achola, J.O. (2007). Male circumcision for HIV prevention in young men in Kisumu, Kenya: a randomised controlled trial. Lancet *369*, 643-656.

Balzarini, J. (2007). Targeting the glycans of glycoproteins: a novel paradigm for antiviral therapy. Nat Rev Microbiol *5*, 583-597.

Banchereau, J., and Steinman, R.M. (1998). Dendritic cells and the control of immunity. Nature *392*, 245-252.

Barber, L.D., Gillece-Castro, B., Percival, L., Li, X., Clayberger, C., and Parham, P. (1995). Overlap in the repertoires of peptides bound in vivo by a group of related class I HLA-B allotypes. Curr Biol *5*, 179-190.

Baribaud, F., Pohlmann, S., Sparwasser, T., Kimata, M.T., Choi, Y.K., Haggarty, B.S., Ahmad, N., Macfarlan, T., Edwards, T.G., Leslie, G.J., *et al.* (2001). Functional and antigenic characterization of human, rhesus macaque, pigtailed macaque, and murine DC-SIGN. J Virol *75*, 10281-10289.

Barresinoussi, F., Chermann, J.C., Rey, F., Nugeyre, M.T., Chamaret, S., Gruest, J., Dauguet, C., Axlerblin, C., Vezinetbrun, F., Rouzioux, C., *et al.* (1983). Isolation of a T-lymphotropic retrovirus from a patient at risk for Acquired Immune-Deficiency Syndrome (AIDS). Science *220*, 868-871.

Barrette, R.W., Metwally, S.A., Rowland, J.M., Xu, L., Zaki, S.R., Nichol, S.T., Rollin, P.E., Towner, J.S., Shieh, W.-J., Batten, B., *et al.* (2009). Discovery of Swine as a Host for the Reston ebolavirus. Science *325*, 204-206.

Becker, S., Spiess, M., and Klenk, H.D. (1995). The asialoglycoprotein receptor is a potential liver-specific receptor for Marburg Virus. J Gen Virol *76*, 393-399.

Becker, Y. (1995). Retrovirus and filovirus "immunosuppressive motif" and the evolution of virus pathogenicity in HIV-1, HIV-2, and Ebola viruses. Virus Genes *11*, 191-195.

Bender, W., and Davidson, N. (1976). Mapping of poly(A) sequences in electron-microscope reveals unusual structure of type-C oncornavirus RNA molecules. Cell *7*, 595-607.

Berger, E.A. (1997). HIV entry and tropism: the chemokine receptor connection. AIDS *11*, S3-S16.

Betts, M.R., Nason, M.C., West, S.M., De Rosa, S.C., Migueles, S.A., Abraham, J., Lederman, M.M., Benito, J.M., Goepfert, P.A., Connors, M., *et al.* (2006). HIV nonprogressors preferentially maintain highly functional HIV-specific CD8+ T cells. Blood *107*, 4781-4789.

Bjorndal, A., Deng, H.K., Jansson, M., Fiore, J.R., Colognesi, C., Karlsson, A., Albert, J., Scarlatti, G., Littman, D.R., and Fenyo, E.M. (1997). Coreceptor usage of primary human immunodeficiency virus type 1 isolates varies according to biological phenotype. J Virol *71*, 7478-7487.

Blankson, J.N., Bailey, J.R., Thayil, S., Yang, H.-C., Lassen, K., Lai, J., Gandhi, S.K., Siliciano, J.D., Williams, T.M., and Siliciano, R.F. (2007). Isolation and characterization of replication-competent human immunodeficiency virus type 1 from a subset of elite suppressors. J Virol *81*, 2508-2518.

Boily-Larouche, G., Milev, M.P., Zijenah, L.S., Labbe, A.C., Zannou, D.M., Humphrey, J.H., Ward, B.J., Poudrier, J., Mouland, A.J., Cohen, E.A., *et al.* (2012). Naturally-occurring genetic variants in human DC-SIGN increase HIV-1 capture, cell-transfer and risk of mother-to-child transmission. PLoS One *7*, e40706.

Borggren, M., Repits, J., Kuylenstierna, C., Sterjovski, J., Churchill, M.J., Purcell, D.F.J., Karlsson, A., Albert, J., Gorry, P.R., and Jansson, M. (2008). Evolution of DC-SIGN use revealed by fitness studies of R5 HIV-I variants emerging during AIDS progression. Retrovirology *5*, doi:10.1186/1742-4690-1185-1128.

Borregaard, N. (2010). Neutrophils, from Marrow to Microbes. Immunity *33*, 657-670.

Bourne, N., Stanberry, L.R., Kern, E.R., Holan, G., Matthews, B., and Bernstein, D.I. (2000). Dendrimers, a new class of candidate topical microbicides with activity against herpes simplex virus infection. Antimicrob Agents Chemother *44*, 2471-2474.

Bowen, E.T., Platt, G.S., Simpson, D.I., McArdell, L.B., and Raymond, R.T. (1978). Ebola haemorrhagic fever: experimental infection of monkeys. Trans R Soc Trop Med Hyg *72*, 188-191.

Bray, M. (2001). The role of the Type I interferon response in the resistance of mice to filovirus infection. J Gen Virol *82*, 1365-1373.

Bunnik, E.M., Euler, Z., Welkers, M.R., Boeser-Nunnink, B.D., Grijsen, M.L., Prins, J.M., and Schuitemaker, H. (2010). Adaptation of HIV-1 envelope gp120 to humoral immunity at a population level. Nat Med *16*, 995-997.

Bunnik, E.M., Pisas, L., van Nuenen, A.C., and Schuitemaker, H. (2008). Autologous neutralizing humoral immunity and evolution of the viral envelope in the course of subtype B human immunodeficiency virus type 1 infection. J Virol *82*, 7932-7941.

Butler, D.M., Smith, D.M., Cachay, E.R., Hightower, G.K., Nugent, C.T., Richman, D.D., and Little, S.J. (2008). Herpes simplex virus 2 serostatus and viral loads of HIV-1 in blood and semen as risk factors for HIV transmission among men who have sex with men. AIDS *22*, 1667-1671.

Cambi, A., Gijzen, K., de Vries l, J., Torensma, R., Joosten, B., Adema, G.J., Netea, M.G., Kullberg, B.J., Romani, L., and Figdor, C.G. (2003). The C-type lectin DC-SIGN (CD209) is an antigen-uptake receptor for Candida albicans on dendritic cells. Eur J Immunol *33*, 532-538.

Cameron, P.U., Freudenthal, P.S., Barker, J.M., Gezelter, S., Inaba, K., and Steinman, R.M. (1992). Dendritic cells exposed to human immunodeficiency virus type-1 transmit a vigorous cytopathic infection to CD4+ T cells. Science *257*, 383-387.

Cao, Y.Z., Qin, L.M., Zhang, L.Q., Safrit, J., and Ho, D.D. (1995). Virological and immunological characterization of long-term survivors of Human Immunodeficiency Virus Type 1 infection. N Eng J Med *332*, 201-208.

Carette, J.E., Raaben, M., Wong, A.C., Herbert, A.S., Obernosterer, G., Mulherkar, N., Kuehne, A.I., Kranzusch, P.J., Griffin, A.M., Ruthel, G., *et al.* (2011). Ebola virus entry requires the cholesterol transporter Niemann-Pick C1. Nature *477*, 340-343.

Carrington, M., Nelson, G.W., Martin, M.P., Kissner, T., Vlahov, D., Goedert, J.J., Kaslow, R., Buchbinder, S., Hoots, K., and O'Brien, S.J. (1999). HLA and HIV-1: heterozygote advantage and B*35-Cw*04 disadvantage. Science *283*, 1748-1752.

Carrington, M., and O'Brien, S.J. (2003). The influence of HLA genotype on AIDS. Annu Rev Med *54*, 535-551.

Casado, C., Pernas, M., Sandonis, V., Alvaro-Cifuentes, T., Olivares, I., Fuentes, R., Martinez-Prats, L., Grau, E., Ruiz, L., Delgado, R., *et al.* (2013). Identification of a cluster of HIV-1 controllers infected with low replicating viruses. PLoS One *8*, e77663.

CDC, C.f.D.C.a.P. (2001). Outbreak of Ebola hemorrhagic fever Uganda, August 2000-January 2001. Morb Mortal Wkly Rep *50*, 73-77.

Clerici, M., Giorgi, J.V., Chou, C.C., Gudeman, V.K., Zack, J.A., Gupta, P., Ho, H.N., Nishanian, P.G., Berzofsky, J.A., and Shearer, G.M. (1992). Cell-mediated immune response to Human-Immunodeficiency-Virus (HIV) Type-1 in seronegative homosexual men with recent sexual exposure to HIV-1. J Infect Dis *165*, 1012-1019.

Coffin, J.M. (1992). Structure and classification of retroviruses (New York: Plenum Press).

Coffin, J.M., Hughes, S.H., and Varmus, H.E. (1997). Retroviruses (New York: Cold Spring Harbor Laboratory Press).

Colmenares, M., Puig-Kroger, A., Pello, O.M., Corbi, A.L., and Rivas, L. (2002). Dendritic cell (DC)-specific intercellular adhesion molecule 3 (ICAM-3)-grabbing nonintegrin (DC-SIGN, CD209), a C-type surface lectin in human DCs, is a receptor for Leishmania amastigotes. J Biol Chem *277*, 36766-36769.

Connor, R.I., Chen, B.K., Choe, S., and Landau, N.R. (1995). Vpr is required for efficient replication of Human-Immuno-Deficiency-Virus Type-1 in mononuclear phagocytes. Virology *206*, 935-944.

Cook, J.D., and Lee, J.E. (2013). The secret life of viral entry glycoproteins: moonlighting in immune evasion. PLoS Pathog *9*, e1003258.

Cote, M., Misasi, J., Ren, T., Bruchez, A., Lee, K., Filone, C.M., Hensley, L., Li, Q., Ory, D., Chandran, K., *et al.* (2011). Small molecule inhibitors reveal Niemann-Pick C1 is essential for Ebola virus infection. Nature *477*, 344-348.

Crozat, K., Vivier, E., and Dalod, M. (2009). Crosstalk between components of the innate immune system: promoting anti-microbial defenses and avoiding immunopathologies. Immunol Rev *227*, 129-149.

Curtis, B.M., Scharnowske, S., and Watson, A.J. (1992). Sequence and expression of a membrane-associated C-type lectin that exhibits CD4-independent binding of Human-Immunodeficiency-Virus envelope glycoprotein-gp120. Proc Natl Acad Sci U S A *89*, 8356-8360.

Chackerian, B., Rudensey, L.M., and Overbaugh, J. (1997). Specific N-linked and O-linked glycosylation modifications in the envelope V1 domain of simian immunodeficiency virus variants that evolve in the host alter recognition by neutralizing antibodies. J Virol *71*, 7719-7727.

Chan, D.C., Fass, D., Berger, J.M., and Kim, P.S. (1997). Core structure of gp41 from the HIV envelope glycoprotein. Cell *89*, 263-273.

Chan, S.Y., Empig, C.J., Welte, F.J., Speck, R.F., Schmaljohn, A., Kreisberg, J.F., and Goldsmith, M.A. (2001). Folate receptor-alpha is a cofactor for cellular entry by Marburg and Ebola viruses. Cell *106*, 117-126.

Chen, Y., Winchester, R., Korber, B., Gagliano, J., Bryson, Y., Hutto, C., Martin, N., McSherry, G., Petru, A., Wara, D., *et al.* (1997). Influence of HLA alleles on the rate of progression of vertically transmitted HIV infection in children: association of several HLA-DR13 alleles with long-term survivorship and the potential association of HLA-A*2301 with rapid progression to AIDS. Long-Term Survivor Study. Hum Immunol *55*, 154-162.

Chertova, E., Bess, J.W., Crise, B.J., Sowder, R.C., Schaden, T.M., Hilburn, J.M., Hoxie, J.A., Benveniste, R.E., Lifson, J.D., Henderson, L.E., *et al.* (2002). Envelope glycoprotein incorporation, not shedding of surface envelope glycoprotein (gp120/SU), is the primary determinant of SU content of purified human immunodeficiency virus type 1 and simian immunodeficiency virus. J Virol *76*, 5315-5325.

Chohan, B., Lang, D., Sagar, M., Korber, B., Lavreys, L., Richardson, B., and Overbaugh, J. (2005). Selection for human immunodeficiency virus type 1 envelope glycosylation variants with shorter V1-V2 loop sequences occurs during transmission of certain genetic subtypes and may impact viral RNA levels. J Virol *79*, 6528-6531.

Chung, N.P., Breun, S.K., Bashirova, A., Baumann, J.G., Martin, T.D., Karamchandani, J.M., Rausch, J.W., Le Grice, S.F., Wu, L., Carrington, M., *et al.* (2010). HIV-1 transmission by dendritic cell-specific ICAM-3-grabbing nonintegrin (DC-SIGN) is regulated by determinants in the carbohydrate recognition domain that are absent in liver/lymph node-SIGN (L-SIGN). J Biol Chem *285*, 2100-2112.

Churchill, M.J., Rhodes, D.I., Learmont, J.C., Sullivan, J.S., Wesselingh, S.L., Cooke, I.R.C., Deacon, N.J., and Gorry, P.R. (2006). Longitudinal analysis of human immunodeficiency virus type 1 nef/long terminal repeat sequences in a cohort of long-term survivors infected from a single source. J Virol *80*, 1047-1052.

Davis, K.J., Anderson, A.O., Geisbert, T.W., Steele, K.E., Geisbert, J.B., Vogel, P., Connolly, B.M., Huggins, J.W., Jahrling, P.B., and Jaax, N.K. (1997). Pathology of experimental Ebola virus

infection in African green monkeys - Involvement of fibroblastic reticular cells. Arch Pathol Lab Med *121*, 805-819.

de Bakker, B.I., de Lange, F., Cambi, A., Korterik, J.P., van Dijk, E.M., van Hulst, N.F., Figdor, C.G., and Garcia-Parajo, M.F. (2007). Nanoscale organization of the pathogen receptor DC-SIGN mapped by single-molecule high-resolution fluorescence microscopy. Chemphyschem *8*, 1473-1480.

de Fougerolles, A.R., Qin, X., and Springer, T.A. (1994). Characterization of the function of intercellular adhesion molecule (ICAM)-3 and comparison with ICAM-1 and ICAM-2 in immune responses. J Exp Med *179*, 619-629.

de Fougerolles, A.R., and Springer, T.A. (1992). Intercellular adhesion molecule 3, a third adhesion counter-receptor for lymphocyte function-associated molecule 1 on resting lymphocytes. J Exp Med *175*, 185-190.

de La Fuente, J.M., Barrientos, A.G., Rojas, T.C., Rojo, J., Canada, J., Fernandez, A., and Penades, S. (2001). Gold Glyconanoparticles as Water-Soluble Polyvalent Models To Study Carbohydrate Interactions. Angew Chem Int Ed Engl *40*, 2257-2261.

de Witte, L., Nabatov, A., and Geijtenbeek, T.B.H. (2008). Distinct roles for DC-SIGN(+)-dendritic cells and Langerhans cells in HIV-1 transmission. Trends Mol Med *14*, 12-19.

de Witte, L., Nabatov, A., Pion, M., Fluitsma, D., de Jong, M.A., de Gruijl, T., Piguet, V., van Kooyk, Y., and Geijtenbeek, T.B. (2007). Langerin is a natural barrier to HIV-1 transmission by Langerhans cells. Nat Med *13*, 367-371.

Deacon, N.J., Tsykin, A., Solomon, A., Smith, K., Ludfordmenting, M., Hooker, D.J., McPhee, D.A., Greenway, A.L., Ellett, A., Chatfield, C., *et al.* (1995). Genomic structure of an attenuated quasi-species of HIV-1 from a blood-transfusion donor and recipients. Science *270*, 988-991.

Deeks, S.G., Schweighardt, B., Wrin, T., Galovich, J., Hoh, R., Sinclair, E., Hunt, P., McCune, J.M., Martin, J.N., Petropoulos, C.J., *et al.* (2006). Neutralizing antibody responses against autologous and heterologous viruses in acute versus chronic human immunodeficiency virus (HIV) infection: evidence for a constraint on the ability of HIV to completely evade neutralizing antibody responses. J Virol *80*, 6155-6164.

Deeks, S.G., and Walker, B.D. (2007). Human immunodeficiency virus controllers: Mechanisms of durable virus control in the absence of antiretroviral therapy. Immunity *27*, 406-416.

den Dunnen, J., Gringhuis, S.I., and Geijtenbeek, T.B. (2010). Dusting the sugar fingerprint: C-type lectin signaling in adaptive immunity. Immunol Lett *128*, 12-16.

Deng, H.K., Liu, R., Ellmeier, W., Choe, S., Unutmaz, D., Burkhart, M., DiMarzio, P., Marmon, S., Sutton, R.E., Hill, C.M., *et al.* (1996). Identification of a major co-receptor for primary isolates of HIV-1. Nature *381*, 661-666.

Dolnik, O., Volchkova, V., Garten, W., Carbonnelle, C., Becker, S., Kahnt, J., Stroher, U., Klenk, H.D., and Volchkov, V. (2004). Ectodomain shedding of the glycoprotein GP of Ebola virus. EMBO J *23*, 2175-2184.

Douek, D.C., Roederer, M., and Koup, R.A. (2009). Emerging concepts in the immunopathogenesis of AIDS. Annu Rev Med *60*, 471-484.

Drickamer, K., and Taylor,M.E (2006). Introduction to Glycobiology 2nd edition edn (USA: Oxford University Press).

Druar, C., Saini, S.S., Cossitt, M.A., Yu, F., Qiu, X., Geisbert, T.W., Jones, S., Jahrling, P.B., Stewart, D.I., and Wiersma, E.J. (2005). Analysis of the expressed heavy chain variable-region genes of Macaca fascicularis and isolation of monoclonal antibodies specific for the Ebola virus' soluble glycoprotein. Immunogenetics *57*, 730-738.

Dustin, M.L., and Chan, A.C. (2000). Signaling takes shape in the immune system. Cell *103*, 283-294.

Elias, C.J., and Coggins, C. (1996). Female-controlled methods to prevent sexual transmission of HIV. AIDS *10*, S43-S51.

Engering, A., Geijtenbeek, T.B.H., van Vliet, S.J., Wijers, M., van Liempt, E., Demaurex, N., Lanzavecchia, A., Fransen, J., Figdor, C.G., Piguet, V., *et al.* (2002). The dendritic cell-specific adhesion receptor DC-SIGN internalizes antigen for presentation to T cells. J Immunol *168*, 2118-2126.

Epstein, M.A., and Barr, Y.M. (1965). Characteristics and mode of growth of tissue culture strain (EB1) of human lymphoblasts from Burkitt´s Lymphoma. J Natl Cancer Inst *34*, 231-240.

Feinberg, H., Mitchell, D.A., Drickamer, K., and Weis, W.I. (2001). Structural basis for selective recognition of oligosaccharides by DC-SIGN and DC-SIGNR. Science *294*, 2163-2166.

Feldmann, H., and Kiley, M.P. (1999). Classification, structure, and replication of filoviruses. Marburg and Ebola Viruses *235*, 1-21.

Feldmann, H., Klenk, H.D., and Sanchez, A. (1993). Molecular biology and evolution of filoviruses. Archives of virology Supplementum *7*, 81-100.

Feldmann, H., Will, C., Schikore, M., Slenczka, W., and Klenk, H.D. (1991). Glycosylation and oligomerization of the spike protein of Marburg Virus. Virology *182*, 353-356.

Feng, Y., Broder, C.C., Kennedy, P.E., and Berger, E.A. (1996). HIV-1 entry cofactor: Functional cDNA cloning of a seven-transmembrane, G protein-coupled receptor. Science *272*, 872-877.

Fenouillet, E., Gluckman, J.C., and Jones, I.M. (1994). Functions of HIV envelope glycans. Trends Biochem Sci *19*, 65-70.

Fiebig, E.W., Wright, D.J., Rawal, B.D., Garrett, P.E., Schumacher, R.T., Peddada, L., Heldebrant, C., Smith, R., Conrad, A., Kleinman, S.H., *et al.* (2003). Dynamics of HIV viremia and antibody seroconversion in plasma donors: implications for diagnosis and staging of primary HIV infection. AIDS *17*, 1871-1879.

Fisher-Hoch, S.P., Perez-Oronoz, G.I., Jackson, E.L., Hermann, L.M., and Brown, B.G. (1992). Filovirus clearance in non-human primates. Lancet *340*, 451-453.

Frost, S.D., Liu, Y., Pond, S.L., Chappey, C., Wrin, T., Petropoulos, C.J., Little, S.J., and Richman, D.D. (2005). Characterization of human immunodeficiency virus type 1 (HIV-1) envelope variation and neutralizing antibody responses during transmission of HIV-1 subtype B. J Virol *79*, 6523-6527.

Gallo, R.C., Salahuddin, S.Z., Popovic, M., Shearer, G.M., Kaplan, M., Haynes, B.F., Palker, T.J., Redfield, R., Oleske, J., Safai, B., *et al.* (1984). Frequent detection and isolation of cytopathic retroviruses (HTLV-III) from patients with AIDS and at risk for AIDS. Science *224*, 500-503.

Gao, X., Nelson, G.W., Karacki, P., Martin, M.P., Phair, J., Kaslow, R., Goedert, J.J., Buchbinder, S., Hoots, K., Vlahov, D., *et al.* (2001). Effect of a single amino acid change in MHC class I molecules on the rate of progression to AIDS. N Engl J Med *344*, 1668-1675.

Garcia-Vallejo, J.J., and van Kooyk, Y. (2013). The physiological role of DC-SIGN: A tale of mice and men. Trends Immunol *34*, 482-486.

Geczy, A.F., Kuipers, H., Coolen, M., Ashton, L.J., Kennedy, C., Ng, G., Dodd, R., Wallace, R., Le, T., Raynes-Greenow, C.H., *et al.* (2000). HLA and other host factors in transfusion-acquired HIV-1 infection. Hum Immunol *61*, 172-176.

Geijtenbeek, T.B., Groot, P.C., Nolte, M.A., van Vliet, S.J., Gangaram-Panday, S.T., van Duijnhoven, G.C., Kraal, G., van Oosterhout, A.J., and van Kooyk, Y. (2002a). Marginal zone macrophages express a murine homologue of DC-SIGN that captures blood-borne antigens in vivo. Blood *100*, 2908-2916.

Geijtenbeek, T.B., Koopman, G., van Duijnhoven, G.C., van Vliet, S.J., van Schijndel, A.C., Engering, A., Heeney, J.L., and van Kooyk, Y. (2001). Rhesus macaque and chimpanzee DC-SIGN act as HIV/SIV gp120 trans-receptors, similar to human DC-SIGN. Immunol Lett *79*, 101-107.

Geijtenbeek, T.B., van Vliet, S.J., Engering, A., t Hart, B.A., and van Kooyk, Y. (2004). Self- and nonself-recognition by C-type lectins on dendritic cells. Annu Rev Immunol *22*, 33-54.

Geijtenbeek, T.B.H., Krooshoop, D., Bleijs, D.A., van Vliet, S.J., van Duijnhoven, G.C.F., Grabovsky, V., Alon, R., Figdor, C.G., and van Kooyk, Y. (2000a). DC-SIGN-ICAM-2 interaction mediates dendritic cell trafficking. Nat Immunol *1*, 353-357.

Geijtenbeek, T.B.H., Kwon, D.S., Torensma, R., van Vliet, S.J., van Duijnhoven, G.C.F., Middel, J., Cornelissen, I., Nottet, H., KewalRamani, V.N., Littman, D.R., *et al.* (2000b). DC-SIGN, a dendritic cell-specific HIV-1-binding protein that enhances trans-infection of T cells. Cell *100*, 587-597.

Geijtenbeek, T.B.H., Torensma, R., van Vliet, S.J., van Duijnhoven, G.C.F., Adema, G.J., van Kooyk, Y., and Figdor, C.G. (2000c). Identification of DC-SIGN, a novel dendritic cell-specific ICAM-3 receptor that supports primary immune responses. Cell *100*, 575-585.

Geijtenbeek, T.B.H., van Duijnhoven, G.C.F., van Vliet, S.J., Krieger, E., Vriend, G., Figdor, C.G., and van Kooyk, Y. (2002b). Identification of different binding sites in the dendritic cell-specific receptor DC-SIGN for intercellular adhesion molecule 3 and HIV-1. J Biol Chem *277*, 11314-11320.

Geijtenbeek, T.B.H., and van Kooyk, Y. (2003). Pathogens target DC-SIGN to influence their fate - DC-SIGN functions as a pathogen receptor with broad specificity. APMIS *111*, 698-714.

Geijtenbeek, T.B.H., van Vliet, S.J., Koppel, E.A., Sanchez-Hernandez, M., Vandenbroucke-Grauls, C., Appelmelk, B., and van Kooyk, Y. (2003). Mycobacteria target DC-SIGN to suppress dendritic cell function. J Exp Med *197*, 7-17.

Geisbert, T.W., and Jahrling, P.B. (1995). Differentiation of filoviruses by electron microscopy. Virus Research *39*, 129-150.

Gelderblom, H.R., Ozel, M., Hausmann, E.H.S., Winkel, T., Pauli, G., and Koch, M.A. (1988). Fine-structure of Human Immunodeficiency Virus (HIV), immunolocalization of structural proteins and virus-cell relation. Micron Microscop *19*, 41-60.

Geyer, H., Will, C., Feldmann, H., Klenk, H.D., and Geyer, R. (1992). Carbohydrate structure of Marburg Virus glycoprotein Glycobiology *2*, 299-312.

Gnanakaran, S., Bhattacharya, T., Daniels, M., Keele, B.F., Hraber, P.T., Lapedes, A.S., Shen, T.Y., Gaschen, B., Krishnamoorthy, M., Li, H., *et al.* (2011). Recurrent Signature Patterns in HIV-1 B Clade Envelope Glycoproteins Associated with either Early or Chronic Infections. Plos Pathogens *7*, doi:10.1371.

Gomez, C., and Hope, T.J. (2005). The ins and outs of HIV replication. Cell Microbiol *7*, 621-626.

Goonetilleke, N., Liu, M.K.P., Salazar-Gonzalez, J.F., Ferrari, G., Giorgi, E., Ganusov, V.V., Keele, B.F., Learn, G.H., Turnbull, E.L., Salazar, M.G., *et al.* (2009). The first T cell response to transmitted/founder virus contributes to the control of acute viremia in HIV-1 infection. J Exp Med *206*, 1253-1272.

Gordon, S. (2002). Pattern recognition receptors: Doubling up for the innate immune response. Cell *111*, 927-930.

Gottlieb, M.S., Schroff, R., Schanker, H.M., Weisman, J.D., Fan, P.T., Wolf, R.A., and Saxon, A. (1981). Pneumocystis-Carinii Pneumonia and mucosal candidiasis in previously healthy homosexual men - Evidence of a new Acuired Cellular Immunodeficiency. N Eng J Med *305*, 1425-1431.

Goulder, P.J., and Watkins, D.I. (2004). HIV and SIV CTL escape: implications for vaccine design. Nat Rev Immunol *4*, 630-640.

Graham, F.L., Smiley, J., Russell, W.C., and Nairn, R. (1977). Characteristics of a human cell line transformed by DNA from human adenovirus type-5. J Gen Virol *36*, 59-72.

Grakoui, A., Bromley, S.K., Sumen, C., Davis, M.M., Shaw, A.S., Allen, P.M., and Dustin, M.L. (1999). The immunological synapse: a molecular machine controlling T cell activation. Science *285*, 221-227.

Gramberg, T., Hofmann, H., Moller, P., Lalor, P.F., Marzi, A., Geier, M., Krumbiegel, M., Winkler, T., Kirchhoff, F., Adams, D.H., *et al.* (2005). LSECtin interacts with filovirus glycoproteins and the spike protein of SARS coronavirus. Virology *340*, 224-236.

Gray, R.H., Kigozi, G., Serwadda, D., Makumbi, F., Watya, S., Nalugoda, F., Kiwanuka, N., Moulton, L.H., Chaudhary, M.A., Chen, M.Z., *et al.* (2007). Male circumcision for HIV prevention in men in Rakai, Uganda: a randomised trial. Lancet *369*, 657-666.

Greatrex, B.W., Brodie, S.J., Furneaux, R.H., Hook, S.M., McBurney, W.T., Painter, G.F., Rades, T., and Rendle, P.M. (2009). The synthesis and immune stimulating action of mannose-capped lysine-based dendrimers. Tetrahedron *65*, 2939-2950.

Gringhuis, S.I., den Dunnen, J., Litjens, M., van der Vlist, M., and Geijtenbeek, T.B. (2009). Carbohydrate-specific signaling through the DC-SIGN signalosome tailors immunity to Mycobacterium tuberculosis, HIV-1 and Helicobacter pylori. Nat Immunol *10*, 1081-1088.

Gringhuis, S.I., den Dunnen, J., Litjens, M., van Het Hof, B., van Kooyk, Y., and Geijtenbeek, T.B. (2007). C-type lectin DC-SIGN modulates Toll-like receptor signaling via Raf-1 kinase-dependent acetylation of transcription factor NF-kappaB. Immunity *26*, 605-616.

Groseth, A., Marzi, A., Hoenen, T., Herwig, A., Gardner, D., Becker, S., Ebihara, H., and Feldmann, H. (2012). The Ebola virus glycoprotein contributes to but is not sufficient for virulence in vivo. PLoS Pathog *8*, e1002847.

Guo, Y., Feinberg, H., Conroy, E., Mitchell, D.A., Alvarez, R., Blixt, O., Taylor, M.E., Weis, W.I., and Drickamer, K. (2004). Structural basis for distinct ligand-binding and targeting properties of the receptors DC-SIGN and DC-SIGNR. Nat Struct Mol Biol *11*, 591-598.

Gupta, R., Jung, E., and Brunak, S. (2004). Prediction of N-glycosylation sites in human proteins. Available at (http://www.cbs.dtu.dk/services/NetNGlyc/).

Haase, A.T. (2005). Perils at mucosal front lines for HIV and SIV and their hosts. Nat Rev Immunol *5*, 783-792.

Haase, A.T. (2010). Targeting early infection to prevent HIV-1 mucosal transmission. Nature *464*, 217-223.

Halary, F., Amara, A., Lortat-Jacob, H., Messerle, M., Delaunay, T., Houles, C., Fieschi, F., Arenzana-Seisdedos, F., Moreau, J.F., and Dechanet-Merville, J. (2002). Human cytomegalovirus binding to DC-SIGN is required for dendritic cell infection and target cell trans-infection. Immunity *17*, 653-664.

Hassaine, G., Agostini, I., Candotti, D., Bessou, G., Caballero, M., Agut, H., Autran, B., Barthalay, Y., Vigne, R., and French, A.L.T.S.G. (2000). Characterization of human immunodeficiency virus type 1 vif gene in long-term asymptomatic individuals. Virology *276*, 169-180.

Hatano, H., Yukl, S.A., Ferre, A.L., Graf, E.H., Somsouk, M., Sinclair, E., Abdel-Mohsen, M., Liegler, T., Harvill, K., Hoh, R., *et al.* (2013). Prospective antiretroviral treatment of asymptomatic, HIV-1 infected controllers. PLoS Pathog *9*, e1003691.

Hendel, H., Caillat-Zucman, S., Lebuanec, H., Carrington, M., O'Brien, S., Andrieu, J.M., Schachter, F., Zagury, D., Rappaport, J., Winkler, C., *et al.* (1999). New class I and II HLA alleles strongly associated with opposite patterns of progression to AIDS. J Immunol *162*, 6942-6946.

Hirbod, T., Bailey, R.C., Agot, K., Moses, S., Ndinya-Achola, J., Murugu, R., Andersson, J., Nilsson, J., and Broliden, K. (2010). Abundant expression of HIV target cells and C-type lectin receptors in the foreskin tissue of young Kenyan men. Am J Pathol *176*, 2798-2805.

Hoffmann, C., and Rockstroh, J.K. (2010). HIV 2010 (Hamburg, Germany: Medizin Fokus Verlag).

Hoffmann, J.A., Kafatos, F.C., Janeway, C.A., and Ezekowitz, R.A.B. (1999). Phylogenetic perspectives in innate immunity. Science *284*, 1313-1318.

Hong, P.W.P., Nguyen, S., Young, S., Su, S.V., and Lee, B. (2007). Identification of the optimal DC-SIGN binding site on human immunodeficiency virus type 1 gp120. J Virol *81*, 8325-8336.

Hsue, P.Y., Hunt, P.W., Schnell, A., Kalapus, S.C., Hoh, R., Ganz, P., Martin, J.N., and Deeks, S.G. (2009). Role of viral replication, antiretroviral therapy, and immunodeficiency in HIV-associated atherosclerosis. AIDS *23*, 1059-1067.

Hughes, A.L., and Yeager, M. (1998). Natural selection at major histocompatibility complex loci of vertebrates. Annu Rev Genet *32*, 415-435.

Hunger, R.E., Sieling, P.A., Ochoa, M.T., Sugaya, M., Burdick, A.E., Rea, T.H., Brennan, P.J., Belisle, J.T., Blauvelt, A., Porcelli, S.A., *et al.* (2004). Langerhans cells utilize CD1a and langerin to efficiently present nonpeptide antigens to T cells. J Clin Invest *113*, 701-708.

Hunt, P.W., Brenchley, J., Sinclair, E., McCune, J.M., Roland, M., Page-Shafer, K., Hsue, P., Emu, B., Krone, M., Lampiris, H., *et al.* (2008). Relationship between T cell activation and CD4+ T cell count in HIV-seropositive individuals with undetectable plasma HIV RNA levels in the absence of therapy. J Infect Dis *197*, 126-133.

Imberty, A., Chabre, Y.M., and Roy, R. (2008). Glycomimetics and glycodendrimers as high affinity microbial anti-adhesins. Chemistry *14*, 7490-7499.

Inaba, K., Inaba, M., Naito, M., and Steinman, R.M. (1993). Dendritic cell progenitors phagocytose particulates, including Bacillus-Calmette-Guerin organisms, and sensitize mice to Mycobacterial antigens in vivo. J Exp Med *178*, 479-488.

Ip, W.K.E., Takahashi, K., Ezekowitz, R.A., and Stuart, L.M. (2009). Mannose-binding lectin and innate immunity. Immunol Rev *230*, 9-21.

Ito, H., Watanabe, S., Takada, A., and Kawaoka, Y. (2001). Ebola virus glycoprotein: proteolytic processing, acylation, cell tropism, and detection of neutralizing antibodies. J Virol *75*, 1576-1580.

Iwasaki, A., and Medzhitov, R. (2010). Regulation of Adaptive Immunity by the Innate Immune System. Science *327*, 291-295.

Jahrling, P.B., Geisbert, T.W., Dalgard, D.W., Johnson, E.D., Ksiazek, T.G., Hall, W.C., and Peters, C.J. (1990). Preliminary report - Isolation of Ebola Virus from Monkeys imported to USA. Lancet *335*, 502-505.

Jahrling, P.B., Nicol,S.T., Rollin,P.E., and Ksiazek,T.G (2003). Manual of Clinical Microbiology, Vol 2, 8th edition edn (Washington, D.C., USA: ASM Press Washington, D.C.).

Janeway, C.A. (1989). Approaching the asymtote - Evolution and revolution in immunology. Cold Spring Harbor Symp Quant Biol *54*, 1-13.

Jeffers, S.A., Sanders, D.A., and Sanchez, A. (2002). Covalent modifications of the Ebola virus glycoprotein. J Virol *76*, 12463-12472.

Ji, X., Olinger, G.G., Aris, S., Chen, Y., Gewurz, H., and Spear, G.T. (2005). Mannose-binding lectin binds to Ebola and Marburg envelope glycoproteins, resulting in blocking of virus interaction with DC-SIGN and complement-mediated virus neutralization. J Gen Virol *86*, 2535-2542.

Joffre, O., Nolte, M.A., Spoerri, R., and Reis e Sousa, C. (2009). Inflammatory signals in dendritic cell activation and the induction of adaptive immunity. Immunol Rev *227*, 234-247.

Johnson, K.M., Lange, J.V., Webb, P.A., and Murphy, F.A. (1977). Isolation and partial characterisation of a new virus causing acute haemorrhagic fever in Zaire. Lancet *1*, 569-571.

Karpova, M.B., Schoumans, J., Ernberg, I., Henter, J.I., Nordenskjold, M., and Fadeel, B. (2005). Raji revisited: cytogenetics of the original Burkitt's lymphoma cell line. Leukemia *19*, 159-161.

Kaslow, R.A., Carrington, M., Apple, R., Park, L., Munoz, A., Saah, A.J., Goedert, J.J., Winkler, C., O'Brien, S.J., Rinaldo, C., *et al.* (1996). Influence of combinations of human major histocompatibility complex genes on the course of HIV-1 infection. Nat Med *2*, 405-411.

Kato, C., and Kojima, N. (2010). SIGNR1 ligation on murine peritoneal macrophages induces IL-12 production through NFkappaB activation. Glycoconj J *27*, 525-531.

Katsnelson, A. (2014). Control issues. Nat Med *20*, 328-330.

Kawamura, T., Cohen, S.S., Borris, D.L., Aquilino, E.A., Glushakova, S., Margolis, L.B., Orenstein, J.M., Offord, R.E., Neurath, A.R., and Blauvelt, A. (2000). Candidate microbicides block HIV-1 infection of human immature Langerhans cells within epithelial tissue explants. J Exp Med *192*, 1491-1500.

Keele, B.F., Giorgi, E.E., Salazar-Gonzalez, J.F., Decker, J.M., Pham, K.T., Salazar, M.G., Sun, C., Grayson, T., Wang, S., Li, H., *et al.* (2008). Identification and characterization of transmitted and early founder virus envelopes in primary HIV-1 infection. Proc Natl Acad Sci U S A *105*, 7552-7557.

Keet, I.P., Tang, J., Klein, M.R., LeBlanc, S., Enger, C., Rivers, C., Apple, R.J., Mann, D., Goedert, J.J., Miedema, F., *et al.* (1999). Consistent associations of HLA class I and II and transporter gene products with progression of human immunodeficiency virus type 1 infection in homosexual men. J Infect Dis *180*, 299-309.

Kiepiela, P., Ngumbela, K., Thobakgale, C., Ramduth, D., Honeyborne, I., Moodley, E., Reddy, S., de Pierres, C., Mncube, Z., Mkhwanazi, N., *et al.* (2007). CD8(+) T-cell responses to different HIV proteins have discordant associations with viral load. Nat Med *13*, 46-53.

Kirchhoff, F., Greenough, T.C., Brettler, D.B., Sullivan, J.L., and Desrosiers, R.C. (1995). Brief report - absence of intact Nef sequences in a Long-Term Survivor with nonprogressive HIV-1 infection. N Eng J Med *332*, 228-232.

Kitajima, T., Ariizumi, K., Bergstresser, P.R., and Takashima, A. (1996). A novel mechanism of glucocorticoid-induced immune suppression: The inhibition of T cell-mediated terminal maturation of a murine dendritic cell line. J Clin Invest *98*, 142-147.

Klenk, H.D., and Garten, W. (1994). Host cell proteases controlling virus pathogenicity. Trends Microbiol *2*, 39-43.

Kuller, L.H., Tracy, R., Belloso, W., De Wit, S., Drummond, F., Lane, H.C., Ledergerber, B., Lundgren, J., Neuhaus, J., Nixon, D.*, et al.* (2008). Inflammatory and coagulation biomarkers and mortality in patients with HIV infection. PLoS Med *5*, e203.

Kuznetsov, Y.G., Victoria, J.G., Robinson, W.E., and McPherson, A. (2003). Atomic force microscopy investigation of human immunodeficiency virus (HIV) and HIV-Infected lymphocytes. J Virol *77*, 11896-11909.

Kwon, D.S., Gregorio, G., Bitton, N., Hendrickson, W.A., and Littman, D.R. (2002). DC-SIGN-mediated internalization of HIV is required for trans-enhancement of T cell infection. Immunity *16*, 135-144.

Kwong, P.D., Wyatt, R., Robinson, J., Sweet, R.W., Sodroski, J., and Hendrickson, W.A. (1998). Structure of an HIV gp120 envelope glycoprotein in complex with the CD4 receptor and a neutralizing human antibody. Nature *393*, 648-659.

Lambotte, O., Boufassa, F., Madec, Y., Nguyen, A., Goujard, C., Meyer, L., Rouzioux, C., Venet, A., Delfraissy, J.F., and Grp, S.-H.S. (2005). HIV controllers: A homogeneous group of HIV-1-infected patients with spontaneous control of viral replication. Clin Infect Dis *41*, 1053-1056.

Lasala, F., Arce, E., Otero, J.R., Rojo, J., and Delgado, R. (2003). Mannosyl glycodendritic structure inhibits DC-SIGN-mediated Ebola virus infection in cis and in trans. Antimicrob Agents Chemother *47*, 3970-3972.

Lassen, K.G., Lobritz, M.A., Bailey, J.R., Johnston, S., Nguyen, S., Lee, B., Chou, T., Siliciano, R.F., Markowitz, M., and Arts, E.J. (2009). Elite Suppressor-Derived HIV-1 Envelope Glycoproteins Exhibit Reduced Entry Efficiency and Kinetics. PLoS Pathog *5*.

Layne, S.P., Merges, M.J., Dembo, M., Spouge, J.L., Conley, S.R., Moore, J.P., Raina, J.L., Renz, H., Gelderblom, H.R., and Nara, P.L. (1992). Factors underlying spontaneous inactivation and susceptibility to neutralization of Human-Immunodeficiency-Virus. Virology *189*, 695-714.

Le Bon, A., Etchart, N., Rossmann, C., Ashton, M., Hou, S., Gewert, D., Borrow, P., and Tough, D.F. (2003). Cross-priming of CD8(+) T cells stimulated by virus-induced type I interferon. Nat Immunol *4*, 1009-1015.

Lee, B., Leslie, G., Soilleux, E., O'Doherty, U., Baik, S., Levroney, E., Flummerfelt, K., Swiggard, W., Coleman, N., Malim, M.*, et al.* (2001). cis Expression of DC-SIGN allows for more efficient entry of human and simian immunodeficiency viruses via CD4 and a coreceptor. J Virol *75*, 12028-12038.

Lee, J.E., Fusco, M.L., Hessell, A.J., Oswald, W.B., Burton, D.R., and Saphire, E.O. (2008). Structure of the Ebola virus glycoprotein bound to an antibody from a human survivor. Nature *454*, 177-U127.

Lefrere, J.J., MorandJoubert, L., Mariotti, M., Bludau, H., Burghoffer, B., Petit, J.C., and RoudotThoraval, F. (1997). Even individuals considered as long-term nonprogressors show biological signs of progression after 10 years of human immunodeficiency virus infection. Blood *90*, 1133-1140.

Leonard, C.K., Spellman, M.W., Riddle, L., Harris, R.J., Thomas, J.N., and Gregory, T.J. (1990). Assignment of intrachain disulphide bonds and characterization of potential glycosylation sites of the type-1 recombinant Human-Immunodeficiency-Virus envelope glycoprotein (gp120) expressed in Chinese Hamster Ovary cells. J Biol Chem *265*, 10373-10382.

Letvin, N.L. (2006). Progress and obstacles in the development of an AIDS vaccine. Nat Rev Immunol *6*, 930-939.

Levy, J.A., Hoffman, A.D., Kramer, S.M., Landis, J.A., and Shimabukuro, J.M. (1984). Isolation of lymphocytopathic retroviruses from San-Francisco patients with AIDS Science *225*, 840-842.

Lewin, S.R., and Rouzioux, C. (2011). HIV cure and eradication: how will we get from the laboratory to effective clinical trials? AIDS *25*, 885-897.

Li, Y., Svehla, K., Mathy, N.L., Voss, G., Mascola, J.R., and Wyatt, R. (2006). Characterization of antibody responses elicited by human immunodeficiency virus type 1 primary isolate trimeric and monomeric envelope glycoproteins in selected adjuvants. J Virol *80*, 1414-1426.

Lodish, H., Berk, A., Zipursky, S.L., et al. (2000). Protein Glycosylation in the ER and Golgi Complex., 4th edition edn (New York, USA: W. H. Freeman).

Lozano, M.E., Enria, D., Maiztegui, J.I., Grau, O., and Romanowski, V. (1995). Rapid diagnosis of Argentine hemorrhagic-fever by reverse transcriptase PCR-based assay. J Clin Microbiol *33*, 1327-1332.

Lu, W., Arraes, L.C., Ferreira, W.T., and Andrieu, J.M. (2004). Therapeutic dendritic-cell vaccine for chronic HIV-1 infection. Nat Med *10*, 1359-1365.

Luczkowiak, J., Munoz, A., Sanchez-Navarro, M., Ribeiro-Viana, R., Ginieis, A., Illescas, B.M., Martin, N., Delgado, R., and Rojo, J. (2013). Glycofullerenes Inhibit Viral Infection. Biomacromolecules *14*, 431-437.

Luczkowiak, J., Sattin, S., Sutkeviciute, I., Reina, J.J., Sanchez-Navarro, M., Thepaut, M., Martinez-Prats, L., Daghetti, A., Fieschi, F., Delgado, R., *et al.* (2011). Pseudosaccharide Functionalized Dendrimers as Potent Inhibitors of DC-SIGN Dependent Ebola Pseudotyped Viral Infection. Bioconjug Chem *22*, 1354-1365.

Lue, J., Hsu, M., Yang, D., Marx, P., Chen, Z.W., and Cheng-Mayer, C. (2002). Addition of a single gp120 glycan confers increased binding to dendritic cell-specific ICAM-3-grabbing nonintegrin and neutralization escape to human immunodeficiency virus type 1. Journal of Virology *76*, 10299-10306.

Lum, J.J., Cohen, O.J., Nie, Z.L., Weaver, J.G., Gomez, T.S., Yao, X.J., Lynch, D., Pilon, A.A., Hawley, N., Kim, J.E., *et al.* (2003). Vpr R77Q is associated with long-term nonprogressive HIV infection and impaired induction of apoptosis. J Clin Invest *111*, 1547-1554.

Ly, A., and Stamatatos, L. (2000). V2 loop glycosylation of the human immunodeficiency virus type 1 SF162 envelope facilitates interaction of this protein with CD4 and CCRS receptors and protects the virus from neutralization by anti-V3 loop and anti-CD4 binding site antibodies. J Virol *74*, 6769-6776.

Madec, Y., Boufassa, F., Porter, K., Meyer, L., and Collaboration, C. (2005a). Spontaneous control of viral load and CD4 cell count progression among HIV-1 seroconverters. AIDS *19*, 2001-2007.

Madec, Y., Boufassa, F., Rouzioux, C., Delfraissy, J.F., Meyer, L., and Grp, S.S. (2005b). Undetectable viremia without antiretroviral therapy in patients with HIV seroconversion: An uncommon phenomenon? Clin Infect Dis *40*, 1350-1354.

Maeda, N., Nigou, J., Herrmann, J.L., Jackson, M., Amara, A., Lagrange, P.H., Puzo, G., Gicquel, B., and Neyrolles, O. (2003). The cell surface receptor DC-SIGN discriminates between Mycobacterium species through selective recognition of the mannose caps on lipoarabinomannan. J Biol Chem *278*, 5513-5516.

Magierowska, M., Theodorou, I., Debre, P., Sanson, F., Autran, B., Riviere, Y., Charron, D., and Costagliola, D. (1999). Combined genotypes of CCR5, CCR2, SDF1, and HLA genes can predict the long-term nonprogressor status in human immunodeficiency virus-1-infected individuals. Blood *93*, 936-941.

Martin, M.P., Lederman, M.M., Hutcheson, H.B., Goedert, J.J., Nelson, G.W., van Kooyk, Y., Detels, R., Buchbinder, S., Hoots, K., Vlahov, D., *et al.* (2004). Association of DC-SIGN promoter polymorphism with increased risk for parenteral, but not mucosal, acquisition of human immunodeficiency virus type 1 infection. J Virol *78*, 14053-14056.

Martinez-Avila, O., Bedoya, L.M., Marradi, M., Clavel, C., Alcami, J., and Penades, S. (2009). Multivalent Manno-Glyconanoparticles Inhibit DC-SIGN-Mediated HIV-1 Trans-infection of Human T Cells. Chembiochem *10*, 1806-1809.

Martinez-Picado, J., Prado, J.G., Fry, E.E., Pfafferott, K., Leslie, A., Chetty, S., Thobakgale, C., Honeyborne, I., Crawford, H., Matthews, P., *et al.* (2006). Fitness cost of escape mutations in p24 Gag in association with control of human immunodeficiency virus type 1. J Virol *80*, 3617-3623.

Maruyama, T., Parren, P.W., Sanchez, A., Rensink, I., Rodriguez, L.L., Khan, A.S., Peters, C.J., and Burton, D.R. (1999). Recombinant human monoclonal antibodies to Ebola virus. J Infect Dis *179 Suppl 1*, S235-239.

Masur, H., Michelis, M.A., Greene, J.B., Onorato, I., Vandestouwe, R.A., Holzman, R.S., Wormser, G., Brettman, L., Lange, M., Murray, H.W., *et al.* (1981). An outbreak of community-acquired Pneumocystis-Carinii Pneumonia - Initial manifestation of cellular immune dysfunction. N Eng J Med *305*, 1431-1438.

Matlin, K.S., Reggio, H., Helenius, A., and Simons, K. (1982). Pathway of Vesicular Stomatitis Virus entry leading to infection. J Mol Biol *156*, 609-631.

McCaffrey, R.A., Saunders, C., Hensel, M., and Stamatatos, L. (2004). N-linked glycosylation of the V3 loop and the immunologically silent face of gp120 protects human immunodeficiency virus type 1 SF162 from neutralization by anti-gp120 and anti-gp41 antibodies. J Virol *78*, 3279-3295.

McDonald, D., Wu, L., Bohks, S.M., KewalRamani, V.N., Unutmaz, D., and Hope, T.J. (2003). Recruitment of HIV and its receptors to dendritic cell-T cell junctions. Science *300*, 1295-1297.

McGovern, R.A., Thielen, A., Mo, T., Dong, W., Woods, C.K., Chapman, D., Lewis, M., James, I., Heera, J., Valdez, H., *et al.* (2010). Population-based V3 genotypic tropism assay: a retrospective analysis using screening samples from the A4001029 and MOTIVATE studies. AIDS *24*, 2512-2520.

McKeating, J.A., and Willey, R.L. (1989). Structure and function of the HIV envelope. AIDS *3*, S35-S41.

McNeil, A.J., Yap, P.L., Gore, S.M., Brettle, R.P., McColl, M., Wyld, R., Davidson, S., Weightman, R., Richardson, A.M., and Robertson, J.R. (1996). Association of HLA types A1-B8-DR3 and B27 with rapid and slow progression of HIV disease. QJM *89*, 177-185.

Medzhitov, R., and Janeway, C.A. (1999). Innate immune induction of the adaptive immune response. Cold Spring Harbor Symp Quant Biol *64*, 429-435.

Mellman, I., Turley, S., and Steinman, R. (1998). Antigen processing for amateurs and professionals. Trends Cell Biol *8*, 231-237.

Migueles, S.A., Laborico, A.C., Shupert, W.L., Sabbaghian, M.S., Rabin, R., Hallahan, C.W., Van Baarle, D., Kostense, S., Miedema, F., McLaughlin, M., *et al.* (2002). HIV-specific CD8(+) T cell proliferation is coupled to perforin expression and is maintained in nonprogressors. Nat Immunol *3*, 1061-1068.

Migueles, S.A., Sabbaghian, M.S., Shupert, W.L., Bettinotti, M.P., Marincola, F.M., Martino, L., Hallahan, C.W., Selig, S.M., Schwartz, D., Sullivan, J., *et al.* (2000). HLA B*5701 is highly associated with restriction of virus replication in a subgroup of HIV-infected long term nonprogressors. Proc Natl Acad Sci U S A *97*, 2709-2714.

Miranda, M.E., Ksiazek, T.G., Retuya, T.J., Khan, A.S., Sanchez, A., Fulhorst, C.F., Rollin, P.E., Calaor, A.B., Manalo, D.L., Roces, M.C., *et al.* (1999). Epidemiology of Ebola (subtype Reston) virus in the Philippines, 1996. J Infect Dis *179*, S115-S119.

Mitchell, D.A., Fadden, A.J., and Drickamer, K. (2001). A novel mechanism of carbohydrate recognition by the C-type lectins DC-SIGN and DC-SIGNR. Subunit organization and binding to multivalent ligands. J Biol Chem *276*, 28939-28945.

Mitchell, D.A., Jones, N.A., Hunter, S.J., Cook, J.M.D., Jenkinson, S.F., Wormald, M.R., Dwek, R.A., and Fleet, G.W.J. (2007). Synthesis of 2-C-branched derivatives of D-mannose: 2-C-aminomethyl-D-mannose binds to the human C-type lectin DC-SIGN with affinity greater than an order of magnitude compared to that of D-mannose. Tetrahedron-Asymmetry *18*, 1502-1510.

Miura, T., Brockman, M.A., Brumme, Z.L., Brumme, C.J., Pereyra, F., Trocha, A., Block, B.L., Schneidewind, A., Allen, T.M., Heckerman, D., *et al.* (2009). HLA-associated alterations in replication capacity of chimeric NL4-3 viruses carrying gag-protease from elite controllers of human immunodeficiency virus type 1. J Virol *83*, 140-149.

Monks, C.R., Freiberg, B.A., Kupfer, H., Sciaky, N., and Kupfer, A. (1998). Three-dimensional segregation of supramolecular activation clusters in T cells. Nature *395*, 82-86.

Montefiori, D.C., Pantaleo, G., Fink, L.M., Zhou, J.T., Zhou, J.Y., Bilska, M., Miralles, G.D., and Fauci, A.S. (1996). Neutralizing and infection-enhancing antibody responses to human immunodeficiency virus type 1 in long-term nonprogressors. J Infect Dis *173*, 60-67.

Montoya, M.C., Sancho, D., Bonello, G., Collette, Y., Langlet, C., He, H.T., Aparicio, P., Alcover, A., Olive, D., and Sanchez-Madrid, F. (2002). Role of ICAM-3 in the initial interaction of T lymphocytes and APCs. Nat Immunol *3*, 159-168.

Moore, C.B., John, M., James, I.R., Christiansen, F.T., Witt, C.S., and Mallal, S.A. (2002). Evidence of HIV-1 adaptation to HLA-restricted immune responses at a population level. Science *296*, 1439-1443.

Munoz, A., Kirby, A.J., He, Y.D., Margolick, J.B., Visscher, B.R., Rinaldo, C.R., Kaslow, R.A., and Phair, J.P. (1995). Long-term survivors with HIV-1 infection - incubation period and longitudinal patterns of CD4(+) lymphocytes. J Acquired Immune Defic Syndr *8*, 496-505.

Nagaoka, K., Takahara, K., Minamino, K., Takeda, T., Yoshida, Y., and Inaba, K. (2010). Expression of C-type lectin, SIGNR3, on subsets of dendritic cells, macrophages, and monocytes. J Leukoc Biol *88*, 913-924.

Navarro-Sanchez, E., Altmeyer, R., Amara, A., Schwartz, O., Fieschi, F., Virelizier, J.L., Arenzana-Seisdedos, F., and Despres, P. (2003). Dendritic-cell-specific ICAM3-grabbing non-integrin is essential for the productive infection of human dendritic cells by mosquito-cell-derived dengue viruses. Embo Reports *4*, 723-728.

Neumann, G., Feldmann, H., Watanabe, S., Lukashevich, I., and Kawaoka, Y. (2002). Reverse genetics demonstrates that proteolytic processing of the Ebola virus glycoprotein is not essential for replication in cell culture. J Virol *76*, 406-410.

Neumann, G., Geisbert, T.W., Ebihara, H., Geisbert, J.B., Daddario-DiCaprio, K.M., Feldmann, H., and Kawaoka, Y. (2007). Proteolytic processing of the Ebola virus glycoprotein is not critical for Ebola virus replication in nonhuman primates. J Virol *81*, 2995-2998.

O'Brien, S.J., Gao, X., and Carrington, M. (2001). HLA and AIDS: a cautionary tale. Trends Mol Med *7*, 379-381.

Ohsugi, Y., Gershwin, M.E., Owens, R.B., and Nelson-Rees, W.A. (1980). Tumorigenicity of human malignant lymphoblasts: comparative study with unmanipulated nude mice, antilymphocyte serum-treated nude mice, and X-irradiated nude mice. J Natl Cancer Inst *65*, 715-718.

Ohtani, M., Iyori, M., Saeki, A., Tanizume, N., Into, T., Hasebe, A., Totsuka, Y., and Shibata, K. (2012). Involvement of suppressor of cytokine signalling-1-mediated degradation of MyD88-adaptor-like protein in the suppression of Toll-like receptor 2-mediated signalling by the murine C-type lectin SIGNR1-mediated signalling. Cell Microbiol *14*, 40-57.

Ohtsubo, K., and Marth, J.D. (2006). Glycosylation in cellular mechanisms of health and disease. Cell *126*, 855-867.

Palucka, K., and Banchereau, J. (2002). How dendritic cells and microbes interact to elicit or subvert protective immune responses. Curr Opin Immunol *14*, 420-431.

Parham, P., and Ohta, T. (1996). Population biology of antigen presentation by MHC class I molecules. Science *272*, 67-74.

Park, C.G., Takahara, K., Umemoto, E., Yashima, Y., Matsubara, K., Matsuda, Y., Clausen, B.E., Inaba, K., and Steinman, R.M. (2001). Five mouse homologues of the human dendritic cell C-type lectin, DC-SIGN. Int Immunol *13*, 1283-1290.

Pereyra, F., Lo, J., Triant, V.A., Wei, J., Buzon, M.J., Fitch, K.V., Hwang, J., Campbell, J.H., Burdo, T.H., Williams, K.C., *et al.* (2012). Increased coronary atherosclerosis and immune activation in HIV-1 elite controllers. AIDS *26*, 2409-2412.

Peters, C.J., Sanchez, A., Rollin, P.E., Ksiazek, T.G., and Murphy, G.A. (1996). Filoviridae: Marburg and Ebola viruses., Vol 1 (Philadelphia: Lippincott-Raven Press).

Phillips, A.N. (1992). CD4 lymphocyte depletion prior to the development of AIDS. AIDS *6*, 735-736.

Pohlmann, S., Zhang, J., Baribaud, F., Chen, Z., Leslie, G.J., Lin, G., Granelli-Piperno, A., Doms, R.W., Rice, C.M., and McKeating, J.A. (2003). Hepatitis C virus glycoproteins interact with DC-SIGN and DC-SIGNR. J Virol *77*, 4070-4080.

Ponten, J., and Macintyre, E.H. (1968). Long term culture of normal and neoplastic human glia. Acta Pathologica Et Microbiologica Scandinavica *74*, 465-486.

Pope, M., Betjes, M.G., Romani, N., Hirmand, H., Cameron, P.U., Hoffman, L., Gezelter, S., Schuler, G., and Steinman, R.M. (1994). Conjugates of dendritic cells and memory T lymphocytes from skin facilitate productive infection with HIV-1. Cell *78*, 389-398.

Powlesland, A.S., Ward, E.M., Sadhu, S.K., Guo, Y., Taylor, M.E., and Drickamer, K. (2006). Widely divergent biochemical properties of the complete set of mouse DC-SIGN-related proteins. J Biol Chem *281*, 20440-20449.

Pulvertaft, J.V. (1964). Cytology of Burkitt´s Tumour (African Lymphoma). Lancet *1*, 238-240.

Qiao, R., Roberts, A.P., Mount, A.S., Klaine, S.J., and Ke, P.C. (2007). Translocation of C-60 and its derivatives across a lipid bilayer. Nano Letters *7*, 614-619.

Rahbari, R., Sheahan, T., Modes, V., Collier, P., Macfarlane, C., and Badge, R.M. (2009). A novel L1 retrotransposon marker for HeLa cell line identification. Biotechniques *46*, 277-+.

Reina, J.J., Sattin, S., Invernizzi, D., Mari, S., Martinez-Prats, L., Tabarani, G., Fieschi, F., Delgado, R., Nieto, P.M., Rojo, J., *et al.* (2007). 1,2-mannobioside mimic: Synthesis, DC-SIGN interaction by NMR and docking, and antiviral activity. Chemmedchem *2*, 1030-1036.

Reis e Sousa, C. (2001). Dendritic cells as sensors of infection. Immunity *14*, 495-498.

Reis e Sousa, C. (2006). Essay - Dendritic cells in a mature age. Nat Rev Immunol *6*, 476-483.

Ribeiro-Viana, R., Sanchez-Navarro, M., Luczkowiak, J., Koeppe, J.R., Delgado, R., Rojo, J., and Davis, B.G. (2012). Virus-like glycodendrinanoparticles displaying quasi-equivalent nested polyvalency upon glycoprotein platforms potently block viral infection. Nat commun *3*, 1303-1303.

Richman, D.D., Wrin, T., Little, S.J., and Petropoulos, C.J. (2003). Rapid evolution of the neutralizing antibody response to HIV type 1 infection. Proc Natl Acad Sci U S A *100*, 4144-4149.

Rizzuto, C., and Sodroski, J. (2000). Fine definition of a conserved CCR5-binding region on the human immunodeficiency virus type 1 glycoprotein 120. AIDS Res Hum Retroviruses *16*, 741-749.

Rizzuto, C.D., Wyatt, R., Hernandez-Ramos, N., Sun, Y., Kwong, P.D., Hendrickson, W.A., and Sodroski, J. (1998). A conserved HIV gp120 glycoprotein structure involved in chemokine receptor binding. Science *280*, 1949-1953.

Rojo, J., and Delgado, R. (2004). Glycodendritic structures: promising new antiviral drugs. J Antimicrob Chemother *54*, 579-581.

Rong, R., Bibollet-Ruche, F., Mulenga, J., Allen, S., Blackwell, J.L., and Derdeyn, C.A. (2007). Role of V1V2 and other human immunodeficiency virus type 1 envelope domains in resistance to autologous neutralization during clade C infection. J Virol *81*, 1350-1359.

Roy, R. (1996). Syntheses and some applications of chemically defined multivalent glycoconjugates. Curr Opin Struct Biol *6*, 692-702.

Royce, R.A. (1997). Sexual transmission of HIV (vol 336, pg 1072, 1997). N Eng J Med *337*, 799-799.

Saah, A.J., Hoover, D.R., Weng, S., Carrington, M., Mellors, J., Rinaldo, C.R., Jr., Mann, D., Apple, R., Phair, J.P., Detels, R., *et al.* (1998). Association of HLA profiles with early plasma viral load, CD4+ cell count and rate of progression to AIDS following acute HIV-1 infection. Multicenter AIDS Cohort Study. AIDS *12*, 2107-2113.

Saez-Cirion, A., Bacchus, C., Hocqueloux, L., Avettand-Fenoel, V., Girault, I., Lecuroux, C., Potard, V., Versmisse, P., Melard, A., Prazuck, T., *et al.* (2013). Post-treatment HIV-1 controllers with a long-term virological remission after the interruption of early initiated antiretroviral therapy ANRS VISCONTI Study. PLoS Pathog *9*, e1003211.

Sagar, M., Laeyendecker, O., Lee, S., Gamiel, J., Wawer, M.J., Gray, R.H., Serwadda, D., Sewankambo, N.K., Shepherd, J.C., Toma, J., *et al.* (2009). Selection of HIV Variants with Signature Genotypic Characteristics during Heterosexual Transmission. J Infect Dis *199*, 580-589.

Sagar, M., Wu, X., Lee, S., and Overbaugh, J. (2006). Human immunodeficiency virus type 1 V1-V2 envelope loop sequences expand and add glycosylation sites over the course of infection, and these modifications affect antibody neutralization sensitivity. J Virol *80*, 9586-9598.

Sallusto, F., Cella, M., Danieli, C., and Lanzavecchia, A. (1995). Dendritic cells use macropinocytosis and the mannose receptor to concentrate macromolecules in the major histocompatibility complex class-II compartment - down-regulation by cytokines and bacterial products. J Exp Med *182*, 389-400.

Sanchez-Navarro, M., and Rojo, J. (2010). Targeting DC-SIGN with carbohydrate multivalent systems. Drug News Perspect *23*, 557-572.

Sanchez, A., Khan, A.S., Zaki, S.R., Nabel, G.J., Ksiazek, T.G., and Peters, C.J. (2001). Filoviridae: Marburg and Ebola viruses, 4th ed edn (Philadelphia, Pa, USA: Lippincott Williams & Wilkins).

Sanchez, A., Trappier, S.G., Mahy, B.W.J., Peters, C.J., and Nichol, S.T. (1996). The virion glycoproteins of Ebola viruses are encoded in two reading frames and are expressed through transcriptional editing. Proc Natl Acad Sci U S A *93*, 3602-3607.

Sanchez, A., Yang, Z.Y., Xu, L., Nabel, G.J., Crews, T., and Peters, C.J. (1998). Biochemical analysis of the secreted and virion glycoproteins of Ebola virus. J Virol *72*, 6442-6447.

Sanders, R.W., Venturi, M., Schiffner, L., Kalyanaraman, R., Katinger, H., Lloyd, K.O., Kwong, P.D., and Moore, J.P. (2002). The mannose-dependent epitope for neutralizing antibody 2G12 on human immunodeficiency virus type 1 glycoprotein gp120. J Virol *76*, 7293-7305.

Sattin, S., Daghetti, A., Thepaut, M., Berzi, A., Sanchez-Navarro, M., Tabarani, G., Rojo, J., Fieschi, F., Clerici, M., and Bernardi, A. (2010). Inhibition of DC-SIGN-Mediated HIV Infection by a Linear Trimannoside Mimic in a Tetravalent Presentation. ACS Chem Biol *5*, 301-312.

Schacker, T., Collier, A.C., Hughes, J., Shea, T., and Corey, L. (1996). Clinical and epidemiologic features of primary HIV infection. Ann Intern Med *125*, 257-264.

Schaefer, M., Reiling, N., Fessler, C., Stephani, J., Taniuchi, I., Hatam, F., Yildirim, A.O., Fehrenbach, H., Walter, K., Ruland, J., *et al.* (2008). Decreased pathology and prolonged survival of human DC-SIGN transgenic mice during mycobacterial infection. J Immunol *180*, 6836-6845.

Schneider, U., Schwenk, H.U., and Bornkamm, G. (1977). Characterization of EBV-genome negative null and T-cell lines derived from children with acute lymphoblastic leukemia and leukemic transformed non-Hodgkin lymphoma. Int J Cancer *19*, 621-626.

Schwartz, A.J., Alvarez, X., and Lackner, A.A. (2002). Distribution and immunophenotype of DC-SIGN-expressing cells in SIV-infected and uninfected macaques. AIDS Res Hum Retroviruses *18*, 1021-1029.

Shattock, R.J., and Rosenberg, Z. (2012). Microbicides: topical prevention against HIV. Cold Spring Harb Perspect Med *2*, a007385.

Shimojima, M., Takada, A., Ebihara, H., Neumann, G., Fujioka, K., Irimura, T., Jones, S., Feldmann, H., and Kawaoka, Y. (2006). Tyro3 family-mediated cell entry of Ebola and Marburg viruses. J Virol *80*, 10109-10116.

Silberman, S. (2010). The woman behind HeLa. Nature *463*, 610.

Skrabal, K., Saragosti, S., Labernardiere, J.L., Barin, F., Clavel, F., and Mammano, F. (2005). Human immunodeficiency virus type 1 variants isolated from single plasma samples display a wide spectrum of neutralization sensitivity. J Virol *79*, 11848-11857.

Srivastava, V., Manchanda, M., Gupta, S., Singla, R., Behera, D., Das, G., and Natarajan, K. (2009). Toll-like receptor 2 and DC-SIGNR1 differentially regulate suppressors of cytokine signaling 1 in dendritic cells during Mycobacterium tuberculosis infection. J Biol Chem *284*, 25532-25541.

Stacey, A.R., Norris, P.J., Qin, L., Haygreen, E.A., Taylor, E., Heitman, J., Lebedeva, M., DeCamp, A., Li, D., Grove, D., *et al.* (2009). Induction of a striking systemic cytokine cascade prior to peak viremia in acute human immunodeficiency virus type 1 infection, in contrast to more modest and delayed responses in acute hepatitis B and C virus infections. J Virol *83*, 3719-3733.

Starcich, B.R., Hahn, B.H., Shaw, G.M., McNeely, P.D., Modrow, S., Wolf, H., Parks, E.S., Parks, W.P., Josephs, S.F., Gallo, R.C., *et al.* (1986). Identification and characterization of conserved and variable regions in the envelope gene of HTLV-III LAV, the retrovirus of AIDS. Cell *45*, 637-648.

Starling, G.C., McLellan, A.D., Egner, W., Sorg, R.V., Fawcett, J., Simmons, D.L., and Hart, D.N. (1995). Intercellular adhesion molecule-3 is the predominant co-stimulatory ligand for leukocyte function antigen-1 on human blood dendritic cells. Eur J Immunol *25*, 2528-2532.

Steinman, R.M., Granelli-Piperno, A., Pope, M., Trumpfheller, C., Ignatius, R., Arrode, G., Racz, P., and Tenner-Racz, K. (2003). The interaction of immunodeficiency viruses with dendritic cells. Curr Top Microbiol Immunol *276*, 1-30.

Sterjovski, J., Churchill, M.J., Ellett, A., Gray, L.R., Roche, M.J., Dunfee, R.L., Purcell, D.F., Saksena, N., Wang, B., Sonza, S., *et al.* (2007). Asn 362 in gp120 contributes to enhanced fusogenicity by CCR5-restricted HIV-1 envelope glycoprotein variants from patients with AIDS. Retrovirology *4*, doi:10.1186/1742-4690-1184-1189.

Sterling, T.R., Lyles, C.M., Vlahov, D., Astemborski, J., Margolick, J.B., and Quinn, T.C. (1999). Sex differences in longitudinal human immunodeficiency virus type 1 RNA levels among seroconverters. J Infect Dis *180*, 666-672.

Stewart, R.J., and Boggs, J.M. (1993). A carbohydrate-carbohydrate interaction between galactosylceramide-containing liposomes and cerebroside sulfate-containing liposomes: dependence on the glycolipid ceramide composition. Biochemistry *32*, 10666-10674.

Sullivan, N.J., Sanchez, A., Rollin, P.E., Yang, Z.Y., and Nabel, G.J. (2000). Development of a preventive vaccine for Ebola virus infection in primates. Nature *408*, 605-609.

Svajger, U., Anderluh, M., Jeras, M., and Obermajer, N. (2010). C-type lectin DC-SIGN: an adhesion, signalling and antigen-uptake molecule that guides dendritic cells in immunity. Cell Signal *22*, 1397-1405.

Tabarani, G., Thepaut, M., Stroebel, D., Ebel, C., Vives, C., Vachette, P., Durand, D., and Fieschi, F. (2009). DC-SIGN neck domain is a pH-sensor controlling oligomerization: SAXS and hydrodynamic studies of extracellular domain. J Biol Chem *284*, 21229-21240.

Takada, A., Fujioka, K., Tsuiji, M., Morikawa, A., Higashi, N., Ebihara, H., Kobasa, D., Feldmann, H., Irimura, T., and Kawaoka, Y. (2004). Human macrophage C-type lectin specific for galactose and N-acetylgalactosamine promotes filovirus entry. J Virol *78*, 2943-2947.

Takada, A., Watanabe, S., Ito, H., Okazaki, K., Kida, H., and Kawaoka, Y. (2000). Downregulation of beta 1 integrins by Ebola virus glycoprotein: Implication for virus entry. Virology *278*, 20-26.

Takahara, K., Arita, T., Tokieda, S., Shibata, N., Okawa, Y., Tateno, H., Hirabayashi, J., and Inaba, K. (2012). Difference in fine specificity to polysaccharides of Candida albicans mannoprotein between mouse SIGNR1 and human DC-SIGN. Infect Immun *80*, 1699-1706.

Takeuchi, Y., Akutsu, M., Murayama, K., Shimizu, N., and Hoshino, H. (1991). Host range mutant of Human Immunodeficiency Virus Type-1 - Modification of cell tropism by a single mutation at the neutralization epitope in the env gene. J Virol *65*, 1710-1718.

Tanne, A., Ma, B., Boudou, F., Tailleux, L., Botella, H., Badell, E., Levillain, F., Taylor, M.E., Drickamer, K., Nigou, J., *et al.* (2009). A murine DC-SIGN homologue contributes to early host defense against Mycobacterium tuberculosis. J Exp Med *206*, 2205-2220.

Thery, C., Zitvogel, L., and Amigorena, S. (2002). Exosomes: Composition, biogenesis and function. Nat Rev Immunol *2*, 569-579.

Torriani, F.J., Komarow, L., Parker, R.A., Cotter, B.R., Currier, J.S., Dube, M.P., Fichtenbaum, C.J., Gerschenson, M., Mitchell, C.K., Murphy, R.L., *et al.* (2008). Endothelial function in human immunodeficiency virus-infected antiretroviral-naive subjects before and after starting potent antiretroviral therapy: The ACTG (AIDS Clinical Trials Group) Study 5152s. J Am Coll Cardiol *52*, 569-576.

Tremblay, M., and Wainberg, M.A. (1990). Neutralization of multiple HIV-1 isolates from a single subject by autologous sequential sera. J Infect Dis *162*, 735-737.

Trumpfheller, C., Park, C.G., Finke, J., Steinman, R.M., and Granelli-Piperno, A. (2003). Cell type-dependent retention and transmission of HIV-1 by DC-SIGN. Int Immunol *15*, 289-298.

Tsegaye, T.S., and Pohlmann, S. (2010). The multiple facets of HIV attachment to dendritic cell lectins. Cell Microbiol *12*, 1553-1561.

Tsunetsugu-Yokota, Y., Yasuda, S., Sugimoto, A., Yagi, T., Azuma, M., Yagita, H., Akagawa, K., and Takemori, T. (1997). Efficient virus transmission from dendritic cells to CD4(+) T cells in response to antigen depends on close contact through adhesion molecules. Virology *239*, 259-268.

Turville, S.G., Santos, J.J., Frank, I., Cameron, P.U., Wilkinson, J., Miranda-Saksena, M., Dable, J., Stossel, H., Romani, N., Piatak, M., *et al.* (2004). Immunodeficiency virus uptake, turnover, and 2-phase transfer in human dendritic cells. Blood *103*, 2170-2179.

Underhill, D.M. (2003). Toll-like receptors: networking for success. Eur J Immunol *33*, 1767-1775.

Usami, K., Matsuno, K., Igarashi, M., Denda-Nagai, K., Takada, A., and Irimura, T. (2011). Involvement of viral envelope GP2 in Ebola virus entry into cells expressing the macrophage galactose-type C-type lectin. Biochem Biophys Res Commun *407*, 74-78.

Valladeau, J., Ravel, O., Dezutter-Dambuyant, C., Moore, K., Kleijmeer, M., Liu, Y., Duvert-Frances, V., Vincent, C., Schmitt, D., Davoust, J., *et al.* (2000). Langerin, a novel C-type lectin specific to Langerhans cells, is an endocytic receptor that induces the formation of Birbeck granules. Immunity *12*, 71-81.

van Die, I., van Vliet, S.J., Nyame, A.K., Cummings, R.D., Bank, C.M., Appelmelk, B., Geijtenbeek, T.B., and van Kooyk, Y. (2003). The dendritic cell-specific C-type lectin DC-SIGN is a receptor for Schistosoma mansoni egg antigens and recognizes the glycan antigen Lewis x. Glycobiology *13*, 471-478.

Van Gulck, E., Bracke, L., Heyndrickx, L., Coppens, S., Atkinson, D., Merlin, C., Pasternak, A., Florence, E., and Vanham, G. (2012). Immune and viral correlates of "secondary viral control" after treatment interruption in chronically HIV-1 infected patients. PLoS One *7*, e37792.

van Kooyk, Y., and Geijtenbeek, T.B. (2003). DC-SIGN: escape mechanism for pathogens. Nat Rev Immunol *3*, 697-709.

Vanham, G., Buve, A., Florence, E., Seguin-Devaux, C., and Saez-Cirion, A. (2014). What is the significance of posttreatment control of HIV infection vis-a-vis functional cure? AIDS *28*, 603-605.

Vanhems, P., Dassa, C., Lambert, J., Cooper, D.A., Perrin, L., Vizzard, J., Hirschel, B., Kinloch-de Loes, S., Carr, A., and Allard, R. (1999). Comprehensive classification of symptoms and signs reported among 218 patients with acute HIV-1 infection. J Acquired Immune Defic Syndr *21*, 99-106.

Vestweber, D., and Blanks, J.E. (1999). Mechanisms that regulate the function of the selectins and their ligands. Physiol Rev *79*, 181-213.

Vivier, E., Raulet, D.H., Moretta, A., Caligiuri, M.A., Zitvogel, L., Lanier, L.L., Yokoyama, W.M., and Ugolini, S. (2011). Innate or adaptive immunity? The example of natural killer cells. Science *331*, 44-49.

Volchkov, V.E., Becker, S., Volchkova, V.A., Ternovoj, V.A., Kotov, A.N., Netesov, S.V., and Klenk, H.D. (1995). GP mRNA of Ebola virus is edited by the Ebola virus polymerase and by T7 and vaccinia virus polymerases. Virology *214*, 421-430.

Volchkov, V.E., Blinov, V.M., and Netesov, S.V. (1992). The envelope glycoprotein of Ebola Virus contains an immunosuppressive-like domain similar to oncogenic retroviruses. Febs Letters *305*, 181-184.

Volchkov, V.E., Volchkova, V.A., Muhlberger, E., Kolesnikova, L.V., Weik, M., Dolnik, O., and Klenk, H.D. (2001). Recovery of infectious Ebola virus from complementary DNA: RNA editing of the GP gene and viral cytotoxicity. Science *291*, 1965-1969.

Volchkov, V.E., Volchkova, V.A., Slenczka, W., Klenk, H.D., and Feldmann, H. (1998). Release of viral glycoproteins during Ebola virus infection. Virology *245*, 110-119.

Volchkova, V.A., Feldmann, H., Klenk, H.D., and Volchkov, V.E. (1998). The nonstructural small glycoprotein sGP of ebola virus is secreted as an antiparallel-orientated homodimer. Virology *250*, 408-414.

Volchkova, V.A., Klenk, H.D., and Volchkov, V.E. (1999). Delta-peptide is the carboxy-terminal cleavage fragment of the nonstructural small glycoprotein sGP of Ebola virus. Virology *265*, 164-171.

Walker, B.D. (2007). Elite Control of HIV infection: Implications for Vaccines and Treatments. Top HIV Med *15*, 134-136.

Wang, B., Ge, Y.C., Palasanthiran, P., Xiang, S.H., Ziegler, J., Dwyer, D.E., Randle, C., Dowton, D., Cunningham, A., and Saksena, N.K. (1996). Gene defects clustered at the C-terminus of the vpr gene of HIV-1 in long-term nonprogressing mother and child pair: In vivo evolution of vpr quasispecies in blood and plasma. Virology *223*, 224-232.

Wang, J.J.G., Steel, S., Wisniewolski, R., and Wang, C.Y. (1986). Detection of antibodies to Human T-Lymphotropic Virus Type-III by using a synthetic peptide of 21 amino acid residues corresponding to a highly antigenic segment of gp41 envelope glycoprotein. Proc Natl Acad Sci U S A *83*, 6159-6163.

Wang, S.-K., Liang, P.-H., Astronomo, R.D., Hsu, T.-L., Hsieh, S.-L., Burton, D.R., and Wong, C.-H. (2008). Targeting the carbohydrates on HIV-1: Interaction of oligomannose dendrons with human monoclonal antibody 2G12 and DC-SIGN. Proc Natl Acad Sci U S A *105*, 3690-3695.

Watts, D.W. (2010). HeLa cancer cells killed Henrietta Lacks. Then they made her immortal. The Virginian-pilot *1*, 12-14.

Wei, X., Decker, J.M., Wang, S., Hui, H., Kappes, J.C., Wu, X., Salazar-Gonzalez, J.F., Salazar, M.G., Kilby, J.M., Saag, M.S., *et al.* (2003). Antibody neutralization and escape by HIV-1. Nature *422*, 307-312.

Weiss, A., Wiskocil, R.L., and Stobo, J.D. (1984). The role of T3 surface molecules in the activation of Human T-cells - A 2-stimulus requirement for Il-2 production reflects events occuring at a pre-translational level. J Immunol *133*, 123-128.

Weiss, R.A. (1993). How does HIV cause AIDS? Science *260*, 1273-1279.

Weiss, R.A., Clapham, P.R., Cheingsong-Popov, R., Dalgleish, A.G., Carne, C.A., Weller, I.V., and Tedder, R.S. (1985). Neutralization of human T-lymphotropic virus type III by sera of AIDS and AIDS-risk patients. Nature *316*, 69-72.

Wieland, C.W., Koppel, E.A., den Dunnen, J., Florquin, S., McKenzie, A.N., van Kooyk, Y., van der Poll, T., and Geijtenbeek, T.B. (2007). Mice lacking SIGNR1 have stronger T helper 1 responses to Mycobacterium tuberculosis. Microbes Infect *9*, 134-141.

Wiley, R.D., and Gummuluru, S. (2006). Immature dendritic cell-derived exosomes can mediate HIV-1 trans infection. Proc Natl Acad Sci U S A *103*, 738-743.

Wilson, J.A., Hevey, M., Bakken, R., Guest, S., Bray, M., Schmaljohn, A.L., and Hart, M.K. (2000). Epitopes involved in antibody-mediated protection from Ebola virus. Science *287*, 1664-1666.

Witvrouw, M., Fikkert, V., Pluymers, W., Matthews, B., Mardel, K., Schols, D., Raff, J., Debyser, Z., De Clercq, E., Holan, G., *et al.* (2000). Polyanionic (i.e., polysulfonate) dendrimers can inhibit the replication of human immunodeficiency virus by interfering with both virus adsorption and later steps (Reverse transcriptase/integrase) in the virus replicative cycle. Mol Pharmacol *58*, 1100-1108.

Wong-Staal, F. (1991). HIVes and their replication (New York, USA: Raven Press, Ltd.).

Wool-Lewis, R.J., and Bates, P. (1998). Characterization of Ebola virus entry by using pseudotyped viruses: identification of receptor-deficient cell lines. J Virol *72*, 3155-3160.

Wu, L., and KewalRamani, V.N. (2006). Dendritic-cell interactions with HIV: infection and viral dissemination. Nat Rev Immunol *6*, 859-868.

Wu, L., Martin, T.D., Carrington, M., and KewalRamani, V.N. (2004). Raji B cells, misidentified as THP-1 cells, stimulate DC-SIGN-mediated HIV transmission. Virology *318*, 17-23.

Wyatt, R., Kwong, P.D., Desjardins, E., Sweet, R.W., Robinson, J., Hendrickson, W.A., and Sodroski, J.G. (1998). The antigenic structure of the HIV gp120 envelope glycoprotein. Nature *393*, 705-711.

Wyatt, R., Moore, J., Accola, M., Desjardin, E., Robinson, J., and Sodroski, J. (1995). Involvement of V1/V2 variable loop structures in the exposure of Human Immunodeficiency Virus Type-1 gp120 epitopes induced by receptor binding. J Virol *69*, 5723-5733.

Wyatt, R., and Sodroski, J. (1998). The HIV-1 envelope glycoproteins: Fusogens, antigens, and immunogens. Science *280*, 1884-1888.

Wyatt, R., Sullivan, N., Thali, M., Repke, H., Ho, D., Robinson, J., Posner, M., and Sodroski, J. (1993). Functional and immunological characterization of Human immunodeficiency Virus Type-1 envelope glycoproteins containing deletions of the major variable regions. J Virol *67*, 4557-4565.

Yaddanapudi, K., Palacios, G., Towner, J.S., Chen, I., Sariol, C.A., Nichol, S.T., and Lipkin, W.I. (2006). Implication of a retrovirus-like glycoprotein peptide in the immunopathogenesis of Ebola and Marburg viruses. FASEB J *20*, 2519-2530.

Yamada, T., and Iwamoto, A. (2000). Comparison of proviral accessory genes between long-term nonprogressors and progressors of human immunodeficiency virus type 1 infection. Arch Virol *145*, 1021-1027.

Yang, S.L., Delgado, R., King, S.R., Woffendin, C., Barker, C.S., Yang, Z.Y., Xu, L., Nolan, G.P., and Nabel, G.J. (1999). Generation of retroviral vector for clinical studies using transient transfection. Hum Gene Ther *10*, 123-132.

Yang, Z., Delgado, R., Xu, L., Todd, R.F., Nabel, E.G., Sanchez, A., and Nabel, G.J. (1998). Distinct cellular interactions of secreted and transmembrane Ebola virus glycoproteins. Science *279*, 1034-1037.

Yang, Z.Y., Duckers, H.J., Sullivan, N.J., Sanchez, A., Nabel, E.G., and Nabel, G.J. (2000). Identification of the Ebola virus glycoprotein as the main viral determinant of vascular cell cytotoxicity and injury. Nat Med *6*, 886-889.

Yu Kimata, M.T., Cella, M., Biggins, J.E., Rorex, C., White, R., Hicks, S., Wilson, J.M., Patel, P.G., Allan, J.S., Colonna, M., *et al.* (2002). Capture and transfer of simian immunodeficiency virus by macaque dendritic cells is enhanced by DC-SIGN. J Virol *76*, 11827-11836.

Zimmerli, S.C., Harari, A., Cellerai, C., Vallelian, F., Bart, P.A., and Pantaleo, G. (2005). HIV-1-specific IFN-gamma/IL-2-secreting CD8 T cells support CD4-independent proliferation of HIV-1-specific CD8 T cells. Proc Natl Acad Sci U S A *102*, 7239-7244.

SUPPLEMENTARY MATERIAL

XI. SUPPLEMENTARY MATERIAL

1. Supplementary material 1: Analysis of subtype B HIV-1 envelopes from Los Alamos data base

The molecular basis for the virus mutations in the envelope sequence, specifically PNGS, which might influence affinity to the lectin DC-SIGN, was also studied in gp160 sequences from the Los Alamos database (http://www.hiv.lanl.gov/ components/ sequence/HIV/search/search.html). The HIV-1 gp160 sequences were obtained from subtype B HIV-1 variants fulfilling one of criteria: documented year of infection or documented time of collected sample from the beginning of the infection.

The following number of gp160 HIV-1 sequences were collected from Los Alamos data base: 31 sequences obtained from patients infected in years 1983-1986, 65 sequences obtained from patients infected in years 2006-2009, 78 sequences from patients in acute infection period, 25 sequences obtained from patients in advance stage of disease, 14 sequences obtained from the same 7 patients, first from acute infection period and second from chronic infection. The length of variable loops (VLs) in gp160 and the number of PNGS were analyzed in each group of patients. The statistical analysis to compare different groups of patients was performed by implying Mann-Whitney test.

A comparison of the length of VLs between the groups of patients with acute infection and between patients with chronic infection did not reveal any statistically significant difference in the length of each VL separately as well as in the length of total VLs or total gp160. Although no statistical significance was found in performed analysis, the mean length of V1 increased from 26.17 aa to 27.28 aa, the mean length of V1V2 increased from 67.64 aa to 68.44 aa, the mean length of all VLs increased from 147.5 aa to 149.52 aa and the mean length of gp160 increased from 854.28 aa to 856.84 aa in virus sequences from acute-chronic infection. The difference in the number of PNGS in both groups of patient was statistically significant in case of V1 and V3 ($p=0.0814$ and

p=0.0009, respectively). The mean number of PNGS in V1 decreased from 2.74 to 2.52 PNGS and the mean number of PNGS in V3 decreased from 1.09 to 0.8 PNGS in virus from chronic infection as compared with acute. The number of PNGS in V2, V4, V5, all VLs and total gp160 did not show any significant difference (Fig. 59).

A subsequent comparison of the length of VLs and the number of PNGS in VLs was performed between patients infected in years 1983-1986 and patients infected in years 2006-2009. The length of VLs did not reveal any significant difference in both groups of patients. However, the number of PNGS varied considerably in V1, V1V2, V3, V5, all VLs and total gp160. The mean number of PNGS in V1 increased from 3.27 to 3.83 PNGS, the mean number of PNGS in V3 increased from 0.92 to 1.06 PNGS, the mean number of PNGS in V5 increased from 1.27 to 1.59 PNGS, the mean number of PNGS in V1V2 increased from 5.61 to 6.22 PNGS, the mean number of PNGS in all VLs increased from 12.47 to 13.22 PNGS and the mean number of PNGS in total gp160 increased from 29.76 to 30.82 PNGS in patients infected in years 2006-2009. The number of PNGS in V2 and V4 did not show any statistical difference. Although the analysis of the HIV-1 envelopes length did not reveal any statistically significant difference, the mean length of V1 increased from 25.88 to 27.49 aa, the mean length of V1V2 increased from 67.83 to 69.53 and the mean length of gp160 increased from 854.57 to 857.43 aa in patients infected in years 2006-2009 (Fig. 60).

The comparison of the length and the number of PNGS was also performed on the sequences obtained from Los Alamos data base from the same patient. Two HIV-1 envelope sequences were obtained for each of 7 patients. The first sequence was obtained at the moment of acute infection of a patient and the second was obtained at the moment of AIDS stage of infection. The comparison of the length of VLs within the same patient at different stage of HIV-1 infection did not show any statistically significant difference. However, the mean length of V1 increased from 21 aa to 23 aa, the mean length of V2 increased from 42.71 aa to 43.43 aa, the mean length of V1V2 increased from 63.71 aa to 66.43 aa, the mean length of all VL increased from 144.57 aa to 146.43 aa and the length of gp160 increased from 852.57 aa to 854.71 aa within the same patient over the

time of HIV-1 infection. The number of PNGS in VLs increased significantly over the course of disease (p=0.0368). The mean number of PNGS in V2 increased from 2 to 3.86 PNGS (p=0.0032), the mean number of PNGS in V1V2 increased from 4.71 to 5.86 PNGS (p=0.0728), the mean number of PNGS in all VLs increased from 11.43 to 13.57 PNGS and the mean number of PNGS in gp160 increased from 28.71 to 31.57 PNGS (p=0.0450) in the same patients along the time of infection. The number of PNGS in V1, V3, V4 and V5 did not reveal any significant difference (Fig. 61).

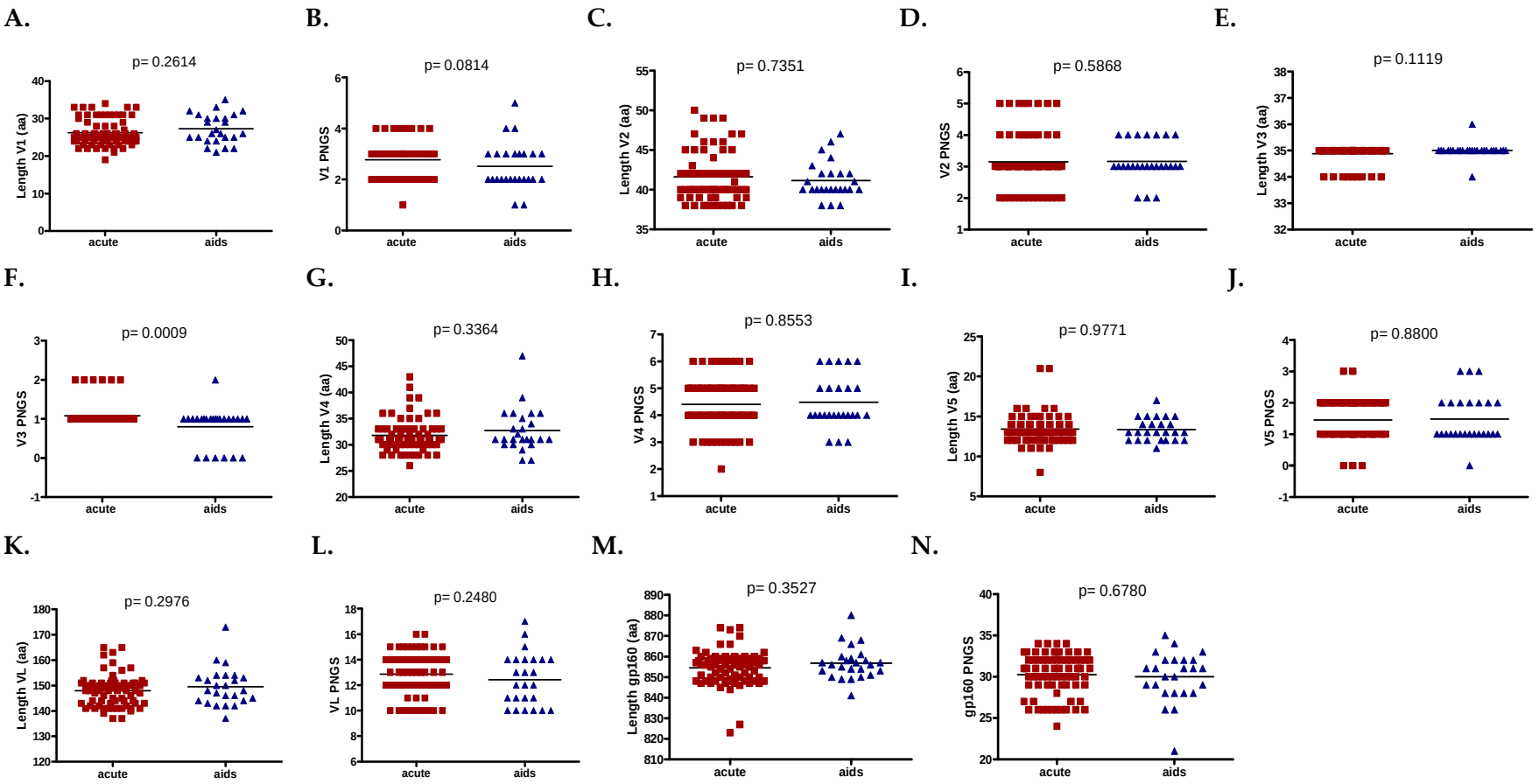

Figure 59. Comparison of the length and the PNGS number in HIV-1 envelopes between patients with acute HIV-1 infection and patients with chronic HIV-1 infection. **A**. Length of V1. **B.** PNGS in V1. **C.** Length of V2. **D.** PNGS in V2. **E.** Length of V3. **F.** PNGS in V3. **G.** Length of V4. **H.** PNGS in V4. **I.** Length of V5. **J.** PNGS in V5. **K.** Length of VLs. **L.** PNGS in VLs. **M.** Length of gp160. **N.** PNGS in gp160. The p values, estimated by Mann-Whitney test, are shown above each graph.

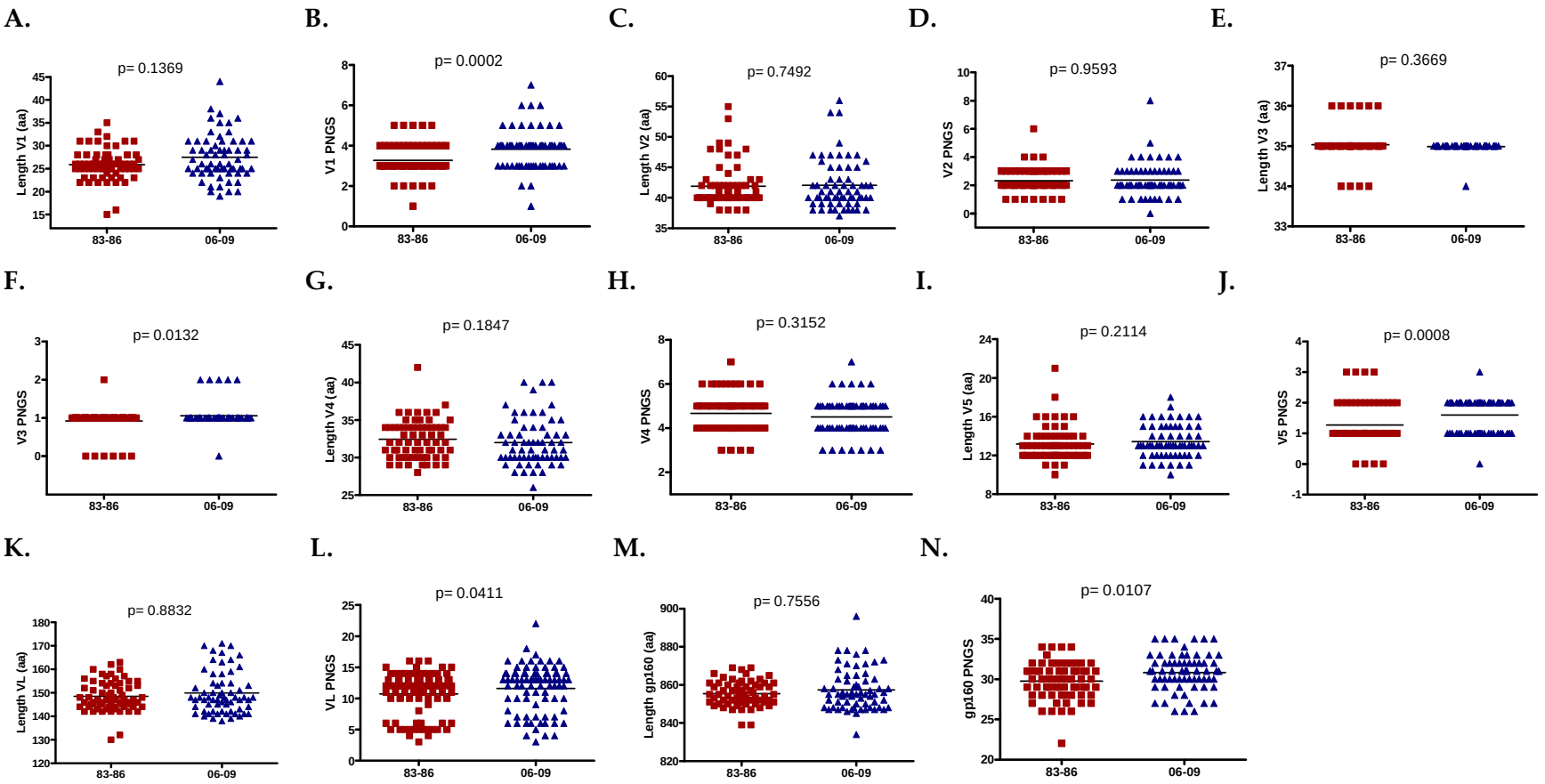

Figure 60. The comparison of the VLs length and the PNGS number between patients infected in years 1983-1986 and patients infected in years 2006-2009. **A**. Length of V1. **B.** PNGS in V1. **C.** Length of V2. **D.** PNGS in V2. **E.** Length of V3. **F.** PNGS in V3. **G.** Length of V4. **H.** PNGS in V4. **I.** Length of V5. **J.** PNGS in V5. **K.** Length of VLs. **L.** PNGS in VLs. **M.** Length of gp160. **N.** PNGS in gp160. The p values, estimated by Mann-Whitney, test are shown above each graph.

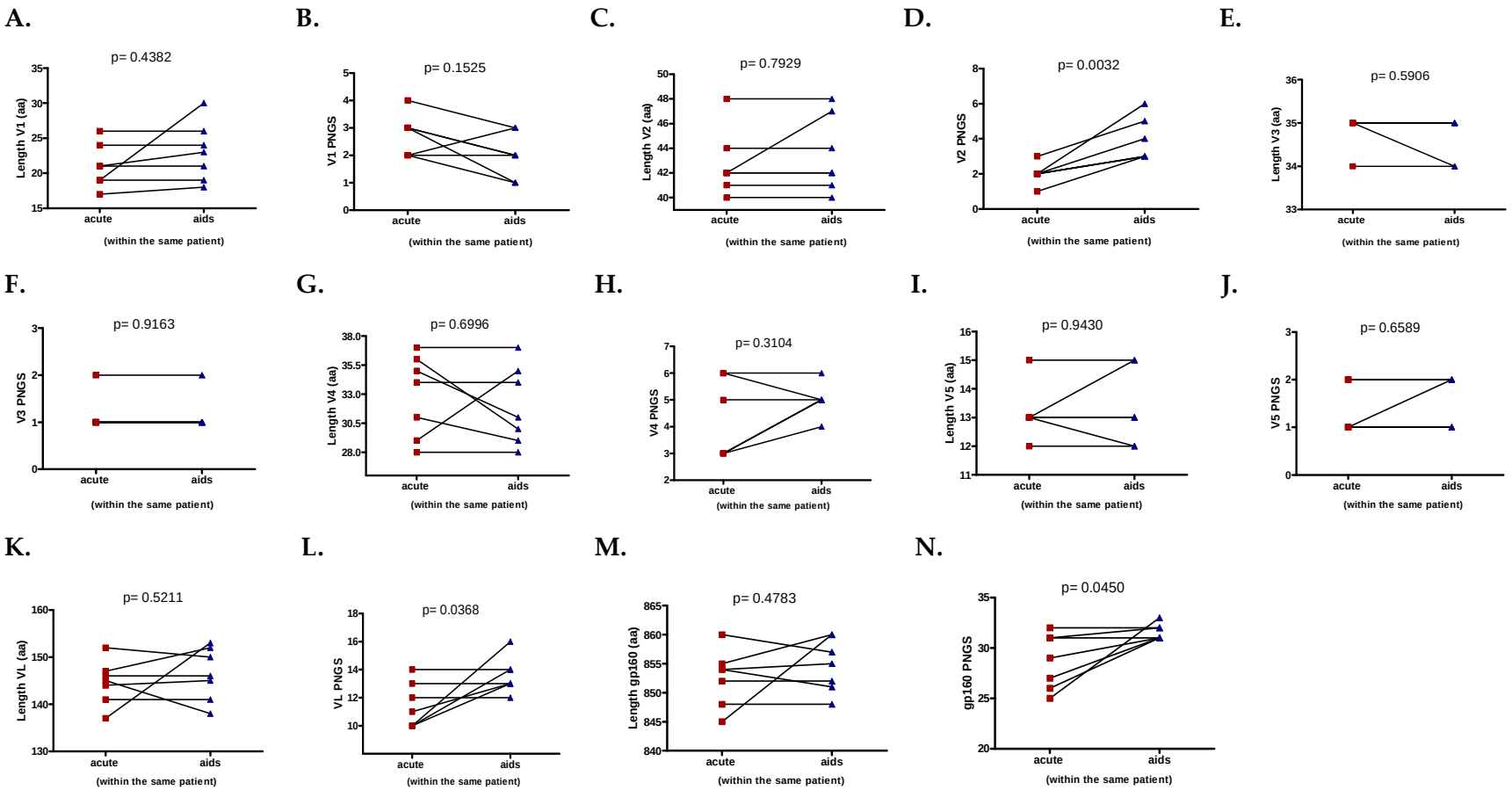

Figure 61. Comparison of the length of VLs and the number of PNGS in the same patient over the time of HIV-1 infection. **A**. Length of V1. **B.** PNGS in V1. **C.** Length of V2. **D.** PNGS in V2. **E.** Length of V3. **F.** PNGS in V3. **G.** Length of V4. **H.** PNGS in V4. **I.** Length of V5. **J.** PNGS in V5. **K.** Length of VLs. **L.** PNGS in VLs. **M.** Length of gp160. **N.** PNGS in gp160. The p values, estimated by Mann-Whitney test, are shown above each graph.

	stage of HIV-1 infection	date of HIV-1 infection	the same patient
	acute vs chronic infection	1983-1986 vs 2006-2009	acute vs chronic infection
V1 length	0.2614	0.1369	0.4382
V1 PNGS	0.0814	**0.0002**	0.1525
V2 length	0.7351	0.7492	0.7929
V2 PNGS	0.5868	0.9593	**0.0032**
V1V2 length	0.6004	0.3774	0.3363
V1V2 PNGS	0.1917	**0.0065**	0.0728
V3 length	0.1119	0.3669	0.5906
V3 PNGS	**0.0009**	**0.0132**	0.9163
V4 length	0.3364	0.1847	0.6996
V4 PNGS	0.8553	0.3152	0.3104
V5 length	0.9771	0.2114	0.9430
V5 PNGS	0.8800	**0.0008**	0.6589
V1-V5 length	0.2976	0.8832	0.5211
V1-V5 PNGS	0.2480	**0.0411**	**0.0368**
gp160 length	0.3527	0.7556	0.4783
gp160 PNGS	0.6780	**0.0107**	**0.0450**

Table 5. Statistical analysis of the length and the PNGS number in 3 groups of patients: 1) individuals with different stage of HIV-1 infection, 2) patients infected in years 1983-1986 or 2006-2009, 3) in the same patient on HIV-1 sequences obtained at different stages of HIV-1 infection. The p values were calculated by GraphPad Prism V4 applying Mann-Whitney test.

PUBLICATIONS AND COMMUNICATIONS RELATED TO THIS THESIS

XII. PUBLICATIONS AND COMMUNICATIONS RELATED TO THIS THESIS

Scientific publications

1) J. Luczkowiak , S. Sattin, I. Sutkevičiūtė, J.J. Reina, M. Sánchez-Navarro, M. Thépaut, L. Martínez-Prats, A. Daghetti, F. Fieschi, R. Delgado, A. Bernardi, J. Rojo. Pseudosaccharide functionalized dendrimers as potent inhibitors of DC-SIGN dependent Ebola pseudotyped viral infection. *Bioconjugate Chemistry*. 2011; 22(7): 1354-1365.

2) R. Ribeiro, M. Sánchez-Navarro, J. Luczkowiak, J.R. Koeppe, R. Delgado, J. Rojo, B.G. Davis. Virus-like glycodendrinanoparticles: highly symmetric polyvalent glycoprotein platforms generate a potent anti-viral activity. *Nature Communications*. 2012; 3:1303. doi: 10.1038/ncomms2302.

3) J. Luczkowiak, A. Muñoz, M. Sánchez-Navarro, R. Ribeiro-Viana, B.M. Illescas,N. Martín, R. Delgado, J. Rojo. Glycofullerenes inhibit viral infection. *Biomacromolecules.* 2013; 14(2): 431-437.

Scientific communications

1) J. Luczkowiak, R. Ribeiro, J. Rojo, R. Delgado. Inhibition of DC-SIGN-mediated Ebola virus infection by carbohydrate-based multivalent compounds. Abstract. *Glycosciences course*. Wageningen. 17-20 Mayo 2010.

2) R. Ribeiro-Viana, J. J. Reína, S. Sattin, J. Luczkowiak, A. Bernardi, R. Delgado, J. Rojo. Synthesis of glycodendrimers bearing pseudo sugars and evaluation of inhibition of Ebola infection in cis throught lectin DC-SIGN. Abstract. *Glycosciences course*. Wageningen. 17-20 Mayo 2010

3) R. Ribeiro-Viana, A. Mascaraque, M. Sánchez-Navarro, J. Luczkowiak, I. Sutkevičiūté, F. Fieschi, R. Delgado, B. Illescas, N. Martin, B. Davis, J. García Vallejo, Y. van Kooyk, J. Rojo. Glycodendritic structures: Synthesis and biological activity. Abstract P602. *26 International Carbohydrate Symposium*. Madrid. 22-27 Julio 2012.

4) J. Luczkowiak, L. Martínez-Prats, O. Sierra, F. Pulido, R. Rubio, R. Delgado. DC-SIGN-mediated trans-infection in HIV-1 clinical isolates: 1988-2011. Abstract P-067. *GeSIDA*. Toledo. 27-30 Noviembre. 2012.

5) J. Luczkowiak, O. Sierra, R. Delgado. Trans-Infección mediada por DC-SIGN y Control Virológico en un grupo de aislamientos clínicos de VIH-1. Abstract P-162. *GeSIDA*. Sitges. 19-22 Noviembre 2013.

Bioconjugate Chemistry

ARTICLE

pubs.acs.org/bc

Pseudosaccharide Functionalized Dendrimers as Potent Inhibitors of DC-SIGN Dependent Ebola Pseudotyped Viral Infection

Joanna Luczkowiak,[§] Sara Sattin,[‡] Ieva Sutkevičiūtė,[∥,#] José Juan Reina,[‡] Macarena Sánchez-Navarro,[†] Michel Thépaut,[∥,⊥] Lorena Martínez-Prats,[§] Anna Daghetti,[‡] Franck Fieschi,[*,∥,#] Rafael Delgado,[*,§] Anna Bernardi,[*,‡,¶] and Javier Rojo[*,†]

[†]Glycosystems Laboratory, Instituto de Investigaciones Químicas, CSIC — Universidad de Sevilla, Américo Vespucio 49, 41092 Seville, Spain

[‡]Università degli Studi di Milano, Dipartimento di Chimica Organica e Industriale, and CISI, Milano, Italy

[§]Laboratorio de Microbiología Molecular, Instituto de Investigación Hospital 12 de Octubre (imas12), 28041 Madrid, Spain

[∥]Institut de Biologie Structurale, CNRS, UMR 5075, 41 rue Jules Horowitz, 38027 Grenoble France

[⊥]CEA, DSV, 38027 Grenoble France

[#]Université Joseph Fourier, Institut Universitaire de France, 38000 Grenoble, France

[¶]CNR-ISTM, Institute of Molecular Sciences and Technologies, Milano, Italy

Supporting Information

ABSTRACT: The development of compounds with strong affinity for the receptor DC-SIGN is a topic of remarkable interest due to the role that this lectin plays in several pathogen infection processes and in the modulation of the immune response. DC-SIGN recognizes mannosylated and fucosylated oligosaccharides in a multivalent manner. Therefore, multivalent carbohydrate systems are required to interact in an efficient manner with this receptor and compete with the natural ligands. We have previously demonstrated that linear pseudodi- and pseudotrisaccharides are adequate ligands for DC-SIGN. In this work, we show that multivalent presentations of these glycomimetics based on polyester dendrons and dendrimers lead to very potent inhibitors (in the nanomolar range) of cell infection by Ebola pseudotyped viral particles by blocking DC-SIGN receptor. Furthermore, SPR model experiments confirm that the described multivalent glycomimetic compounds compete in a very efficient manner with polymannosylated ligands for binding to DC-SIGN.

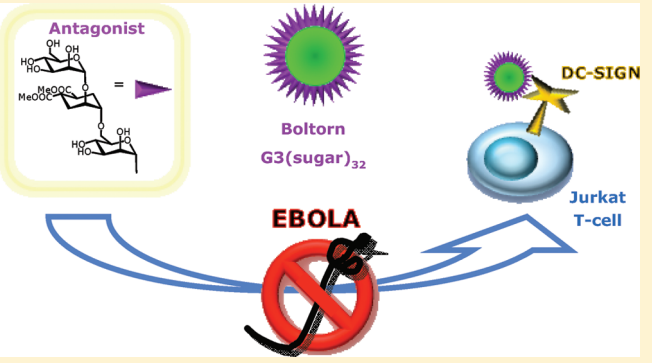

INTRODUCTION

Carbohydrates are involved in several biological processes including cell-differentiation, migration, tumor progression and metastasis, inflammation, pathogen infection, and so forth.[1] Carbohydrates participate in these events through complex and selective recognition processes triggered by interaction with receptors.

One of the processes that initialize immune response to pathogen invasion is the interaction of the pathogen surface glycans with C-type lectin receptors expressed on the antigen-presenting cells (APCs), such as dendritic cells (DCs). Although usually individual carbohydrate unit binding to lectin is weak (K_D in millimolar range), the clustered organization of these receptors as well as high glycosylation of their ligands create the conditions for more specific multivalent interactions, and thus overcome low affinity problems.[2−5] The use of scaffolds to prepare carbohydrate multivalent systems is nowadays a very useful and common approach to develop tools to understand and intervene in these biological processes where carbohydrates play a key role.[6,7]

The lack of design in these multivalent systems is partly a result of the often scarce information about the structural details of the multivalent presentation of the corresponding receptors at the cell surface. However, even if these details were known, topological design of large, multivalent molecules would still not be straightforward and the valency and 3D structures required to achieve a strong cluster effect on a given receptor cannot be estimated a priori. These facts explain the huge number of examples illustrating different strategies to target cellular receptors in a multivalent manner. In this context, our research is focused on the development of glycodendrimers to block a C-type lectin, DC-SIGN, which recognizes glycoconjugates present on the surfaces of several pathogens including viruses (HIV, Ebola, Cytomegalovirus, Dengue, SARS), bacteria (*M. tuberculosis, S. pneumoniae*) fungi (*C. albicans, A. fumigatus*), and

Received: January 21, 2011
Revised: March 31, 2011
Published: June 08, 2011

ACS Publications © 2011 American Chemical Society

parasites (*Leishmania, S. mansoni*).[8−14] It has been proven that this lectin plays a key role in the early stages of the infection processes caused by some of these pathogens. Therefore, DC-SIGN can be selected as a new therapeutic target for the design of antiviral drugs.[15−18] Previous results from our groups indicate that glycodendrimers based on Boltorn-type structures bearing mannoses exhibit a strong antiviral activity in a pseudotype Ebola viral particles infection model both for in *cis* and in *trans* infection.[19−21] Additionally, we have demonstrated that carbohydrate mimics such as a pseudomannobioside present an activity around 1 order of magnitude higher than mannose in such infection studies.[22,23] These new glycomimetics are more stable against enzymatic degradation than the corresponding natural counterparts, and therefore, they are more adequate compounds to be used in clinical applications.

In this study, we combined the improved binding properties of these new pseudomannoside ligands with the potency of multivalent presentation on Boltorn scaffolds. Indeed, nanomolar inhibition levels have been reached in a pseudotyped Ebola viral particles infection model. Binding properties between these compounds and their receptor, DC-SIGN, have been analyzed at the molecular level using biosensors with surface plasmon resonance (SPR) detection method. Altogether, this work opens road to new compounds in antiviral strategy.

MATERIALS AND METHODS

Reagents were purchased from Sigma-Aldrich, Senn Chemicals, Flucka and were used without purification. Solvents were dried by standard procedures. Reactions requiring anhydrous conditions were performed under nitrogen. Synthetic compounds were purified by flash chromatography using medium or fine silica gel or by Sephadex (LH20, G25). Thin layer chromatography (TLC) was carried out with precoated Merck F_{254} silica gel plates. Flash chromatography (FC) was carried out with Macherey-Nagel silica gel 60 (230−400 mesh). Reaction completion was observed by TLC using as development reagents phosphomolibdic acid, 10% sulfuric acid in methanol or anisaldehyde. ^{1}H and ^{13}C spectra were recorded at 400 MHz on Bruker Avance DPX 300, DRX 400, and DRX 500 MHz spectrometers. Chemical shifts (δ) for ^{1}H and ^{13}C spectra are expressed in ppm relative to internal TMS (tetramethylsilane) using manufacturer indirect referencing method. Signals were abbreviated as s, singlet; bs, broad singlet; d, doublet; t, triplet; q, quartet; and m, multiplet. Mass spectra were obtained with a Bruker ion-trap Esquire 3000 or 6000 apparatus (ESI ionization) and Microflex apparatus (MALDI ionization) from Bruker. HRMS (FT-ICR, ESI) were obtained with an Apex II instrument. Infrared spectra were recorded with a Bruker Vector 22 FT-IR spectrometer. Elemental analyses were obtained with a Leco CNHS instrument. All hydrogenation reactions were carried out under H_2 atmosphere at atmospheric pressure.

Synthesis of Compounds. Compounds **G1(Bn)$_4$**,[24] **G1-(OH)$_8$**,[25] **1**,[26] **2**,[27] **3**,[28] **6**,[29] **11**,[23] **13**,[22] and **14**−**15**[23] were prepared as described previously in the literature.

Synthesis of G2(Bn)$_8$. G1(OH)$_8$ (100 mg, 0.17 mmol) and DMAP (70 mg) were dissolved in dry pyridine (1 mL) and then diluted with CH_2Cl_2 (2 mL). Anhydride **1** (812 mg, 2.04 mmol) was added and the reaction mixture was stirred at room temperature for 15 h. Then, the excess of anhydride **1** was quenched by stirring the reaction mixture with 1 mL of pyridine/H_2O (1:1) solution overnight. The organic phase was diluted with CH_2Cl_2 (100 mL), and washed with $NaHSO_4$ 1 M (2 × 40 mL), Na_2CO_3 (10%) (2 × 40 mL), and NaCl sat. (40 mL). The organic phase was dried using $MgSO_4$ anh., and the solvent was evaporated under vacuum. The residue was recrystallized from CH_2Cl_2/hexane to give **G2(Bn)$_8$** (370 mg, 97%) as white crystals. ^{1}H NMR (300 MHz, $CDCl_3$): δ (ppm) 7.40−7.38 (m, 16 H, H_{Ar}), 7.32−7.26 (m, 30H, H_{Ar}), 5.36 (s, 8H, 8 × CH_{Bn}), 4.53 (d, 16H, J = 11.7 Hz, CH_{2G2}), 4.36 (d, 8H, J = 11.4 Hz, CH_{2G1}), 4.29 (d, 8H, J = 11.4 Hz, CH_{2G1}), 3.89 (s, 8H, $CH_{2Pentaerythritol}$), 3.52 (d, 16H, J = 11.7 Hz, CH_{2G2}), 1.15 (s, 12H, CH_{3G1}), 0.88 (s, 24H, CH_{3G1}); ^{13}C NMR (100 MHz, $CDCl_3$) δ (ppm) 175.9 (COO_{G2}), 174.1 (COO_{G1}), 140.2 (C_{Ph}), 131.2 (C_{Ph}), 130.4 (CH_{Ph}), 128.5 (CH_{Ph}), 104.0 (CH_{Bn}), 75.7, 75.7, 67.2, 63.6, 49.2, 44.8, 36.2, 20.0 (CH_{3G2}), 19.9 ($CH_{3\ G1}$); ESI-MS for $C_{121}H_{140}O_{40}$; calcd 2232.9 $[M]^+$; found 2256.7 $[M+Na]^+$ and 1139.8 $[M+2Na]^{2+}$; Elemental analysis calcd (%) for $C_{121}H_{140}O_{40}$: C, 65.04%; H, 6.32%; found: C, 65.32%; H, 6.31%.

Synthesis of G2(OH)$_{16}$. G2(Bn)$_8$ (3.8 g, 1.70 mmol) was dissolved in CH_2Cl_2 (50 mL) and diluted with MeOH (50 mL). A catalytic amount of Pd(C) was added to the solution and the reaction mixture was hydrogenated under vigorous stirring for 12 h. Then, the reaction mixture was filtered over a pad of Celite. The solvent was evaporated to give **G2(OH)$_{16}$** (860 mg, 95%) as a white solid. ^{1}H NMR (300 MHz, CD_3OD): δ (ppm) 4.39 (d, 8H, J = 11.1 Hz, CH_{2G1}), 4.30 (d, 8H, J = 11.1 Hz, CH_{2G1}), 4.29 (s, 8H, $CH_{2Pentaerythritol}$), 3.70 (d, 16H, J = 10.8 Hz, CH_{2G2}), 3.61 (d, 16H, J = 10.8 Hz, CH_{2G2}), 1.35 (s, 12H, CH_{3G1}), 1.17 (s, 24H, CH_{3G2}); ^{13}C NMR (75 MHz, CD_3OD): δ (ppm) 176.0 (COO_{G2}), 173.8 (COO_{G1}), 66.1 ($CH_{2Pentaerythritol}$), 65.9 (CH_{2G2}), 63.6 (C_{G2}), 51.8 (CH_{2G1}), 44.3 (C_{G1}), 18.3 (CH_{3G1}), 17.4 (CH_{3G2}); ESI-MS for $C_{65}H_{108}O_{40}$; calcd: 1528.6 $[M]^+$; found: 1551.4 $[M+Na]^+$.

Synthesis of G3(Bn)$_{16}$. G2)OH)$_{16}$ (1.00 g, 0.654 mmol) and DMAP (445 mg) were dissolved in dry pyridine (20 mL) and then diluted with CH_2Cl_2 (40 mL). Anhydride **1** (6.02 g, 14.13 mmol) was added, and the reaction mixture was stirred at room temperature for 15 h. Then, the excess of anhydride **1** was quenched by stirring the reaction mixture with 20 mL of pyridine/H_2O (1:1) solution overnight. The organic phase was diluted with CH_2Cl_2 (300 mL), and washed with $NaHSO_4$ 1 M (2 × 150 mL), Na_2CO_3 (10%) (2 × 150 mL), and NaCl sat. (150 mL). The organic phase was dried using $MgSO_4$ anh., and the solvent was evaporated under vacuum. The residue was recrystallized from CH_2Cl_2/MeOH to give **G3(Bn)$_{16}$** (2.7 g, 97%) as white crystals. ^{1}H NMR (500 MHz, $CDCl_3$): δ (ppm) 7.37−7.34 (m, 32H, CH_{Ph}), 7.27−7.21 (m, 48H, CH_{Ph}), 5.32 (s, 16H, CH_{Bn}), 4.49 (d, 32H, CH_{2G3}), 4.34−4.25 (m, 32H, 2 × 16 CH_{2G2}), 4.12 (d, 8H, CH2$_{G1}$), 4.11 (s, 8H, $CH_{2Pentaerythritol}$), 4.02 (d, 8H, CH_{2G1}), 3.55−3.51 (m, 32H, CH_{2G3}), 1.18 (s, 24H, CH_{3G2}), 1.08 (s, 12H, CH_{3G1}), 0.88 (s, 48H, CH_{3G3}); ^{13}C NMR (125 MHz, $CDCl_3$): δ (ppm) 173.2 (COO_{G3}), 171.9 (COO_{G2}), 171.5 (COO_{G1}), 138.0 (C_{Ph}), 128.8 (CH_{Ph}), 128.1 (CH_{Ph}), 126.2 (CH_{Ph}), 101.6 (CH_{Bn}), 73.4, 73.3, 64.9, 46.9, 46.6, 42.5 (CH_{2G3}), 34.0, 25.0, 17.7 (CH_{3G2}), 17.6 (CH_{3G3}), 17.2 (CH_{3G1}); ESI-MS for $C_{257}H_{300}O_{88}$; calcd: 4793.9 $[M]^+$; found: 2420.5 $[M+2Na]^{2+}$ and 1621.8 $[M+3Na]^{3+}$; Elemental analysis calcd (%) for $C_{257}H_{300}O_{88}$: C, 64.34%; H, 6.30%; found: C, 64.07%; H, 6.46%.

Synthesis of G3(OH)$_{32}$. G3(Bn)$_{16}$ (1.7 g, 0.354 mmol) was dissolved in CH_2Cl_2 (30 mL) and diluted with MeOH (30 mL). A catalytic amount of Pd(C) was added to the solution and the reaction mixture was hydrogenated under vigorous stirring for 12 h. Then, the reaction mixture was filtered over a pad of Celite. The solvent was evaporated to give **G3(OH)$_{32}$** (1.14 g, 95%) as a white solid. ^{1}H NMR (500 MHz, CD_3OD): δ (ppm) 4.36−4.22 (m, 56H, $CH_{2Pentaerythritol}$ + CH_{2G1} + CH_{2G2}), 3.68 (m, 32H, CH_{2G3}), 3.58 (d, 32H, J = 10.0 Hz, CH_{2G3}), 3.39 (s, 32H, CH_2OH), 1.34 (s, 12H,

CH_{3G1}), 1.30 (s, 24H, CH_{3G2}), 1.12 (s, 48H, CH_{3G3}); ^{13}C NMR (75 MHz, CD_3OD): δ (ppm) 176.0 (COO_{G2}), 173.8 (COO_{G1}), 66.1 ($CH_{2Pentaerythritol}$), 65.9 (CH_{2G2}), 63.6 (C_{G2}), 51.8 (CH_{2G1}), 44.3 (C_{G1}), 18.3 (CH_{3G1}), 17.8 (CH_{3G3}), 17.4 (CH_{3G2}); ESI-MS for $C_{65}H_{108}O_{40}$; calcd: 3385.4 $[M]^+$; found: 1716.0 $[M+2Na]^{2+}$ and 1151.0 $[M+3Na]^{3+}$.

Synthesis of G3(sucBn)$_{32}$. (460 mg, 1.36 mmol), succinic acid derivate **2** (1.086 g, 5.22 mmol) and DPTS (512 mg, 1.74 mmol) were disolved in CH_2Cl_2 (15 mL) under argon atmosphere. DCC (1.433 g, 6.96 mmol) was added and the reaction mixture was stirred for 24 h at room temperature. Then, the reaction mixture was diluted with (6 mL), filtered over a pad of Celite, and the solvent was evaporated. The residue was purified by flash chromatography on silica gel (Hex-AcOEt, 1:1.2), to afford **G3(sucBn)$_{32}$** (1.10 g, 81%) as an oil. ^{1}H NMR (500 MHz, $CDCl_3$): δ (ppm) 7.41−7.33 (m, 160H, CH_{Ar}), 5.13 (bs, 64H, $CH2_{Bn}$), 4.50−4.21 (m, 120H, $CH_{2dendrimer}$), 2.63 (bs, 128H, CH_{2suc}), 1.39 (bs, 12H, CH_{3G1}), 1.31 (bs, 24H, CH_{3G2}), 1.23 (bs, 48H, CH_{3G3}); ^{13}C NMR (125 MHz, $CDCl_3$) δ (ppm) 171.9 (COO_{G3}), 171.7 (COO_{G2}), 171.6 (COO_{G1}), 135.9 (C_{ArBn}), 128.5 (CH_{ArBn}), 128.4 (CH_{ArBn}), 128.2 (CH_{ArBn}), 66.4 (CH_{2Bn}), 65.1, 64.9 ($CH_{2dendrimer}$), 46.7 (C_{G1}), 46.6 (C_{G2}), 46.3 (C_{G3}), 28.9 (CH_{2suc}), 28.8 (CH_{2suc}), 17.7 (CH_{3G3}), 17.6 (CH_{3G2}), 17.4 (CH_{3G1}); ESI-MS for $C_{497}H_{556}O_{184}$; calcd: 9467.4 $[M]^+$; found: 4758.5 $[M+2Na]^{2+}$ and 3185.3 $[M+3Na]^{3+}$; Elemental analysis calcd (%) for $C_{497}H_{556}O_{184}$: C, 63.01%; H, 5.92%; found: C, 62.54%; H, 6.00%.

Synthesis of G3(suc)$_{32}$. **G3(sucBn)$_{32}$** (87 mg, 9.19×10^{-3} mmol) was dissolved in CH_2Cl_2 (3 mL) and diluted with MeOH (6 mL). A catalytic amount of Pd(C) was added to the solution and the reaction mixture was hydrogenated under vigorous stirring for 12 h. Then, the reaction mixture was filtered over a pad of Celite. The solvent was evaporated to give **G3(suc)$_{32}$** (79 mg, quant.) as a white solid. ^{1}H NMR (300 MHz, D_2O): δ (ppm) 4.50−4.20 (m, 120, 60 × CH_2OCO), 2.70−257 (m, 128H, 64 × CH_{2suc}), 1.42 (s, 12H, 4 × CH_{3G1}), 1.35 (s, 32H, 8 × CH_{3G2}), 1.28 (s, 52H, 16 × CH_{3G3}); ^{13}C NMR (125 MHz, CD_3CN): δ (ppm) 174.2 (COO), 173.0 (COO), 172.9 (COO), 66.3 (CH_2O), 47.4 (C), 29.1 (CH_{2suc}), 17.9 (CH_3).

G3(pseudodi)$_{32}$. To a solution of **G3(suc)$_{32}$** (3.5 mg, 5.31×10^{-4} mmol, 1 equiv) in dry DMA (100 μL) under nitrogen atmosphere, HATU (13 mg, 0.034 mmol, 64 equiv) and DIPEA (12 μL, 0.068 mmol, 128 equiv) were added. After 15 min a solution of **13** (16.0 mg, 0.037 mmol, 69 equiv) in dry DMA (170 μL) was added. The reaction was stirred at room temperature for 1 day. MALDI mass analysis of a sample of the reaction mixture showed the completion of the reaction. The reaction mixture was diluted in methanol and charged directly onto a Sephadex LH-20 column in methanol. Slow elution led to the purification of the product **G3(pseudodi)$_{32}$** that was isolated in good yield (9.2 mg, 88%). ^{1}H NMR (400 MHz, D_2O): δ (ppm) 5.00 (s, H_{1M}), 4.43−4.14 (m, CH_2O_{G1} + CH_2O_{G2} + CH_2O_{G3}), 4.02−3.95 (m, H_{D2} + H_{2M}), 3.92 (s, H_{2M}), 3.86 (d, J = 11.2 Hz, H_{6MB}), 3.81 (dd, J = 3.2 and 8.8 Hz, H_{3M}), 3.78−3.56 (m, H_{6MA} + H_{D1} + H_{4M} + H_{5M} + H_7), 3.69 (s, $COOCH_3$), 3.69 (s, $COOCH_3$), 3.42−3.32 (m, H_8), 2.97−2.81 (m, H_{D4} + H_{D5}), 2.72−2.61 (m, CH_2COO), 2.61−2.49 (m, CH_2CONH), 2.16−2.03 (m, H_{D6eq} + H_{D3eq}), 1.89−1.71 (m, H_{D6ax} + H_{D3ax}), 1.39−1.18 (m, CH_{3G1} + CH_{3G2} + CH_{3G3}); ^{13}C NMR (100 MHz, D_2O): 177.1, 176.8, 173.4 ($COOCH_3$, $COOCH_2$, CONH), 98.7 (C_{1M}), 73.9 (C_{D1}), 73.6 (C_{4M}), 71.1 (C_{D2}), 70.6 (C_{2M} + C_{3M}), 67.1 (C_7), 66.9 (C_{5M}), 65.5 (CH_2O_{G1} + CH_2O_{G2} + CH_2O_{G3}), 61.1 (C_{6M}), 52.5 (CH_3O), 46.5 (C_{quatG1} + C_{quatG2} + C_{quatG3}), 39.5 (C_8), 39.1 (C_{D4}, C_{D5}), 30.2 (CH_2CONH), 29.3 (CH_2COO), 27.3, 26.9 (C_{D6}, C_{D3}), 17.3 (CH_{3G1} + CH_{3G2} + CH_{3G3}); MALDI-ToF MS (matrix, SA): distribution centered on 31 sugar loaded, for 31 sugars $[M+Na]^+$ calculated: 19614.8, found: 19689.5.

G3(pseudotri)$_{32}$. To a solution of **G3(suc)$_{32}$** (7.6 mg, 1.15×10^{-3} mmol, 1 equiv) in 100 μL of dry DMA under nitrogen atmosphere, HATU (28.1 mg, 0.074 mmol, 64 equiv) and DIPEA (26 μL, 0.148 mmol, 128 equiv) were added. After 15 min, a solution of **15** (35.7 mg, 0.06 mmol, 52 equiv) in dry DMA (230 μL) was added. The reaction was stirred at room temperature for 2 days. MALDI mass analysis of a sample of the reaction mixture showed the completion of the reaction. The reaction mixture was diluted in methanol and charged directly onto a Sephadex LH-20 column in methanol. Slow elution led to the purification of the product **G3(pseudotri)$_{32}$** that was isolated in good yield (25.5 mg, 88% yield). ^{1}H NMR (400 MHz, D_2O): δ (ppm) 5.00 (s, $H_{1M'}$), 4.84 (s, H_{1M}), 4.40−4.10 (m, CH_2O_{G1} + CH_2O_{G2} + CH_2O_{G3}), 4.04 (s, H_{D2}), 3.97 (bs, $H_{2M'}$), 3.92 (s, H_{2M}), 3.89−3.53 (m, $H_{3M'}$ + $H_{6M'B}$ + H_{6MB} + H_{D1} + $H_{6M'A}$ + H_{6MA} + H_{3M} + H_{4M} + $H_{4M'}$ + H_7 + H_{5M} + $H_{5M'}$), 3.69 (s, $COOCH_3$), 3.68 (s, $COOCH_3$), 3.49−3.34 (m, H_8), 3.00−2.85 (m, H_{D4} + H_{D5}), 2.73−2.59 (m, CH_2COO), 2.59−2.46 (m, CH_2CONH), 2.27−2.03 (m, H_{D6eq} + H_{D3eq}), 1.89−1.71 (m, H_{D6ax} + H_{D3ax}), 1.40−1.15 (m, CH_{3G1} + CH_{3G2} + CH_{3G3}); ^{13}C NMR (100 MHz, D_2O): δ (ppm) 177.3, 177.0, 173.5, 173.0 ($COOCH_3$, $COOCH_2$, CONH), 99.9 (C_{1M}), 98.7 ($C_{1M'}$), 74.7 (C_{D1}), 73.5, 72.2 (C_{4M} + $C_{4M'}$), 71.0 (C_{D2}), 70.9, 70.7, 70.6 ($C_{2M'}$ + C_{3M} + $C_{3M'}$), 70.2 (C_{2M}), 68.2 (C_{6M}), 67.1, 66.9 (C_{5M} + $C_{5M'}$), 66.2 (C_7), 65.4 (CH_2O_{G1} + CH_2O_{G2} + CH_2O_{G3}); 61.1 ($C_{6M'}$), 52.6 (CH_3O), 46.4 (C_{quatG1} + C_{quatG2} + C_{quatG3}), 39.1, (C_{D4}, C_{D5}), 39.0 (C_8), 30.1 (CH_2CONH), 29.2 (CH_2COO), 27.2, 26.9 (C_{D6}, C_{D3}), 17.3 (CH_{3G1} + CH_{3G2} + CH_{3G3}). MALDI-ToF MS (matrix: SA): distribution centered on 31 sugar loaded, for 31 sugar $[C_{1041}H1_{612}N_{32}O_{664}Na]^+$ calcd: 25222.75, found: 25227.9.

2-Azidoethyl Isopropylidene-2,2-bis(oxymethyl)propionate (4). 2-Bromoethanol (1.2 mL, 17.0 mmol) and DMAP (0.325 g, 2.6 mmol) were dissolved in pyridine (25 mL), followed by the addition of CH_2Cl_2 (70 mL). The anhydride of isopropylidene-2,2-bis(oxymethyl)propionic acid **6** (7.4 g, 22.4 mmol) was added slowly. The solution was stirred at room temperature overnight and then was quenched with water (1 mL) under vigorous stirring, followed by dilution with of CH_2Cl_2 (200 mL), and the solution was washed with 10% of $NaHSO_4$ (3 × 40 mL), 10% of Na_2CO_3 (3 × 40 mL), and brine (20 mL). The organic phase was dried with $MgSO_4$, filtered, and concentrated. The crude product was purified by flash chromatography on silica gel, eluting with hexane (100 mL) and gradually increasing the polarity to EtOAc/hexane (9:1; 6:1) to give 2-bromoethyl isopropylidene-2,2-bis(oxymethyl)propionate as colorless oil (4.9 g, 86%). This bromo derivative (4.9 g, 14.6 mmol) and NaN_3 (2.6 g, 40.0 mmol) were dissolved in dry DMF (50 mL) and the reaction mixture was stirred at 50 °C for 15 h. The solvent was removed under high vacuum and AcOEt was added to the residue. The NaN_3 on excess was taken off by filtration, and the solvent was removed to obtain **4** as colorless oil (3.53 g, 99%). ^{1}H NMR (300 MHz, $CDCl_3$) δ: 4.30 (t, 2H, J = 5.1 Hz, $CH_2CH_2N_3$), 4.18 (d, 2H, J = 11.9 Hz, CH_2OCO), 3.64 (d, 2H, J = 11.9 Hz, CH_2OCO), 3.67 (t, 2H, J = 5.1 Hz, $CH_2CH_2N_3$), 1.41 (s, 3H, CH_3), 1.36 (s, 3H, CH_3), 1.19 (s, 6H, 2 × CH_3); ^{13}C NMR (100 MHz, $CDCl_3$) δ: 173.8 (COO), 98.0 (C_{ipr}), 65.8 (CH_2OCO), 63.5 ($CH_2CH_2N_3$), 49.7 ($CH_2CH_2N_3$), 41.9 (C), 24.8, 22.2 (CH_3), 17.7 (CH_3); ESI-MS for

$C_9H_{15}N_3O_4$; calcd: 243.1, $[M]^+$; found 266.1 $[M+Na]^+$. IR (υ, cm^{-1}): 3448 (bs), 2992, 2940, 2105, 1734, 1638.

2-Azidoethyl 2,2-Bis(hydroxymethyl)propionate (5). Azido derivative **4** (11.0 g, 45.2 mmol) was dissolved in MeOH (50 mL). One teaspoon of a Dowex, H+ resin was added, and the reaction mixture was stirred at 40 °C until complete disappearance of starting material. When the reaction was complete, the Dowex H+ resin was filtered off in a glass filter and carefully washed with methanol. The methanol was evaporated to give **5** as colorless oil (9.0 g, 98%). ^{1}H NMR ($CDCl_3$, 300 MHz) δ: 4.34 (t, 2H, J = 5.1 Hz, $CH_2CH_2N_3$), 3.92 (d, 2H, J = 11.2 Hz, CH_2OCO), 3.74 (d, 2H, J = 11.2 Hz, CH_2OCO), 3.52 (t, 2H, J = 5.1 Hz, $CH_2CH_2N_3$), 3.02 (bs, 2H, *OH*), 1.12 (s, 3H, CH_3); ^{13}C NMR ($CDCl_3$, 100 MHz) δ: 175.3 (COO), 67.8 (CH_2OCO), 63.5 ($CH_2CH_2N_3$), 49.8 ($CH_2CH_2N_3$), 49.4 (C), 17.0 (CH_3); ESI-MS for $C_7H_{13}N_3O_4$; calcd: 203.1 $[M]^+$; found: 226.0 $[M+Na]^+$. IR (υ, cm^{-1}): 3405 (bs), 2945, 2885, 2105, 1729, 1660, 1459. Elemental analysis calcd. (%) for $C_7H_{13}N_3O_4$: C, 41.38%, H, 6.45%; N, 20.68%; found: C, 41.83%; H, 6.79%; N, 20.50%.

Compound 7. Azido derivative **5** (2.4 g, 11.8 mmol) and DMAP (0.43 g, 3.54 mmol) were dissolved in pyridine (6 mL), followed by the addition of CH_2Cl_2 (12 mL). The anhydride of isopropylidene-2,2-bis(hydroxymethyl)propionic acid **6** (9.3 g, 30.7 mmol) was added slowly. The solution was stirred at room temperature until completion. The reaction was quenched with water (1 mL) under vigorous stirring, followed by dilution with CH_2Cl_2 (50 mL), and the solution was washed with 10% of $NaHSO_4$ (3 × 20 mL), 10% of Na_2CO_3 (3 × 20 mL), and brine (10 mL). The organic phase was dried with $MgSO_4$, filtered, and concentrated. The crude product was purified by flash chromatography on silica, eluting with hexane (100 mL) and gradually increasing the polarity to EtOAc/hexane (1:3) to give **7** as colorless oil (4.4 g, 73%). ^{1}H NMR ($CDCl_3$, 300 MHz) δ: 1.17 (s, 6H, CH_3), 1.34 (s, 3H, CH_3), 1.38 (s, 6H, CH_3), 1.43 (s, 6H, CH_3), 3.51 (t, J = 5.1 Hz, 2H, $CH_2CH_2N_3$), 3.64 (d, J = 11.9 Hz, 4H, CH_2OCO), 4.17 (d, J = 11.8 Hz, 4H, CH_2OCO), 4.34−4.28 (t, J = 5.1 Hz, 2H, $CH_2CH_2N_3$), 4.36 (s, 4H, CH_2OCO); ^{13}C NMR ($CDCl_3$, 75.5 MHz) δ: 173.5, 172.3 (COO), 98.1 (C^ipr), 66.0, 66.0, 65.3 (CH_2OCO), 63.9 ($CH_2CH_2N_3$), 49.6 ($CH_2CH_2N_3$), 46.9, 42.1 (C), 25.3, 22.0 (CH_3^ipr), 18.0, 17.0 (CH_3); ESI-EM calc for $C_{23}H_{37}N_3O_{10}$(m/z): 515.2; found 538.2 $[M+Na]^+$. IR (υ, cm^{-1}): 3453 (bs), 2991, 2940, 2876, 2106, 1738, 1643, 1455.

Compound 8. Azido derivative **7** (4.3 g, 8.4 mmol) was dissolved in MeOH (20 mL). One teaspoon of a Dowex H+ resin was added, and the reaction mixture was stirred at 40 °C until complete disappearance of starting material by TLC. When the reaction was complete, the Dowex H+ resin was filtered off in a glass filter and carefully washed with methanol. The methanol was evaporated to give **8** as colorless oil (3.5 g, 97%). ^{1}H NMR ($CDCl_3$, 300 MHz) δ: 4.46 (d, J = 11.1 Hz, 2H, CH_2OCO), 4.36−4.26 (m, 4H, CH_2OCO, $CH_2CH_2N_3$), 3.90−3.78 (m, 4H, CH_2OCO), 3.76−3.67 (m, 4H, CH_2OCO), 3.51 (t, J = 5.1 Hz, 2H, $CH_2CH_2N_3$), 3.19−2.87 (bs, 4H), 1.36 (s, 3H, CH_3), 1.08 (s, 6H, CH_3); ^{13}C NMR ($CDCl_3$, 75.5 MHz) δ: 175.0, 175.0, 172.8 (COO), 67.3, 67.2, 67.2, 64.8 (CH_2OCO), 64.0 ($CH_2CH_2N_3$), 49.8 ($CH_2CH_2N_3$), 49.8, 49.6 (C), 18.0, 17.0 (CH_3); ESI-EM calcd for $C_{17}H_{29}N_3O_{10}$ (m/z): 435.2; found 458.2 $[M+Na]^+$. IR (υ, cm^{-1}): 3405 (bs), 2943, 2886, 2108, 1731, 1469.

Compound 10. 4-Oxo-4-(2-(trimethylsilyl)ethoxy)butanoic acid (**9**) (1.43 g, 6.57 mmol), tetraol **8** (0.50 g, 1.09 mmol), and DPTS (0.65 g, 2.18 mmol) were mixed in CH_2Cl_2 anhydrous (10 mL). Then, the reaction flask was flushed with argon and DCC (1.35 g, 6.57 mmol) was added. Stirring at 40 °C was continued for 15 h under argon atmosphere. Once the reaction was complete, the formed urea was filtered off on a glass filter and washed with a small volume of CH_2Cl_2. The crude product was purified by liquid chromatography Sephadex LH20 (CH_2Cl_2/MeOH; 1:1) to give **10** as colorless viscous oil (1.11 g, 81%). ^{1}H NMR ($CDCl_3$, 300 MHz) δ: 4.43−3.97 (m, 14H, 4 CH_{2G1}, 8 CH_{2G2}, 2 $CH_2CH_2N_3$, 8 $CH_2CH_2COCH_2$), 3.53−3.43 (t, J = 5.1 Hz, 2H, $CH_2CH_2N_3$), 2.65−2.47 (m, 16H, CH_2suc), 1.26 (s, 3H, $CH_{3\ G1'}$), 1.20 (s, 6H, $CH_{3\ G2'}$), 1.00−0.88 (t, J = 8.5 Hz, 8H, CH_2-TMS), 0.00 (s, 36 H, CH_3TMS); ^{13}C NMR ($CDCl_3$, 75.5 MHz) δ: 172.1, 171.9, 171.9, 171.7 (COO), 65.6, 65.3, 64.0, 62.9 (CH_2OCO, $CH_2CH_2N_3$, $CH_2CH_2COCH_2$), 49.6 ($CH_2CH_2N_3$), 46.7, 46.4 (CCH_2O), 29.1, 28.8 (CH_2suc), 17.7, 17.4 (CH_2-TMS, CH_3), 17.2, −1.5, −1.9 (CH_3TMS); ESI-HRMS calcd for $C_{53}H_{93}N_3O_{22}Si_4Na$ (m/z): 1258.5291; found: 1258.5226. IR (υ, cm^{-1}): 2955, 2898, 2104, 1730, 1471.

Compound 11. TFA (5 mL) was added to a solution of **10** (142 mg, 0.115 mmol) in CH_2Cl_2 (5 mL). The mixture was stirred at room temperature for 2 h. After complete conversion, the solvent was evaporated and dried in high vacuum to afford **11** as pale yellow syrup (96 mg, 100%). The compound was used in the next step without purification. ^{1}H NMR (MeOH-d_4, 400 MHz) δ: 4.30 (m, 28H, 4$CH_{2\ G1}$ 8$CH_{2\ G2}$, 2$CH_2CH_2N_3$), 3.57 (t, J = 5.1 Hz, 2H, $CH_2CH_2N_3$), 2.62 (m, 16H, CH_2CONH, CH_2COO), 1.34 (s, 3H, $CH_{3G1'}$), 1.27 (s, 6H, $CH_{3G2'}$); ^{13}C NMR ($CDCl_3$, 100 MHz) δ: 174.4, 172.2, 172.2, 172.0 (COO), 65.5, 65.3, 65.2, 64.0 (CH_2OCO, $CH_2CH_2N_3$, $CH_2CH_2COCH_2$), 49.4 ($CH_2CH_2N_3$), 46.9, 46.5, 46.3 (CCH_2O), 28.6, 28.5, 28.3, 28.2 (CH_2CONH, CH_2COO), 16.7, 16.5 (CH_3); ESI-HRMS calcd for $[M+Na]$ $C_{33}H_{45}N_3O_{22}Na$ (m/z): 858.2392; found: 858.2435.

Compound 12. To a solution of the scaffold dendron **11** (6.0 mg, 0.00718 mmol, 1 equiv) in 150 μL of dry DMA under nitrogen atmosphere, HATU (22 mg, 0.0575 mmol, 8 equiv) and DIPEA (20 μL, 0.1157 mmol, 16 equiv) were added. After 15 min, a solution of **13** (23.4 mg, 0.05349 mmol, 8 equiv) in dry DMA (210 μL) was added. The reaction was stirred at room temperature for 3 days. MALDI mass analysis of a sample of the reaction mixture showed the completion of the reaction. The reaction mixture was diluted in methanol and charged directly onto a Sephadex LH-20 column (methanol). Slow elution led to the purification of the product **12** that was isolated in good yield (16.9 mg, 94%). ^{1}H NMR (400 MHz, D_2O): δ (ppm) 4.93 (s, 4H, H_1), 4.27 (bs, 6H, $OCH_2CH_2N_3$, CH_2O_{G1}), 4.18 (bs, 8H, CH_2O_{G2}), 3.91 (bs, 8H, D_2, H_2), 3.78 (d, 4H, H_6B, J = 12 Hz), 3.76−3.71 (m, 4H, H_3), 3.69−3.59 (m, 8H, H_{6A}, H_{D1}), 3.63 (s, 24H, OCH_3), 3.59−3.49 (m, 18H, H_4, H_5, H_7, CH_2N_3), 3.30 (bt, 8H, H_8), 2.91−2.72 (m, 8H, H_{D4}, H_{D5}), 2.65−2.56 (m, 8H, CH_2COO), 2.54−2.45 (m, 8H, CH_2CONH), 2.10−1.99 (m, 8H, H_{D6eq}, H_{D3eq}), 1.81−1.64 (m, 8H, H_{D6ax}, H_{D3ax}), 1.26 (s, 3H, $CH_{3G1'}$), 1.19 (s, 6H, CH_{3G2}); ^{13}C NMR (100 MHz, D_2O): 177.4, 177.2, 174.1, 174.0, 173.8, 173.7 ($COOCH_3$, $COOCH_2$, CONH), 98.6 (C_{1M}), 73.8 (C_{D1}), 73.5 (C_{4M}), 71.0, 70.5 (C_{D2}, C_{2M}, C_{3M}), 66.9 (C_7), 66.8 (C_{5M}), 65.9 (OCH_{2G1}, OCH_{2G2}), 64.8 ($OCH_2CH_2N_3$), 61.0 (C_{6M}); 52.6 (CH_3O); 49.4 (CH_2N_3); 46.6, 46.4 ($C_{quat\ G1,\ G2}$); 39.4 (C_8); 39.0 (C_{D4}, C_{D5}); 30.1 (CH_2CONH); 29.3 (CH_2COO); 27.0, 26.7 (C_{D6}, C_{D3}); 16.9 ($CH_{3G1,G2}$); ESI-MS calcd for $[C_{105}H_{161}N_7O_{62}Na_2]^{+2}$ 1279.7, found: 1279.2; MALDI-ToF MS (matrix DHB) $[C_{105}H_{161}N_7O_{62}Na]^+$ calcd: 2536.4, found: 2537.2.

Production of Recombinant Viruses. Recombinant viruses were produced in 293 T cells. The viral construction was pseudotyped with Ebola virus envelope glycoprotein (EboGP) and

Scheme 1. Synthesis of Compound G3(suc)$_{32}$ from Pentaerythritol

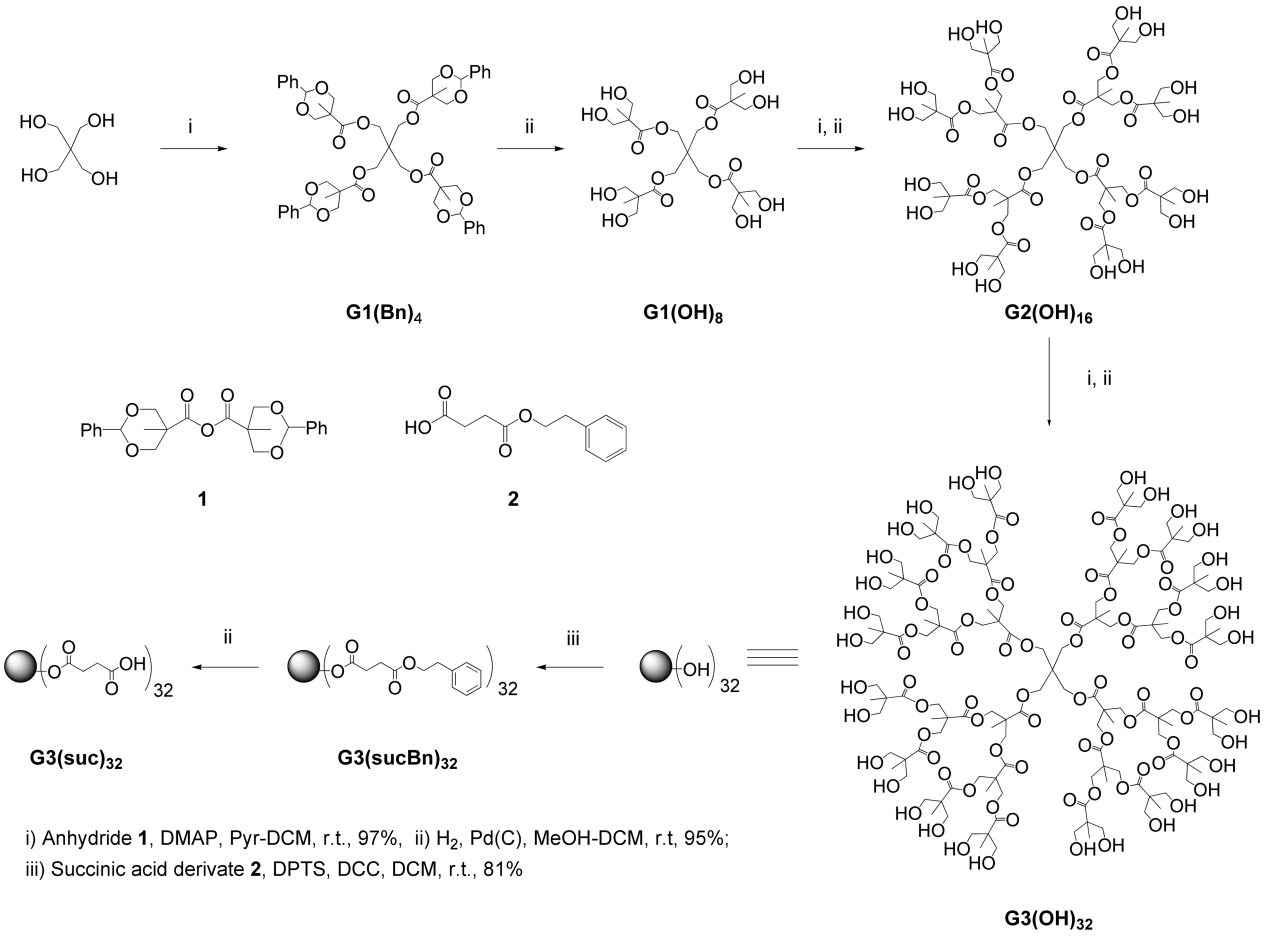

expressed luciferase as a reporter of the infection. The infection of Jurkat cells (a CD+ T-lymphocyte cell line) by EboGP is absolutely dependent on virus envelope interaction with DC-SIGN. As a control of DC-SIGN independent infection, we produced recombinant viruses pseudotyped with vesicular stomatitis virus envelope glycoprotein (VSV-G).

One day (18−24 h) before transfection, 6×10^6 293 T cells were seeded onto 10 cm plates. Cells were cultured in DMEM medium supplemented with 10% heat-inactivated FBS, 25 mg Gentamicin, and 2 mM L-glutamine. Few minutes before transfection, the medium on transfection plates was changed to 9 mL DMEM and 25 μM chloroquine. Transfection reaction with all reagents at room temperature (r.t.) was prepared in 15 mL tubes: 183 μL of 2 M $CaCl_2$, 450 ng of Ebola virus envelope, 21 μg of pNL4−3 luc, and 1200 μL of H_2O. Next, 1.5 mL of 2×HBS (Hepes Buffer Saline) pH 7.00 was added quickly to the tubes and bubbled for 30 s. HBS/DNA solution was dropwise added onto medium. After 8 h of incubation at 37 °C with 5% CO_2, medium on transfection plates was changed to 10 mL DMEM and once again one day after transfection to 7 mL DMEM. Transfection supernatants were harvested after 48 h, centrifuged at 1200 rpm for 10 min at r.t. to remove cell debris, and stored frozen at −80 °C.

Infection Assay. *Infection in cis.* Infection was performed on Jurkat cells expressing DC-SIGN. Since Ebola virus does not infect T-lymphocytes, its entry into Jurkat cells is absolutely dependent on the interaction with DC-SIGN.[30]

DC-SIGN$^+$ Jurkat cells (2.5×10^5) were incubated with carbohydrate multivalent compounds on 24-well suspension plates for 30 min at r.t. and then challenged with 10 000 tissue culture infective dose (TCID) of recombinant viruses. After 48 h of incubation, cells were washed twice with PBS and lysed with 100 μL of 1× Lysis Buffer for luciferase assay (Promega).

Infection control experiment was performed with VSV-G pseudoviruses under the same conditions.

Infection in trans. DC-SIGN$^+$ Jurkat cells (2.5×10^5) were preincubated for 20 min at r.t. with carbohydrate multivalent compounds. Then, they were challenged with 10 000 TCID of recombinant viruses and incubated for 2 h at r.t. with rotation. After 2 h, cells were centrifuged at 1000 rpm for 5 min and washed twice with 1 mL of PBS supplemented with 0.5% bovine serum albumin (BSA) and 1 mM $CaCl_2$. DC-SIGN$^+$ Jurkat cells were resuspended in 500 μL of RPMI medium and co-cultivated with adherent HeLa cells (10^5 cells/well) on 24-well plate. After 48 h, supernatant was removed and monolayer of HeLa was washed twice with 1 mL of PBS and lysed with 100 μL of 1× Lysis Buffer for luciferase assay.

As control experiment, *trans*-infection test with VSV-G pseudoviruses was performed.

Surface Plasmon Resonance. Extracellular domain (ECD) of DC-SIGN protein (residue 66−404) has been overexpressed and purified as described previously.[31] All experiments were performed on a Biacore 3000 using functionalized CM4 sensor chips and the corresponding reagents from BIAcore. Two flow

Scheme 2. Synthesis of Tetravalent Compounds 12 and 14

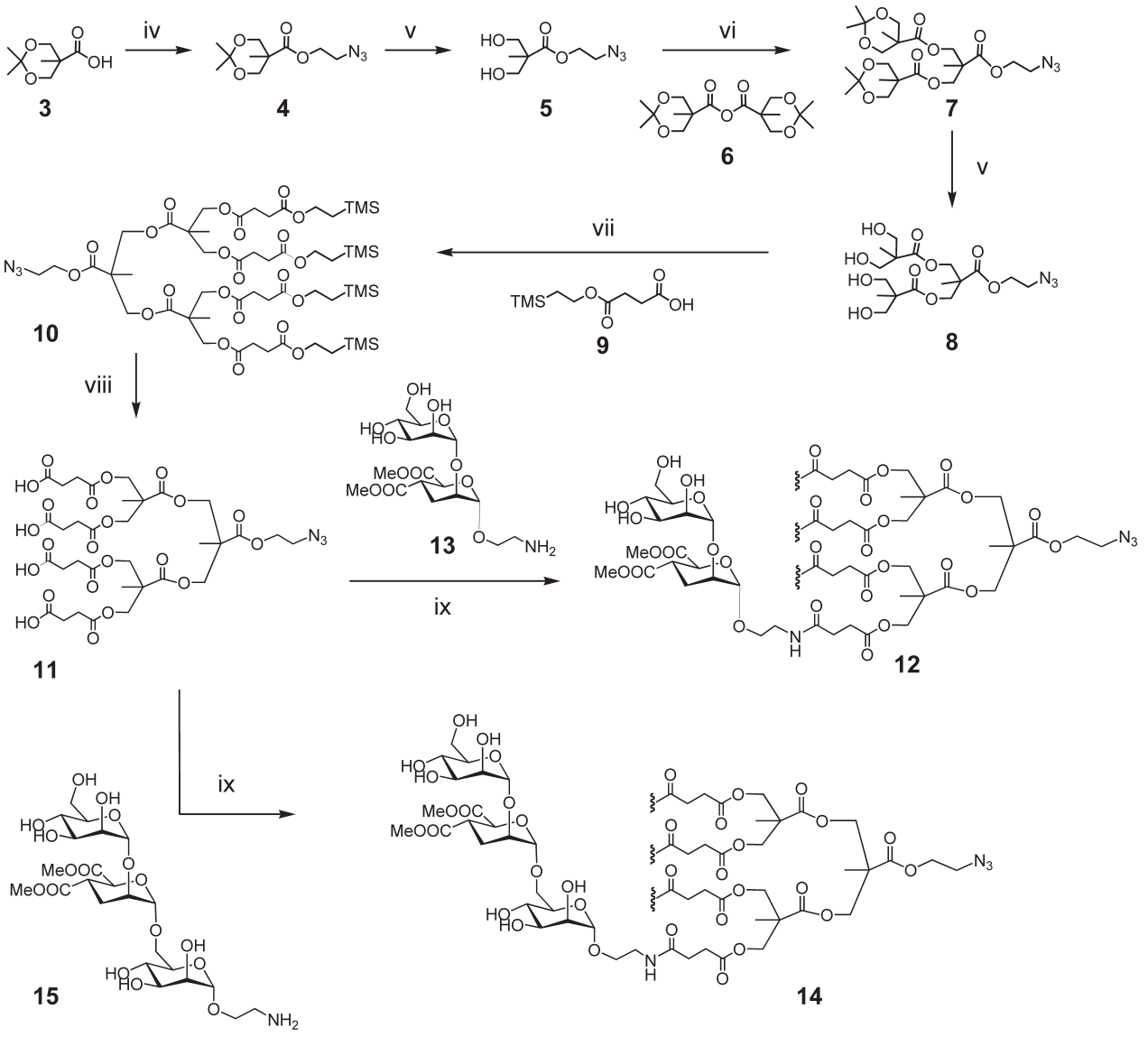

iv) a) 2-bromoethanol, DMAP, DCM, r.t.; b) NaN_3, DMF, 86%; v) Dowex, H+ resin, MeOH, r.t., 98%; vi) DMAP, Anhydride **6**, DCM, r.t., 73%, vii) Acid **9,** DPTS, DCC, DCM, 40ºC, 81%; viii) TFA, DCM, r.t., quant.; ix) pseudomannobioside **13** or pseudomannotrioside **15**, HATU, DIPEA, DMA, r.t., 94%

cells were activated as previously described.[32] Flow cell one was then blocked with 30 μL of 1 M ethanolamine and used as a control surface. The second one was treated with BSA-Manα1−3[Manα1−6]Man (BSA-Mannotriose, Dextra) (60 μg/mL) in 10 mM acetate buffer, pH 4. Remaining activated groups were blocked with 30 μL of 1 M ethanolamine. The final density immobilized on the surface of the second flow cell was 1200 RU. The BSA-Mannotriose used to functionalize CM4 chip harbors 12 glycosylation sites according to manufacturer. The affinity of the various sugars and mimics was then estimated through a DC-SIGN ECD binding inhibition assay. The ECD of DC-SIGN was injected onto the BSA-Mannotriose surface, at 20 μM alone or in presence of an increasing concentration of the sugar derivatives. Injections were performed at 20 μL/min using 25 mM Tris-HCl, pH 8, 150 mM NaCl, 4 mM $CaCl_2$, and 0.005% of P20 surfactant as running buffer. The original sensorgrams are reported as Supporting Information.

To determine IC_{50} values for sugar derivatives, the steady state binding responses of DC-SIGN ECD to BSA-Mannotriose surface were obtained from sensorgrams and converted to relative residual activity values. Relative IC_{50} values were determined from the plots of sugar derivative concentration vs relative residual DC-SIGN ECD activity by fitting four-parameter logistic model (see eq 1 in SI) to the experimental data.

RESULTS

In previous works, we have demonstrated that the commercially available and very cheap third generation of a Boltorn

dx.doi.org/10.1021/bc2000403 |*Bioconjugate Chem.* 2011, 22, 1354–1365

Scheme 3. Coupling of Glycomimetics 13 and 15 on G3(suc)$_{32}$

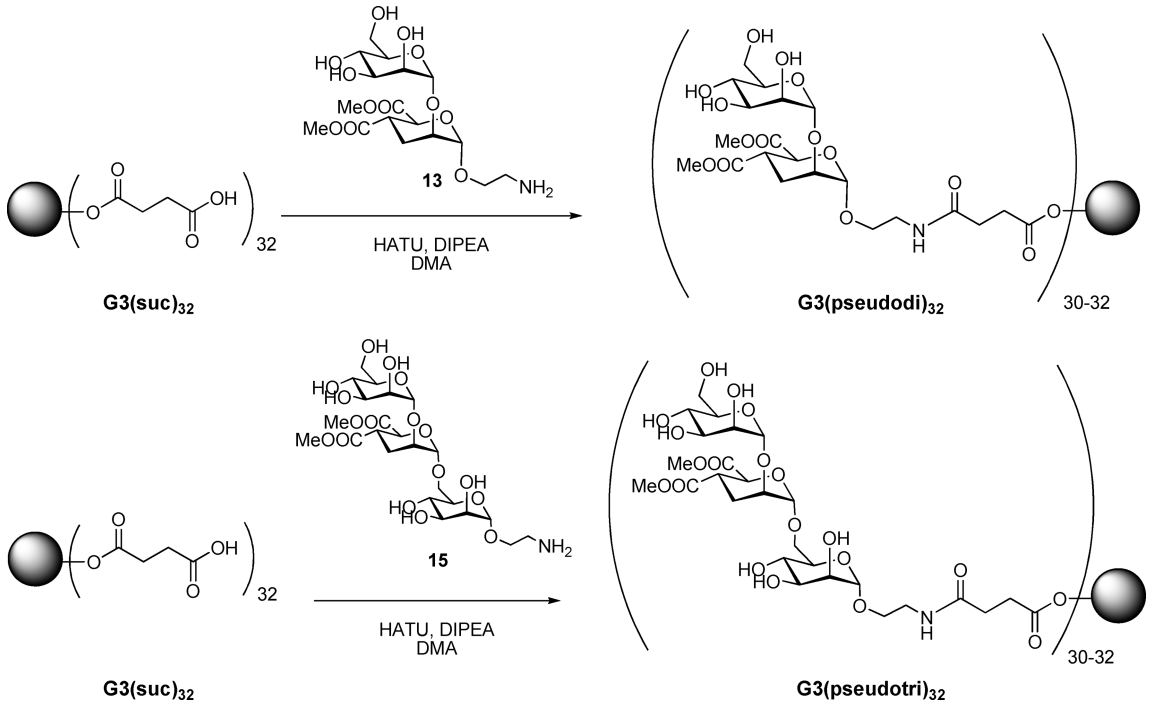

dendritic polymer was a very convenient platform for a multivalent presentation of carbohydrates.[19] This polydisperse dendritic polymer, bearing 32 copies of mannose, exhibited a high antiviral activity (IC_{50} = 0.3 μM) in an Ebola infection model.[20] The polydispersity of the commercial Boltorn scaffold is a major drawback of this strategy. On the basis of these preliminary results, we decided to prepare a Boltorn-type polyester dendrimer in a completely monodisperse manner. To approach this synthesis, we used a divergent strategy based on the anhydride **1** as a building block monomer and pentaerythritol as a central core, a strategy previously used to prepare polyester dendrons.[26] A sequential set of two reactions was employed as described in Scheme 1. A coupling reaction with anhydride **1** to grow to the next generation, followed by hydrogenolysis using palladium on carbon as catalyst to remove the benzylidene protecting groups, yielded the first (G1(OH)$_8$), second (G2(OH)$_{16}$), and third (G3(OH)$_{32}$) generations of the polyester dendrimers in a very efficient way and with complete monodispersity, as shown by mass spectrometry. These dendrimers were prepared in multigram-scale and purified by recrystallization in a very straightforward way.

Carboxylic acids were introduced as functional groups at the surface of the third-generation dendrimer G3(OH)$_{32}$ to allow coupling with conveniently functionalized ligands by the formation of amide bonds. In contrast to our previous experience, where the carboxylic acids were introduced by reaction of G3(OH)$_{32}$ with a large excess of succinic anhydride, succinic acid monobenzyl ester and DCC were used for the coupling reaction (Scheme 1). Using this strategy, the resulting compound G3(sucBn)$_{32}$ was soluble in organic solvents and very easy to purify by flash chromatography on silica gel. Again, a complete analysis of the compound, especially by MS, confirmed the monodispersity of the molecule. After a simple step of benzyl ester deprotection by hydrogenolysis at atmospheric pressure using Pd(C) (10%) at room temperature, the dendrimer G3(suc)$_{32}$ with 32 carboxylic acids was obtained almost quantitatively.

To evaluate the importance of the valency, a tetravalent system also based on 2,2′-bis(hydroxymethyl) propionic acid (bis-MPA) (Scheme 2) was considered as a scaffold for presentation of four copies of selected ligands.

Starting from the isopropylidene-2,2-bis(methoxy)propionic acid (**3**) prepared as reported in the literature[28] and following the experimental procedure described in Scheme 2, we obtained **4** in good yields with adequate functionalization. As a protecting group of the carboxylic acid, the azidoethanol was used. This terminal azide has been used in our laboratory in a convergent strategy to create higher valency compounds applying a click chemistry Cu catalyzed cycloaddition (unpublished results). Compound **4** was prepared in good yields by reaction of **3** with 2-bromoethanol in the presence of DCC and 4-(dimethylamino)pyridinum 4-toluenesulfonate (DPTS) followed by treatment with sodium azide in DMF at 40 °C. After deprotection of the hydroxyl groups using an acidic resin in methanol, the tetraol **8** was prepared using a two-step synthetic sequence reported in the literature to prepare similar polyester dendrons.[28,29,33] This synthetic sequence begun coupling **5** with 2 equiv of anhydride **6** which, in turn, was prepared in one step from acid **3** using DCC,[29] in pyridine and dimethylaminopyridine as catalyst. The second step was the deprotection of the isopropylidene acetals of **7** using Dowex H+. Tetraol **8** was obtained in good yield after chromatographic purification. The introduction of the carboxylic acid linkers on **8** was performed using the trimethylsilylethanol monosuccinate **9** prepared by ring-opening of succinic anhydride by trimethylsilylethanol as described in the literature.[34] In this way, the silyl protected compound was prepared in good yields and easily purified. After deprotection using trifluoroacetic acid at room temperature, the tetraacid **11** was obtained in very good yield and was used in the next step without any further purification.

Our previous studies have demonstrated that compounds **13** and **15**, linear glycomimetics of the disaccharide Manα1,2Man and of the trisaccharide Manα1,2Manα1,6Man, respectively, were

dx.doi.org/10.1021/bc2000403 |*Bioconjugate Chem.* 2011, 22, 1354–1365

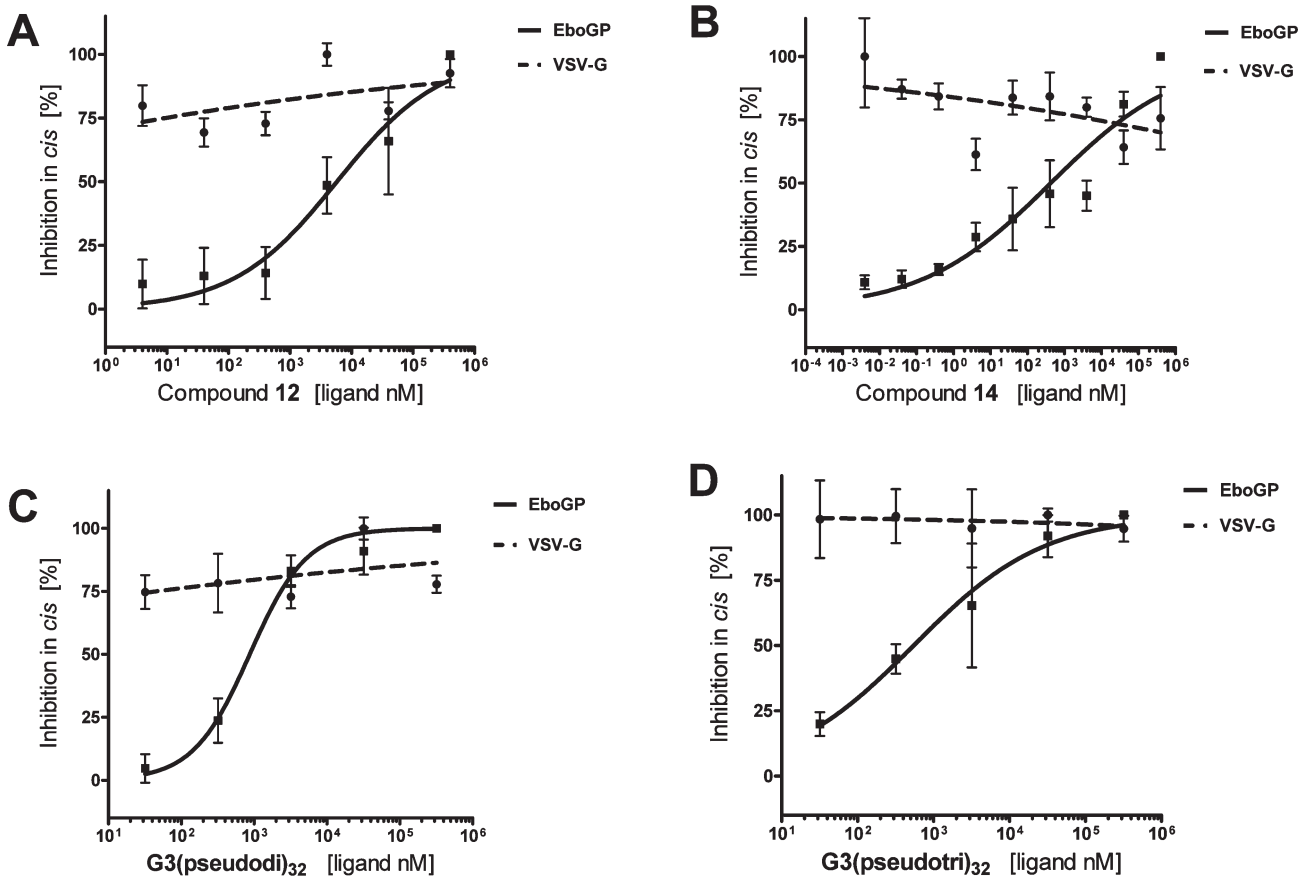

Figure 1. Infection results of the *cis*-experiments using **12**, **14**, G3(pseudodi)$_{32}$, and G3(pseudotri)$_{32}$ compounds as inhibitors. Concentrations are expressed based on ligand concentration.

very adequate ligands for DC-SIGN providing better stability against enzymatic degradation than the corresponding natural counterparts. The synthesis of these glycomimetics has been previously described.[22,23]

Conjugation of **13** and **15** on the tetra- and multivalent scaffolds was performed using HATU as an activating reagent in the presence of DIPEA at room temperature and afforded the corresponding multivalent systems with high yields after purification by size exclusion chromatography as described in Schemes 2 and 3.

The tetravalent compounds were fully characterized by NMR, IR, and MS analysis. MALDI-MS of the compounds G3(pseudodi)$_{32}$ and G3(pseudotri)$_{32}$ using sinapinic acid (SA) as matrix allowed to observe a complex signal centered on the molecular weight corresponding to the 31-loaded dendrimer both for pseudodi- and pseudotrimultivalent systems (see SI for MS spectra). This is consistent with the number of 30−32 ligands which could be estimated based on the integration of significant signals in the ^{1}H NMR spectrum (see SI). Although the MS spectra were not conclusive, we concluded that almost all the reactive sites of the scaffold were conjugated with ligands to obtain a high load narrowly disperse system.

Infection Studies. The antiviral activity of these tetra- and multivalent systems was tested using pseudotyped viral particles presenting the EboGP and Jurkat cell line expressing DC-SIGN on the surface. Two kinds of experiments were set up: a *cis*-infection assay of DC-SIGN+ Jurkat cells with this artificial Ebola virus, and a *trans*-infection experiment of HeLa cells using DC-SIGN+ Jurkat cells as viral particle transporters.

We have used these infection models previously to test the activity of mannosylated Boltorn-type hyperbranched dendritic polymers.[20] The DC-SIGN blocking efficiency has been evaluated as dependence of multivalency and of the different pseudomannoside ligands used in the compounds synthesized. The infection inhibition analysis has been done as a function of compound concentration. All compounds were used in at least 3 independent experiments. The results of the infection assays are represented as a percentage of infection inhibition compared with DC-SIGN+ Jurkat cells infected by pseudoviruses without addition of any compound (blank experiment). The IC_{50} values were calculated with the 95% confidence intervals. Control experiment with VSV-G pseudoviruses was performed with final concentrations of 10 nM and 10 μM (negative control).

The results obtained in the *cis* infection experiments indicate that the tetravalent systems presenting four copies of the pseudomannotrioside, **14**, show an IC_{50} 1 order of magnitude lower than the system with four pseudomannobiosides, **12** (Figure 1). In a previous publication, we have shown that the tetravalent system **14** bearing four copies of linear pseudomannotrioside **15** was an effective inhibitor of T-cell *trans* infection by HIV.[23]

Multivalent systems with an average of 30−32 copies of glycomimetic ligands were tested. In this case, no significant differences were found as a function of the pseudosaccharide presented. The IC_{50} values found for the multivalent systems were around 20 nM (around 0.5 μM, based on ligand concentration), which shows that their inhibitory potency is between

dx.doi.org/10.1021/bc2000403 |*Bioconjugate Chem.* 2011, 22, 1354–1365

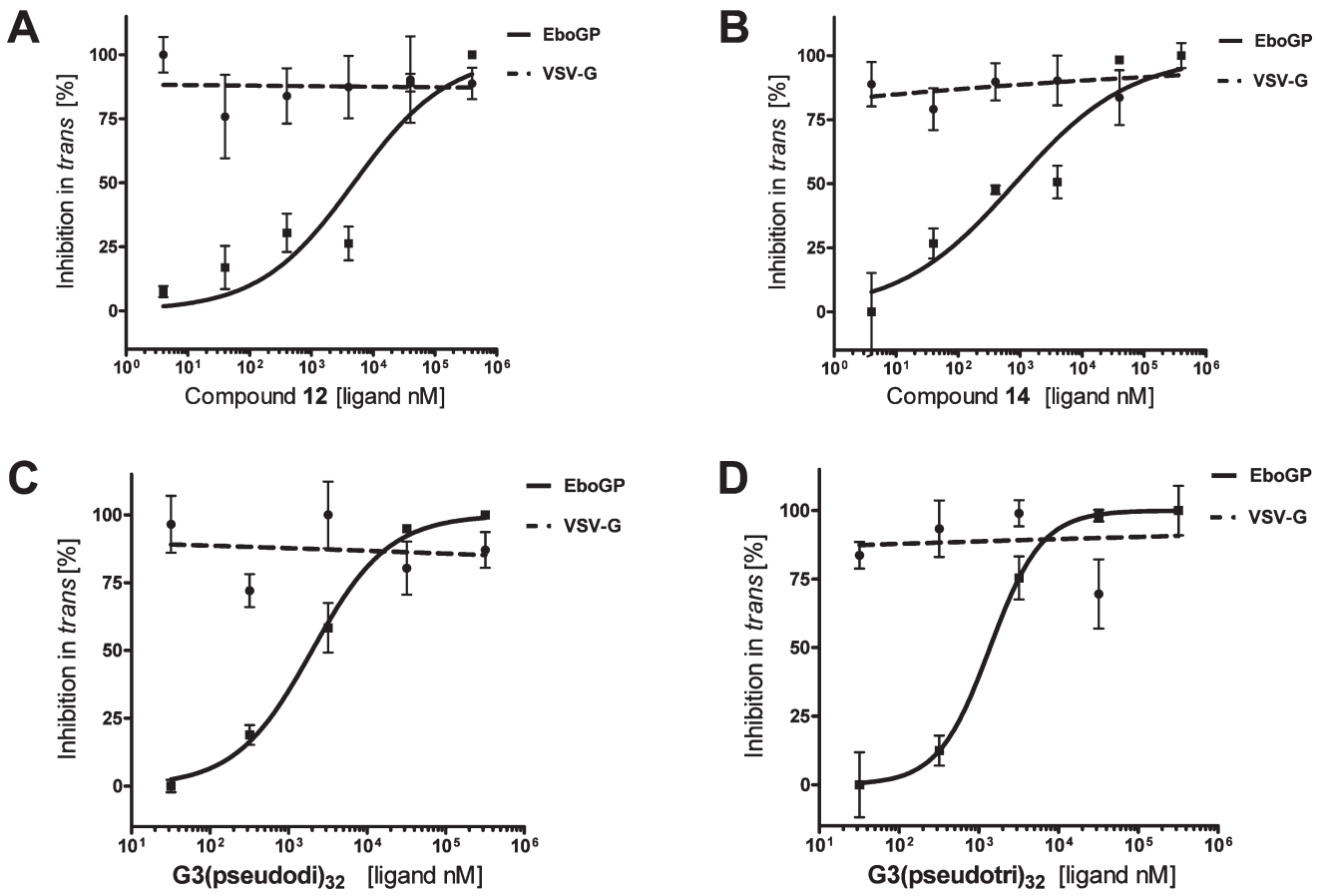

Figure 2. Infection results of the *trans* experiments using **12**, **14**, G3(pseudodi)$_{32}$, and G3(pseudotri)$_{32}$ compounds as inhibitors. Concentrations are expressed based on ligand concentration.

1 to 2 orders of magnitude higher than that of the corresponding tetravalent systems.

Similar results were obtained in the *trans* infection experiments (Figure 2). The IC_{50} of 32-valent systems bearing pseudomannobioside **13** or pseudomannotrioside **15** were 62 nM and 31.5 nM, respectively (2 and 1 μM, based on ligand concentration, respectively). The tetravalent dendron **14** with four copies of pseudomannotrioside showed an IC_{50} of 203 nM (0.8 μM, based on ligand concentration), and the tetravalent dendron **12** with four copies of pseudomannobioside was 1 order of magnitude less potent with an IC_{50} of 1.22 μM (4.9 μM, based on ligand concentration) (Figure 2).

SPR Studies. Competition experiments using Biacore SPR were performed to analyze the interaction of these glycomimetic tetra- and multivalent systems with the receptor DC-SIGN and to characterize the interaction at the molecular level.

For this aim, Biacore CM4 sensor chip was functionalized as described in the experimental section with BSA-Mannotriose. A fixed amount of DC-SIGN ECD was injected over the sensor chip flow cells in the presence or absence of different concentrations of the glycodendritic compounds to be evaluated. Analysis of the sensorgrams (see Supporting Information) allowed estimating IC_{50} for the monovalent, tetravalent, and multivalent compounds. At the monovalent level, strong differences were found (almost 1 order of magnitude) between the IC_{50} of monovalent pseudodi- and pseudotrisaccharides (IC_{50} 1.19 mM for the pseudodisaccharide **13** and 0.16 mM for the pseudotrisaccharide **15**). However, these differences decrease notably when the ligands are presented on the tetravalent scaffold (IC_{50} 227 μM for the tetravalent pseudodi **12** and 120 μM for the tetravalent pseudotri **14**) and are very similar when a dendrimer of third generation is used as multivalent platform (IC_{50} 2 μM for the multivalent pseudodi G3(pseudodi)$_{32}$ and 1.25 μM for the multivalent pseudotri G3(pseudotri)$_{32}$. (Figure 3)

These data show that tetravalent presentation of the pseudodisaccharide **13** on dendron **12** affords a very modest (1.3 per pseudosugar), if any, polyvalency effect (β), which improves significantly (18 per pseudosugar) in the full dendrimer G3-(pseudodi)$_{32}$. Strikingly, the tetravalent presentation of the pseudotrisaccharide **15** on dendron **14** does not afford any affinity increase (β = 0.3 per pseudosugar) and only a modest improvement (4 per pseudosugar) is observed for the full dendrimer G3(pseudotri)$_{32}$.

DISCUSSION

DC-SIGN is considered a very interesting therapeutic target for the design of new antiviral drugs. In addition, the ability of DC-SIGN to trigger signaling pathways that lead to a specific immune response has attracted attention on this lectin.[35−42] The development of specific tools to interact with and to understand the role and function of this lectin is of great interest. Furthermore, specific ligands designed to block the carbohydrate recognition domain of this lectin could be good candidates to be tested as antimicrobial agents.

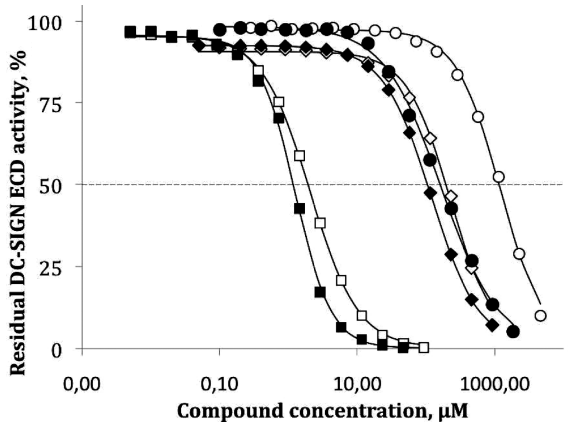

Figure 3. Inhibition of DC-SIGN ECD interaction with BSA-Mannotriose surface. DC-SIGN ECD (20 μM) was incubated with pseudomannobioside and pseudomannotrioside compounds at increasing concentrations: from 0 to 5000 μM and to 2000 μM for monovalent pseudomannobioside and pseudomannotrioside, respectively, from 0 to 1000 μM for compounds **12** and **14**, and from 0 to 100 μM for G3(pseudodi)$_{32}$, and G3(pseudotri)$_{32}$. The samples were coinjected over BSA-Mannotriose surface (1200 RU functionalization level). The steady state responses were extracted from the sensorgrams (see Supporting Information), converted to DC-SIGN ECD residual activity, and plotted against corresponding compound concentration. ○,● – monovalent, ◊,♦ – tetravalent, and □,■ – multivalent compounds; the empty and filled symbols represent pseudomannobioside and pseudomannotrioside compounds, respectively.

In this context, we have selected two linear pseudosaccharides **13** and **15** with good affinity for this receptor. The affinity has been remarkably enhanced *via* a multivalent presentation of these ligands. Tetra- and multivalent scaffolds based on bis-MPA as building block have been prepared with adequate functionalization on the surface for attachment of the selected ligands. The corresponding glycoconjugates with 4 and 32 copies of these ligands were prepared in good yields and were characterized using typical spectroscopic methods. MS analysis demonstrated the monodispersity of the tetravalent systems (compounds **12** and **14**). Higher valency systems obtained from monodisperse G3 Boltorn-type dendrimer G3(OH)$_{32}$ did not give good MS spectra and by analysis of the NMR spectra could only be described as systems with 30−32 ligands as an average loading; therefore, the monodispersity of these systems was not confirmed.

These tetra- and multivalent systems were tested *in vitro* as antiviral compounds in a well-established infection model based on pseudotyped viral particles with the Ebola virus envelope glycoprotein GP1. This infection system is a very efficient and "clean" model where the infection is exclusively dependent on DC-SIGN.[20] Cells that do not express the receptor and viruses able to infect the cells independently of DC-SIGN have been used as controls in these experiments. The results obtained have clearly demonstrated inhibition of the infection through blockage of the DC-SIGN receptor. The tetravalent systems **12** and **14** were very active in the low micromolar range, and the multivalent systems G3(pseudosugar)$_{32}$ showed a very strong inhibition effect with IC$_{50}$ in the nanomolar range. These systems could be considered as very potent inhibitors to be tested in further experiments. On the other hand, relatively small differences were observed between the two selected monovalent ligands the pseudodi **13** and the pseudotrisaccharide **15**.

In order to analyze this in more detail and to have additional molecular-level data on the interaction of these compounds with DC-SIGN, competition experiments using a biosensor with SPR detection were performed. A chip functionalized with mannosylated BSA was used to compete with our ligands for DC-SIGN. Analysis of the results obtained in these competition experiments demonstrates that the pseudosugars are good ligands for DC-SIGN, and that the pseudotrisaccharide **15** is 1 order of magnitude better than the pseudodisaccharide **13** when used as monovalent units. Surprisingly, this trend was not observed when the ligands are used in multivalent presentations: they both present a similar affinity when are exposed on the multivalent scaffolds. A plausible explanation for these facts could be the loss of different binding modes of the ligands when they are linked to a scaffold. In the particular case of DC-SIGN, it has been experimentally determined by X-ray[43] and also by NMR[44] that different binding modes are possible for carbohydrate ligands. These binding modes were observed for free ligands, but once they are conjugated to scaffolds, some or all of these alternative binding modes could become inaccessible; consequently, this could notably influence binding affinity. As a consequence, despite the improved affinity of the pseudomannotrioside at the monovalent level, our data suggest that the pseudomannobioside is the effective lead compound to use for further improvement of our multivalent pseudosaccharide compounds.

More structural experiments are currently being carried out in our laboratory at the monovalent level to obtain more detailed information and to investigate the factors that govern this phenomenon.

In summary, we present in this work the preparation of carbohydrate mimics on a tetra- and multivalent presentations and the analysis of their antiviral activity using a pseudotyped Ebola virus infection model. A strong inhibitory activity was found for the higher valency compounds with IC$_{50}$ in the nanomolar range. Competition experiments using SPR have also demonstrated the ability of these compounds to interact with DC-SIGN and compete for this receptor. Our results confirm pseudoglycosylated multivalent systems as very promising antiviral drugs with strong activities and encourage us to pursue more *in vitro* and *in vivo* studies concerning the potential biomedical applications.

■ ASSOCIATED CONTENT

Supporting Information. Additional information as described in the text. This material is available free of charge via the Internet at http://pubs.acs.org.

■ AUTHOR INFORMATION

Corresponding Author

*E-mail: franck.fieschi@ibs.fr (F.F); rdelgado.hdoc@salud.madrid.org (R.D.); anna.bernardi@unimi.it (A.B.); javier.rojo@iiq.csic.es (J.R.).

■ ACKNOWLEDGMENT

We would like to acknowledge the financial support by the MICINN of Spain CTQ2008-01694, the EU RTN CARMUSYS (PITN-GA-2008-213592), Comune di Milano (Convenzione 55/2008), Sidaction – Ensemble contre le Sida, Fundación Mutua Madrileña (FMM2007-700) and the European FEDER funds. The

expression plasmid for the glycoprotein of the Zaire strain of Ebola virus was kindly provided by Dr. A. Sanchez, Centers for Disease Control and Prevention, Atlanta, GA.

REFERENCES

(1) Varki, A. (1993) Biological roles of oligosaccharides: all of the theories are correct. *Glycobiology 2*, 97–130.

(2) Lundquist, J. J., and Toone, E. J. (2002) The cluster glycoside effect. *Chem. Rev. 102*, 555–578.

(3) Lee, R. T., and Lee, Y. C. (2000) Affinity enhacement by multivalent lectin-carbohydrate interaction. *Glycoconj. J. 17*, 543–551.

(4) Mammen, M., Choi, S.-K., and Whitesides, G. M. (1998) Polyvalent interactions in biological systems: implications for design and use of multivalent ligands and inhibitors. *Angew. Chem., Int. Ed. 37*, 2754–2794.

(5) Lee, Y. C., and Lee, R. T. (1995) Carbohydrate-protein interactions: basis of glycobiology. *Acc. Chem. Res. 28*, 321–327.

(6) Chabre, Y. M., and Roy, R. (2010) Designs and creativity in synthesis of multivalent neoglycoconjugates. *Adv. Carb. Chem. Biochem. 63*, 168–393.

(7) Lahmann, M. (2009) Architectures of multivalent glycomimetics for probing carbohydrate-lectin interactions. *Top. Curr. Chem. 288*, 17–65.

(8) Curtis, B. M., Scharnowske, S., and Watson, A. J. (1992) Sequence and expression of a membrane-associated C-type lectin that exhibits CD4-independent binding of human immunodeficiency virus envelope glycoprotein gp120. *Proc. Natl. Acad. Sci. U.S.A. 89*, 8356–8360.

(9) Geijtenbeek, T. B. H., Kwon, D. S., Torensma, R., Van Vliet, S. J., Van Duijnhoven, G. C. F., Middel, J., Cornelissen, I. L. M. H. A., Nottet, H. S. L. M., KewalRamani, V. N., Littman, D. R., Figdor, C. G., and Van Kooyk, Y. (2000) DC-SIGN, a dendritic cell-specific HIV-1-binding protein that enhances *trans*-infection of T Cells. *Cell 100*, 587–597.

(10) Geijtenbeek, T. B. H., Torensma, R., Van Vliet, S. J., Van Duijnhoven, G. C. F., Adema, G. J., Van Kooyk, Y., and Figdor, C. G. (2000) Identification of DC-SIGN, a novel dendritic cell−specific ICAM-3 receptor that supports primary immune responses. *Cell 100*, 575–585.

(11) Feinberg, H., Mitchell, D. A., Drickamer, K., and Weis, W. (2001) Structural basis for selective recognition of oligosaccharides by DC-SIGN and DC-SIGNR. *Science 294*, 2163–2166.

(12) Mitchell, D. A., Fadden, A. J., and Drickamer, K. (2001) A novel mechanism of carbohydrate recognition by the C-type lectins DC-SIGN and DC-SIGNR. *J. Biol. Chem. 276*, 28939–28945.

(13) van Kooyk, Y., Geijtenbeek, T. B. H. (2003) DC-SIGN: escape mechanism for pathogens. *Nat. Rev. Immunol. 3*, 697−709.

(14) Geijtenbeek, T. B. H., and van Kooyk, Y. (2003) Pathogens target DC-SIGN to influence their fate DC-SIGN functions as a pathogen receptor with broad specificity. *APMIS 111*, 698–714.

(15) Rojo, J., and Delgado, R. (2004) Glycodendritic structures: promising new antiviral drugs. *J. Antimicrob. Chemother. 54*, 579–581.

(16) Borrok, M. J., and Kiessling, L. L. (2007) Non-carbohydrate inhibitors of the lectin DC-SIGN. *J. Am. Chem. Soc. 129*, 12780–12785.

(17) Becer, C. R., Gibson, M. I., Geng, J., Ilyas, R., Wallis, R., Mitchell, D. A., and Haddleton, D. M. (2010) High-affinity glycopolymer binding to human DC-SIGN and disruption of DC-SIGN interactions with HIV envelope glycoprotein. *J. Am. Chem. Soc. 132*, 15130–15132.

(18) Sánchez-Navarro, M., and Rojo, J. (2010) Targeting DC-SIGN with multivalent systems. *Drug News and Perspectives 23*, 557–572.

(19) Arce, E., Nieto, P. M., Díaz, V., Castro, R. G., Bernad, A., and Rojo, J. (2003) Glycodendritic structures based on Boltorn hyperbranched polymers and their interactions with Lens Culinaris lectin. *Bioconjugate Chem. 14*, 817–823.

(20) Lasala, F., Arce, E., Otero, J. R., Rojo, J., and Delgado, R. (2003) Mannosyl glycodendritic structure inhibits DC-SIGN-mediated Ebola virus infection in cis and in trans. *Antimicrob. Agents Chemother. 47*, 3970–3972.

(21) Rojo, J., and Delgado, R. (2007) Dendrimers and dendritic polymers as anti-infective agents: new antimicrobial strategies for therapeutic drugs. *Anti-infect. Agents Med. Chem. 6*, 151–174.

(22) Reina, J. J., Sattin, S., Invernizzi, D., Mari, S., Martinez-Prats, L., Tabarani, G., Fieschi, F., Delgado, R., Nieto, P. M., Rojo, J., and Bernardi, A. (2007) 1,2-Mannobioside mimic: synthesis, DC-SIGN interaction by NMR and docking, and antiviral activity. *ChemMedChem 2*, 1030–1036.

(23) Sattin, S., Daghetti, A., Thépaut, M., Berzi, A., Sánchez-Navarro, M., Tabarani, G., Rojo, J., Fieschi, F., Clerici, M., and Bernardi, A. (2010) Inhibition of DC-SIGN-mediated HIV infection by a linear trimannoside mimic in a tetravalent presentation. *ACS Chem. Biol. 3*, 301–312.

(24) Annby, U., Malmberg, M., Pettersson, B., and Rehnberg, N. (1998) Benzylidene protected Bis-MPA A convenient dendrimer building block. *Tetrahedron Lett. 39*, 3217–3220.

(25) Goodwin, A. P., Lam, S. S., and Fréchet, J. M. J (2007) Rapid, efficient synthesis of heterobifunctional biodegradable dendrimers. *J. Am. Chem. Soc. 129*, 6994–6995.

(26) Ihre, H., Padilla de Jesús, O. L., and Fréchet, J. M. J. (2001) Fast and convenient divergent synthesis of aliphatic ester dendrimers by anhydride coupling. *J. Am. Chem. Soc. 123*, 5908–5917.

(27) Isomura, S., Wirsching, P., and Janda, K. D. (2001) An immunotherapeutic program for the treatment of nicotine addiction: hapten design and synthesis. *J. Org. Chem. 66*, 4115–4121.

(28) Ihre, H, Hult, A., Fréchet, J. M. J., and Gitsov, I. (1998) Double-stage convergent approach for the synthesis of functionalized dendritic aliphatic polyesters based on 2,2-Bis(hydroxymethyl)propionic acid. *Macromolecules 31*, 4061–4068.

(29) Malkoch, M., Malmström, E., and Hult, A. (2002) Rapid and efficient synthesis of aliphatic ester dendrons and dendrimers. *Macromolecules 35*, 8307–8314.

(30) Alvarez, C. P., Lasala, F., Carrillo, J., Muñiz, O., Corbí, A. L., and Delgado, R. (2002) C-Type lectins DC-SIGN and L-SIGN mediate cellular entry by ebola virus in *cis* and in *trans*. *J. Virol. 76*, 6841–6844.

(31) Tabarani, G., Thepaut, M., Stroebel, D., Ebel, C., Vives, C., Vachette, P., Durand, D., and Fieschi, F. (2009) DC-SIGN neck domain is a pH-sensor controlling oligomerization: SAXS and hydrodynamic studies of extracellular domain. *J. Biol. Chem. 284*, 21229–21240.

(32) Halary, F., Amara, A., Lortat-Jacob, H., Messerie, M., Delaunay, T., Houlès, C., Fieschi, F., Arenzana-Seisdedos, F., Moreaus, J.-F., and Déchanet-Merville, J. (2002) Human cytomegalovirus binding to DC-SIGN is required for dendritic cell infection and target cell *trans*-infection. *Immunity 17*, 653–664.

(33) Yim, S.-H., Huh, J., Ahn, C.-H., and Park, T. G. (2007) Development of a novel synthetic method for aliphatic ester dendrimers. *Macromolecules 40*, 205–210.

(34) Anderson, G. T., Alexander, M. D., Taylor, S. D., Smithrud, D. B., Benkovic, S. J., and Weinreb, S. M. (1996) Catalytic antibodies in synthesis: design and synthesis of a hapten for application to the preparation of a scalemic pyrrolidine ring synthon for Ptilomycalin A. *J. Org. Chem. 61*, 125–132.

(35) Zhou, T., Chen, Y., Hao, L., and Zhang, Y. (2006) DC-SIGN and immunoregulation. *Cell. Mol. Immunol. 3*, 279–283.

(36) Caparrós, E., Muñoz, P., Sierra-Filardi, E., Serrano-Gómez, D., Puig-Kröger, A., Rodríguez-Fernández, J. L., Mellado, M., Sancho, J., Zubiaur, M., and Corbí, A. L. (2006) DC-SIGN ligation on dendritic cells results in ERK and PI3K activation and modulates cytokine production. *Blood 107*, 3950–3958.

(37) Shan, M., Klasse, P. J., Banerjee, K., Dey, A. K., Iver, S. P., Dionisio, R., Charles, D., Campbell-Gardener, L., Olson, W. C., Sanders, R. W., and Moore, J. P. (2007) HIV-1 gp120 mannose induce immunosupresive responses from dendritic cells. *PLoS Pathogens 3*, e169.

(38) van Kooyk, Y. (2008) C-type lectins on dendritic cells: key modulators for the induction of immune responses. *Biochem. Soc. Trans. 36*, 1478–1481.

(39) den Dunnen, J., Gringhuis, S. I., and Geijtenbeek, T. B. H. (2009) Innate signaling by the C-type lectin DC-SIGN dictates immune responses. *Cancer Immunol. Immunother. 58*, 1149–1157.

(40) Geijtenbeek, T. B. H., den Dunnen, J., and Gringhuis, S. I. (2009) Pathogen recognition by DC-SIGN shapes adaptive immunity. *Future Microbiol. 4*, 879–890.

(41) Gringhuis, S. I., den Dunnen, J., Litjens, M., van der Vlist, M., and Geijtenbeek, T. B. H. (2010) Carbohydrate-specific signaling through the DC-SIGN signalosome tailors immunity to Mycobacterium tuberculosis, HIV-1 and Helicobacter pylori. *Nat. Immunol. 10*, 1081–1089.

(42) den Dunnen, J., Gringhuis, S. I., and Geijtenbeek, T. B. H. (2010) Dusting the sugar fingerprint: C-type lectin signaling in adaptive immunity. *Immunol. Lett. 128*, 12–16.

(43) Feinberg, H., Castelli, R., Drickamer, K., Seeberger, P. H., and Weis, W. I. (2007) Multiple modes of binding enhance the affinity of DC-SIGN for high mannose *N*-linked glycans found on viral glycoproteins. *J. Biol. Chem. 282*, 4202–4209.

(44) Angulo, J., Reina, J. J., Tabarani, G., Fieschi, F., Rojo, J., and Nieto., P. M. (2008) Saturation transfer difference (STD) NMR spectroscopy characterization of dual binding mode of a mannose disaccharide to DC-SIGN. *ChemBioChem 9*, 2225–2227.

■ NOTE ADDED AFTER ASAP PUBLICATION

This paper was published on the Web on June 20, 2011 with a production error, the omission of the reagent lists in Schemes 1 and 2. The corrected version was reposted on June 23, 2011.

Article

pubs.acs.org/Biomac

Glycofullerenes Inhibit Viral Infection

Joanna Luczkowiak,[†] Antonio Muñoz,[‡] Macarena Sánchez-Navarro,[§] Renato Ribeiro-Viana,[§] Anthony Ginieis,[§] Beatriz M. Illescas,[‡] Nazario Martín,*[,‡,∥] Rafael Delgado,*[,†] and Javier Rojo*[,§]

[§]Glycosystems Laboratory, Instituto de Investigaciones Químicas (IIQ), CSIC − Universidad de Sevilla, Av. Américo Vespucio 49, Seville 41092 Spain

[†]Laboratorio de Microbiología Molecular, Instituto de Investigación Hospital, 12 de Octubre (imas12), 28041 Madrid, Spain

[‡]Departamento de Química Orgánica, Facultad de Química, Universidad Complutense, 28040 Madrid, Spain

[∥]IMDEA-Nanoscience, Campus Cantoblanco, 28049 Madrid, Spain

Supporting Information

ABSTRACT: Water-soluble glycofullerenes based on a hexakis-adduct of [60]fullerene with an octahedral addition pattern are very attractive compounds providing a spherical presentation of carbohydrates. These tools have been recently described and they have been used to interact with lectins in a multivalent manner. Here, we present the use of these glycofullerenes, including new members with 36 mannoses, as compounds able to inhibit a DC-SIGN-dependent cell infection by pseudotyped viral particles. The results obtained in these experiments demonstrate for the first time that these glycoconjugates are adequate to inhibit efficiently an infection process, and therefore, they can be considered as very promising and interesting tools to interfere in biological events where lectins such as DC-SIGN are involved.

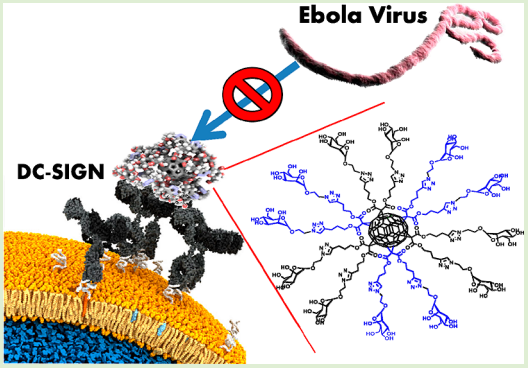

INTRODUCTION

Carbohydrate−protein interactions govern many biological processes including inflammation, embryogenesis, tumor progression and metastasis, pathogen infection, and so on.[1−3] These interactions are characterized by a high selectivity, metal ion dependence, and a low affinity compensated in nature by multivalency.[4,5] The search for adequate systems to achieve a multivalent presentation of sugars is a topic of extensive research.[6−9] The lack of information about the adequate orientation of ligands required to obtain the strongest interaction has induced chemists to try any possible and accessible scaffold. Calixarenes,[10] gold-nanoparticles,[11] polymers,[12] liposomes,[13,14] and dendrimers[15] are among the most studied and frequent structures used for constructing multivalent glycoconjugates.

Since its discovery in 1985,[16] biochemical and biomedical applications of fullerenes, and specially C_{60}, have attracted much attention. Biological properties of fullerenes have been tested in different areas such as DNA photocleavage, neuroprotection, antibacterial and antiviral activity, antioxidation, and drug delivery.[17−22]

Carbohydrate derivatives of fullerenes, glycofullerenes, had been previously studied due to the combination of interesting biological properties.[23−31] However, most of these derivatives showed an amphiphilic character with the fullerene being the lipophilic part of the structures. Recently, we have shown that this amphiphilic character of sugar-fullerene conjugates can be avoided by obtaining hexakis-adducts of [60]fullerene in which the C_{60} sphere is completely surrounded by sugar moieties in a *T*-symmetrical octahedral addition pattern.[32] In fact, some of the advantages of fullerenes in comparison to other carbon nanostructures are related to its 3D structure and the possibility to functionalize different positions of the C_{60} cage in a controlled fashion.[33] In this sense, fullerenes can be considered very attractive spherical scaffolds for a multivalent presentation of ligands in a globular shape.

By employing a Cu(I)-catalyzed azide−alkyne cycloaddition (CuAAC) methodology to click sugar residues to alkyne-substituted Bingel-Hirsch hexakis-adducts, we have obtained glycofullerenes with up to 24 sugar moieties on the periphery of C_{60}.[34] These compounds are water soluble and interact with Concanavalin A in a multivalent manner, demonstrating the accessibility of these sugars on the fullerene surface to be recognized by a lectin. Moreover, the compounds show a good stability and low toxicity which confirm the appropriate features to be used in cellular assays. This kind of fullerene glycoclusters have recently been investigated as inhibitors of various glycosidases,[35] FimH, a bacterial adhesin,[36] PA-IL, a bacterial lectin from *Pseudomonas aeruginosa*,[37] and WaaC, a glycosyltransferase.[38] Many of these enzymes play key roles in the infection processes caused by several pathogens and are, therefore, therapeutic targets for the search for new drugs.

Received: October 30, 2012
Revised: December 21, 2012
Published: January 1, 2013

 © 2013 American Chemical Society

We have proved that dendritic molecules decorated with carbohydrates (mannoses or fucoses) can be considered as good ligands to interact with and block the receptor DC-SIGN.[39−45] DC-SIGN is a C-type lectin able to interact with glycoconjugates present on the surface of several pathogens, including viruses like HIV or Ebola. Due to the important role of this lectin in infection processes, the discovery of new compounds with an adequate affinity for this receptor is of great interest. We have envisaged that the globular presentation of carbohydrates provided by the fullerene as scaffold could afford interesting glycomimetics to achieve this goal. This rigid spherical scaffold permitted reaching a distance between two ligands on this multivalent presentation (at least 1 nm of diameter for the fullerene plus the distance provided by the dendritic moiety), increasing the chances to get an efficient multivalent interaction. Additionally, the 3D presentation of these ligands on 360° could better mimic the surface of pathogens such as HIV having more possibilities for encountering a receptor due to the symmetry of the multivalent system.

In this work, we would like to present the preparation of globular glycofullerenes with higher valency by a convergent strategy combining trimannosylated glycodendrons with a Bingel-Hirsch hexakis-adduct [60]fullerene to obtain glycodendrofullerenes with 36 mannoses and two different spacers. Also, we introduce for the first time the biological activity of these compounds in a cellular infection model providing important information about the potential use of these new glycomimetics as antiviral agents.

MATERIALS AND METHODS

Reagents were purchased from Sigma-Aldrich, Senn Chemicals, and Flucka and were used without purification. Solvents were dried by standard procedures. Reactions requiring anhydrous conditions were performed under argon. Synthetic compounds were purified by flash chromatography using medium or fine silica gel or by sephadex (LH20, G25). Thin layer chromatography (TLC) was carried out with precoated Merck F_{254} silica gel plates. Flash chromatography (FC) was carried out with Macherey-Nagel silica gel 60 (230−400 mesh). Reaction completion was observed by TLC using as development reagents phosphomolibdic acid, 10% sulfuric acid in methanol or anisaldehyde. ^{1}H, and ^{13}C spectra were recorded on Bruker Avance DPX 300, DRX 400, DRX 500, and AVIII 700 MHz spectrometers. Chemical shifts (δ) for ^{1}H and ^{13}C spectra are expressed in ppm relative to the residual solvent signal using manufacturer indirect referencing method. Signals were abbreviated as s, singlet; bs, broad singlet; d, doublet; t, triplet; q, quartet; m, multiplet. Mass spectra were obtained with a Bruker ion-trap Esquire 6000 apparatus (ESI) and a Bruker ULTRAFLEX III (MALDI-ToF) from Bruker Daltonics; HRMS were obtained with an Apex II instrument (FT-ICR, ESI) and with a Micromass Autospec-Q (FAB).

Synthesis. Compounds **3**−**8** have been previously reported.[32,45]

Glycofullerene ***1***. Alkyne-functionalized hexakis-adduct **5** (7.4 mg, 3.5×10^{-3} mmol) was dissolved in 2 mL of DMSO under an argon atmosphere, and sugar-dendron **6** (70 mg, 0.063 mmol), CuBr·S-$(CH_3)_2$ (4 mg, 0.018 mmol), and a piece of Cu metal wire were added. The mixture was vigorously stirred over a period of 72 h. The green crude was purified using a short chromatographic column with QuadraSil Mercaptopropyl (2 g) in DMSO as solvent, obtaining a red solution. The product was isolated by precipitation and centrifugation with AcOEt (15−20 mL) as a red solid (47 mg, 87%).

^{1}H NMR (DMSO-d_6, 700 MHz): δ 8.02 (s, 36H), 7.82 (s, 12H), 5.12 (m, H), 5.01 (m, H), 4.76−4.59 (m, H), 4.27 (m, H), 3.95 (m, H), 3.89 (m, H), 3.78 (m, H), 3.62−3.55 (m, H), 3.18−3.04 (m, H), 2(s, H). ^{13}C NMR (DMSO-d_6, 175 MHz): δ 162.79, 147.71, 145.60, 145.42, 141.15, 124.49, 122.74, 102.25, 100.26, 75.94, 74.55, 73.13, 71.27, 70.53, 69.25, 69.06, 67.19 65.35, 64.59, 61.58, 60.24, 55.39, 49.70, 49.07, 45.39, 28.17, 21.25. IR (neat): 3308, 3137, 2881, 2821, 1742, 1607, 1427, 1354, 1223, 1136, 1093, 1059, 878, 814, 777, 674, 520, 477 cm^{-1}. MS (MALDI-TOF) Calcd for $[M]^+$ $C_{606}H_{936}N_{144}O_{300}$, 15450.147; found, 15450 $[M]^+$.

Glycofullerene ***2***. Alkyne-functionalized hexakis-adduct **5** (11.8 mg, 5.5×10^{-3} mmol) was dissolved in 2 mL of DMSO under an argon atmosphere, and sugar-dendron **10** (120 mg, 0.1 mmol), CuBr·S-$(CH_3)_2$ (5 mg, 0.020 mmol), sodium ascorbate (12 mg, 0.06 mmol), and a piece of Cu metal wire were added. The mixture was vigorously stirred over a period of 72 h. After this time, the green crude was purified using a short chromatographic column with QuadraSil Mercaptopropyl (2 g) in DMSO as solvent, obtaining a red solution. The product was isolated by precipitation and centrifugation with AcOEt (15−20 mL) as a red sticky solid (71 mg, 78%).

^{1}H NMR (DMSO-d_6, 700 MHz): δ 8.16 (s, 36H), 7.75 (s, 12H), 5.19−4.97 (m, H), 4.76−4.59 (m, H), 4.31−4.21 (m, H), 3.90−3.70 (m, H), 3.65−3.54 (m, H), 3.18−3.04 (m, H), 2.07−1.98 (m, H). ^{13}C NMR (DMSO-d_6, 175 MHz): δ 169.8, 161.0, 147.7, 146.2, 144.9, 141.3, 131.4, 131.1, 128.5, 125.6, 122.7, 102.0, 101.6, 100.2, 75.9, 75.3, 74.5, 73.1, 71.1, 70.5, 69.2, 69.0, 67.2, 66.6, 65.3, 65.0, 64.6, 64.2, 63.4, 61.5, 60.3, 54.6, 49.7, 49.1, 46.7, 36.1, 31.2, 28.2, 21.2, 20.9. IR (KBr): 3311, 3177, 3099, 2881, 2864, 1731, 1620, 1503, 1431, 1378, 1223, 1207, 1136, 1081, 1059, 878, 817, 757, 672, 526, 504, 458 cm^{-1}. MS (MALDI-TOF) Calcd for $[M]^+$ $C_{690}H_{1032}N_{144}O_{324}$, 16506.776; found, 16506 $[M]^+$.

Glycodendron ***9***. 2-Azidoethyl-α-D-mannopyranoside **8** (50 mg, 0.2 mmol), [2-[2-(2-chloroethoxy)ethoxy]ethoxy]ethoxymethyl trikis(2-propyniloxymethyl)methane **7** (27 mg. 0.06 mmol), $CuSO_4 \cdot 5H_2O$ (1.5 mg, 0.006 mmol), TBTA (6.5 mg, 0.01 mmol), and sodium ascorbate (4.8 mg, 0.024 mmol) were dissolved in 1 mL of THF/H_2O (1:1). The solution was heated at 60 °C in a microwave oven for 25 min. A metal scavenger resin, QuadrasilMP, was added to the reaction solution and stirred for 5 min. After that, the mixture was filtered and the resulting solution was purified by size-exclusion chromatography (Sephadex LH-20 MeOH 100%), furnishing the glycodendron **9** as a white foam (61 mg, 85%).

^{1}H NMR (D_2O, 400 MHz): δ 8.07 (s, 3H, $H_{triazol}$), 4.83−4.75 (m, 3H, $H_{1\text{-man}}$), 4.72−4.62 (m, 6H, $NC\underline{H}_2CH_2O$), 4.59 (s, 6H, $OC\underline{H}_2C_{triazol}$), 4.15−4.05 (m, 3H, $NCH_2C\underline{H}_2O$), 3.98−3.90 (m, 3H, $NCH_2C\underline{H}_2O$), 3.90−3.54 (m, 31H, $H_{2\text{-man}}$, $H_{3\text{-man}}$, $H_{5\text{-man}}$, $H_{6\text{-man}}$, $OC\underline{H}_2CH_2O$, $OCH_2C\underline{H}_2O$, $C\underline{H}_2CH_2Cl$, $CH_2C\underline{H}_2Cl$), 3.47 (s, 6H, $C\underline{H}_2O_{pentaerythritol}$), 3.42 (s, 2H, $CH_2O_{pentaerythritol}$), 3.14−3.06 (m, 3H, $H_{4\text{-man}}$). ^{13}C NMR (D_2O, 400 MHz): δ 145.0 ($C_{triazol}$), 125.3 ($\underline{C}H_{triazol}$), 99.5 ($C_{1\text{-man}}$), 72.7 ($C_{4\text{-man}}$), 70.7 ($\underline{C}H_2O$), 70.5 ($C_{3\text{-man}}$), 70.4 ($\underline{C}H_2O$), 69.8 ($C_{2\text{-man}}$), 69.6 ($\underline{C}H_2O$, $\underline{C}H_2O$), 69.5 ($\underline{C}H_2O$), 69.4 ($\underline{C}H_2O_{pentaerythritol}$), 68.3 ($\underline{C}H_2O_{pentaerythritol}$), 66.3 ($C_{5\text{-man}}$), 65.4 ($O\underline{C}H_2CH_2N$), 63.5 ($O\underline{C}H_2C_{triazol}$), 60.6 ($C_{6\text{-man}}$), 50.0 ($OCH_2\underline{C}H_2N$), 44.7 ($C_{pentaerythritol}$), 43.1 ($CH_2\underline{C}H_2Cl$). MS (ESI) Calcd for $[M]^+$ $C_{46}H_{78}ClN_9O_{25}$, 1191.5; found, 1214.1 $[M + Na]^+$. HRMS (CI) Calcd for $C_{46}H_{78}ClN_9O_{25}Na$: 1214.4659. Found: 1214.4695 $[M + Na]^+$.

Glycodendron ***10***. Glycodendron **9** (99 mg, 0.083 mmol) and sodium azide (54 mg, 0.83 mmol) were dissolved in DMF (2 mL). The mixture was stirred at 60 °C for 4 days. After consumption of the starting material, the solvent was concentrated and the crude was purified by size-exclusion chromatography (Sephadex G-25 H_2O/MeOH 9:1), furnishing glycondendron **10** (86 mg, 86%) of as a white foam.

^{1}H NMR (D_2O, 400 MHz): δ 8.04 (s, 3H, $H_{triazol}$), 4.84−4.76 (m, 3H, $H_{1\text{-man}}$), 4.73−4.64 (m, 6H, $NC\underline{H}_2CH_2O$), 4.56 (s, 6H, $OC\underline{H}_2C_{triazol}$), 4.13−4.05 (m, 3H, $NCH_2C\underline{H}_2O$), 3.95−3.87 (m, 3H, $NCH_2C\underline{H}_2O$), 3.86−3.83 (m, 3H, $H_{2\text{-man}}$), 3.76−3.56 (m, 28H, $H_{3\text{-man}}$, $H_{5\text{-man}}$, $H_{6\text{-man}}$, $OC\underline{H}_2CH_2O$, $OCH_2C\underline{H}_2O$, $C\underline{H}_2CH_2N_3$, $CH_2C\underline{H}_2N_3$), 3.43 (m, 6H, $C\underline{H}_2O_{pentaerythritol}$), 3.39 (s, 2H, $C\underline{H}_2O_{pentaerythritol}$), 3.1−3.04 (m, 3H, $H_{4\text{-man}}$). ^{13}C NMR (D_2O, 400 MHz): δ 144.2 ($C_{triazol}$), 125.4 ($\underline{C}H_{triazol}$), 99.5 ($C_{1\text{-man}}$), 72.7 ($C_{4\text{-man}}$), 70.5 ($\underline{C}H_2CH_2N_3$), 70.4 ($C_{3\text{-man}}$), 69.8 ($C_{2\text{-man}}$), 69.6 ($\underline{C}H_2O$, $\underline{C}H_2O$), 69.5 ($\underline{C}H_2O$, $\underline{C}H_2O$), 69.2 ($\underline{C}H_2O_{pentaerythritol}$), 69.0 ($\underline{C}H_2O$), 68.2 ($\underline{C}H_2O_{pentaerythritol}$), 66.3 ($C_{5\text{-man}}$), 65.4 ($O\underline{C}H_2CH_2N$), 63.5 ($O\underline{C}H_{2triazol}$), 60.6 ($C_{6\text{-man}}$), 50.1

dx.doi.org/10.1021/bm3016658 | Biomacromolecules 2013, 14, 431−437

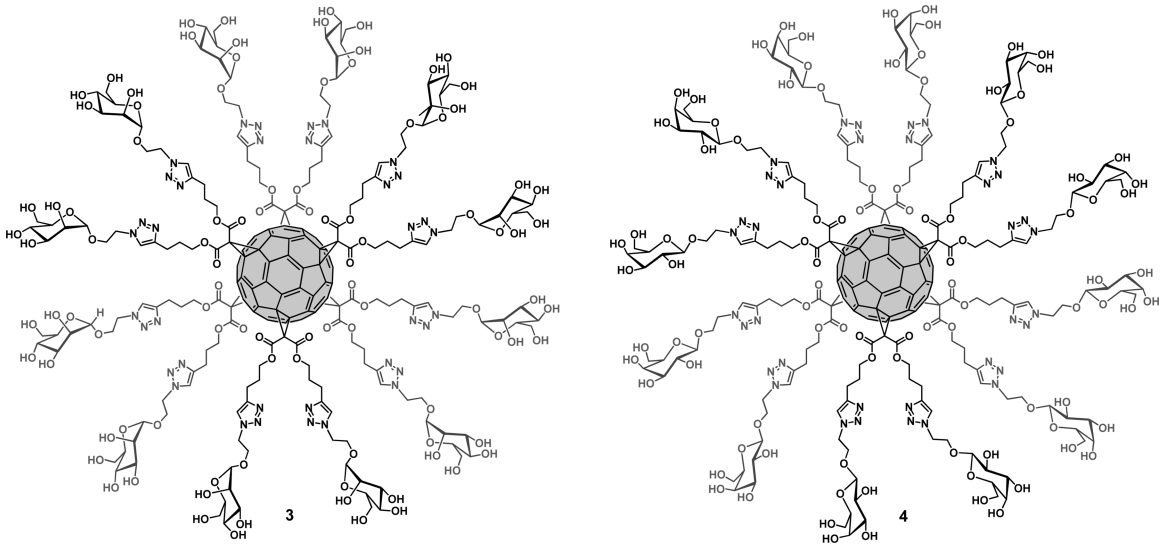

Figure 1. Structures of mannose (**3**) and galactose (**4**) glycofullerenes.

($CH_2\underline{C}H_2N_3$), 50.0 ($OCH_2\underline{C}H_2N$), 44.7 ($C_{pentaerythritol}$). MS (ESI) Calcd for $[M]^+$ $C_{46}H_{78}N_{12}O_{25}$, 1198.5; found, 1221.4 $[M + Na]^+$. HRMS (CI) Calcd for $C_{46}H_{78}N_{12}O_{25}Na$: 1221.5115; found, 1221.5099 $[M + Na]^+$.

Production of Recombinant Viruses. Recombinant viruses were produced in 293T cells. The viral construction was pseudotyped with EboGP or VSV-G and expressed luciferase as a reporter of the infection.[46] One day (18−24 h) before transfection, 5×10^6 293T were seeded onto 10 cm plates. Cells were cultured in DMEM medium supplemented with 10% heat-inactivated FBS, 25 μg/mL gentamycin, and 2 mM L-glutamine. Few minutes before transfection, the medium on transfection plates was changed to 9 mL DMEM and chloroquine was added to 25 μM final concentration. Transfection reaction with all reagents at room temperature (RT) was prepared in 15 mL tubes: 500 ng of Ebola virus envelope plasmid, 21 μg of pNL4−3Luc,[47] 183 μL of 2 M $CaCl_2$, 1300 μL of H_2O, and 1.5 mL of 2 × HBS (Hepes buffer saline) pH 7.00. HBS/DNA solution was bubbled for 30 s and gently dropped onto the plates. After 8 h of incubation at 37 °C with 5% CO_2, medium on transfection plates was changed to 10 mL of DMEM and once again 1 day after transfection to 7 mL of DMEM. Transfection supernatants were harvested after 48 h, centrifuged at 1200 rpm for 10 min at RT to remove cell debris, and stored frozen at −80 °C.[40,48]

Infection in *cis* Experiment. Infection was performed on Jurkat cells (A $CD4^+$ T-lymphocyte cell line) expressing the receptor DC-SIGN on its surface.[49] Because the Ebola virus does not infect T-lymphocytes, Ebola virus entry is absolutely dependent on DC-SIGN for infection of Jurkat cells.[39,49] On a day of infection assay, 5×10^4 of Jurkat DC-SIGN cells were plated into each well of 96-well plate. Cells were incubated at RT for 20 min with the carbohydrate-based compounds and then challenged with 5000 TCID of recombinant viruses. After 48 h of incubation, cells were washed twice with PBS, lysed, and assayed for luciferase activity. VSV-G-pseudotyped viruses were used as controls, of DC-SIGN independent infection under the same conditions. The values of inhibition of infection presented in Figure 2 correspond to the mean of six experiments performed in two independent assays. Error bars correspond to the standard errors of the mean. The IC_{50} values were estimated using GraphPad Prism v6.0 with a 95% confidence interval and settings to normalize dose−response curves.

RESULTS AND DISCUSSION

Glycofullerenes endowed with 12 (**3**) and 24 copies of mannoses have previously been prepared in our laboratory using a straightforward strategy based on a Cu(I)-catalyzed azide−alkyne cycloaddition (CuAAC), so named click chemistry, for the conjugation of sugars onto a Bingel-Hirsch hexakis-adduct [60]fullerene.[32,34] This strategy affords compounds very efficiently in few steps with good yields. Also, a [60]fullerene with 12 copies of galactose (**4**) has been prepared as negative control for experiments involving DC-SIGN as target molecule, since this lectin is not able to recognize galactose. (Figure 1) Due to the success of this synthetic approach, we decided to address the preparation of glycofullerenes with higher valency. Two [60]fullerenes bearing 36 copies of mannoses (**1** and **2**) have been prepared based on a convergent strategy using small mannosylated glycodendrons (**6** or **10**) and the hexakis-adduct **5** depicted in Scheme 1. Glycodendron **6**, which presents a short linker at the focal position had been previously prepared in large scale using a conveniently functionalized mannose with an azido group and it is a suitable building block to create highly multivalent species.[45]

For the preparation of glycodendrofullerene **1**, the conjugation of this key glycodendron **6** with the hexakis-adduct **5** was performed using $CuBr{\cdot}SMe_2$ and Cu(0) as copper source in DMSO affording the glycodendrofullerene with 36 mannoses **1** in good yield (Scheme 1). The compound was precipitated and washed extensively. To remove all traces of copper metal, a commercially available resin (QuadraSil Mercaptopropyl) was used. We have observed that considerable amounts of copper can be retained into the glycodendrofullerene inducing high cellular toxicity (data not shown). In fact, cell death has been detected in experiments using glycodendrofullerene without the resin treatment. Consequently, this removal of copper was always done previous to the use of these fullerenes in biological assays. ICP analysis allowed determining the amount of copper present into the samples (copper concentration below 0.1%). The use of QuadraSil Mercaptopropyl resin prevents the presence of copper and reduces completely the toxicity of these fullerene derivatives.

Compound **1** was completely characterized by using standard spectroscopic and analytical techniques (see Supporting Information). In particular, analysis of the IR data evidence the absence of the signals corresponding to the C−H stretching band of terminal alkyne and the C≡C band (3289 and 2117 cm^{-1}, respectively) present in compound **5**. This experimental finding unambiguously indicates that all alkyne moieties have

dx.doi.org/10.1021/bm3016658 | Biomacromolecules 2013, 14, 431−437

Scheme 1. Synthesis of Glycofullerenes 1 and 2[a]

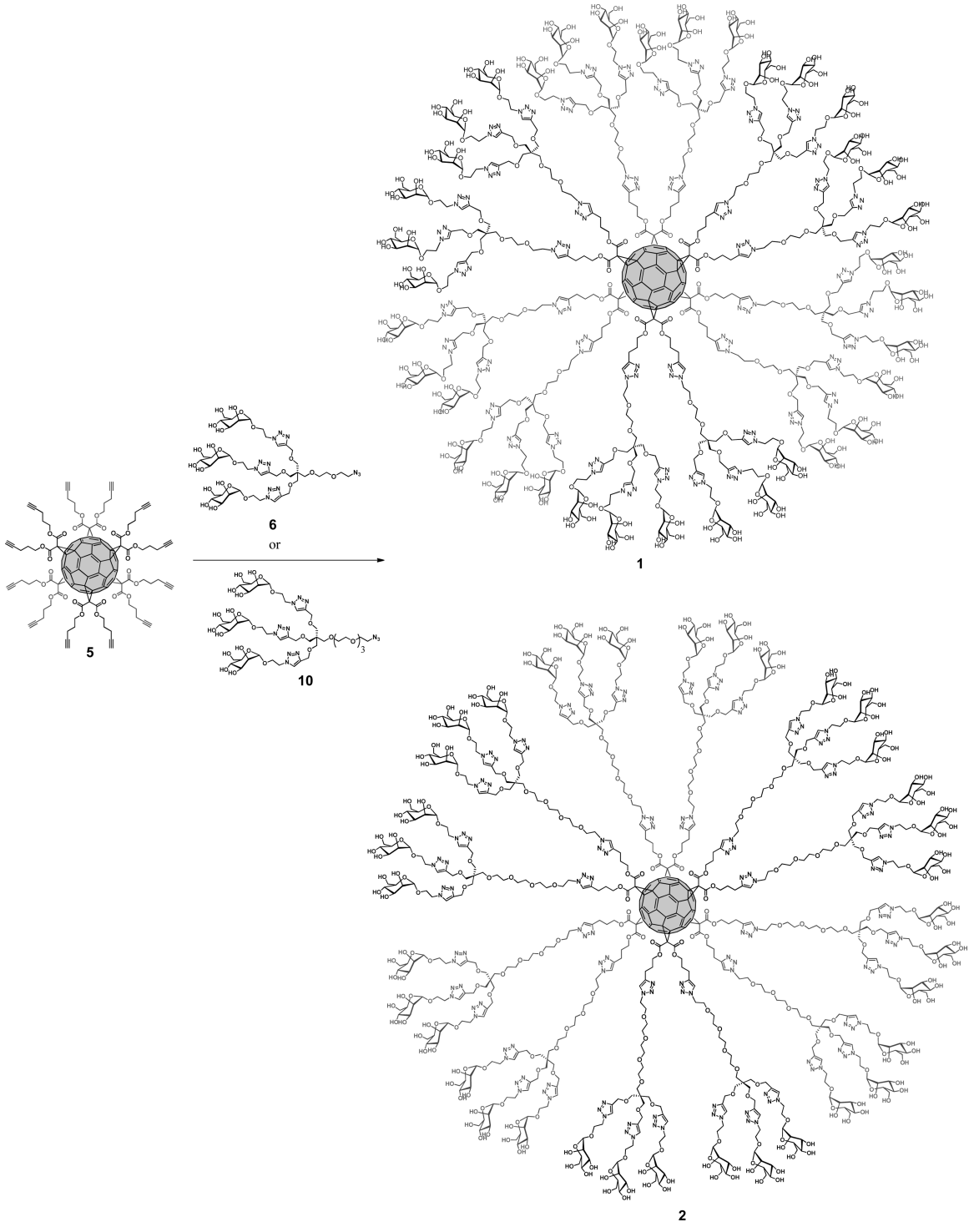

[a]Reagents and conditions: $CuBr{\cdot}SMe_2$, Cu(0), DMSO, 72 h, rt, 88%.

reacted. ^1H NMR spectrum showed the characteristic signals for the triazole protons at $\delta \sim 8.02$ and 7.82 in a 3:1 proportion, attending to the chemical structure of glycofullerene **1**. ^{13}C NMR is particularly useful for demonstrating both the full functionalization of the alkyne moieties and the *T* symmetry of the structure. Thus, the signals corresponding to the alkyne in the precursor **5** (at around 69.0 and 83.3 ppm) are not observed for the final compound **1**, and only two signals appear for the sp^2 carbons of the C_{60} cage (at around 145 and 147 ppm), together with the signal at $\delta \sim 69$ for the two sp^3 carbons of the C_{60} core. In the ^{13}C NMR spectrum, we can also observe one signal for the 12 carbonyl groups at $\delta \sim 162.8$. The C atoms of the triazole rings are observed at $\delta \sim 141.1$ and 124.5 for the peripheral triazole rings and at $\delta \sim 147.1$ and 122.7 for the 12 inner triazole rings. The anomeric carbon of the sugar moieties is observed at $\delta \sim 100.2$.

Using the same strategy, we have synthesized the glycodendrofullerene **2** (Scheme 1). This compound contains

dx.doi.org/10.1021/bm3016658 | *Biomacromolecules* 2013, 14, 431−437

Scheme 2. Synthesis of Glycodendron 10

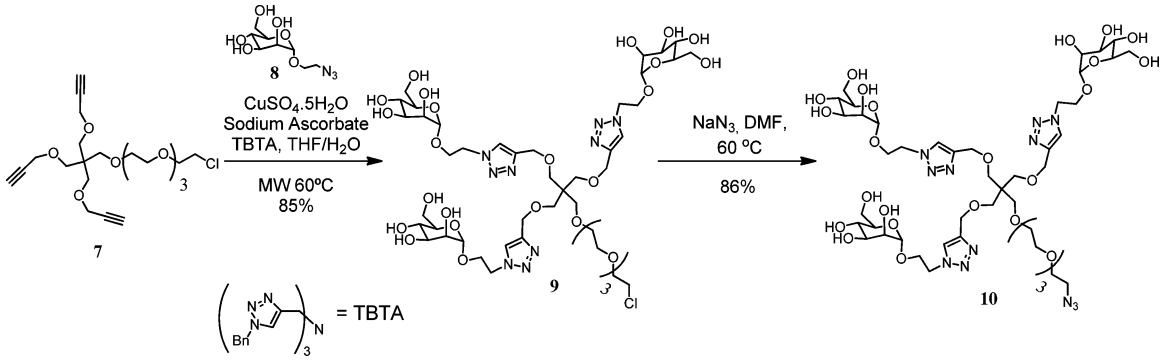

a larger spacer between the carbohydrate ligands and the fullerene scaffold. The aim of this tetraethylenglycol based linker is the increment of the flexibility of the carbohydrate ligands on the fullerene surface allowing a better accessibility and availability of ligands to be recognized by the receptor. For this aim, a trivalent mannosylated dendron **10** was prepared in two steps using the previously described trivalent scaffold **7**[44,45] and the conveniently functionalized mannose derivative **8** (Scheme 2). Trialkynylated dendron **7** has been conjugated with three copies of mannose using a click chemistry reaction. In particular, we employed $CuSO_4$ as copper salt, sodium ascorbate to reduce in situ Cu(II) to Cu(I) and TBTA as additive to stabilize Cu(I). Under these conditions, the glycodendron **9** was obtained in good yield after sephadex and QuadraSil Mercaptopropyl purification. In a second step, the chlorine atom was substituted by an azido group using sodium azide in DMF at 60 °C to afford the glycodendron **10** conveniently functionalized to be conjugated with the hexakis-adduct **5**.

Glycodendrofullerene **2** was prepared using the same conditions as those used for glycofullerene **1**. After QuadraSil Mercaptopropyl purification compound **2** was obtained in 78% yield. The characterization of this compound was performed by NMR, IR, and MS. The same parameters described above for glycodendrofullerene **1** were used to confirm the structure of glycodendrofullerene **2**.

Initial binding studies with glycofullerenes using Concanavalin A and isothermal titration calorimetry (ITC) demonstrated that mannoses on the surface of these glycofullerene systems were recognized by this lectin in a multivalent manner.[34] These studies were a proof of the adequate presentation of carbohydrates on the spherical platform. With the aim to know the efficiency of these mannosylated systems in cellular experiments we addressed an infection study assay using Ebola virus glycoprotein (EboGP) pseudotyped viral particles as infectious agents. This is a very robust and clean infection assay to test the capability of molecules to interfere with lectin-mediated viral infection since the Ebola pseudovirus, in this experimental model, is absolutely dependent on interaction with DC-SIGN for viral entry and infection.[49] This infection assay has been previously used to test the antiviral activity of glycodendritic structures prepared in our laboratory.[39,40,50] Therefore, these experiments will allow the comparison of the results with those previously obtained. In this way the relevance of the globular presentation of carbohydrates in the fullerene scaffold could be analyzed.

Briefly, infection was performed on Jurkat cells expressing DC-SIGN. Because Ebola virus does not infect T-lymphocytes, Ebola virus entry is absolutely dependent on DC-SIGN for infection of Jurkat cells. Infection by Vesicular Stomatitis Virus Glycoprotein (VSV-G) pseudoviruses was performed in the same conditions as the negative control because infection with VSV-G is independent of the presence of DC-SIGN receptor. Also, Jurkat cells not expressing DC-SIGN were used as negative control of infectivity. Cells were incubated at RT for 20 min with the carbohydrate-based compounds and then challenged with recombinant viruses. After 48 h of incubation the inhibition of infection was evaluated for each compound.

The results obtained in these experiments show the dependence of the inhibition effect on the mannoses (Figure 2). Galactosyl fullerene **4** was not able to inhibit the infection

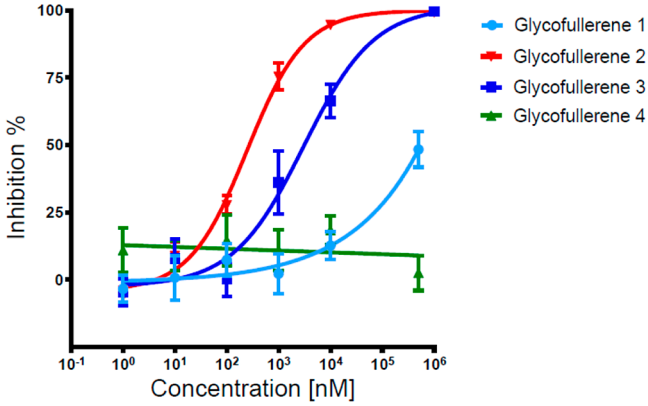

Figure 2. Inhibition of infection by pseudotyped Ebola virus infection of Jurkat DC-SIGN+ cells using mannosylated glycofullerenes **1**, **2**, **3**, and negative control **4**.

process mediated by DC-SIGN, as expected. The comparison of the mannosylated compounds **1** and **3** with different valency (12 and 36) showed an important decrease of activity with the increase of valency. Glycofullerene **3** with 12 mannoses showed an IC_{50} of 2 μM, which is very promising; however, an unexpected result was obtained for the activity of the glycodendrofullerene **1** with 36 mannoses. The IC_{50} found for this compound was 68 μM, or in other words, 34-fold less activity than the fullerene with 12 mannoses. In this case, the increase of the valency produced a decrease in the activity. The introduction of a longer spacer in glycodendrofullerene **2** has a very important effect, recovering the activity of this compound with an IC_{50} around 0.3 μM, (more than 200-fold increase in comparison with glycodendrofullerene **1**, which is present in the same valency). This value was basically the same to the previously obtained with a glycodendrimer based on a polyester

dx.doi.org/10.1021/bm3016658 | *Biomacromolecules* 2013, 14, 431−437

scaffold of similar valency in the same infection assay.[39] In this case, a clear multivalent effect was observed and this new glycodendrofullerene can be considered as a very active inhibitor of the DC-SIGN-dependent infection process.

CONCLUSIONS

We have prepared mannosylated fullerenes containing several copies of carbohydrates in a globular presentation. These multivalent systems have a good solubility in aqueous media and a low cytotoxicity against several cell lines. Preliminary binding studies using the model lectin Concanavalin A demonstrated the potency of these glycodendrofullerenes to interact with lectins in a multivalent manner.

In this work, we have shown for the first time the potential application of glycodendrofullerenes as antiviral agents. The antiviral activity of these compounds in an Ebola pseudotyped infection model were in the low micromolar range for fullerenes with 12 mannoses, a very promising data. Interestingly, the increase of valency in glycofullerene **1** induced a loss of antiviral effect. This could be probably related to steric congestion of sugars at the surface of the fullerene. One important factor to achieve high affinity in binding processes is not only the spatial presentation of the ligand but also the adequate accessibility of these ligands to interact with the corresponding receptor. Using the glycodendrofullerene **2** showing the same valency as compound **1** but including a longer spacer, we have increased remarkably the inhibitory activity of these compounds with IC_{50} in the nanomolar range, probably due to a more efficient interaction with DC-SIGN. This result highlights the importance to combine an adequate scaffold to achieve the multivalency (the spherical fullerene) with the right ligand accessibility and flexibility. The valency of the compound is an important factor to obtain good affinities in a carbohydrate−lectin interaction, but as it has been shown in these experiments, it is not the only factor to be taken into account.

Based on these results, we can consider fullerenes as very attractive scaffolds for a globular multivalent presentation of sugars. These promising results prompt us to search new approaches addressing the preparation of glycodendritic key building blocks to conjugate on fullerenes avoiding steric hindrance with the aim to achieve better antiviral activities.

ASSOCIATED CONTENT

Supporting Information

^{1}H NMR, ^{13}C NMR, FTIR, and MS spectra for glycofullerene **1** and **2**, and ^{1}H and ^{13}C NMR spectra for glycodendrons **9** and **10**. This material is available free of charge via the Internet at http://pubs.acs.org.

AUTHOR INFORMATION

Corresponding Author

*E-mail: nazmar@quim.ucm.es (N.M); rdelgado.hdoc@salud.madrid.org (R.D.); javier.rojo@iiq.csic.es (J.R.).

Notes

The authors declare no competing financial interest.

ACKNOWLEDGMENTS

Ebola GP was kindly provided by Dr. Anthony Sanchez, Centers for Disease Control, Atlanta, GA. The plasmid pNL4-3.Luc.R-E- was obtained from the AIDS Reagents Program. We would like to acknowledge the financial support by the MICINN of Spain CTQ2008-01694, by MINECO of Spain (CTQ2011-23410, CTQ2011-24652 and Consolider-Ingenio CSD2007-00010), and CAM (MADRISOLAR-2 S2009/PPQ-1533), the EU RTN CARMUSYS (PITN-GA-2008-213592), Instituto de Salud Carlos III (FIS01101580), and the European FEDER funds.

REFERENCES

(1) Varki, A. *Glycobiology* **1993**, *3*, 97−130.
(2) Feizi, T. *Curr. Opin. Struct. Biol.* **1993**, *3*, 701−710.
(3) Bertozzi, C. R.; Kiessling, L. L. *Science* **2001**, *291*, 2357−2364.
(4) Lundquist, J. J.; Toone, E. J. *Chem. Rev.* **2002**, *102*, 555−578.
(5) Lee, Y. C.; Lee, R. T. *Acc. Chem. Res.* **1995**, *28*, 321−327.
(6) Chabre, Y. M.; Roy, R. *Adv. Carbohydr. Chem. Biochem.* **2010**, *63*, 165−393.
(7) Pieters, R. J. *Org. Biomol. Chem.* **2009**, *7*, 2013−2025.
(8) Houseman, B. T.; Mrksich, M. *Top. Curr. Chem.* **2002**, *218*, 1−44.
(9) Martos, V.; Castreno, P.; Valero, J.; de Mendoza, J. *Curr. Opin. Chem. Biol.* **2008**, *12*, 698−706.
(10) Dondoni, A.; Marra, A.; Scherrmann, M.-C.; Casnati, A.; Sansone, F.; Ungaro, R. *Chem.—Eur. J.* **1997**, *3*, 1774−1782.
(11) de la Fuente, J. M.; Barrientos, A. G.; Rojas, C. T.; Rojo, J.; Cañada, J.; Fernández, A.; Penadés, S. *Angew. Chem., Int. Ed.* **2001**, *40*, 2257−2261.
(12) Roy, R. *Curr. Opin. Struct. Biol.* **1996**, *6*, 692−702.
(13) Stewart, R. J.; Boggs, J. M. *Biochemistry* **1993**, *32*, 10666−10674.
(14) Brewer, G. J.; Matinyan, N. *Biochemistry* **1992**, *31*, 1816−1820.
(15) Imberty, A.; Chabre, Y. M.; Roy, R. *Chem.—Eur. J.* **2008**, *14*, 7490−7499.
(16) Kroto, H. W.; Heath, J. R.; O'Brien, S. C.; Curl, R. F.; Smalley, R. E. *Nature* **1985**, *318*, 162−163.
(17) Pantarotto, D.; Tagmatarchis, N.; Bianco, A.; Prato, M. *Mini-Rev. Med. Chem.* **2001**, *1*, 339−348.
(18) Bosi, S.; Da Ros, T.; Spalluto, G.; Prato, M. *Eur. J. Med. Chem.* **2003**, *38*, 913−923.
(19) Partha, R.; Conyers, J. L. *Int. J. Nanomed.* **2009**, *4*, 261−275.
(20) Nakamura, E.; Isobe, H. *Chem. Rec.* **2010**, *10*, 260−270.
(21) Montellano, A.; Da Ros, T.; Bianco, A.; Prato, M. *Nanoscale* **2011**, *3*, 4035−4041.
(22) Bianco, A.; Da Ros, T. In *Fullerenes: Principles and Applications*, 2nd ed.; De La Puente, F. L., Nierengarten, J.-F., Eds.; Royal Society of Chemistry: London, 2011; pp 507−545.
(23) Cardullo, F.; Diederich, F.; Echegoyen, L.; Habicher, T.; Jayaraman, N.; Leblanc, R. M.; Stoddart, J. F.; Wang, S. *Langmuir* **1998**, *14*, 1955−1959.
(24) Kato, H.; Yashiro, A.; Mizuno, A.; Nishida, Y.; Kobayashi, K.; Shinohara, K. *Bioorg. Med. Chem. Lett.* **2001**, *11*, 2935−2939.
(25) Mikata, Y.; Takagi, S.; Tanahashi, M.; Ishii, S.; Obata, M.; Miyamoto, Y.; Wakita, K.; Nishisaka, T.; Hirano, T.; Ito, T.; Hoshino, M.; Ohtsuki, C.; Tanihara, M.; Yano, S. *Bioorg. Med. Chem. Lett.* **2003**, *13*, 3289−3292.
(26) Ito, H.; Tada, T.; Sudo, M.; Ishida, Y.; Hino, T.; Saigo, K. *Org. Lett.* **2003**, *5*, 2643−2645.
(27) Nishida, Y.; Mizuno, A.; Kato, H.; Yashiro, A.; Ohtake, T.; Kobayashi, K. *Chem. Biodiversity* **2004**, *1*, 1452−1464.
(28) Enes, R. F.; Tomé, A. C.; Cavaleiro, J. A. S.; El-Agamey, A.; McGarvey, D. J. *Tetrahedron* **2005**, *61*, 11873−11881.
(29) Kato, H.; Kaneta, N.; Nii, S.; Kobayashi, K.; Fukui, N.; Shinohara, H.; Nishida, Y. *Chem. Biodiversity* **2005**, *2*, 1232−1241.
(30) Isobe, H.; Cho, K.; Solin, N.; Werz, D. B.; Seeberger, P. H.; Nakamura, E. *Org. Lett.* **2007**, *9*, 4611−4614.
(31) Kato, H.; Böttcher, C.; Hirsch, A. *Eur. J. Org. Chem.* **2007**, 2659−2666.
(32) Nierengarten, J.-F.; Iehl, J.; Oerthel, V.; Holler, M.; Illescas, B. M.; Munoz, A.; Martin, N.; Rojo, J.; Sanchez-Navarro, M.; Cecioni, S.; Vidal, S.; Buffet, K.; Durka, M.; Vincent, S. P. *Chem. Commun.* **2010**, *46*, 3860−3862.
(33) Hirsch, A.; Vostrowsky, O. *Eur. J. Org. Chem.* **2011**, 829−848.

(34) Sanchez-Navarro, M.; Munoz, A.; Illescas, B. M.; Rojo, J.; Martin, N. *Chem.—Eur. J.* **2011**, *17*, 766−769.
(35) Compain, P.; Decroocq, C.; Iehl, J.; Holler, M.; Hazelard, D.; Mena Barragán, T.; Ortiz Mellet, C.; Nierengarten, J.-F. *Angew. Chem., Int. Ed.* **2010**, *49*, 5753−5756.
(36) Durka, M.; Buffet, K.; Iehl, J.; Holler, M.; Nierengarten, J.-F.; Taganna, J.; Bouckaert, J.; Vicent, S. P. *Chem. Commun.* **2011**, *49*, 1321−1323.
(37) Cecioni, S.; Oertherl, V.; Iehl, J.; Holler, M.; Goyard, D.; Praly, J.-P.; Imberty, A.; Nierengarten, J.-F.; Vidal, S. *Chem.—Eur. J.* **2011**, *17*, 3252−3261.
(38) Durka, M.; Buffet, K.; Iehl, J.; Holler, M.; Nierengarten, J.-F.; Vincent, S. P. *Chem.—Eur. J.* **2012**, *18*, 641−651.
(39) Lasala, F.; Arce, E.; Otero, J. R.; Rojo, J.; Delgado, R. *Antimicrob. Agents Chemother.* **2003**, *47*, 3970−3972.
(40) Luczkowiak, J.; Sattin, S.; Sutkeviciute, I.; Reina, J. J.; Sanchez-Navarro, M.; Thepaut, M.; Martinez-Prats, L.; Daghetti, A.; Fieschi, F.; Delgado, R.; Bernardi, A.; Rojo, J. *Bioconjugate Chem.* **2011**, *22*, 1354−1365.
(41) Arce, E.; Nieto, P. M.; Diaz, V.; Castro, R. G.; Bernad, A.; Rojo, J. *Bioconjugate Chem.* **2003**, *14*, 817−823.
(42) Sattin, S.; Daghetti, A.; Thepaut, M.; Berzi, A.; Sanchez-Navarro, M.; Tabarani, G.; Rojo, J.; Fieschi, F.; Clerici, M.; Bernardi, A. *ACS Chem. Biol.* **2010**, *5*, 301−312.
(43) Tabarani, G.; Reina, J. J.; Ebel, C.; Vives, C.; Lortat-Jacob, H.; Rojo, J.; Fieschi, F. *FEBS Lett.* **2006**, *580*, 2402−2408.
(44) Ribeiro-Viana, R.; García-Vallejo, J. J.; Collado, D.; Pérez-Inestrosa, E.; Bloem, K.; van Kooyk, Y.; Rojo, J. *Biomacromolecules* **2012**, *13*, 3209−3219.
(45) Ribeiro-Viana, R.; Sánchez-Navarro, M.; Luczkowiak, J.; Koeppe, J. R.; Delgado, R.; Rojo, J.; Davis, B. G. *Nat. Commun.* **2012**, *3*, 1303 DOI: 10.1038/ncomms2302.
(46) Yang, Z.; Delgado, R.; Xu, L.; Todd, R. F.; Nabel, E. G.; Sanchez, A.; Nabel, G. J. *Science* **1998**, *279*, 1034−1037.
(47) He, J.; Choe, S.; Walker, R.; Di Marzio, P.; Morgan, D. O.; Landau, N. R. *J. Virol.* **1995**, *69*, 6705−6711.
(48) Yang, S.; Delgado, R.; King, S. R.; Woffendin, C.; Barker, C. S.; Yang, Z. Y.; Xu, L.; Nolan, G. P.; Nabel, G. J. *Hum. Gene Ther.* **1999**, *10*, 123−132.
(49) Álvarez, C. P.; Lasala, F.; Carrillo, J.; Muñiz, O.; Corbí, A. L.; Delgado, R. *J. Virol.* **2002**, *76*, 6841−6844.
(50) Reina, J. J.; Sattin, S.; Invernizzi, D.; Mari, S.; Martinez-Prats, L.; Tabarani, G.; Fieschi, F.; Delgado, R.; Nieto, P. M.; Rojo, J.; Bernardi, A. *ChemMedChem* **2007**, *2*, 1030−1036.

nature COMMUNICATIONS

ARTICLE

Received 13 Jun 2012 | Accepted 15 Nov 2012 | Published 18 Dec 2012

DOI: 10.1038/ncomms2302 OPEN

Virus-like glycodendrinanoparticles displaying quasi-equivalent nested polyvalency upon glycoprotein platforms potently block viral infection

Renato Ribeiro-Viana[1,2], Macarena Sánchez-Navarro[1], Joanna Luczkowiak[3], Julia R. Koeppe[1], Rafael Delgado[3], Javier Rojo[2] & Benjamin G. Davis[1]

Ligand polyvalency is a powerful modulator of protein–receptor interactions. Host–pathogen infection interactions are often mediated by glycan ligand–protein interactions, yet its interrogation with very high copy number ligands has been limited to heterogenous systems. Here we report that through the use of nested layers of multivalency we are able to assemble the most highly valent glycodendrimeric constructs yet seen (bearing up to 1,620 glycans). These constructs are pure and well-defined single entities that at diameters of up to 32 nm are capable of mimicking pathogens both in size and in their highly glycosylated surfaces. Through this mimicry these glyco-dendri-protein-nano-particles are capable of blocking (at picomolar concentrations) a model of the infection of T-lymphocytes and human dendritic cells by Ebola virus. The high associated polyvalency effects ($\beta > 10^6$, $\beta/N \sim 10^2$–10^3) displayed on an unprecedented surface area by precise clusters suggest a general strategy for modulation of such interactions.

[1] Department of Chemistry, University of Oxford, Chemistry Research Laboratory, 12 Mansfield Road, Oxford OX1 3TA, UK. [2] Glycosystems Laboratory, Instituto de Investigaciones Químicas (IIQ), CSIC—Universidad de Sevilla, Américo Vespucio 49, Seville 41092, Spain. [3] Laboratorio de Microbiología Molecular, Instituto de Investigación Hospital 12 de Octubre (imas12), Madrid 28041, Spain. Correspondence and requests for materials should be addressed to R.D. (email: rdelgado.hdoc@salud.madrid.org) or to J.R. (email: javier.rojo@iiq.csic.es) or to B.G.D. (email: ben.davis@chem.ox.ac.uk).

© 2012 Macmillan Publishers Limited. All rights reserved.

The initial stages of an infectious process are crucial for subsequent immune response and elimination of pathogens[1]. The innate immune system comprises mechanisms and specialized cells responsible for first contact with external biological agents[2]. Detection of invaders via pathogen recognition receptors and subsequent activation of antimicrobial defences triggers specific antigen responses[3]. DC-SIGN (dendritic cell-specific intercellular adhesion molecule-3-grabbing nonintegrin) receptor is one of the most important pathogen recognition receptor. It is expressed mainly on the surface of dendritic cells (DCs), and some subtypes of macrophages[4]. DC-SIGN recognizes in a multivalent manner mannose and fucose containing glycoproteins[5], such as ICAM-3 (intercellular adhesion molecule 3) present in T cells, and envelope glycoproteins found on pathogens[6]. By using DC-SIGN as an entry point some viruses are capable of escaping from the processing and degradation events carried out by the immune defence machinery at antigen-presenting cells[7]. Therefore, the inhibition of pathogen entry through the blockade of this receptor at early stages of infection is one strategy for new antiviral agents.

Several studies have been directed towards the preparation of synthetic carbohydrate systems able to block or stimulate DC-SIGN[8–21]. Despite their elegant design, one of the problems that these artificial systems face is achieving adequate size and multivalency to sufficiently mimic natural systems such as viruses or other pathogens while maintaining full control of shape and structure[16]. Indeed, ligand valencies beyond 32 (refs 9,18) have not been possible before with full control (Indeed, valencies >100 are rare in any glycodendrimeric structure. See the following references André *et al.*[22] and Camponovo *et al.*[23] for examples of 128-mer lactoside and 243-mer xyloside display, respectively.)[22,23].

We have previously demonstrated that symmetrically multivalent glycan ligands mounted on protein platforms (glycodendriproteins) are useful tools to study carbohydrate–protein interactions and are able to control or modulate a desired response[24–27]. Other dendrimeric displays on proteins have also been explored subsequently[28–30]. However, to date, this approach has provided only limited carbohydrate valency levels on single protein platforms. We envisaged that a controlled design for a highly polyvalent protein display of sugars might be achieved through a novel strategy of 'nested polyvalency' (polyvalent display of polyvalency) (Fig. 1a).

We describe here the realization of this approach through the multivalent assembly of protein monomers themselves carrying polyvalent glycan display motifs (glycodendrons). The resulting glycodendriprotein homomultimers display many glycans in a precise manner. Consistent with associated guiding physical principles[31–33], these constructs therefore display symmetry and pseudosymmetry at both the level of protein assembly and glycodendron. These synthetic glycoprotein assemblies display the highest known number of glycans ($n=1{,}620$) yet presented in a homogeneous manner. We have applied this idea (Fig. 1) here to the inhibitory immunomodulation of a DC-SIGN-pathogen glycoprotein interaction (Fig. 1b).

Results

Construction of glyco-dendri-protein-nano-particles. We reasoned that assembly of an entity with similar dimensions (in the form of a self-assembled protein sphere-like icosahedron Qβ[34], ~28 nm in diameter) might mimic the display in target pathogens (Ebola pseudotyped virus particles have ~90 nm in diameter). Using a tag-and-modify[27] strategy, we chose to selectively introduce a non-natural amino acid (tag) on the protein that could be used for the attachment (modify) of the selected glycodendrons appropriately functionalized at the focal position. As a stringent test of this approach we chose to mimic the highly glycosylated pathogen envelopes of Ebola virus. We selected a monomer Qβ[34,35] protein as carrier, which assembles into a 180-copy multimer. Qβ multimer has been used by us and others to display glycans for other purposes but in these prior experiments only partial levels of nonspecific modification were achieved (see Supplementary Discussion). The result of these prior incomplete reactions was a formation of mixtures and not the desired homogeneous and (pseudo)symmetrical display required for this study[36,37]. This proteic platform provided the necessary viral mimic scaffold (core diameter, ~28 nm)[34] to construct the desired multivalent systems.

The designed glycodendrons were prepared in a straightforward manner by the Cu(I)-catalysed modification[38,39] of the Huisgen cycloaddition as depicted in Fig. 2. α-D-Mannose was chosen to be introduced onto the dendritic scaffolds as a relevant ligand that is recognized by DC-SIGN[5]. Synthesis of glycodendron **4** was accomplished using a modular strategy that advantageously avoided the need for carbohydrate protection. First, unprotected azidoethyl mannoside **3** (see Supplementary Methods)[8] was coupled to the trialkynyl pentaerythritol core **2** using $CuSO_4$ and sodium ascorbate in a 1:1 mixture of water:THF (tetrahydrofuran) at room temperature (RT)[40]. The focal azido group required for subsequent site-specific conjugation to the protein tag, was introduced by reaction with sodium azide to give **5**. The designed modular strategy also allowed use of **5** in the construction of higher generation glycodendron **8**. Thus, coupling of **5** with the trialkynyl core **6** gave **7** (Fig. 2), which was similarly converted to an azide **8** for protein modification.

Unnatural alkyne-containing amino acid L-homopropargylglycine (Hpg) was site-specifically introduced into the protein that would make up the proteic scaffold (Qβ) to serve as an alkyne 'tag' through the expression of corresponding gene sequences in an auxotrophic strain of *E. coli* (B834(DE3))[41]. Gene sequences were designed to create a protein displaying alkyne at a site on the outer surface of the eventual icosahedral platform (Hpg16) for which the position could simply be controlled by the 'Met' triplet codon ATG. Replacement of wildtype methionine (Met) residues, with near-isosteric amino acid isoleucine allows reassignment of the codons in the gene sequence to allow incorporation instead of Hpg as a 'tag' (see Supplementary Methods for full details). The resulting Qβ-$(Hpg16)_{180}$ was characterized, including by mass spectrometry and dynamic light scattering (Fig. 3 and see Supplementary Methods and Supplementary Fig. S1), demonstrating the introduction of the Hpg amino acid into the sequence. On the basis of previous results[42,43], Qβ-$(Hpg16)_{180}$ was modified using a reaction mixture of Cu(I)Br complexed by tris[(1-ethylacetate-1*H*-1,2,3-triazol-4-yl) methyl]amine in acetonitrile (Fig. 3a). It should be noted that the presence of Hpg on the protein results in slower Huisgen cycloaddition reaction rates in comparison with those obtained when azide in the form of azidohomoalanine (Aha) is present in the protein[42,43]. Optimization of the reaction conditions by varying catalyst loading and stepwise addition, afforded the desired glycodendron-bearing virus-like particles. Thus, reaction of Qβ-$(Hpg16)_{180}$ with trivalent glycodendron **5** afforded Qβ-$(Man_3)_{180}$ bearing 540 terminal mannosyl residues and reaction with second-generation nonavalent glycodendron **8** gave Qβ -$(Man_9)_{180}$. Both reactions proceeded with >95% conversion; consistent with greater bulk a longer reaction time (up to 7.5 h) was required for reaction of **8** to form 1,620-mer Qβ- $(Man_9)_{180}$. Increasing particle diameter was observed, Qβ (27.6 nm) → Qβ-$(Man_3)_{180}$ (29.8) → Qβ-$(Man_9)_{180}$ (32.0), consistent with the controlled introduction of 'shells' of glycosylation ~1.1 nm thick (Fig. 3b and see Supplementary Table S1 for rough estimate of dendron length)

© 2012 Macmillan Publishers Limited. All rights reserved.

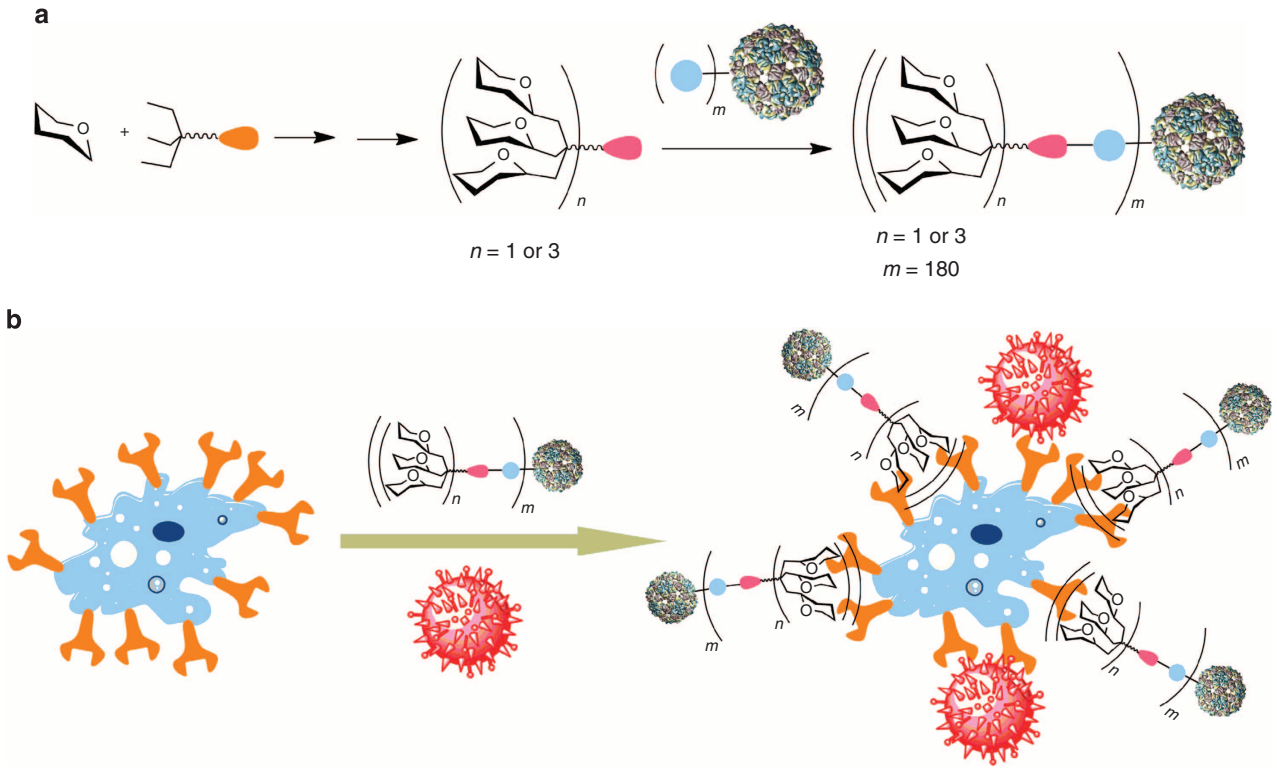

Figure 1 | Schematic representation of the nested polyvalency strategy. (**a**) Nested symmetrical assembly of virus-like glycodendrinanoparticles using a tag-and-modify strategy. Glycodendrons are created through iterative multivalent assembly and then attached to multiple tags, each in a monomer protein. (**b**) Ebola (shown in red) infection model and its competitive inhibition with virus-like glycodendrinanoparticles.

for each dendron generation. To the best of our knowledge, this is the first synthesis reported of such highly functionalized monodisperse glycodendriproteins (bearing up to 1,620 terminal sugar moieties) using a convergent approach.

Inhibition of DC-SIGN *in vitro* and on T lymphocytes. The inhibitory function of these glycodendriprotein particles was tested in several ways. Competition ELISA assay (See Supplementary Methods and Supplementary Figs S2 and S3) revealed that Qβ-$(Man_3)_{180}$ could completely inhibit the binding of DC-SIGN (as an Fc chimera) to a synthetically mannosylated glycoprotein (albumin bearing Manα1–3(Manα1–6)Man) with an estimated IC_{50} ~35–40 nM. A complete lack of inhibition by control, non-glycosylated Qβ confirmed dependence of this promisingly potent inhibition upon glycan.

Next, an Ebola viral infection model[44], was explored using mammalian T-lymphocyte (Jurkat) cells displaying DC-SIGN. Recombinant viruses were produced in HEK 293 T cells; the viral construction was pseudotyped with Ebola virus envelope GP (EboGP) or the vesicular stomatitis virus envelope glycoprotein (VSV-G) and expressed luciferase as a reporter of the infection[45]. The inhibition of DC-SIGN-dependent infection of T-lymphocyte Jurkat cells (examined in at least three independent experiments) demonstrated that unglycosylated Qβ reduced infection minimally (Fig. 4a). In contrast, Qβ-$(Man_3)_{180}$ and Qβ-$(Man_9)_{180}$ showed strong dose-dependent inhibition of the infection process (Fig. 4a–c). Indeed, Qβ-$(Man_9)_{180}$ presented a notable antiviral activity, inhibiting infection by ~80% at 5 nM; estimated IC_{50}s = 9.62 nM for β-$(Man_3)_{180}$ and = 910 pM for Qβ-$(Man_9)_{180}$.

VSV-G is able to infect T-lymphocyte Jurkat cells independently of DC-SIGN[44] and provided a positive control in infection experiments; consistent with the proposed model of inhibition (Fig. 1) this glycan-independent pathway for VSV-G was completely uninhibited (Fig. 4b,c). In this model, the Ebola infection process is absolutely dependent on the presence of DC-SIGN on the cell surface. Jurkat cells not expressing DC-SIGN were used as a negative control in the infection studies and showed no infection by Ebola pseudovirus (See Supplementary Fig. S4). The ratio of infection *in cis* between Jurkat DC-SIGN + and Jurkat cells was ~2,600 for Ebola virus infection and 0.96 for VSV infection.

Blocking of DC infection by pseudotyped Ebola. Having shown such potent inhibition of infection of a stable cell line that displays DC-SIGN, we next evaluated inhibition in the perhaps more relevant and more demanding context of inhibition of primary cells. DCs are a primary target of Ebola infection; these display multiple C-type lectins that could provide a different or modulated route for infection with potentially higher affinty for virus. Accordingly, DCs were generated from isolated human peripheral blood mononuclear cells (PBMCs) and tested. We were pleased to find that as for the stable Jurkat cell line presenting DC-SIGN alone, Qβ-$(Man_9)_{180}$ displayed potent activity (Fig. 4d), inhibiting infection by >80% at 5 nM and >95% at 25 nM (estimated IC_{50} ~2 nM for Qβ-$(Man_9)_{180}$). Excitingly, these data indicate that the mode of inhibition of these synthetic glycodendrinanoparticles translates into cellular contexts relevant to human infection and are consistent with the mode of action suggested in Fig. 1.

Discussion

Although the evaluation of the number of monomer units interacting during these inhibitory processes is complicated by quasi-equivalence[32], the data obtained indicate that these systems afford a clear polyvalency effect (β)[46] when compared with the

© 2012 Macmillan Publishers Limited. All rights reserved.

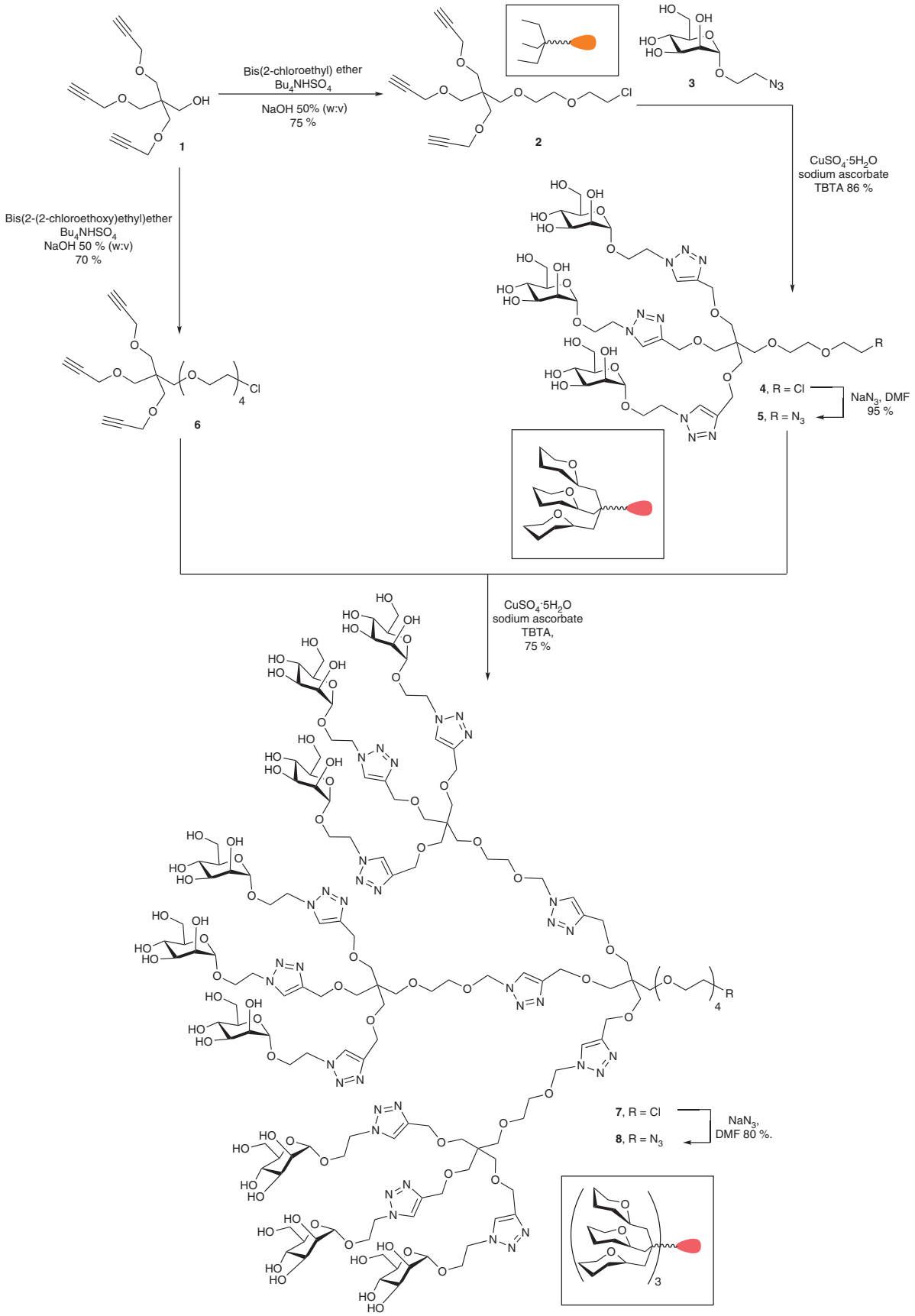

Figure 2 | Creation of polyvalent mannose-terminated glycodendrons. Synthesis of the glycondendron reagents **5** and **8** used in the assembly of virus-like glycodendri-nano-particles (see Fig. 3). TBTA, tribenzyl(tris)triazoylamine; DMF, *N*,*N*-dimethylformamide.

© 2012 Macmillan Publishers Limited. All rights reserved.

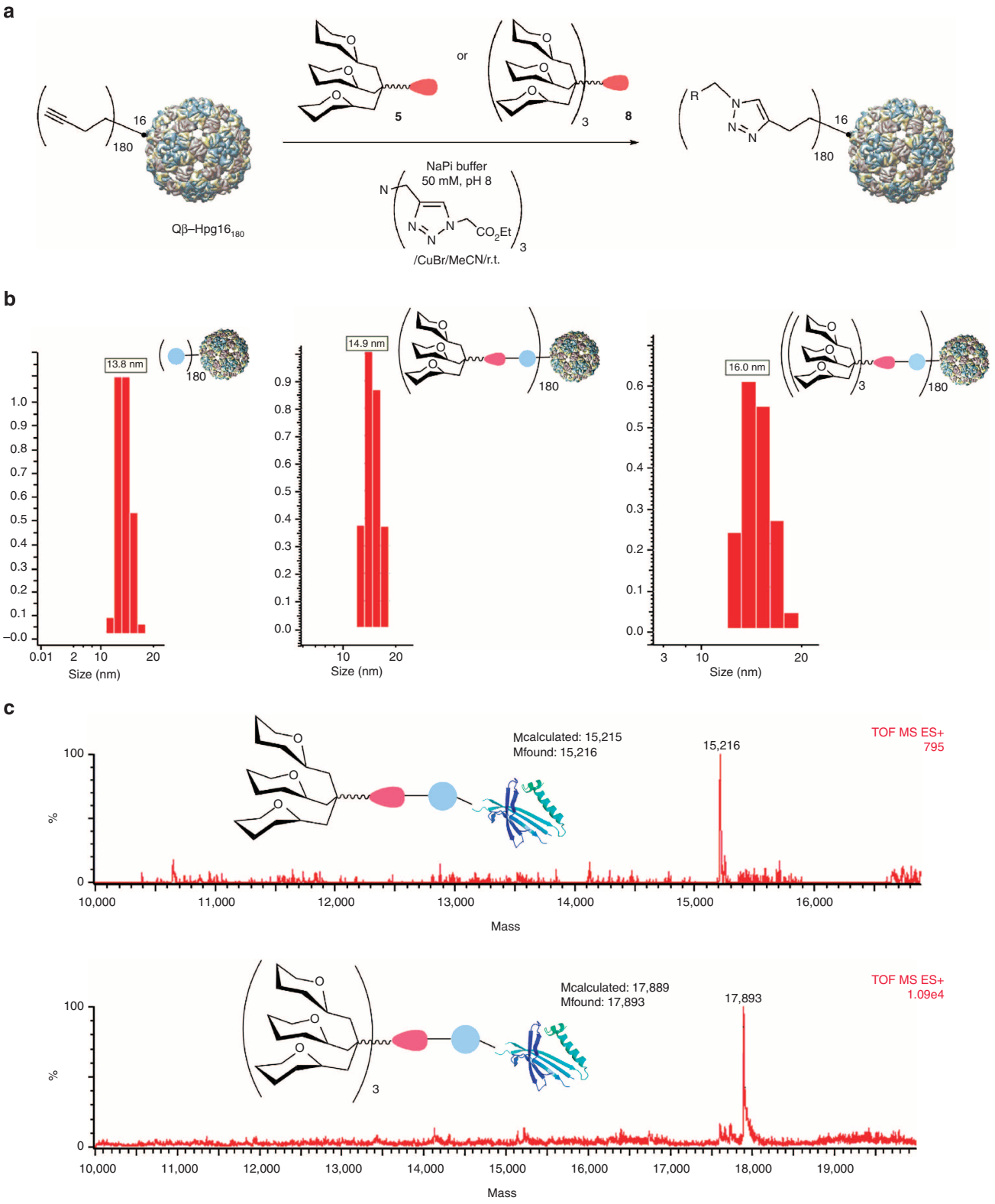

Figure 3 | Controlled assembly and characterization of virus-like glycodendri-nano-particles. (**a**) A tag-and-modify strategy allowed the generation of the second nested layer of multivalency from Qβ-$(Hpg16)_{180}$ using glycondendron reagents **5** and **8**. R = corresponding glycodendron. (**b**) Dynamic light scattering histograms showing the hydrodynamic radius of Qβ (radius 13.8 nm), Qβ-$(Man_3)_{180}$ (radius 14.9) and Qβ-$(Man_9)_{180}$ (radius 16.0). (**c**) Mass spectrometric analysis of monomer proteins of the particles. P_i, phosphate.

monomer methyl α-D-mannopyranoside) (see Supplementary Table S2). The inhibitory properties of each mannoside monomer unit can therefore be considered[46] to be ~250-fold and ~860-fold (as judged by β/N, see Supplementary Table S2) more potent when displayed in Qβ$(Man_3)_{180}$ and Qβ-$(Man_9)_{180}$, respectively, than when displayed alone. The efficiency of this system therefore

© 2012 Macmillan Publishers Limited. All rights reserved.

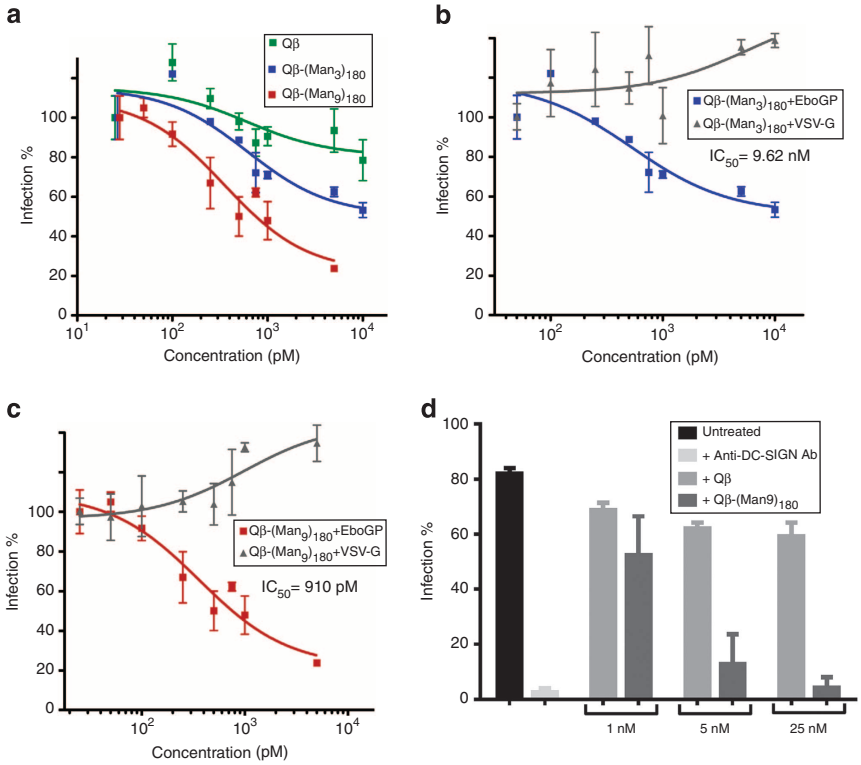

Figure 4 | Inhibition of viral infection of mammalian cells. (**a**) Comparison of infection rates of T-lymphocyte (Jurkat) cells displaying DC-SIGN by EboGP pseudovirus in the presence of Qβ, Qβ-$(Man_3)_{180}$, Qβ-$(Man_9)_{180}$; (**b**) Inhibition by Qβ-$(Man_3)_{180}$ of EBOV-GP (EboG) pseudovirus and vesicular stomatitis psuedovirus (VSV-G) in the infection (% infection)of T-lymphocyte (Jurkat) cells displaying DC-SIGN; (**c**) as for (**b**) using Qβ-$(Man_9)_{180}$. Values correspond to means of three experiments with s.e.m. shown; the IC_{50}s were estimated using Graphpad Prism v4.0 at 95% with a 95% confidence interval (4.43–20.9 nM for Qβ-$(Man_3)_{180}$ and 651 pM–1.3 nM for Qβ-$(Man_9)_{180}$) and settings for normalized dose-response curves. See the Supplementary Fig. S5 for duplicated inhibition assays. (**d**) Inhibition of infection in *cis* of human DCs by EBOV-GP (EboG) using Qβ-$(Man_9)_{180}$. Anti-DC-SIGN Ab is an antibody that blocks DC-SIGN. Immature DCs were generated from isolated human PBMCs. Blockade with anti-DC-sign antibody was used as a positive control.

relies upon a vital combination of not only a high number of displayed ligands but also display size and geometry. To date, no homogeneous polyvalent systems have been described that can generate such a large surface area (solvent-accessible surface area ~725,000 Å^2[47]) as the systems we have described here. The system we describe here is based on an icosahedral scaffold ($T=3$, triakis iscosahedral) that generates several underlying quasi-symmetry elements including those that relate the displayed glycodendrons in a two-fold, three-fold and six-fold manner (see Supplementary Movie 1). It is tempting to speculate that this, in turn, allows the simultaneous display of many distinct putative global glycan clusters where the glycan 'tips' are also quasi-equivalent (for example, 6-fold-related faces displaying a resultant 54-mer in Qβ-$(Man_9)_{180}$ or a 3-fold-related 9-mer in Qβ-$(Man_3)_{180}$, see Supplementary Movie 1). In this way, the nested glycan polyvalency that we have developed here may allow many subtly varying polyvalent combinations to be displayed, each of which (or even a combination of which) might give rise to optimal biological function (here inhibition of Ebola binding). These constructs are therefore not 'balls of sugar' but homogenous constructs that array varying faces with different polyvalent glycan arrangements. Thus, their most relevant structural features may well not be simply their average glycan-to-glycan distance (as estimated, say, from Cα-to-Cα residue distances of ~28–40 Å for 2-fold up to 6-fold quasi-symmetry) but instead the specific topology of glycan display and how that relates to both the inter-domain distances in the DC-SIGN tetramer[48] as well as its organization on cell surfaces.[49] Moreover, initial inspection of other viral surfaces suggests that such topologies might effectively out-compete not only Ebola but also other human pathogens. The striking β values that we have discovered here may well arise from such specific 'optimal' faces (see Supplementary Movie 1 for illustrative examples of these quasi-symmetrical faces). Indeed, although direct comparison with non-viral systems is not possible, non-viral particles displaying multiple mannosyl residues in a less ordered manner are notably less potent and show much lower multivalency effects ($\beta \leq 20$, see Supplementary Table S2).

In summary, a novel nested polyvalency approach combined with tag-and-modify site-selective protein synthesis has allowed the creation of homogeneous protein platforms bearing glycodendrons. These well-defined polyvalent glycoprotein assemblies present on their surface up to 1,620 copies of glycan, a remarkably high valency never obtained before using a fully controlled strategy. These glycodendriprotein particles show exciting antiviral activity, preventing mammalian cell infection by Ebola pseudotyped virus through competitive blockade of the DC-SIGN receptor in the nanomolar to picomolar range. These results clearly indicate the efficiency of these systems to interact with this pattern recognition receptor and to compete with pathogens during their entry into target cells. Their *in vivo* activity remains to be tested and it is possible that such constructs, if used in this context, could elicit humoral responses that might potentially neutralize some of the interactions studied here. The high activity and fascinating (quasi)symmetric, high surface area morphology of these new glycoconjugates provides promising candidates for the development of both new antiviral agents as well as probes of larger-scale biological events.

© 2012 Macmillan Publishers Limited. All rights reserved.

Methods

Synthesis of glycodendrons. *Glycodendron* **4**: 2-Azidoethyl α-D-mannopyranoside (306 mg, 1.2 mmol), 2-(2-chloroethoxy)ethoxymethyl trikis(2-propynyloxymethyl)methane (128 mg. 0.37 mmol), $CuSO_4 \cdot 5H_2O$ (9 mg, 0.04 mmol), tribenzyl(tris)triazoylamine (39 mg, 0.07 mmol) and sodium ascorbate (29 mg, 0.15 mmol) were dissolved in 2 ml of THF/H_2O (1:1). After consumption of the starting material (3 h), the solvent was evaporated and the crude was purified by size-exclusion chromatography (Sephadex LH-20 MeOH 100%), furnishing the glycondendron **4** as a white foam (347 mg, 86%).

Glycodendron **5**: Glycodendron **4** (80 mg, 0.07 mmol) and sodium azide (47 mg, 0.7 mmol) were dissolved in *N*,*N*-dimethylformamide (2 ml). The mixture was stirred at 60 °C for 4 days. After consumption of the starting material, the solvent was concentrated and the crude was purified by size-exclusion chromatography (Sephadex G-25 H_2O/MeOH 9:1), furnishing glycondendron **5** (76 mg, 95%) as a white foam.

Glycodendron **7**: Glycodendron **5** (30 mg, 0.03 mmol), [2-[2-(2-chloroethoxy)ethoxy]ethoxy]ethoxymethyl tris(2-propynyloxymethyl)methane (3.6 mg, 0.008 mmol), $CuSO_4 \cdot 5H_2O$ (0.5 mg, 0.002 mmol), tribenzyl(tris)triazoylamine (1.7 mg, 0.003 mmol) and sodium ascorbate (1.3 mg, 0.006 mmol) were dissolved in THF/H_2O (1:1, 1 ml). After consumption of the starting material, the solvent was evaporated and the crude was purified by size-exclusion chromatography (Sephadex LH-20 MeOH 100%), furnishing glycondendron **7** (22 mg, 75%) as a white foam.

Glycodendron **8**: Glycodendron **7** (25 mg, 0.007 mmol) and sodium azide (4 mg, 0.07 mmol) were dissolved in *N*,*N*-dimethylformamide (1 ml). The mixture was stirred at 60 °C for 4 days. After that, the solvent was concentrated and the crude was purified by size-exclusion chromatography (Sephadex G-25 H_2O/MeOH 9:1), furnishing glycondendron **8** (20 mg, 80%) as a white foam.

Synthesis of virus-like glycodendrinanoparticles. *Glycoprotein Qβ-$(Man_3)_{180}$*: Glycodendron **5** (2.84 mg, 0.002 mmol) was dissolved in sodium phosphate buffer (50 mM, pH = 8, 200 µl). Protein solution (180 µg, 100 µl) was added to the above solution and mixed thoroughly. A freshly prepared solution of copper (I) bromide (99.999%) in acetonitrile (32.6 µl of 10 mg ml^{-1}) was premixed with an acetonitrile solution of tris[(1-ethylacetate-1*H*-1,2,3- triazol-4-yl)methyl] amine (12.6 µl of 100 mg ml^{-1}). The preformed Cu-complex solution (25 µl) was added to the mixture and the reaction was agitated on a rotator for at RT. After 4 h, 150 µl of buffer and 50 µl of fresh Cu-complex solution were added to the mixture again and the reaction was agitated for a further 1.5 h. The resulting mixture was purified in PD-MiniTrap (G-25) twice and concentrated on a vivaspin membrane concentrator (30 KDa molecular weight cut off) to 400 µl. To a virus-like particle aliquot (20 µl) was added 1 µl of TCEP (1 M) to allow the protein to denature before analysis by liquid chromatography–mass spectrometry. Electrospray Ionization Mass Spectrometry (TOF ES+) (*m/z*): calc. 15,215; found 15,216.

Glycoprotein Qβ-$(Man_9)_{180}$: Glycodendron **8** (4.8 mg, 0.001 mmol) was dissolved in sodium phosphate buffer (50 mM, pH = 8, 50 µl). Protein solution (90 µg, 50 µl) was added to the above solution and mixed thoroughly. A freshly prepared solution of copper (I) bromide (99.999%) in acetonitrile (32.6 µl of 10 mg ml^{-1}) was premixed with an acetonitrile solution tris[(1-ethylacetate-1*H*-1,2,3- triazol-4-yl)methyl] amine, (12.6 µl of 100 mg ml^{-1}). The preformed Cu-complex solution (25 µl) was added to the mixture and the reaction was agitated on a rotator at RT. After 3 and 6 h, 50 µl of buffer and 12.5 µl of fresh Cu-complex solution were added to the mixture again (each time) and the reaction was agitated for further 1.5 h. The resulting mixture was purified in PD-MiniTrap (G-25) twice and concentrated on a vivaspin membrane concentrator (30 KDa molecular weight cut off) to 400 µl. To a virus-like particle aliquot (20 µl) was added 1 µl of TCEP (1M) to allow the protein to denature before analysis by liquid chromatography–mass spectrometry. ESI-MS (TOF ES+) (*m/z*): calc. 17,889; found 17,893.

Production of recombinant viruses. Recombinant viruses were produced in 293T cells. The viral construction was pseudotyped with EboGP or VSV-G and expressed luciferase as a reporter of the infection[45]. One day (18–24 h) before transfection, 6×10^6 293T were seeded onto 10 cm plates. Cells were cultured in DMEM medium supplemented with 10% heat-inactivated FBS, 25 mg gentamycin, 2 mM L-glutamine. A few minutes before transfection, the medium on transfection plates was changed to 9 ml DMEM and chloroquine was added to 25 µM final concentration. Transfection reaction with all reagents at RT was prepared in 15 ml tubes: 183 µl of 2M $CaCl_2$, 450 ng of Ebola virus envelope, 21 µg of pNL4-3 luc[50], 1,300 µl of water. Next, 1.5 ml of 2xHBS (hepes buffer saline) pH 7.0 was added quickly to the tubes and bubbled for 30 s. HBS/DNA solution was gently dropped onto medium. After 8 h of incubation at 37 °C with 5% CO_2, medium on transfection plates was changed to 10 ml DMEM and once again 1 day after transfection to 7 ml DMEM. Transfection supernatants were collected after 48 h, centrifuged at 1,200 rpm for 10 min at RT to remove cell debris, and stored frozen at −80 °C (ref. 51).

Infection of Jurkat cells displaying DC-SIGN in cis. Infection was performed on Jurkat cells (T-lymphocyte cell line) expressing receptor DC-SIGN on their surface. One day before infection, 5×10^4 of Jurkat DC-SIGN cells were plated into each well of 96-well plate. Cells were incubated at RT for 20 min with the carbohydrate-based compounds and then challenged with 5000 Tissue Culture Infective Dose of recombinant viruses. After 48 h of incubation cells were washed twice with PBS and lysed for luciferase assay. The range of concentrations tested for compounds Qβ and Qβ-$(Man_3)_{180}$ was 100 pM–50 nM and for compound Qβ-$(Man_9)_{180}$ was 50 pM–50 nM. As a control, an experiment of infection with VSV-G pseudoviruses was performed under the same conditions. Infection with VSV-G is independent of the presence of DC-SIGN receptor.

Generation of monocyte-derived DCs (DCs). PBMCs were isolated from buffy coats from healthy human donors (Hospital 12 de Octubre, Madrid, Spain) by Ficoll-Paque (Pharmacia, Uppsala, Sweden) density-gradient centrifugation. Following the centrifugation of 40 ml of whole blood samples on Ficoll-Paque at 2,000 rpm for 30 min, the cells from interface were collected and washed five times with PBS at 1,500 rpm for 5 min at RT. PBMCs were then resuspended in RPMI medium supplemented with 10% heat-inactivated FBS, 25 mg gentamycin, 2 mM L-glutamine at concentration 2×10^6 cells per ml and placed onto 24-well plate for 1 h at 37 °C with 5% CO_2. The adherent monolayer of monocytes were then washed twice with PBS and resuspended in RPMI medium supplemented with cytokines granulocyte–macrophage colony-stimulating factor (200 ng ml^{-1}) and IL-4 (10 ng ml^{-1}). For the differentiation of immature monocyte-derived DCs, cells were incubated at 37 °C with 5% CO_2 for 7 days and subsequently activated with cytokines on day 2 and 5 (refs 44,52,53).

Infection of immature monocyte-derived DCs in cis. Immature monocyte-derived DCs were incubated at RT for 20 min with the carbohydrate-based compounds and then challenged with 5000 TCID of EBOV-GP recombinant pseudoviruses. After 48 h of incubation cells were washed twice with PBS and lysed for luciferase assay. The range of concentrations tested for Qβ-$(Man_9)_{180}$ was 1, 5 and 25 nM. As a control, experiment of inhibition of infection of EBOV-GP was performed in the presence of antibody anti-DC-SIGN and mannan at concentration of 25 µg ml^{-1}.

Statistical methods. *Dynamic light scattering*: Dynamic light scattering values represent the average of 10 independent measurements, where 10 individual acquisitions were taken per measurement the results analysed using OmniSIZE software.

Infection assays: Statistical analysis was performed using GraphPad Prism v6.0.

Infection of mammalian Jurkat cells displaying DC-SIGN by EboV-GP pseudotyped viruses: The values of percentage of infection presented on the graph correspond to the mean of six independent experiments with error bars corresponding to the s.e.m. The IC_{50} values were estimated using GraphPad Prism v6.0 with a 95% confidence interval and settings to normalize dose-response curves.

Infection of primary monocyte-derived DC by EboV-GP pseudotyped viruses: The values of percentage of infection correspond to the mean of two independent experiments (error bars describe the range between the two values obtained).

References

1. Neyrolles, O., Gicquel, B. & Quintana-Murci, L. Towards a crucial role for DC-SIGN in tuberculosis and beyond. *Trends Microbiol.* **14,** 383–387 (2006).
2. Gordon, S. Pattern recognition receptors: doubling up for the innate immune response. *Cell* **111,** 927–930 (2002).
3. Medzhitov, R. Recognition of microorganisms and activation of the immune response. *Nature* **449,** 819–826 (2007).
4. Geijtenbeek, T. B. H. *et al.* Identification of DC-SIGN, a novel dendritic cell specific ICAM-3 receptor that supports primary immune responses. *Cell* **100,** 575–585 (2000).
5. Guo, Y. *et al.* Structural basis for distinct ligand-binding and targeting properties of the receptors DC-SIGN and DC-SIGNR. *Nat. Struct. Mol. Biol.* **11,** 591–598 (2004).
6. Steinman, R. M. DC-SIGN: a guide to some mysteries of dendritic cells. *Cell* **100,** 491–494 (2000).
7. van, K. Y. & Geijtenbeek, T. B. H. DC-SIGN: escape mechanism for pathogens. *Nat. Rev. Immunol.* **3,** 697–709 (2003).
8. Arce, E. *et al.* Glycodendritic structures based on Boltorn hyperbranched polymers and their interactions with Lens culinaris lectin. *Bioconjugate Chem.* **14,** 817–823 (2003).
9. Lasala, F., Arce, E., Otero, J. R., Rojo, J. & Delgado, R. Mannosyl glycodendritic structure inhibits DC-SIGN-mediated ebola virus infection in cis and in trans. *Antimicrob. Agents Chemother.* **47,** 3970–3972 (2003).
10. Borrok, M. J. & Kiessling, L. L. Non-carbohydrate inhibitors of the lectin DC-SIGN. *J. Am. Chem. Soc.* **129,** 12780–12785 (2007).
11. Reina, J. J. *et al.* 1,2-Mannobioside mimic: synthesis, DC-SIGN interaction by NMR and docking, and antiviral activity. *ChemMedChem* **2,** 1030–1036 (2007).
12. Mitchell, D. A. *et al.* Synthesis 2-C-branched derivatives of D-mannose: 2-C-aminomethyl-D-mannose binds to the human C-type lectin DC-SIGN with affinity greater than an order of magnitude compared to that of D-mannose. *Tetrahedron Asymmetry* **18,** 1502–1510 (2007).

© 2012 Macmillan Publishers Limited. All rights reserved.

13. Martínez-Ávila, O. *et al.* Multivalent manno-glyconanoparticles inhibit DC-SIGN-mediated HIV-1 trans-infection of human T cells. *ChemBioChem* **10,** 1806–1809 (2009).
14. Martínez-Ávila, O. *et al.* Gold manno-glyconanoparticles: multivalent systems to block HIV-1 gp120 binding to the lectin DC-SIGN. *Chem. Eur. J.* **15,** 9874–9888 (2009).
15. Sattin, S. *et al.* Inhibition of DC-SIGN-mediated HIV infection by a linear trimannoside mimic in a tetravalent presentation. *ACS Chem. Biol.* **5,** 301–312 (2010).
16. Sanchez-Navarro, M. & Rojo, J. Targeting DC-SIGN wih carbohydrate multivalent systems. *Drug News Perspect.* **23,** 557–572 (2010).
17. Wang, S.-K. *et al.* Targeting the carbohydrates on HIV-1: interaction of oligomannose dendrons with human monoclonal antibody 2G12 and DC-SIGN. *Proc. Natl Acad. Sci. USA* **105,** 3690–3695 (2008).
18. Greatrex, B. W. *et al.* The synthesis and immune stimulating action of mannose-capped lysine-based dendrimers. *Tetrahedron* **65,** 2939–2950 (2009).
19. Luczkowiak, J. *et al.* Pseudosaccharide functionalized dendrimers as potent inhibitors of DC-SIGN dependent Ebola pseudotyped viral infection. *Bioconjugate Chem.* **22,** 1354–1365 (2011).
20. Andreini, M. *et al.* Second generation of fucose-based DC-SIGN ligands: affinity improvement and specificity versus Langerin. *Org. Biomol. Chem.* **9,** 5778–5786 (2011).
21. Prost, L. R., Grim, J. C., Tonelli, M. & Kiessling, L. L. Noncarbohydrate glycomimetics and glycoprotein surrogates as DC-SIGN antagonists and agonists. *ACS Chem. Biol.* **7,** 1603–1608 (2012).
22. André, S., Ortega, P. J. C., Perez, M. A., Roy, R. & Gabius, H.-J. Lactose-containing starburst dendrimers: influence of dendrimer generation and binding-site orientation of receptors (plant/animal lectins and immunoglobulins) on binding properties. *Glycobiology* **9,** 1253–1261 (1999).
23. Camponovo, J. *et al.* 'Click' glycodendrimers containing 27, 81, and 243 modified xylopyranoside termini. *J. Org. Chem.* **74,** 5071–5074 (2009).
24. Davis, B. G. The controlled glycosylation of a protein with a bivalent glycan: towards a new class of glycoconjugates, glycodendriproteins. *Chem. Commun.* 351–352 (2001).
25. Rendle, P. M. *et al.* Glycodendriproteins: a synthetic glycoprotein mimic enzyme with branched sugar-display potently inhibits bacterial aggregation. *J. Am. Chem. Soc.* **126,** 4750–4751 (2004).
26. Robinson, M. A. *et al.* LEAPT: lectin-directed enzyme-activated prodrug therapy. *Proc. Natl Acad. Sci. USA* **101,** 14527–14532 (2004).
27. Chalker, J. M., Bernardes, G. J. L. & Davis, B. G. A 'tag-and-modify' approach to site-selective protein modification. *Acc. Chem. Res.* **44,** 730–741 (2011).
28. Sato, M. *et al.* Glycoinsulins: dendritic sialyloligosaccharide-displaying insulins showing a prolonged blood-sugar-lowering activity. *J. Am. Chem. Soc.* **126,** 14013–14022 (2004).
29. Ni, J., Song, H., Wang, Y., Stamatos, N. M. & Wang, L. -X. Toward a carbohydrate-based HIV-1 vaccine: synthesis and immunological studies of oligomannose-containing glycoconjugates. *Bioconjugate Chem.* **17,** 493–500 (2006).
30. Kostiainen, M. A., Szilvay, G. R., Smith, D. K., Linder, M. B. & Ikkala, O. Multivalent dendrons for high-affinity adhesion of proteins to DNA. *Angew. Chem. Int. Ed.* **45,** 3538–3542 (2006).
31. Crick, F. H. C. & Watson, J. D. The structure of small viruses. *Nature* **177,** 473–475 (1956).
32. Caspar, D. L. D. & Klug, A. Physical principles in the construction of regular viruses. *Cold Spring Harbor Symp. Quant. Biol.* **27,** 1–24 (1962).
33. Johnson, J. E. & Speir, J. A. Quasi-equivalent viruses: a paradigm for protein assemblies. *J. Mol. Biol.* **269,** 665–675 (1997).
34. Kozlovska, T. M. *et al.* Recombinant RNA phage Qβ capsid particles synthesized and self-assembled in *Escherichia coli*. *Gene* **137,** 133–137 (1993).
35. Strable, E. *et al.* Unnatural amino acid incorporation into virus-like particles. *Bioconjugate Chem.* **19,** 866–875 (2008).
36. Astronomo, R. *et al.* Defining criteria for oligomannose immunogens for HIV using icosahedral virus capsid scaffolds. *Chem. Biol.* **17,** 357–370 (2010).
37. Doores, K. J. *et al.* A nonself sugar mimic of the HIV glycan shield shows enhanced antigenicity. *Proc. Natl Acad. Sci. USA* **107,** 17107–17112 (2010).
38. Tornøe, C. W., Christensen, C. & Meldal, M. Peptidotriazoles on solid phase: [1,2,3]-triazoles by regiospecific copper(I)-catalyzed 1,3-dipolar cycloadditions of terminal alkynes to azides. *J. Org. Chem.* **67,** 3057–3064 (2002).
39. Rostovtsev, V. V., Green, L. G., Fokin, V. V. & Sharpless, K. B. A stepwise huisgen cycloaddition process: copper(I)-catalyzed regioselective 'ligation' of azides and terminal alkynes. *Angew. Chem. Int. Ed.* **41,** 2596–2599 (2002).
40. Ortega-Muñoz, M., Lopez-Jaramillo, J., Hernandez-Mateo, F. & Santoyo-Gonzalez, F. Synthesis of glyco-silicas by Cu(I)-catalyzed 'click-chemistry' and their applications in affinity chromatography. *Adv. Synth. Catal.* **348,** 2410–2420 (2006).
41. Van, H. J. C. M., Kiick, K. L. & Tirrell, D. A. Efficient incorporation of unsaturated methionine analogues into proteins *in vivo*. *J. Am. Chem. Soc.* **122,** 1282–1288 (2000).
42. van Kasteren, S. I., Kramer, H. B., Gamblin, D. P. & Davis, B. G. Site-selective glycosylation of proteins: creating synthetic glycoproteins. *Nat. Protoc.* **2,** 3185–3194 (2007).
43. van Kasteren, S. I. *et al.* Expanding the diversity of chemical protein modification allows post-translational mimicry. *Nature* **446,** 1105–1109 (2007).
44. Alvarez, C. P. *et al.* C-type lectins DC-SIGN and L-SIGN mediate cellular entry by Ebola virus in cis and in trans. *J. Virol.* **76,** 6841–6844 (2002).
45. Yang, Z.-y. *et al.* Distinct cellular interactions of secreted and transmembrane Ebola virus glycoproteins. *Science* **279,** 1034–1037 (1998).
46. Mammen, M., Choi, S.-K. & Whitesides, G. M. Polyvalent interactions in biological systems: implications for design and use of multivalent ligands and inhibitors. *Angew. Chem. Int. Ed.* **37 (1998).**
47. Golmohammadi, R., Fridborg, K., Bundule, M., Valegard, K. & Liljas, L. The crystal structure of bacteriophage Q beta at 3.5 A resolution. *Structure* **4,** 543 (1996).
48. Tabarani, G. *et al.* DC-SIGN neck domain is a pH-sensor controlling oligomerization. *J. Biol. Chem.* **284,** 21229–21240 (2009).
49. de Bakker, B. I. *et al.* Nanoscale organization of the pathogen receptor DC-SIGN mapped by single-molecule high-resolution fluorescence microscopy. *ChemPhysChem* **8,** 1473–1480 (2007).
50. He, J. *et al.* Human immunodeficiency virus type 1 viral protein R (Vpr) arrests cells in the G2 phase of the cell cycle by inhibiting p34cdc2 activity. *J. Virol.* **69,** 6705–6711 (1995).
51. Yang, S. *et al.* Generation of retroviral vector for clinical studies using transient transfection. *Hum. Gene Ther.* **10,** 123–132 (1999).
52. Puig-Kroger, A. *et al.* Maturation-dependent expression and function of the CD49d integrin on monocyte-derived human dendritic cells. *J. Immunol.* **165,** 4338–4345 (2000).
53. Relloso, M. *et al.* DC-SIGN (CD209) expression is IL-4 dependent and is negatively regulated by IFN, TGF-β, and anti-inflammatory agents. *J. Immunol.* **168,** 2634–2643 (2002).

Acknowledgements

We acknowledge the financial support by the MICINN of Spain CTQ2008-01694 and CTQ2011-23410, the EU RTN CARMUSYS (PITN-GA-2008-213592), Instituto de Salud Carlos III (FIS PI080806 and PI1101580) and Fundación para la Investigación y Prevención del SIDA (FIPSE 36749) and the European FEDER funds. We thank Professors A. Sánchez (Centers for Disease Control and Prevention, Atlanta, GA) and M.G. Finn (TSRI, La Jolla, CA) for providing Zaire Ebola Virus glycoprotein and p75m/Qβ plasmids, respectively. MSN thanks Fundación Ramón Areces for funding, BGD is a Royal Society Wolfson Research Merit Award recipient and is supported by an EPSRC LSI Platform grant.

Author contributions

R.R.-V. and M.S.N. synthesized the glycodendrons and the glycodendriproteins, J.L. carried out the Ebola infection experiments. J.R.K. expressed and purified Qβ. M.S.N., R.D., J.R. and B.G.D. designed the experiments. All the authors discussed results and analysed the data. M.S.N. and B.G.D. wrote the manuscript. Correspondence and requests for materials should be addressed to R.D., J.R. and B.G.D.

Additional information

Supplementary Information accompanies this paper at http://www.nature.com/naturecommunications

Competing financial interests: The authors declare no competing financial interests.

Reprints and permission information is available online at http://npg.nature.com/reprintsandpermissions/

How to cite this article: Ribeiro-Viana, R. *et al.* Virus-like glycodendrinanoparticles displaying quasi-equivalent nested polyvalency upon glycoprotein platforms potently block viral infection. *Nat. Commun.* 3:1303 doi: 10.1038/ncomms2302 (2012).

This work is licensed under a Creative Commons Attribution-NonCommercial-NoDerivs 3.0 Unported License. To view a copy of this license, visit http://creativecommons.org/licenses/by-nc-nd/3.0/

© 2012 Macmillan Publishers Limited. All rights reserved.